



Universitat
de les Illes Balears

DOCTORAL THESIS

2019

**ROLE OF MEMBRANE LIPIDS IN COLON
DIFFERENTIATION UNRAVELLED BY MASS
SPECTROMETRY IMAGING: ARACHIDONIC ACID
BEYOND INFLAMMATION**

Joan Bestard Escalas



Universitat
de les Illes Balears

DOCTORAL THESIS

2019

Doctoral Programme of Neuroscience

**ROLE OF MEMBRANE LIPIDS IN COLON
DIFFERENTIATION UNRAVELLED BY MASS
SPECTROMETRY IMAGING: ARACHIDONIC ACID
BEYOND INFLAMMATION**

Joan Bestard Escalas

Thesis Supervisor: Gwendolyn Barceló Coblijn

Thesis tutor: Jerònia Lladó Vich

Doctor by the Universitat de les Illes Balears

A handwritten signature in blue ink, appearing to be "Gwendolyn", with a long horizontal flourish extending to the right.

A handwritten signature in blue ink, appearing to be "Jerònia", with a long horizontal flourish extending to the right.

Role of membrane lipids in colon
differentiation unravelled by mass
spectrometry imaging: arachidonic
acid beyond inflammation

A m'un pare, a mu mare i a na Mar

Per suportarme i confiar sempre amb jo

Agraïments

Primer de tot he d'agraïr haver pogut realitzar aquesta tesi a m'un pare Toni, a mu mare Carme, a n'es meu germà Toni, sa meva predina Enriqueta i sa resta de sa meva família. Encara que en general no tenien molt clar de que va això de fer ciència ni si s'hi pot viure, sempre han estat convençuts de que me les arreglaria per tirar-ho envant.

Evidentment, també he d'agraïr a na Mar, sa meva companya de vida, sa seva confiança en que ho aconseguiria. Malgrat ella sí que té ben clar lo fotut que és treure coses en aquest gremi (ja siguin experiments o contractes).

No puc estar més agraït a n'es meus companys d'es laboratori de Lípids en Patologia Humana; na Rebe, n'Albert, en Dani, en Karim, en Ramon, na Maria i n'Alice. Aquests grans companys no només m'han aguantat durant es moments d'estrés, també he pogut treure envant sa meva feina amb sa seva inestimable ajuda. També he d'agraïr a na Gwendolyn per donar-me s'oportunitat de fer sa tesi doctoral amb ella, atribuint-me unes grans capacitats malgrat un expedient que semblava afirmar tot just lo contrari.

També he d'agraïr a n'es companys i companyes d'es grup de Micro, que m'han demostrat (malgrat algunes vegades de ses maneres més estranyes imaginables) es seu suport i sa seva solidaritat i comprensió. En Biel Cabot, na Sara, na Bel, na Irina, en Biel Torrens, en Tomeu, na Laura, na Elena, en Carles i tots es alumnes i companys que han passat per allà. M'entristeix bastant no poder posar sa llista sencera de companys i companyes de s'IdISBa que m'han ajudat escoltant-me i ajudant-me amb es seus consells al llarg d'es meus anys aquí. Malgrat això he d'anomenar al manco a en Javi, n'Amanda, na Esther, n'Antònia, na Laura, n'Aina, na Bàrbara, sa gent Predimed, na Marga Ensenyat, n'Eva, n'Emi, n'Andreas, n'Anna, na Maria, en Carlos Rio, na Cati, en Víctor i en Tòfol. He de fer una menció especial a n'Àngel i na Meri, dos sants que per molt tort que tenguin es dia sempre tenen un moment i un somriure per fer-te un favor, sou dues persones extraordinàries. A més he d'agraïr a n'es personal d'administració de s'IdISBa, pot ser no sempre ens duim bé, però sense sa vostra feina, nosaltres no podríem fer sa nostra. En aquest sentit, he d'estar especialment agraït a na Marga Frontera i en David, gràcies a voltros al manco en un temps, jo i altres podrem fer lo que ens agrada a ca nostra. Moltíssimes gràcies a tots.

Evidentment, no tot a sa vida és fer feina, i per això estan es amics. Per escoltar-te prenent cervesses mentres remugues d'es teu dia. Malgrat molts d'es meus companys s'han convertit en grans amics meus, sense es amics de fora d'es laboratori no crec que hagués aguantat aquests durs anys. Gràcies de tot cor a n'Ana, en Lluís, en Juanjo, en Miguel, na Cata, na Neus i na Joana, que sempre que m'han vist malament m'han donat una abraçada, una cervesa i ànims per seguir. També he d'agraïr i demanar perdó a n'es amics de Canamunt i Canavall, en Jordi, en Rober, n'Aurèlia, n'Àitor na Maria i en Pau. Perdó per lo pesat que hagi pogut ser durant aquests anys amb aquesta feina que pot ser m'ha absorbit tant que vos he deixat inmerescudament un poc de costat, i gràcies per malgrat això, haver seguit estimant-me i fent-me cas.

Abbreviations	1
Abstract	3
Resum.....	4
Resumen.....	5
1 Introduction	7
1.1 Lipids: a basic classification	9
1.2 Lipid nomenclature	13
1.3 Membrane heterogeneity	14
1.4 Membrane phospholipid metabolism.....	17
1.4.1 <i>De novo</i> or Kennedy pathway	17
1.4.2 Fatty acid remodeling or Land's cycle	21
1.5 Lipid analysis	23
1.5.1 Before analysis: the lipid extraction.....	24
1.5.2 Membrane lipid analysis by chromatographic techniques.....	24
1.5.3 Mass Spectrometry techniques.....	24
1.6 Colon as a proliferation and differentiation model	27
1.7 Introduction to colon signaling	31
1.8 Arachidonic acid derivatives and prostaglandin signaling	33
1.9 Lipid biomarkers.....	39
1.9.1 Extracellular vesicles as non-invasive biomarkers	40
2 Hypothesis and aim of the study.....	43
3 Results: Chapter 1: Exploring the cell membrane lipidome as colorectal cancer biomarker	45
3.1.1 Lipid biomarkers for cellular malignization in cell culture model	45
3.1.2 Lipid biomarkers for cellular malignization in human tissue	57
3.1.3 Extracellular vesicles lipids as biomarkers of malignization in cell culture model	67

3.1.4	Extracellular vesicles lipidome as clinical colorectal cancer biomarker.....	72
3.2	Chapter 2: Lipid metabolism in the colonocytes proliferation and differentiation process	79
3.2.1	Lipidome as biomarker of the physiopathological state of the cell.....	79
3.2.2	Prostaglandin signaling in colon proliferation.....	94
4	General discussion	113
5	Conclusions	118
6	Experimental procedures.....	120
6.1	Chapter 1.....	120
6.1.1	Commercial cell lines culture conditions	120
6.1.2	Extracellular vesicles isolation.....	120
6.1.3	Cells and cell-derived EVs lipid composition.....	120
6.1.4	Principal component analysis.....	122
6.1.5	Protein quantification	123
6.1.6	Western Blot	123
6.1.7	RNA isolation protocol	124
6.1.8	Quantitative Reverse Transcription-Polymerase Chain Reaction (qRT-PCR)	124
6.1.9	Tissue samples processing for imaging techniques	124
6.1.10	MALDI-IMS analysis.....	125
6.1.11	Plasma-derived EVs lipid composition	126
6.2	Chapter 2.....	126
6.2.1	Immunofluorescence in colon tissue	126
6.2.2	Organoid cell culture	128
6.2.3	Organoid MTT assays	129
6.2.4	PLA ₂ and COX inhibition assessment.....	129
6.2.5	Digital Droplet PCR.....	130

6.2.6	Nuclear colocalization of prostaglandin receptors in colonocytes by IF	130
6.3	Statistical analysis	131
7	Bibliography	133
8	Supplemental material.....	178
3.1.1	Lipid markers for cellular malignization in cell culture model	178
3.1.2	Lipid markers for cellular malignization in human tissue	184

Abbreviations

AA	Arachidonic acid
ACS	Acyl-CoA synthetase
AECC	Asociación española contra el cáncer
Cer	Ceramide
COX	Cyclooxygenase
CRC	Colorectal cancer
DAG	Diacylglycerol
DESI	Desorption/electrospray ionisation
ER	Endoplasmic reticulum
ESI	Electrospray ionisation
EV	Extracellular vesicles
FOBT	Fecal occult blood test
GC	Gas chromatography
GPCR	G-protein-coupled receptor
HexCer	Hexosylceramide
HPLC	High-Performance Liquid Chromatography
IF	Immunofluorescence
IMS	Imaging Mass Spectrometry
LPA	Lysophosphatidic acid
LPC	Lysophosphatidyl choline
LPLAT	Lysophospholipid acyltransferase
MALDI	Matrix-Assisted Laser Desorption Ionisation
MS	Mass spectrometry
MUFA	Monounsaturated fatty acid
MVBs	Multivesicular bodies
NSAID	Non-steroidal antiinflammatory drug
PA	Phosphatidic acid
PC	Phosphatidylcholine
PE	Phosphatidylethanolamine
PG	Prostaglandins
PI	Phosphatidylinositol
PIP	Phosphatidylinositol phosphate
PLA₁	Phospholipase A1
PLA₂	Phospholipase A2
PLB	Phospholipase B
PLC	Phospholipase C
PLD	Phospholipase D
PS	Phosphatidylserine
PUFA	Polyunsaturated fatty acid
RI	Relative intensity
SEOM	Sociedad española de oncología médica
SIMS	Secondary ion mass spectrometry

SM Sphingomyelin
TA cells Transit-amplifying cells
TLC Thin-layer chromatography

Abstract

The presence of thousands of lipid species in nature (to date around 21500 molecular species) opens the question of why life needs this high variety if to generate membranes only a few species are really needed. The systematic study of the lipidome has helped in defining lipids not just as building blocks and providers of the right environment for proteins to function, but also as direct participants in many biological processes and as precursors of other signaling molecules. In this thesis, we took advantage of the last advances in lipid analytical techniques to study the lipid changes occurring in colon pathophysiology and to identify potential new lipid biomarkers for colorectal cancer (CRC).

Analyzing commercial cell lines lipidome by HPLC-mass spectrometry, we demonstrated that the lipidome was able to distinguish between healthy primary and CRC cell lines. Further, we assessed the difference in lipid composition in human tissue sections, analyzing them by imaging mass spectrometry techniques (IMS). This technique allows describing two-dimensionally the lipid distribution along tissue sections. The images obtained showed that the lipidome was sensitive enough to discriminate between the different cell types conforming colon mucosa first, and then between healthy and tumor tissue. Among the multiple changes detected, it was remarkable how different arachidonic acid (AA) species were handled by the epithelial cells compared to stromal cells. While AA changed precisely along the colon crypt according to the differentiation state of the epithelial cells, in the stroma, the changes surfaced the immunological response naturally occurring in a healthy colon. In order to delve into the role of AA metabolism in proliferation and differentiation processes, we used colon organoids to investigate how changes in prostaglandins (PG) metabolism influenced colonocytes development.

Given the sensitivity showed by the lipidome to the pathophysiological state of colon cells, we next explored the possibility of using the lipid composition of extracellular vesicles (EVs) as non-invasive biomarkers. We confirmed that the lipid composition of these vesicles was sensitive enough to stratify them according to their cell of origin in model systems and according to the patients group (healthy vs. adenomatous polyps/invasive neoplasia). These analyzes showed that the lipid composition of plasma-derived EVs reflects the colon tumor development by a significant proportion of patients with colon tumors.

In summary, this thesis proved that the lipidome is highly sensitive to the pathophysiological state of cells in the colon, establishing the comprehensive lipid analysis as a feasible and reliable tool to detect pathological states as CRC. Furthermore, this study provided solid evidence to investigate lipid metabolism as a source of potential new drug targets.

Resum

La presència de milers d'espècies de lípids en la natura (a dia d'avui al voltant de 21500 espècies moleculars) fa qüestionar el perquè la vida necessita aquesta gran varietat si per generar membranes bastarien unes quantes espècies. L'estudi sistemàtic del lipidoma ha ajudat a definir els lípids no només com a blocs de construcció i proveïdors de l'ambient necessari per fer funcionar les proteïnes, sinó a més com a participants en múltiples processos biològics i com a precursors d'altres molècules senyal. En aquesta tesi, hem aprofitat els darrers avenços en tècniques d'anàlisi de lípids per estudiar els canvis que es donen en la fisiopatologia del colon i per identificar nous potencials biomarcadors de càncer colorectal (CCR).

Amb l'anàlisi lipídica de línies comercials per HPLC acoblada a espectrometria de masses, hem demostrat que el lipidoma era capaç de distingir entre cèl·lules primàries sanes i línies cel·lulars de càncer colorectal. A més, comprovarem les diferències en composició lipídica en talls histològics de teixit humà usant tècniques d'imatge acoblada a espectrometria de masses (IMS). Aquesta tècnica permet descriure en dues dimensions la distribució dels lípids al llarg de les seccions histològiques. Les imatges obtingudes mostraren que el lipidoma era suficientment sensible per discriminar primer entre les diferents cèl·lules que conformen la mucosa del colon, i després entre el teixit sà i tumoral. Entre els múltiples canvis detectats, fou remarcable com les espècies que contenien àcid araquidònic (AA) eren usades de forma diferent entre les cèl·lules epitelials i les estromals. Mentre que l'AA canviava al llarg de la cripta en funció del seu estat de diferenciació, al llarg de l'estroma els canvis concordaven en la resposta immunològica que es dona fisiològicament en el colon sà. Per tal d'aprofundir en el paper del metabolisme de l'AA en processos de diferenciació i proliferació, usarem organoides de colon per investigar com els canvis en el metabolisme de les prostaglandines podria influir en el desenvolupament dels colonòcits.

Donada la sensibilitat mostrada pel lipidoma en la fisiopatologia de les cèl·lules del colon, a continuació explorarem la possibilitat d'usar la composició lipídica de vesícules extracel·lulars (EVs) com a biomarcadors no invasius. Confirmarem que la composició lipídica d'aquestes vesícules era suficientment sensible per estratificar-les depenent de la seva cèl·lula d'origen en sistemes model i d'acord amb el grup de pacients corresponent (sans vs. pòlips adenomatosos/neoplàsies invasives). Aquestes anàlisis mostraren que la composició lipídica de EVs aïllades de plasma de pacients reflectien el desenvolupament de tumors a una proporció significativa de pacients amb tumors al colon.

En resum, aquesta tesi prova que el lipidoma és altament sensible a l'estat fisiopatològic de les cèl·lules en el colon, establint les anàlisis lipídiques exhaustives com una eina viable i reproduïble capaç de detectar estats patològics com el càncer colorectal. A més, aquest estudi proporcionarà evidències sòlides per investigar el metabolisme lipídic com a font de noves dianes terapèutiques.

Resumen

La presencia de miles de especies de lípidos en la naturaleza (a día de hoy alrededor de 21500 especies moleculares) hace cuestionar el porqué la vida necesita esta gran variedad si para generar membranas bastarían unas pocas especies. El estudio sistemático del lipidoma ha ayudado a definir los lípidos no solo como bloques de construcción y proveedores del ambiente necesario para hacer funcionar las proteínas, si no además como participantes en múltiples procesos biológicos y como precursores de otras moléculas señal. En esta tesis, hemos aprovechado los últimos avances en técnicas de análisis de lípidos para estudiar los cambios que se dan en la fisiopatología del colon y para identificar nuevos potenciales biomarcadores de cáncer colorectal (CCR).

Con el análisis lipídico de líneas comerciales por HPLC acoplada a espectrometría de masas, hemos demostrado que el lipidoma era capaz de distinguir entre células primarias sanas y líneas celulares de cáncer colorectal. Además, comprobamos las diferencias en composición lipídica en cortes histológicos de tejido humano usando técnicas de imagen acopladas a espectrometría de masas (IMS). Esta técnica permite describir en dos dimensiones la distribución de los lípidos a lo largo de secciones histológicas. Las imágenes obtenidas mostraron que el lipidoma era suficientemente sensible para discriminar primero entre las diferentes células que conforman la mucosa del colon, y después entre el tejido sano y el tumoral. Entre los múltiples cambios detectados, fue remarcable como las especies que contenían ácido araquidónico (AA) eran usadas de forma diferente entre las células epiteliales y las estromales. Mientras que el AA cambiaba a lo largo de la cripta en función de su estado de diferenciación, a lo largo del estroma los cambios concordaban con la respuesta inmunológica que se da fisiológicamente en el colon sano. Para profundizar en el papel del metabolismo del AA en procesos de diferenciación y proliferación, usamos organoides de colon para investigar como los cambios en el metabolismo de las prostaglandinas podría influir en el desarrollo de los colonocitos.

Dada la sensibilidad mostrada por el lipidoma en la fisiopatología de las células del colon, a continuación exploramos la posibilidad de usar la composición lipídica de vesículas extracelulares (EVs) como biomarcadores no invasivos. Confirmamos que la composición lipídica de estas vesículas era suficientemente sensible para estratificarlas dependiendo de su origen celular en sistemas modelo y de acuerdo con el grupo de pacientes correspondiente (sanos vs. pólipos adenomatosos/neoplasias invasivas). Estos análisis mostraron que la composición lipídica de EVs aisladas de plasma de pacientes reflejaban el desarrollo de tumores a una proporción significativa de pacientes con tumor en el colon.

En resumen, esta tesis prueba que el lipidoma es altamente sensible al estado fisiopatológico de las células en el colon, estableciendo los análisis de lípidos exhaustivos como una herramienta viable y reproducible capaz de detectar estados patológicos como el cáncer colorectal. Además, este estudio proporcionó evidencias sólidas para investigar el metabolismo lipídico como una fuente de nuevas dianas terapéuticas.

INTRODUCTION

1 Introduction

The term lipid encompasses a broad family of biomolecules with different characteristics, although a common feature shared by all is their hydrophobicity, a property necessary for their biological roles as main membrane components and as an energy reservoir. Lipidomic techniques provide comprehensive lipid characterization of samples, allowing understanding the multiple roles of lipids beyond the separation of aqueous solutions by forming membranes. To date, around 21.500 lipid species from biological sources have been identified, which are classified into the six categories included in figure 1-1. Bearing this in mind, the obvious question would be: if an isolating barrier can be generated using few, or even a single, phospholipid species, why do cells generate such a complex lipid repertoire?

Mammalian lipid categories

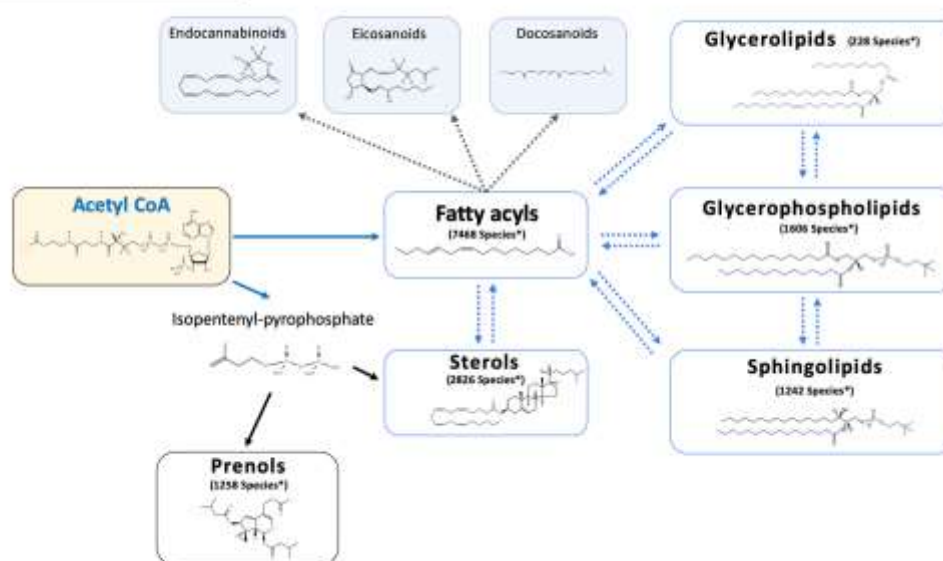


Figure 1-1. Metabolic interactions between the relevant lipid classes in mammals, including the number of lipid species defined so far in each class. Information on lipid species was obtained from the Lipid Maps Structure Database¹.

The lipid composition is completely dependent on the function to be carried out; in fact, different cell types and even organelles possess unique membrane composition²⁻⁴. Thus, many biological processes like cell division⁵⁻¹¹, differentiation¹²⁻¹⁴, modulation of the inflammatory response¹⁵⁻¹⁹ or cytochrome c activity²⁰ depend on specific membrane lipid composition. Delving in this topic, the description of specific regions of membranes able to affect enzyme location and activity adds further complexity to lipid membrane metabolism²¹⁻²⁶. In this context, the lipid membrane environment is not just an invariable scaffold where static proteins exert their functions, but a fast adaptable ocean that responds to the cell physiological requirements. Given the great number of membrane lipid molecular species, is not a surprise the still scarce knowledge about each one function and regulation. Hence, the reason why life requires this plethora of diverse lipids for many different biological locations and situations is still an unanswered question. However, their participation in any biological process raised membrane lipids as useful biomarkers and their metabolism as a promising target for many pathological conditions.

The diversity of these biomolecules forces to the application of multiple techniques to obtain a complete lipidome. For many years, the difficulty in identifying all lipid species due to

a lack of massive analysis techniques had dragged the advances in lipid knowledge. However, the development of mass spectrometry (MS) and its coupling to chromatographic techniques in the late 1950s²⁷ boosted significantly the interest in studying the complete lipidome in multiple tissues and contexts (Figure 1-2). Although was their broad application to lipid analysis from the 2000s which lead spectacularly to the emergence of lipid-related works.

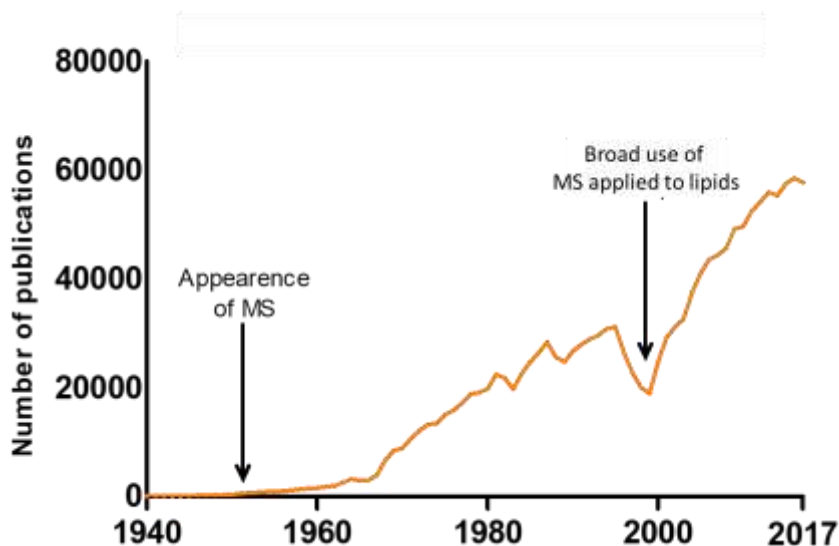


Figure 1-2: Number of publications related with lipids. Information obtained from Web of Science database (accessed 23/07/2018).

The possibility of characterizing whole lipidomes with higher precision increased drastically the knowledge about lipid participation in pathophysiological processes. In fact, MS have been indispensable to understand the relevance of lipid diversity in life. The lipidomic techniques applied in this thesis exemplify how the use of comprehensive lipid knowledge provides important information about tissue physiological states and how it can be used to reveal biomarkers in pathological situations.

However, without tools characterizing their distribution within tissues, the biological meaning of a lipidome remained unclear. Protein and nucleic acid visualization by microscopy revealed the biological relevance of confining enzyme activity to delimited tissue and cell locations. Unfortunately, without any feasible probe to mark specific lipids in tissues, the lipidomic field suffered more limitations. These limitations were overcome by the development of MS imaging (IMS) applied to lipid analysis, leading the field to new and exciting possibilities in this research field. Thus, using these techniques it is possible to obtain complete profiles of molecules along with two-dimensional samples like histological tissues. The application of lipid IMS techniques allows the description of lipidomes in tissues preserving their original distribution, with almost no manipulation and, most importantly, with absolute independence of probes.

Lipid imaging gave us the information that many specific lipid molecular species change along colon mucosa. The most relevant change was the increase in AA of the epithelial stem cells which reside at the mucosa base in contrast of increased AA at the luminal site of the connective tissue. This result alone raises the AA as a marker for proliferation and differentiation in colon epithelial cells and of inflammation in the colon mucosa connective tissue. Also, this tight gradient was completely disturbed in adenomatous polyps (pre-cancer

lesions). We further studied the role of AA-derived molecules in the colon physiology in the context of colon epithelial cells differentiation process.

The AA is transformed by COX enzymes to eicosanoids, varied bioactive molecules usually related to pathologies with an inflammatory component like cancer. This relation based many works that tried to use COX enzymes inhibitors (mainly Nonsteroidal Antiinflammatory Drugs) to treat CRC. Unfortunately, the high cardiotoxicity of these compounds and the relative low effects of these drugs over CRC size reduction challenge the effectiveness of these drugs to treat this disease. To understand better how alterations in lipid and PG metabolism may affect to colonocytes, the final part of this work explored the role of PGs in the colon epithelial cell proliferation and differentiation. Using *ex vivo* colonocytes culture we tested the different capacities of three PGs and their receptors in cell proliferation. These results alert on the action of NSAIDs as the diverse COX products exert completely different effects over colon epithelial cell fate. Therefore, suggests that more specific therapies limited to only a few eicosanoid receptors could potentially be an effective therapeutic approach for CRC.

The use of lipidomic techniques applied in this thesis identified biomarkers for CRC and set the base to understand the mechanisms involved in colon epithelium physiology and the alterations present when colon tumors are developed.

1.1 Lipids: a basic classification

Cell membranes are ≈ 4 nm thick structures that separate the different cell organelles from the cytoplasm and provide an adequate enzymatic environment. Furthermore, biological membranes not only separate the different cell aqueous environments, but they also provide the necessary plastic scaffold for the correct protein location and function^{24,25,28}. This protein regulation by membrane lipids occurs through direct interaction with specific lipids²⁸ or to the surrounding lipid context through changes in their biophysical properties (like membrane curvature and polarity)^{24,25}. Finally, lipid products can serve as ligands and bioactive molecules precursors placing membranes as a hub of signaling molecules.

With the rise of lipidomics, there was a need to standardize the nomenclature and lipid classification. Currently one of the largest lipid databases LIPID MAPS (<https://www.lipidmaps.org>) established the following classification²⁹: glycerophospholipids (referred phospholipids hereafter), fatty acids, sterols, sphingolipids, glycerolipids, prenol lipids, saccarolipids, and polyketides.

Fatty acids:

Fatty acids are carboxylic acids with an aliphatic chain, constituted, in most cases, by an even number of carbons that may range from 2 up to more than 30 carbons.

Fatty acids are classified according to the number of carbons in the following categories: short-chain (C2-4), medium-chain (C6-10), long-chain (C12-20), very-long-chain (C22-24), and ultra-long chain (C>26) fatty acids. While the last two categories are highly enriched only in certain tissues, like skin, retina, meibomian gland, testes, and brain, the rest of fatty acids are ubiquitous^{30,31}.

Further, fatty acids might be saturated or unsaturated, with the number of double bonds ranging from 1 (monounsaturated fatty acids, MUFA) to more than 6 (polyunsaturated fatty acids, PUFA). The number of unsaturations affects membrane physical properties. Thus, PUFA-membranes are more flexible than MUFA-membranes as PUFAs reduce the energy necessary for deformation^{32,33}. Figure 1-3 shows examples of two common fatty acids, the hexadecanoic acid (C16:0), a saturated fatty acid, and the AA (C20:4), a PUFA. While most natural fatty acids have from 0 to 6 double bonds, it is possible to find higher unsaturation levels. In mammals, the most frequent double bonds are cis (Z), while trans (E) fatty acids are

1. Introduction

mostly incorporated from diet³⁴. Mammals are unable to synthesize fatty acids with unsaturations more proximal to the methyl end than the ninth carbon, like in the n-3 and n-6 fatty acids (where n indicates the position of the first double bond starting from the methyl end). For this reason, linoleic acid (18:2n-6) and linolenic acid (18:3n-3) are considered essential fatty acids (precursors of AA and docosahexaenoic acid (DHA, 22:6n-3), respectively) and they must be incorporated from the diet. Fatty acids are mainly straight chains, although branched fatty acids are present in very low levels in the skin of newborns³⁵. In humans, increases in branched fatty acids may be indicative of severe peroxisomal diseases, like Refsum disease, characterized by the accumulation of these fatty acids and phytanic acid due to α -oxidation impairment³⁶.

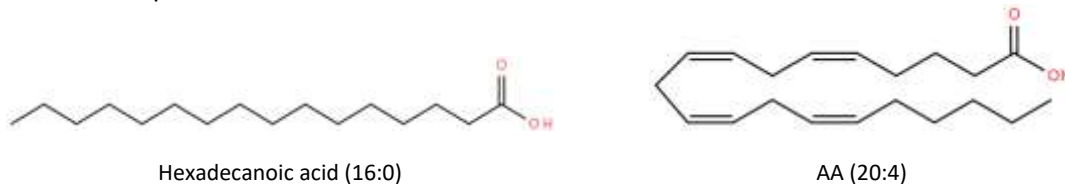


Figure 1-3: Left, hexadecanoic acid, a 16 carbon fatty acid with no unsaturations, as example of saturated fatty acid. Right, AA a 20-carbon fatty acid with 4 unsaturations, as example of PUFA.

Phospholipids:

Phospholipids are by far the main component of cell membranes in prokaryotic and eukaryotic cells. Their structure is based on a glycerol backbone esterified to two fatty acids at sn-1 and sn-2 positions and a phosphate group at sn-3. The sn-1 position is usually occupied by a saturated or a MUFA, while PUFAs usually occupy the sn-2 position. The phosphate group is linked to different moieties being ethanolamine, choline, serine, inositol (generating PE, PC, phosphatidylserine, and PI respectively) the most abundant in mammalian cells; phosphatidic acid (PA) instead is bound to a hydrogen atom (Figure 1-4). Besides these main phospholipids, there are other presents in a lesser amount in cells but with specific locations and functions. This is the case of the cardiolipin, a lipid composed of three glycerol backbones, 2 phosphates, and four acyl chains. Cardiolipin present only at the mitochondrial membranes where is essential in stabilizing enzymes and complexes involved in energy production and mitochondrial apoptotic processes³⁷. Bis(monoacylglycerol) phosphate (BMP) is another minor lipid with a non-conventional structure, composed by two monoacylglycerols bound to a phosphate group. BMP have been related to a normal lysosomal function³⁸.

Further, phospholipids can be classified according to the nature of the bond at the sn-1 position, which may be: an ester, ether or vinyl-ether linkage, giving rise to diacyl-, alkyl- and alkenyl-glycerophospholipids (or plasmalogens), respectively (Figure 1-4). Ether lipids have many peculiarities as the specific synthesis pathway (initiated at the peroxysomes and finished at the endoplasmic reticulum) and their enrichment in PUFA³⁹⁻⁴¹, the reason why plasmalogens are considered second messengers reservoirs⁴²⁻⁴⁴. The vinyl ether linkage confers specific curvature properties as well as a greater reactivity towards reactive oxygen species⁴⁵⁻⁴⁷. Plasmalogens participate in processes as membrane fusion⁴⁸, membrane trafficking⁴⁹, and T-cell activation⁵⁰, although their exact biological roles of these lipids remain unknown. However, it is clear that alterations on their synthesis pathways are the cause of severe pathological conditions. Rhizomelic Chondrodysplasia Punctata (RCDP) and Zellweger Disease, both showing extremely low levels of ether lipids, are the two inherited diseases associated with impaired biosynthesis of plasmalogens⁵¹⁻⁵³.

In turn, each class of membrane phospholipids comprises a broad family of molecular species differing in their fatty acyl composition. Acyl chains are very unevenly distributed among lipids of different classes: PC is highly enriched in 16:0/18:1, while it contains a very low

amount of docosahexaenoic acid (22:6n-3). Conversely, the latter is highly present in both diacyl- and alkenyl- PE, as well as phosphatidylserine, whereas PI is highly enriched in 18:0/20:4. The individual functions of these different molecular species are poorly understood and only recently are the factors establishing the specific incorporation of particular acyl chains into certain lipids attracting more attention⁵⁴. Figure 1-4 presents the different possible combinations of fatty acids and polar heads of the main phospholipid classes.

Phospholipids

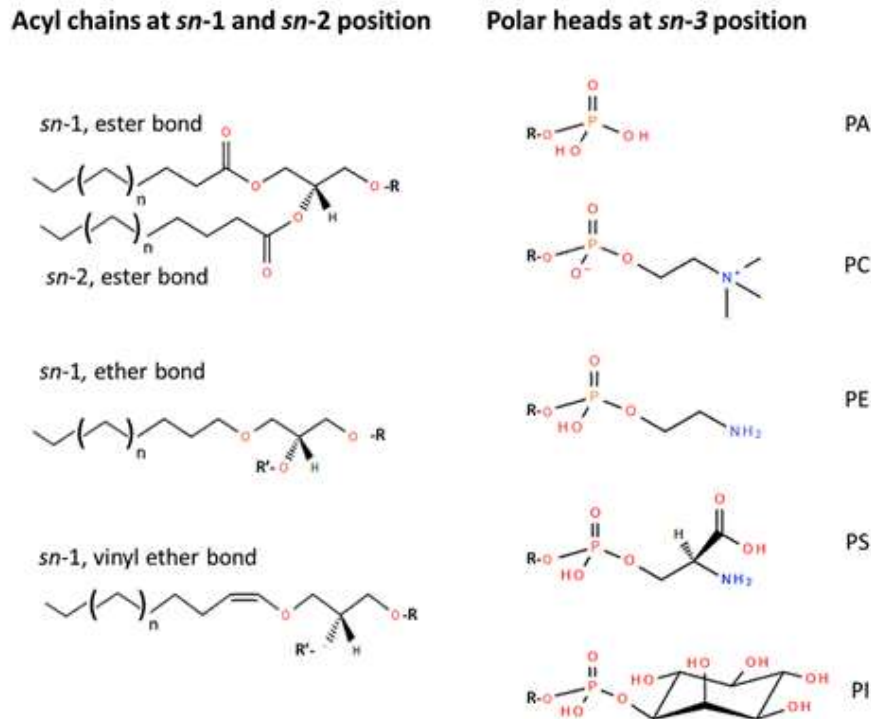


Figure 1-4: Structural elements of glycerophosphate-based lipids. On the left, the different acyl chain types of linkage established at the *sn*-1 position between the fatty acid and the glycerophosphate backbone are shown. Thus, it is possible to establish three subgroups depending on the nature of the bond at *sn*-1 position, which may be: an ester, ether, or vinyl-ether linkage, giving rise to diacyl-, alkyl- (O-alkyl, -O-CH₂-) and alkenyl- (O-alk-1-enyl (-O-CH=CH-)) glycerophospholipids, respectively. Most of the O-alkyl moieties occur as plasmalogen lipids, whereas the O-alk-1-enyl group is mainly associated with plasmalogen lipids (also called PE plasmalogens)⁵⁵. Conversely, the *sn*-2 position is occupied by a fatty acid linked via an ester bond. On the right, the most common polar heads found in mammalian cell membranes: phosphatidic acid (PA), phosphatidylcholine (PC), phosphatidylethanolamine (PE), phosphatidylserine (PS), and phosphatidylinositol (PI).

Sterols and cholesterol:

Steroids are molecules from 27 to 29 carbons derived from the sterol, a molecule of 17 carbons composed by three hexagonal and one pentagonal rings (Figure 1-5). Cholesterol is the most studied member of the sterol family because of the impact on human health that elevated circulating levels of this lipid have⁵⁶. Commonly thought to be found only in animals, cholesterol has been also found in plants⁵⁷. In addition, cholesterol is a main component of myelin sheaths, in fact, 20% of the total cholesterol in the body is present in the brain⁵⁸. Besides, cholesterol is the precursor molecule of the bile acids, Vitamin D and steroid hormones. In membranes, these highly hydrophobic molecules are intermingled with the fatty

acid tails of the phospholipids increasing membrane fluidity, where also modulates the fluidity of the membrane⁵⁹ and regulates the activity of membrane proteins⁶⁰.

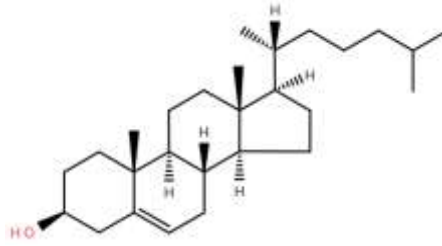


Figure 1-5: Structure of cholesterol, the most common sterol present in mammalian cells.

In agreement with its importance, defects in the cholesterol synthesis pathway are responsible for several inherited disorders with severe neurodevelopmental defects, such as Smith-Lemli-Opitz syndrome, desmosterolosis, and Niemann-Pick type C disease⁵⁸. However, impaired cholesterol metabolism has also been linked to non-inherited neurodegenerative diseases like Alzheimer disease, Huntington's disease, Parkinson's disease, depression, amyotrophic lateral sclerosis, stroke, head trauma, and also normal aging^{61,62}.

Sphingolipids:

As phospholipids, sphingolipids are also amphipathic molecules, although in this case, the hydrophobic moiety is a sphingoid long-chain base, the result of palmitic acid (16:0) and L-serine condensation. This reaction is catalyzed by serine palmitoyl acyltransferase (SPT). Further, an amide bond to a saturated or monounsaturated fatty acid may be established at carbon 2 leading to a ceramide (Cer) core. Different moieties can be linked to position 1 leading to Cer 1-phosphate if linked to a phosphate group, SM if bound to phosphocholine, or glycosphingolipids and gangliosides if bound to saccharides (Figure 1-6). Sphingolipids are considered mainly eukaryotic lipids as only a few bacteria species like the *Bacteroides* genus present them at their membranes⁶³. In contrast to phospholipids, sphingolipids are quite stable regarding their fatty acid composition, and remodeling is restricted essentially to the polar head.

- **Ceramide:**

Cer is the sphingolipids metabolic hub and considered as the precursor of the other sphingolipids and an important player in cell signaling, especially mediating apoptosis⁶⁴⁻⁶⁹.

- **Sphingomyelin:**

SM is the most abundant sphingolipid and one of the major components in mammalian cell plasma membranes. Described for the first time in the brain⁷⁰, SM is a distinctive component of myelin accounting for the 5-9% of its total membrane lipids^{71,72}. At the cellular level is mostly located at the outer leaflet of the membrane^{73,74} and forming part of the nucleohistones⁷⁵⁻⁷⁷. SM is synthesized through the union of a choline to the hydroxyl group of a Cer. To be transformed into SM, Cer are transported from the ER to the Golgi by the CERT transfer protein⁷⁸. Once in the Golgi, a phosphocholine head from a PC is transferred by the phosphatidylcholine:ceramide choline-phosphotransferase, or SMS⁷⁹. This enzyme can also perform the reverse reaction, yielding PC and Cer from SM and diacylglycerol⁸⁰. However, SM degradation is mostly done by specific sphingomyelinases that produce Cer. Depending on the site of action, exist the acidic sphingomyelinase which acts at the outer leaflet of the membrane and the neutral sphingomyelinase, resident at the inner leaflet of the bilayer⁸¹.

- **Glycosphingolipids:**

These lipids bond a monosaccharide or an oligosaccharide through a glycosidic bond. There are three main types: cerebrosides, globosides, and gangliosides (if contain one or more

sialic acid residues)⁸². These lipids play important roles in cellular interaction and recognition, their best-known role is as responsible for erythrocytes blood group ABH⁸³.

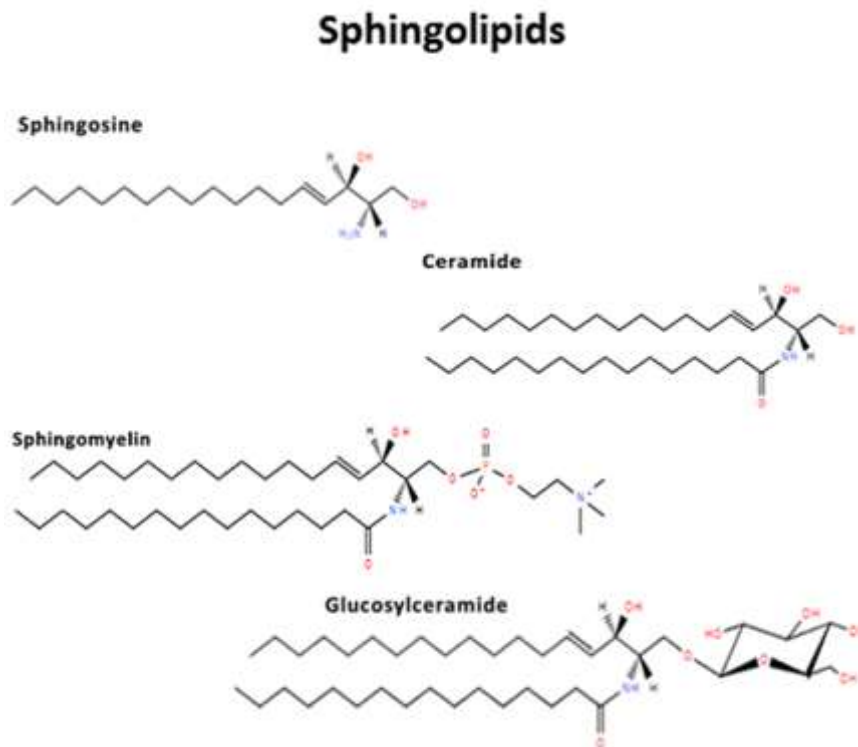


Figure 1-6: Structural elements of sphingoid-based lipids. The most frequent sphingoid base is sphingosine, although there are also other structures such as sphinganine and 4-hydroxysphinganine. Depending on the polar head attached to the ceramide, different molecules are generated, such as sphingomyelins (phosphocholine), cerebroside (glucose, galactose...), and gangliosides (oligosaccharides or sialic acid). In terms of the fatty acyl chain, in sphingolipids it is highly common to find saturated or monounsaturated fatty acids, which often contain a hydroxyl group at C2-position.

1.2 Lipid nomenclature

Many fatty acids have common names, such as oleic acid (C18:1), palmitic acid (C16:0), and AA (C20:4), which are still heavily used at all scientific levels despite the existing systematic nomenclature. The abbreviated form includes two numbers separated by a colon: the first one indicating the total number of carbons and the second, the total number of double bonds. Depending on the nature of the work, nomenclature may become more complex, including the exact position of double bonds, their stereochemistry (cis (Z) or trans (E)), or indicating the position of the first double bond starting from the methyl end (i.e. n-3). The latter is relevant to differentiate between n-3 and n-6 fatty acid acids.

For more complex molecules like phospholipids, it is important to be aware of the different nomenclature a lipid species may receive, particularly if the abbreviated form is used. Thus, in glycerolipids (mono-, di-, and tri-acylglycerides) and phospholipids, the simplest way to abbreviate their content is by adding the number of carbons of each of the acyl chains as well as the number of double bonds (ΣC : Σ unsaturation). However, it is essential to bear in mind that by using this form, important information is missing. Thus, PI 36:2 could correspond to a PI esterified to 18:0 (saturated fatty acid) + 18:2n-6 (essential fatty acid) but it could also

be esterified to 18:1+18:1. In turn, 18:1 could have the double bond at position n-9 (oleic acid) or n-7 (vaccenic acid). Finally, such abbreviation does not provide information regarding the position at which the fatty acid is esterified (sn-1 or sn-2). In an effort to define a more descriptive nomenclature, the following was proposed depending on the degree of structural detail provided: a) number of C-atoms:number of double bonds, if the esterified fatty acids are not known; b) fatty acids separated by an underscore (_), if they are known but the sn-position is not established; and, finally, c) fatty acids separated by a forward slash (/), if both fatty acid and sn-position are known (Table 1-1)⁸⁴. The degree of detail provided will depend on the analytical efforts applied to analyze the sample. Despite rapid advances in the field to determine the specific fatty acyl chain composition of each lipid class or their backbone binding position, rather time-consuming and technically challenging methods are still required. Nonetheless, there is no doubt that the better the characterization of species, the more precise experiments can be designed.

	Free Fatty acid	Phospholipid	Sphingolipid
Systematic Name	12E-octadecenoic acid	1-octadecanoyl-2-(4Z,7Z,10Z,13Z,16Z,19Z-docosahexaenoyl)-sn-glycero-3-phosphoethanolamine	N-(tetracosanoyl)-sphinganine-1-phosphocholine
Common Name	trans-12-elaidic acid	PE(18:0/22:6(4Z,7Z,10Z,13Z,16Z,19Z))	C24DH SM
Abbreviated form	C18:1n-6 ^a	PE(40:6) ^b PE(18:0_22:6) PE(18:0/22:6)	SM(d18:0/24:0) ^c

Table 1-1. Nomenclature of fatty acid-containing lipid species.

^aThe number 6 indicates where the first double bond is found starting from the methylene end.

^bBased on [40], briefly explained in the main text.

^cLetter "d" indicates the number of hydroxy (-OH) groups present in the sphingoid backbone (m:1, d: 2, t:3).

1.3 Membrane heterogeneity

The amphipathic nature of phospholipid and sphingolipids because of the presence of hydrophobic (fatty acid tails) and hydrophilic (head groups) domains induces the spontaneous self-association of fatty acid tails in aqueous solution. In this way, the total surface in contact with water is minimized, establishing a hydrophobic core, while polar head groups face the aqueous environments directly. This key feature allows biological membranes not only to segregate the intracellular milieu into sub-compartments (organelles) but also to provide the hydrophobic environment needed for the activity of transmembrane proteins.

	%*	SM	PC	PI	PS	PE	CL	Others
Subcellular fraction ⁸⁵	Endoplasmic Reticulum	ND	51	14	4	28	ND	4
	Plasma membrane	24	39	4	10	23	ND	1
	Mitochondria	ND	46	11	1	30	10	2
	Golgi	13	50	8	4	18	ND	7
	Late Endosomes	10	48	3	1	23	ND	16
Human cell types and tissues	Erythrocytes	25	32	ND	16	27	ND	ND
	Platelets ⁸⁶	15	35	10	12	23	ND	ND
	Epidermic cells ⁸⁷	21	39	10	4	19	4	2
	Brain ⁷²	18	34	6	7	11	ND	23

Table 1-2. Cellular and subcellular composition in terms of membrane lipid classes * Values are expressed as a percentage of total phospholipids. To help comparison within subcellular fractions or within human cell types, cells were colored with increasing intensity according to their value. ND: non-detected or not described its value in the corresponding study.

Table 1-2 shows how specific lipid composition is in terms of lipid families depending on the tissue or subcellular organelle. However, this specificity goes beyond tissue identity, as each of the subcellular organelle membranes shows particularities at the compositional level⁸⁸. Whereas SM is absent in the endoplasmic reticulum (ER), cardiolipin and cholesterol are exclusively found in mitochondria and plasma membrane, respectively^{89,90}. In fact, there is a compositional gradient along the secretory pathway in terms of lipid composition which has a profound functional impact. Taking into account the fact that most lipids are synthesized in the ER, it is clear that there should be a wide variety of mechanisms able to concentrate specific lipids at specific cellular locations⁸⁹. In turn, the same cell organelle shows a different composition according to its tissue origin. Thus cardiolipin, which contains four fatty acids in its structure, has a rather homogeneous composition that is highly enriched in linoleic acid (18:2n-6). However, this applies to heart and liver cardiolipin – wherein this fatty acid accounts for approx. 70% and 90%, respectively – but not to brain cardiolipin where it accounts for only 10%⁹¹.

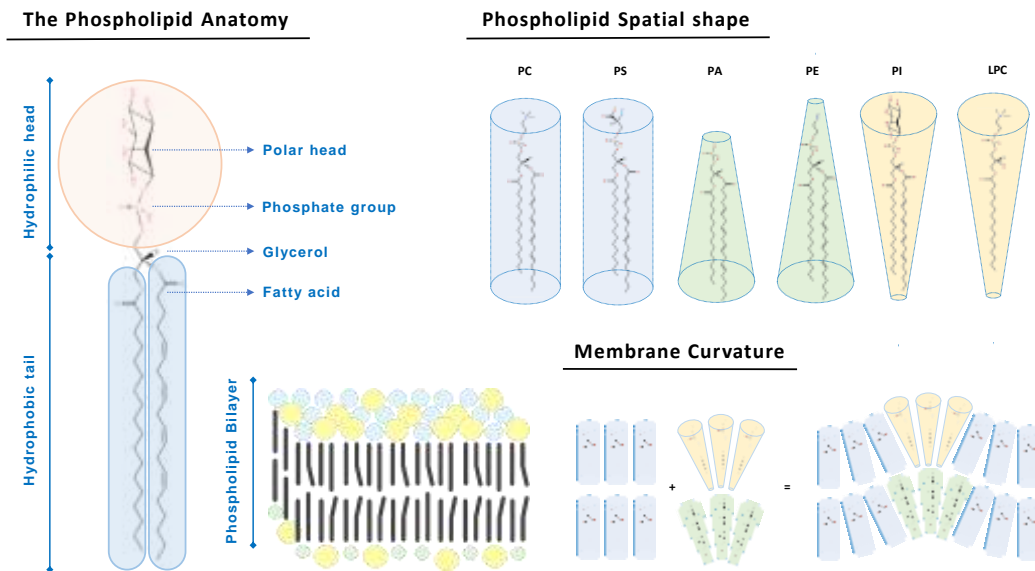
For a long time, it was assumed that lipids were randomly distributed within the membrane leaflets, and were incapable of adopting a coherent lateral structure. Now we know that there are at least two additional levels of organization in terms of lipid distribution: 1) between the two leaflets, so-called transverse asymmetry; and 2) within each leaflet, the lateral asymmetry, i.e., the formation of microdomains. Transverse asymmetry refers to the differences in composition existing between the two leaflets, thereby affecting various bilayer properties, including membrane potential, surface charge, permeability, and shape, as well as stability⁹²⁻⁹⁴. Consistent with these critical functions, asymmetry is maintained by a complex enzymatic network, consisting of flippases (out-to-in), floppases (in-to-out), and scramblases (bidirectional), which mediate lipid translocation⁹⁵. One of the most studied examples is phosphatidylserine translocation to the outer leaflet, a process that acts as a susceptibility signal involved in blood clotting⁹⁶, membrane trafficking⁹⁷, apoptosis⁹⁸, and cancer⁹⁹. In most characterized eukaryotic cells, PC and sphingolipids are found in the extracellular leaflet; whereas PS, PE, PI, and phosphoinositides are preferentially restricted to the cytosolic leaflet^{100,101}. Yet the latter applies basically to the plasma membrane. Within any cell, membrane asymmetry is far from a homogenous characteristic, as there exists a vital gradient along the secretory pathway, from the ER (symmetric and loosely packed) to the plasma membrane (asymmetric, thick, and rigid). This asymmetry is achieved by increasing the

1. Introduction

content in sterols, sphingolipids, and phosphatidylserine, which has a definitive impact not only on membrane thickness but also on membrane electrostatics^{89,90,102}. The mechanisms regulating all these processes are complex, involving specific lipid-protein interactions, and are the object of active research¹⁰³⁻¹⁰⁵.

Over the years, different types of membrane domains have been described, such as caveolae¹⁰⁶⁻¹⁰⁸, clathrin-coated pit^{106,109}, ceramide platforms¹¹⁰, and lipid rafts¹¹¹. The latter are defined as dynamic sterol-sphingolipid-enriched assemblies and are established in the outer leaflet. Lipid rafts have been proposed as regulators of signaling pathways, because of the specific lipid-lipid, protein-lipid, and protein-protein interactions occurring within these domains²¹. Interestingly, it seems that lipid rafts somehow influence the organization of inner leaflet-associated proteins during signal transduction^{22,26}, suggesting the existence of inter-leaflet communication⁹².

A final concept that needs introducing is the intrinsic molecular geometry of membrane lipids, determined by the size of the head group and the acyl chain composition (Figure 1-7). Thus, PC and phosphatidylserine adopt a cylindrical form; PE and PA assume a conical molecular geometry because of the relatively small size of their polar head group; and lysophospholipid (lacking a fatty acid) and phosphoinositides (having an inositol ring) have the shape of an inverted cone. Also, the fatty acid composition does have a certain impact on membrane conformation as well. For instance, the presence of a double bond induces the straight-chain to bend, thereby increasing the space it occupies. Hence, the combination of molecules with different geometry within the bilayer imposes membrane defects and curvature stress, which is used for budding (vesicles), fission (during cell division), and fusion (e.g. during secretory pathway)^{112,113}. Cells are able to sense and regulate the shape of membranes. For example, cytidine triphosphate:phosphocholine cytidyltransferase (CCT), the rate-limiting enzyme in PC biosynthesis, can adapt its activity according to the level of cylindrical or conical phospholipids present in the membrane^{114,115}.



Impact of lipid composition on membrane biophysical properties. Membranes are established because of the amphipathic nature of their components, particularly phospholipids and sphingomyelin. Lipids are asymmetrically distributed between the two leaflets and, in turn, within each of the leaflets. Each phospholipid has a particular shape depending on the polar head and its fatty acid composition. Lipid composition determines many properties of the membrane, such as thickness, fluidity, and surface charge. Thus, membrane thickness can

be modified by altering its composition. Thus, while short, unsaturated fatty acids increase fluidity, saturated fatty acids and sterols decrease it. Conversely, surface charge is determined by the presence or absence of anionic lipids, such as phosphatidylserine (positively charged) and phosphoinositides (negatively charged). Finally, changes in phospholipid intrinsic geometrical shape also impact membrane curvatures and regulate vesicle formation^{89,116}.

In summary, a rather complex scenario is depicted in which, in addition to all the regulatory mechanisms on lipid synthetic pathways, the membrane lipidome is also regulated between leaflets and even within each of the leaflets. This complexity makes it quite difficult to take all these elements into account in a single experiment. Although significant improvements have been made in this sense, such as the generation of asymmetric model membranes⁹², it is still not possible to reproduce *in vitro* the complexity of the cell membrane at the composition level, making it difficult to fully evaluate the real impact of an altered lipidome on cell functioning.

1.4 Membrane phospholipid metabolism

The cell membrane lipidome is highly dynamic, with lipid pools being continuously modified to adjust to environmental changes and cell requirements. Cells possess two pathways to maintain the membrane lipid pools, a *de novo* (named Kennedy¹¹⁷) pathway, and the remodeling (named Land's cycle) pathway.

1.4.1 *De novo* or Kennedy pathway

The *de novo* synthesis of lipids was the first lipid synthesis pathway described. Despite being mainly used by the cells to synthesize triacylglycerides, it is also used for phospholipid synthesis. In this pathway, all phospholipids are synthesized from the main pool of cellular PA, being the interchange of polar heads and acyl chains the main source of phospholipid pools. PA can be synthesized mainly through two possible paths (Figure 1-8). In the *de novo* pathway, the molecule synthesized has a palmitate (16:0) at the sn-1 position and oleate (18:1) or linoleate (18:2) acid at the sn-2 position. Highly unsaturated fatty acids like the PUFA, will be incorporated in later reactions through fatty acid remodeling reactions in the Land's cycle. Finally, PA may be converted into CDP-diacylglycerol and use it in PI and cardiolipin synthesis, or it can be dephosphorylated to diacylglycerol for the synthesis of PC and PE as well of triacylglycerol¹¹⁸ (Figure 1-8).

1. Introduction

Mammalian Membrane Lipid Biosynthesis

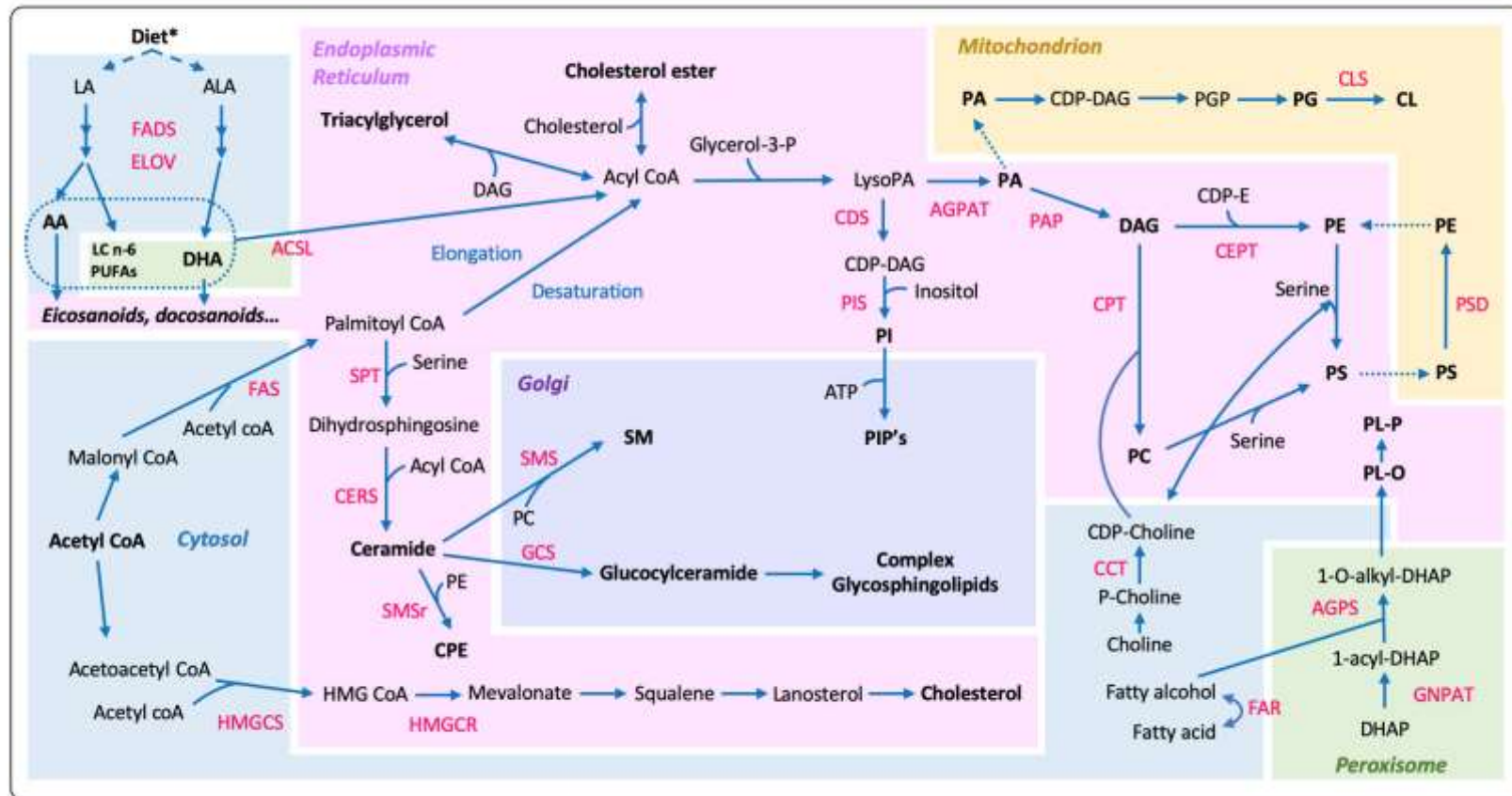


Figure 1-8: Principal pathways on membrane lipid biosynthesis in mammals. Phospholipids and triacylglycerides can be synthesized de novo from common diacylglycerol or phosphatidic acid precursors by the so-called ‘Kennedy pathway’¹¹⁷. Briefly, phosphatidic acid is synthesized by the successive addition of two fatty acyl-CoAs (fatty acid activated form) to glycerol-3-phosphate, a product of glycolysis. Then, phosphatidic acid may be converted into CDP-diacylglycerol, which is used in the synthesis of phosphatidylinositol and cardiolipin, or dephosphorylated to diacylglycerol for the synthesis of phosphatidylcholine and phosphatidylethanolamine as well as triacylglycerol¹¹⁸. Phosphatidylethanolamine – choline and serine polar heads – may be interconverted by exchange, decarboxylation, and methylation reactions¹¹⁹. The equilibrium between phosphatidic acid (PA) and diacylglycerol (DAG) is a metabolic hub linking the synthesis of major phospholipids and triacylglycerides. However, the module with the highest modification rate is fatty acid moiety, and both acyltransferases and phospholipases are critical for this¹²⁰⁻¹²³. The first PA path begins with the formation of the lysophosphatidic acid (LPA) through the link of one fatty acid and a phosphate to the sn-1 and sn-3 position of a glycerol, respectively. This first reaction is exerted at the ER by acyltransferases with high affinity for saturated fatty acids. Once LPA is synthesized, a second fatty acid is bonded to the sn-2

1. Introduction

position. In contrast with the first acyltransferase, the one binding the sn-2 fatty acid has higher affinity for unsaturated fatty acids. The second most common PA synthesis pathway requires the phosphorylation of a diacylglycerol by a diacylglycerol kinase. The ether lipids metabolism is ruled by four rate limiting enzymes: the AGPS, the GNPAT¹²⁴ (also named DHAPAT or DAPAT) and the fatty alcohol reductase 1 and 2 enzymes (FAR1 and FAR2)¹²⁵. Once the fatty alcohols are synthesized, they enter into the peroxisomes lumen where the other two limiting enzymes, GNPAT and AGPS, are¹²⁶. GNPAT acylates dihydroxyacetone phosphate in the first reaction, and is followed by the exchange of the acyl group for a fatty alcohol by the AGPS^{127,128}. The limiting step for PC *de novo* synthesis is catalyzed by the CTP phosphocholine cytidyltransferase which activity is highly enhanced when is translocated from the cytosol to a lipid bilayer^{114,129}. Phosphocholine is then transferred from the CDP-choline to diacylglycerol by the CDP-choline:1,2-diacylglycerol phosphocholinetransferase. Similarly to PC, PE rate-limiting step is catalysed by the CTP:phosphoethanolamine cytidyltransferase which converts phosphoethanolamine to CDP-ethanolamine. Then, PE is transferred to a diacylglycerol or a 1-alkenyl-2-acyl glycerol by a phosphoethanolamine transferase¹³⁰. Additionally to the *de novo* synthesis, PE can also be synthesized from PS decarboxylation in the mitochondria, a process highly dependent on the cell type and on the PS and ethanolamine availability¹³¹. Phosphatidylserine can serve as precursor of other phospholipids by its decarboxylation and methylation, a process specially relevant for PC and PE synthesis¹¹⁹. Both PS and PI are synthesized from the CDP-diacylglycerol through the CTP:phosphatidate cytidyltransferase, located in the mitochondria and endoplasmic reticulum¹³². PS is mainly generated through base exchange reactions while PI through the condensation of the inositol to a diacylglycerol by the CDP-diacylglycerol:inositol phosphatidyltransferase enzyme¹³³. **AGPAT**, 1-acylglycerol-3-phosphate-O-acyltransferase; **AGPS**, alkylglycerone phosphate synthase; **ALA**: alpha-linolenic acid, **CCT**, CTP: phosphocholine cytidyltransferase; **CDP-Choline**, cytidine diphosphate choline; **CDP-DAG**, cytidine diphosphate-diacylglycerol; **CDP-E**, cytidine diphosphate ethanolamine; **CDS**, cytidine diphosphate diacylglycerol synthase; **CEPT**, choline/ethanolamine phosphotransferase; **CERS**, ceramide synthase; **CL**, cardiolipin; **CLS**, cardiolipin synthase; **CPE**, ceramide phosphoethanolamine; **CPT**, cholinephosphotransferase; **DHAP**, dihydroxyacetone phosphate; **ELOVL** Fatty Acid Elongases; **FADS**: fatty acids desaturases; **FAR**, fatty acyl co-A reductase **FAS**, fatty acid synthase; **GCS**, glucosylceramide synthase; **GNPAT**, glyceronephosphate O-acyltransferase **HMGCS**, hydroxymethylglutaryl coenzyme A (CoA) synthase; **HMGCR**, 3-hydroxy-3-methylglutaryl-CoA reductase; **LA**: linoleic acid; **PA**, phosphatidic acid; **PAP**, phosphatidic acid phosphatase; **P-Choline**, phosphocholine; **PG**, phosphatidylglycerol; **PGP**, phosphatidylglycerolphosphate; **PIP**, phosphoinositide; **PC**, phosphatidylcholine; **PE**, phosphatidylethanolamine; **PIS**, phosphatidylinositol synthase; **PS**, phosphatidylserine; **SMS**, sphingomyelin synthase; **SMSr**, sphingomyelin synthase-related enzyme; **SPT**, serine palmitoyltransferase (adapted from Holthuis⁸⁹). * Essential fatty acids; LA (n-6) and ALA (n-3), mammals cannot insert double bonds more proximal to the methyl end than the ninth carbon atom (D-9 desaturase), n-3 and n-6 fatty acids cannot be synthesized *de novo*, consequently these fatty acids have to be present in the diet¹³⁴. For simplicity, lysophosphatidylacyltransferases were not included.

- **Synthesis of ether lipids:**

Ether lipids present a different synthesis pathway due to the link of a fatty alcohol instead of a fatty acid at the sn-1 position. The fatty alcohol synthesis is catalyzed by specific peroxisomal enzymes, where the ether lipid synthesis begins. The modification of a fatty acid into fatty alcohol is performed by one of the two FAR enzymes described so far, the FAR1 and FAR2, both located at the peroxisomal membrane. While both enzymes share the same affinity for 16 and 18 carbon acyl chains, FAR1 can bind both saturated and unsaturated fatty acids while FAR2 has only affinity for the saturated ones¹²⁵ (Figure 1-9). The next steps, which are common to those for diacyl-glycerophospholipids, occurs in the endoplasmic reticulum. Despite the relevance and abundance of plasmalogen species, there is still scarce knowledge on the specificity of these lipid-synthetic enzymes towards plasmalogen or diacyl species.

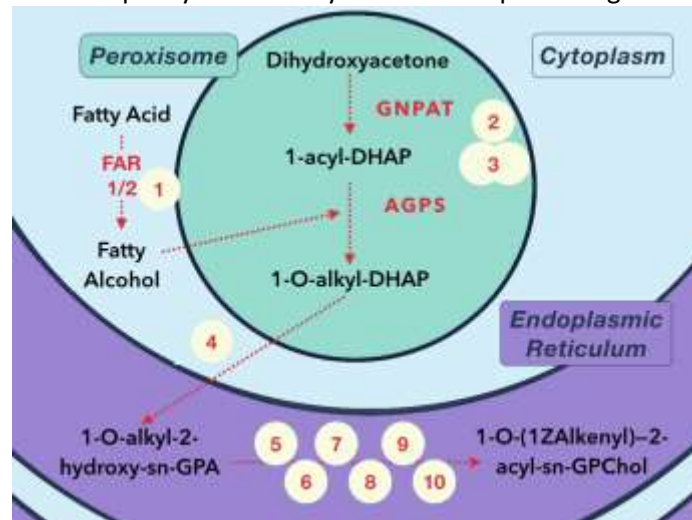


Figure 1-9: Scheme of the pathway for plasmalogen synthesis. Plasmalogen synthesis is a multi-step process initiated in the peroxisomes and ended in the endoplasmic reticulum. The synthesis is catalyzed by the following enzymes (1) FAR1 and 2, fatty acyl-CoA reductase 1 and 2, (2) GNPAT, glycerone phosphate O-acyltransferase (also known DHAPAT, dihydroxyacetone-phosphate acyltransferase); (3) AGPS, alkylglycerone phosphate synthase (also known ADAPS, alkyl dihydroxyacetone phosphate synthase); (4) alkyl/acyl DHAP reductase, (5) alkyl/acyl glycerophosphate acyltransferase, (6) phosphatidic acid phosphatase, (7) ethanolamine (choline) phosphotransferase (8) plasmenylethanolamine desaturase, (9) phospholipase C, (10) choline phosphotransferase. Adapted from Braveman et. al.⁴². Species indicated by (Cho) represent the choline equivalent of the corresponding GPEthanolamine species.

As the metabolic hub of the other phospholipids, PA modifications are the basic process required for the *de novo* synthesis of the other major phospholipid classes: PC, PE, phosphatidylserine, and PI.

PC is the most abundant phospholipid in most biological membranes being especially present in the outer leaflet of the plasma membrane^{100,101}.

PE is usually the second more abundant phospholipid in eukaryotic organisms and, in contrast to PC, is more present at the inner leaflet of the plasma membrane^{100,101}.

PS despite accounting for less than 10% of the total phospholipids, plays important roles in blood coagulation and apoptosis. In healthy cells, PS is more concentrated at the inner leaflet of the plasma membrane^{100,101}, and is translocated to the outer leaflet during apoptosis where it is recognized by macrophages¹³⁵⁻¹³⁷.

PI is present mainly at membranes inner leaflet^{100,101}. The main fatty acid associated with PI is the AA, a key precursor of inflammatory molecules¹³⁸. Also, its phosphorylation leads to the synthesis of phosphoinositides (PIPs), important bioactive molecules¹³⁹⁻¹⁴¹. One of the most studied PIP is PIP3, synthesized through the action of PI3K¹⁴²⁻¹⁴⁸. Once generated, PIP3 can stimulate AKT signaling which in turn fuels proliferation and inhibits apoptosis¹⁴⁹⁻¹⁵⁴. Despite

knowing deeply the effects on different phosphorylation sites, the effects of specific FA composition in PI it has been barely studied and only is known to affect the cellular location of PIPs¹⁵⁵. On the other hand, the phosphorylated inositol head of PIP2 can be cleaved by PLC generating IP₃ (inositol-3-phosphate) and DAG (diacylglycerol). IP₃ induces Ca²⁺ release from the ER^{156,157} which at the end stimulates target expression mainly through CREB activation¹⁵⁸⁻¹⁶¹.

1.4.2 Fatty acid remodeling or Land's cycle

Rapid lipid fatty acid composition changes are necessary to perform processes like cell fission or protein complex formation at any cell level either bacteria¹⁶², protozoa¹⁶³ or mammals^{11,164}. Thus, cells do not rely on the *de novo* pathway to modify the phospholipid pools, but instead, they interchange fatty acids amid phospholipid classes in the named Land's cycle^{120,165}. Acyl chain interchange requires separating the fatty acid of one phospholipid by a phospholipase A enzyme (PLA) before the esterification of another fatty acid by a lysophosphatidyl acyltransferase (LPLAT)¹⁶⁶⁻¹⁷⁰ (Figure 1-10). Despite most of the phospholipid synthesis and modification enzymes shares affinity for different substrates, each one has more activity towards one specific reaction. For example, PLA₂GIV enzymes are able to release any fatty acid in the sn-2 position of any phospholipid, but with much more affinity for the AA bonded to PIP₂¹⁷¹.

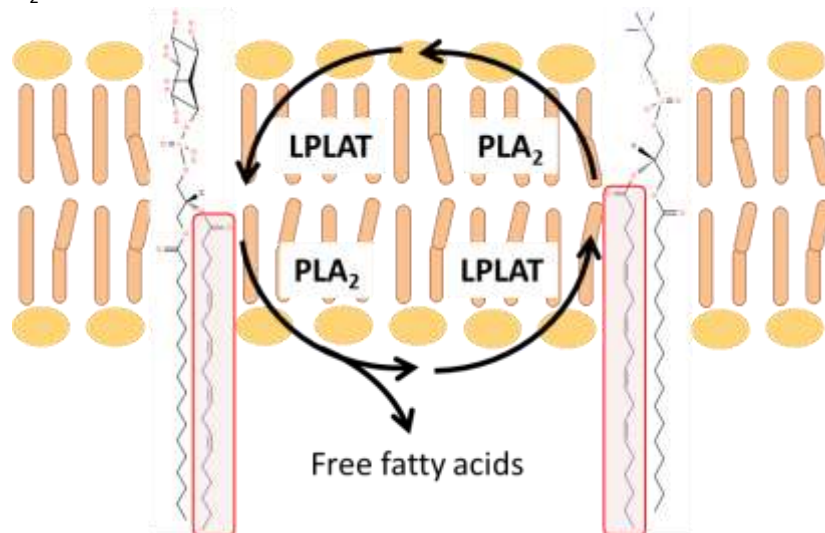


Figure 1-10: Scheme of the Land's cycle. PLA₂ enzymes catalyze the release of fatty acids at sn-2 position of phospholipids. The released phospholipids can be used in other metabolic pathways or can be transacylated to other phospholipid after its activation by the union of a CoA residue through acyl CoA synthase enzymes (ACS).

The term phospholipase refers to any enzyme able to hydrolyze part of a phospholipid. Their functions include the maintenance of the cell homeostasis, the release of bioactive molecules, nutrients digestion and even are a common component of snake poison and bactericidal fluids. To avoid unspecific phospholipid degradation, their regulation is highly dependent on their functional coupling to membranes¹³¹. Phospholipases are classified depending on their site of action on the phospholipid. PLA act on the ester bond of the fatty acid with the glycerol of the sn-1 position (PLA₁) or sn-2 position (PLA₂). Phospholipases able to attack both positions are named PLB. Lysophospholipases act on lysophospholipids hydrolyzing the remaining fatty acid. Although not participating in the Land's cycle, PLC and PLD are also relevant phospholipases in cell metabolism. PLC cleaves the glycerophosphate bond while the

1. Introduction

removal of the polar head is catalyzed by the PLD, therefore both C and D are in fact phosphodiesterases (Figure 1-11)¹⁷².

PLA₂ activity was described for the first time in 1877 by Bokay, who observed the degradation of PC by some component of the pancreatic fluid. During the next years, many secreted PLA (sPLA₂) were identified in venoms and pancreatic juices and classified according to their structure¹⁷³⁻¹⁷⁸. These sPLA₂ were small and Ca²⁺-dependent and contained many disulfide bonds, catalytic histidine, and aspartate residues¹⁷⁴. In the late '80s, PLA₂ activity was also described in neutrophils¹⁷⁹ and platelets¹⁸⁰ forcing the revision of the classification in 1991 with their sequencing and clonation^{181,182}. These newly described PLA₂ were bigger, contained a serine catalytic domain, and no disulfide bonds.

Despite this, it is frequent to divide PLA into Ca²⁺-dependent and Ca²⁺-independent PLA. In the group of the Ca²⁺-dependent PLA₂, the named Group IV PLA₂ (PLA₂GIV) is one of the most relevant phospholipases in cell metabolism and inflammation because of its high specificity for AA-containing phospholipids¹⁸³⁻¹⁸⁵. Interestingly, Ca²⁺ is not required for their catalytic activity, but is necessary for the union of the N-terminal tail to the plasma or intracellular membranes where is active¹⁸⁶⁻¹⁹¹. In phagocytes, AA release by PLA₂GIV is directly channeled to eicosanoid production¹⁹²⁻¹⁹⁴, while macrophages activation involves the specific mobilization of AA-containing PC mobilization¹⁶. Regarding Ca²⁺-independent PLA₂ activity, Group VI PLA₂ (iPLA₂GVI) has a potent AA specificity and supply Ca²⁺-independent activity in Ca²⁺ absence¹⁹⁵. At least in macrophages, iPLA₂ is a major enzyme responsible for the AA remodeling^{190,196,197}.

Despite that multiple PLA₂ inhibitors have been designed, their inespecificity and the promiscuity intrinsically associated with lipid enzymes hamper the study of these enzymes. Thus, arachidonyl trifluoromethyl ketone, broadly used to inhibit Ca²⁺-dependent PLA₂, inhibits to a lesser extent iPLA₂ activities¹⁹⁸. On the other hand, bromoenol lactone, despite inhibiting specifically the iPLA₂ activity, also inhibits PA dephosphorylation, and therefore DAG generation¹⁹⁹.

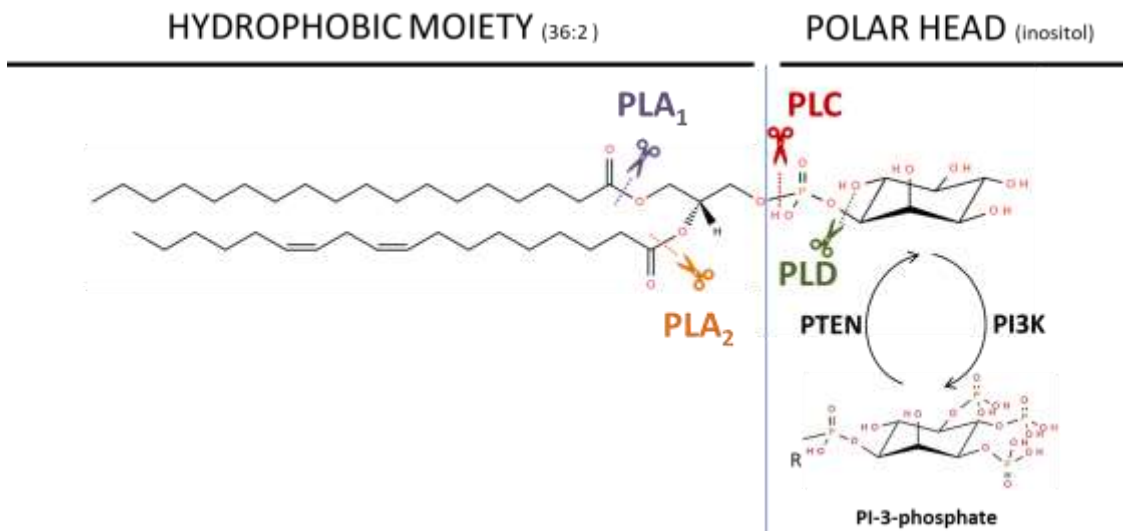


Figure 1-11: Scheme of phospholipases sites of action. On the left PLA₁ and PLA₂ cleaves the fatty acid linked at the sn-1 and sn-2 position of a phospholipid respectively. PLC acts on the bond between the phosphate group and the glycerol releasing IP₃. PLD cleaves the polar head producing also PA which, in addition to being a phospholipid precursor, can act as an intracellular mediator. PI3K phosphorylates PI at the inositol polar head generating phosphoinositides, a family of highly bioactive compounds. PI3K action can be reversed by the action of the phosphatase PTEN.

LPLAT enzymes can be classified by their affinity for phospholipids polar head. According to this classification five LPCAT²⁰⁰⁻²⁰⁶, two LPEAT^{202,204} and one LPIAT²⁰⁷ enzymes have been described so far. Regardless of this classification and as in the case of PLA₂ enzymes, LPLAT enzymes are able to bond multiple substrates both polar heads and fatty acids. Thus, there is scarce knowledge about LPLAT activity and regulation. This lack of works addressing phospholipid remodeling is especially manifest regarding PI fatty acid regulation. The LPIAT1 (also named MBOAT7) is the acyltransferase with higher activity towards PI²⁰⁷, unfortunately, little is known about its role in cell metabolism and its regulation.

Taking into account that lipid-related enzymes are able to act on multiple substrates, the lipid homeostasis seems to be controlled more through the coupling of the different acyltransferases to PLA₂ and acyl-CoA synthases^{208,209}.

1.5 Lipid analysis

Membrane lipid analysis is a challenging field due to their similar chemical structures that hamper their unequivocal identification. Thus, due to their intrinsic chemical properties, the development of probes is not a viable approach for lipid analysis; instead, lipid identification relies on separation by their polarity (chromatography) and fragmentation pattern through ionization (MS). MS-based techniques generate massive information on the lipid composition of a biological sample, the so-called lipidome. Therefore, to obtain a complete sample lipidome requires the combination of various chromatographic and MS techniques. All lipid classes encompass multiple molecular species depending on the fatty acids attached to their lipid backbone. Different fatty acid composition of molecular species implies differences of tens of daltons. For example, the mass difference between PC 16:0/18:1 (759.5778 Da) and PC 16:0/20:4 (781.5622 Da) is of around 22 Da as the second possesses 6 more carbons and three more double bonds. Despite small, this slight difference is translated in a complete different use of both lipids in cells. Therefore, an accurate lipid identification is mandatory to obtain feasible results and to withdraw the correct conclusions.

Chromatography is a general term referring to the separation of complex mixtures into simpler groups or individual components taking advantage of the molecules chemical properties²¹⁰. Briefly, in a chromatographic technique, the sample is placed over a stationary phase before the application of a mobile phase that flows dragging the sample analytes within the stationary phase. The time it takes for a molecule to go through the chromatography system depends on the affinity between the stationary phase and the molecule. The higher the affinity between them the longer it will take. In the case of lipids, chromatography is based on the polarity of the molecules. Of the main membrane lipids, cholesterol is the less polar, phospholipids the second ones and SM the most polar of them. Chromatography techniques allow the separation of complex lipid mixtures, although the identification of molecular species requires tedious and elaborate protocols.

MS techniques enable the identification through fragmentation of molecules simplifying the protocols and in principle introducing fewer errors in the analysis. The sample ionization generates fragments that are ultimately identified by their mass/charge ratio. As the same mass ions can be generated from different lipids, some settings are usually applied to correctly identify the contribution of each lipid to the whole spectra. Coupling a chromatographic technique to a mass spectrometer allows separating the different lipid classes first and then identifying the specific lipid species. Another approach is to take advantage of the ease of each class to generate positive or negative ions, which allows discriminating classes by using different settings. For example, PCs ionize better to positive ions while PE and PI to negative ones. Setting a detector to detect only positive or only negative ions simplifies the spectra by reducing the number of molecules to analyze.

1.5.1 Before analysis: the lipid extraction

To analyze a lipidome, it is usually necessary to separate first the lipid fraction from the rest of the biomolecules. Any lipid extraction uses organic solvents, which besides separating lipids also denaturalize lipases, preventing major lipid degradation and PUFA oxidation. Due to the high differences in lipid polarity within the lipid families²¹¹, there is no universal lipid extraction technique that acts as effectively overall lipid classes. Therefore, particular protocols are used depending on the lipid category to study. Two broadly used protocols allow extracting the main membrane lipid classes like phospholipids and sphingolipids: the Folch²¹² and Blight & Dyer²¹³ methods. Over the years, many variants that favor the extraction of specific lipid subfamilies have been developed.

1.5.2 Membrane lipid analysis by chromatographic techniques

Thin-layer chromatography (TLC) was the first and most used technique applied to analyze lipid extracts. It was widely used during the XX century and currently, it is still useful in particular situations. In TLC, the lipid extract is placed over the stationary phase (usually silica) distributed over a plate, then, part of the plate is submerged in a solvent system. While the mobile phase migrates towards the top of the plate, lipids separate according to their affinity to the mobile and stationary phases. Afterward, the lipid bands are usually visualized using chemical treatments and/or exposure to high temperatures. Different separations can be achieved depending on the solvent system used as the mobile phase. TLC allows separating the major lipid classes: phospholipids, sphingolipids, and neutral lipids, but usually, each TLC band contains numerous molecular species being exceptional its use to separate individual molecular species.

Gas-Liquid Chromatography (GC) uses a carrier gas (the mobile phase) to separate analytes along a thin capillary (the stationary phase). In general, GC is suitable for neutral lipids of less than 500 Da. More complex molecules like phospholipids and triglycerides are unable to become gas without degradation due to their high mass. Once injected, the sample is heated (up to 200-330°C) becoming gas when begins migrating through the capillary. The migration of each molecule depends on its physicochemical properties like the boiling point or the affinity for the solid phase²¹⁰. The main disadvantage of this technique is that the use of high temperatures usually leads to the thermal decomposition of the sample. Regarding this limitation, any compound with charged sites (as fatty acids) cannot become gas without decomposition¹³¹. To overcome this limitation the analytes are chemically modified prior analysis in a process called derivatization, which introduces additional residues to the molecules. The most common fatty acid derivatization method involves their methylation into neutral molecules called fatty acid methyl esters (FAME).

In liquid chromatography (LC), the use of a liquid mobile phase at a much lower temperature allows separating temperature-sensitive molecules without risk of thermal degradation. The development of compact columns used at high pressure leads to the development of High-Performance Liquid Chromatography (HPLC), improving the mass resolution. The most common mobile phases are composed of multiple solvents combinations, which usually include water and organic solvent. The stationary phase is a small column filled with silica, which can be modified in, from its composition to the length and particle size. After the sample injection, the mobile phase can be held constant (isocratic elution) or change along time depending on the desired separation of the sample components. The great variety of settings modifiable in HPLC allows researchers to separate complex mixtures of analytes.

1.5.3 Mass Spectrometry techniques

MS techniques identify hundreds of lipid species with low cost and relatively short times. Although also applied to protein analysis, lipids present more suitable properties for these techniques as they generate fewer fragments and therefore simpler spectra. The development and optimization of MS allowed overcoming the previous lipid analysis techniques limitations, letting to the complete identification of the specific molecular species. MS techniques usually begin with the analytes fragmentation by ionization. The application of an electric potential gradient accelerates the molecules depending on their mass/charge ratio (m/z), reaching the detector at different times²¹⁴. The identification of the molecule can be initially done by the comparison of the m/z with databases, being www.lipidmaps.org the most currently used in the lipid field^{84,215-218}. In terms of sample ionization, the three most common desorption ionization MS techniques applied to lipid analysis are Electrospray Ionization (ESI), Secondary Ion Mass Spectrometry (SIMS) and Matrix-Assisted Laser Desorption Ionisation (MALDI).

Electrospray ionization (ESI) uses an intense electric field at atmospheric pressure to ionize the sample. The intense ion charge generated repels the ions producing ionic evaporation of the sample in the form of an aerosol. ESI-MS analysis usually requires a previous separation (with LC or HPLC for example) to enhance the detection resolution. A variant of the method is the Desorption/Electrospray Ionisation (DESI), which uses the ESI as ionization method²¹⁹. In this case, the charged droplets and ions of solvent produced in an electrospray jet are directed to the sample to desorb their ions²²⁰. The main advantage of these techniques is that the analysis occurs at atmospheric pressure^{220,221}, which make suitable for *in situ* MS or even in living biological systems²²². Unfortunately, this system requires relatively high amounts of the sample due to its low sensitivity²²³.

SIMS ionizes the sample using a focused ion beam of high-energy particles generated by primary ions collisions directed to its surface^{224,225}. This type of ionization allows the detection of concentrations even at attomolar (10^{-18}) range²²⁶. However, the extreme analyte fragmentation limits its mass sensitivity to <500 Da constraining the lipid analysis to small molecules like fatty acids²²⁷.

MALDI is an upgrade of Laser Desorption Ionisation (LDI) which uses laser radiation at a specific wavelength to ionize the sample. The use of some chemical compound named matrix mixed with the sample eases the photon absorbance and therefore the mixture ionization. The matrix absorbs the laser radiation assisting in the emission of molecular and fragment ions^{228,229}. Depending on the matrix used, the ionization of particular molecules may change; therefore, knowing their properties is crucial for a proper sample analysis²³⁰. According to the type of matrix, exist various LDI like the Desorption/ionization on silicon (DIOS)²³¹ and the MALDI^{228,229}. The vacuum necessary for this technique avoids sample oxidation and enzymatic degradation by the sample own enzymes.

In addition, the environment provided by the matrix, acidic or basic depending if the ions generated are positive or negative respectively, averts aggregation between the different analytes^{232,233}. Unlike ESI, MALDI usually does not charge the molecules with more than one charge making simpler spectra however, some molecules present in the sample can ionize with matrix fragments, adding confusing ions to the spectra. Also, the laser energy fluctuation and the heterogeneous matrix crystallization elicits a poor ion-signal reproducibility making the MALDI unsuitable to obtain quantitative results²³². Despite this, this technique has a high mass resolution for even 10^{-21} mol²³⁴.

In any case, any of the ionization techniques described (DESI, SIMS, and MALDI) requires accurate mass determination and tandem MS/MS for exact molecule identification. Tandem MS/MS identifies the first ionization fragments and submits them to a new fragmentation. The second fragmentation into smaller molecules allows detecting more subtle differences and identifying the molecule. The smaller the molecule is to fragment, the fewer

1. Introduction

species coincides with the same mass so its identification is easier and more accurate. This methodology requires specific settings and is difficult to apply, but currently is the only way to obtain the exact lipidome of a sample.

Finally, all these ionization techniques can be coupled to imaging software allowing to obtain images of the analyte distribution²³². The setting to obtain images is done by moving the ionization source (laser beam, ion current...) across one sample, to obtain the lipidome distribution along the sample. After the molecule profile is determined at each point of the sample, a software can assemble the pixels providing the image of the spectra within the sample. These MS-imaging techniques (IMS) unveiled the high correlation between the molecular images and the histology of tissues^{217,235,236} (Figure 1-12).

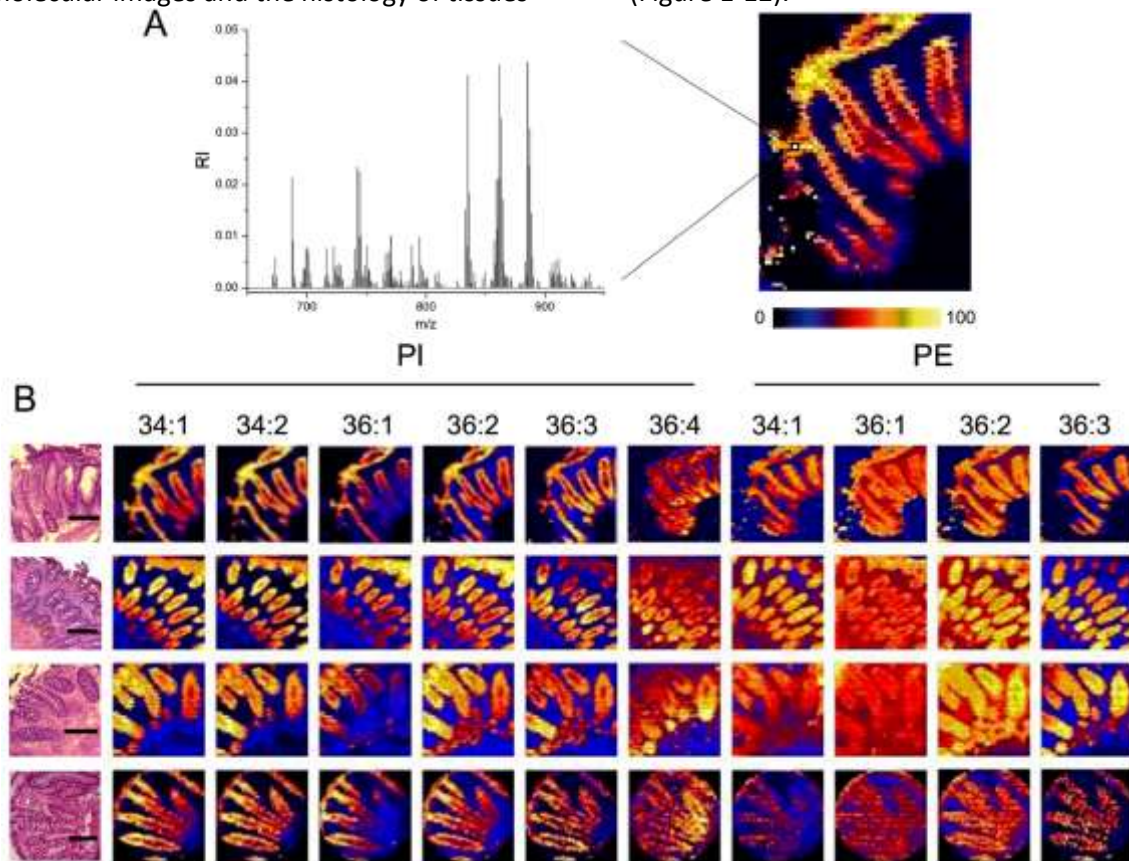


Figure 1-12: Example of MS imaging technique, in this case MALDI-IMS, applied to colon. A) Representative MS spectra associated to one of the pixels defining an MALDI-IMS image. Each m/z peak is integrated and the value is represented according a color scale vs. the coordinates where the spectrum was recorded. **B)** First column: HE staining of colonoscopy biopsies included for comparison, the rest of columns shows the distribution of some of the lipid species displaying a gradient in intensity. Scale bar = 150 μ m. All spectra showed were recorded in negative-ion mode and at 10 μ m of spatial resolution.

Despite the limitations regarding the number of analytes able to identify, SIMS is by far the one MS technique with better lateral resolution. SIMS provides 50 nm of spatial resolution images for elemental ions and few organic fragments^{237,238} and some hundreds of nanometers for biological surfaces²³⁹⁻²⁴⁴. On the other side, the lower spatial resolution of MALDI (5-100 μ m)²⁴⁵⁻²⁴⁸ and DESI (200 μ m)²⁴⁹ is compensated by the higher amount of molecules able to detect due to softer ionization sources²³².

Ion detection

Once the samples are ionized, each ion must be identified by some ion analyzing method. The most common are the Time of Flight (TOF) and the Ionic Trap, which are

commonly combined to overcome their specific limitations. Thus, the ionic trap can be used to filter the ions that will finally arrive at a TOF, so that the sample complexity is reduced.

Importantly for this study, the application of the different lipidomic techniques to biological samples has highlighted the relevance of lipids in complex biological processes like differentiation and proliferation. In the colon, the study of epithelial cells brings a good opportunity to study those processes due to the dynamic in proliferation and differentiation present in their cells cycle.

1.6 Colon as a proliferation and differentiation model

The human large intestine, or colon, begins at the ileocecal valve which connects with the small intestine. The colon diameter is approximately double that of the small intestine and diminishes progressively except for the region of the ampulla of the rectum. It is between 120 and 150 cm long and is anatomically divided into four regions: ascending, transverse, and descending colon, and the rectum (Figure 1-13).

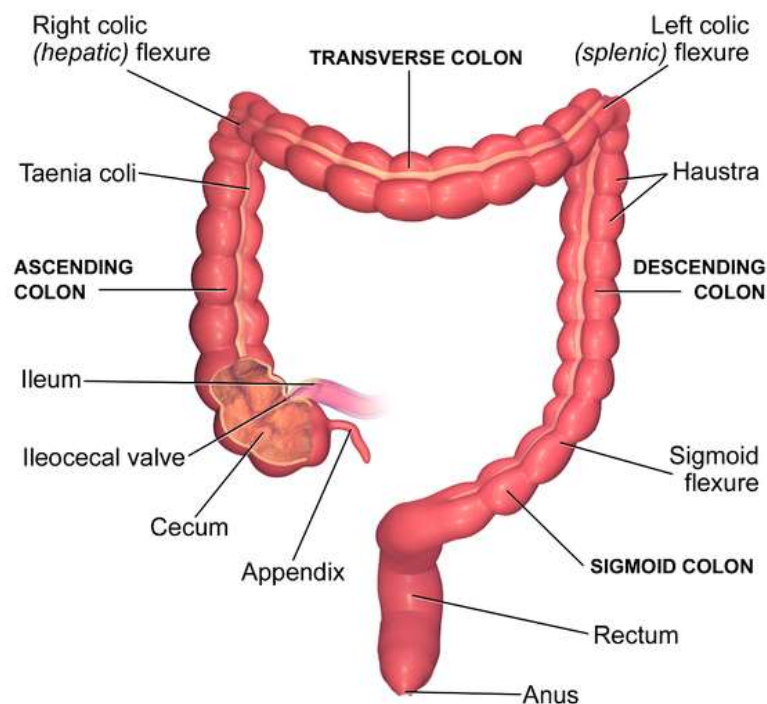


Figure 1-13: General anatomy of the large intestine. The ascending colon is composed of the cecum and the ascending colon. The ascending colon is 15-20cm length, at the hepatic flexure became the transverse colon of 30-60cm. The left colon is composed of the descending and the sigmoid colon. The splenic flexure defines the beginning of the descending colon for 20-25cm, but after crossing the pelvic brim is named sigmoid colon. The rectosigmoid junction indicates the beginning of the rectum, the final part of the intestine²⁵⁰. Adapted from www.teachmeanatomy.info.

At the microscopic level, the colon is composed of four layers: the mucosa, the submucosa, the muscularis and the adventitia (Figure 1-14 A). In turn, the mucosa comprises the epithelial layer, the lamina propria and the muscularis of the mucosa (Figure 1-14 B). The physiologic function of colon epithelium (composed by the colonocytes) is the absorption of water, electrolytes, bile salts and other substances produced by bacterial degradation²⁵⁰; which basically forms the stool. The lamina propria is the connective tissue nutritionally and metabolically supporting the epithelial layer, and where are located the lymphatic nodules and

immune infiltrates. Finally, the muscularis mucosa is the muscular layer that produces the micro-movements necessary to move the stool²⁵¹.

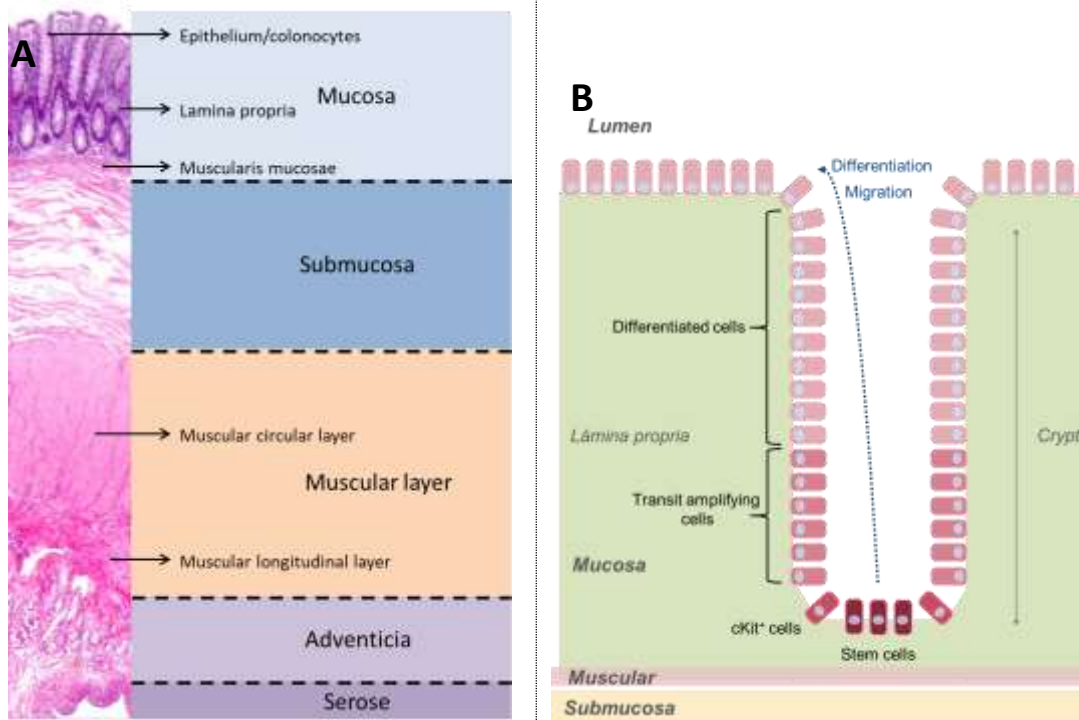


Figure 1-14: A) Histological section of human colon. The figure indicates the layers of the colon tissue, namely: mucosa, submucosa, muscular layer, adventitia and serosa. The mucosa, the functional part of the gastrointestinal tract, occupies around one-fourth of the total colon thickness. The submucosa is the poor-cell and collagen-enriched part of the colon that gives physical support to the tissue thanks to their differently orientated fibers, composing a flexible honeycomb²⁵². The submucosa presents arterial and blood plexuses, adipose accumulations and neural ganglions²⁵⁰. Muscular layers, internal circular and external longitudinal, are perpendicularly oriented and are the main responsible for colon peristaltic movements. Finally, adventitia and serose layers provide physical anchorage points between the bowel and the abdomen. **B) Scheme of the mucosa layer.** Colon crypts are composed of epithelial cells that can be divided into different populations, namely: stem cells, cKit⁺ cells, TA cells and differentiated cells. In turn, colon crypts are surrounded by the lamina propria or stroma, the supporting tissue in charge of supplementing the epithelium with growth factors as well as of the immunological responses of the colon.

The epithelial layer is formed by tubular parallel crypts, its functional unit, surrounded and supported by the lamina propria²⁵¹ (Figure 1-14 B). The main nutrition source of colonocytes comes from the bacterial fermentation of starch and proteins leading to the generation of short-chain fatty acids^{253,254}. Colon crypts renew the colonocytes population from the residing colon stem cells, which lie at the crypt base and become high rapid dividing cells named transit-amplifying (TA) cells^{255,256}. The colon stem cells are supported by Paneth-like cells identified by the expression of the cKit marker²⁵⁷⁻²⁵⁹. Colonocytes positioned at the mid and luminal segments of the crypts acquire their final phenotype and spatial position as migrating towards the colon lumen. Differentiated colonocytes cell types include columnar absorptive cells, goblet cells, and endocrine cells²⁶⁰⁻²⁶². Once colonocytes reach the lumen, cells are flaked off by the stool and dying by anoikis, the programmed cell death induced by detachment²⁶³⁻²⁶⁵. The process of proliferation and differentiation requires strict growth factors secretion in a gradient along the crypts. Thus, disruption of this subtle mechanism leads to tumors and cancer development²⁶⁶⁻²⁶⁹.

According to the Spanish association against cancer (AECC) and the Spanish society of medical oncology (SEOM), in the last 20 years the cancer incidence has increased due to the lifespan extension of the population as the probability to develop cancer increases exponentially with age from 30 years. Thus, studies driven by the Global Cancer Observatory (GCO) indicated that in 2012, new 1.4 million cases were diagnosed with 700000 deaths worldwide caused by CRC^{270,271}. Thus, was expected an incidence increase by 60% respect total cancer deaths by 2013^{270,271}. In addition to the patient incidence, the burden of cancer in health institutions is undeniable as cancer-related causes are the third cause of hospitalization. Once a tumor is able to break through the basal membrane, malignant cells disperse through the body in the process called metastasis. For many cancer types, the development of a complete neoplastic lesion from its incipient state range from 20 to 30 years and is just during the final 5 years that the cells present high proliferation rate and finally invasion capacities²⁷²⁻²⁷⁶. If the pathologic proliferation is detected in its early stages, the disease is still treatable and effective in 50% of cases, but once tumors metastasize, therapies are rarely effective²⁷⁶⁻²⁷⁹. In fact, tumors recur in more than one third of patients with localized disease within 5 years after surgery due to the residual malignant cells²⁸⁰ disseminated to other tissues. Hence, despite being an inefficient process^{281,282} the metastasis is the main cause of cancer mortality²⁸³. CRC is the malignant tumor with most incidences in Spain, in addition, the main survival rate in Spain is 64% while in Europe it is 57%. Figure 1-15 schematizes the different types of possible tumor lesions present in the colon. In this context, early stages of CRC are easily treatable with surgical resection; in fact, colon tumors detected by colonoscopy are routinely removed with no more consequences for the patients. Unfortunately, colon tumors do not produce clear symptoms until the disease is at advanced stages, when the surgical resection is more aggressive and is more probable to not remove all cancer cells. Paradoxically these particular characteristics of CRC make this disease one of the most preventable but one of the less detectable cancers.

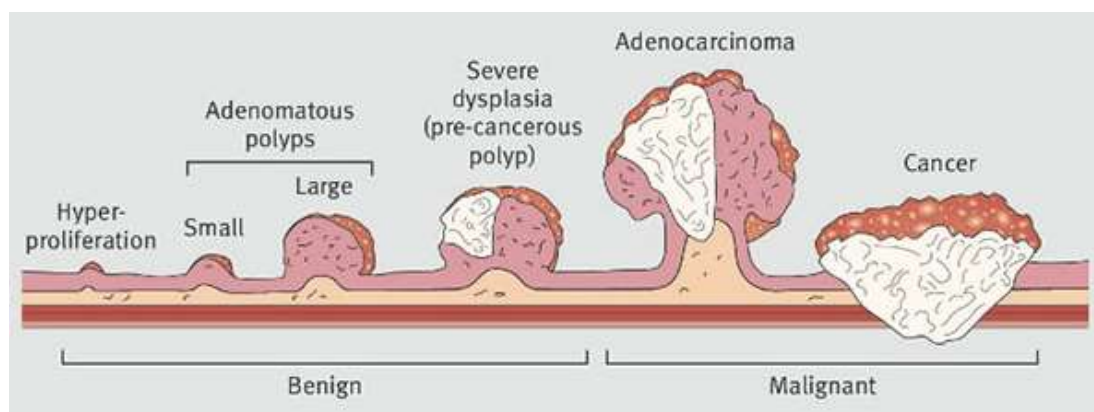


Figure 1-15: Schematic representation of the different polyp types of the colon. Adapted from <http://www.hopkinscoloncancercenter.org>.

Routinely, tumor lesions are classified according to the so-called TNM system which classifies a tumor by the extent of the tumor (T), the number of affected lymph nodes (N) and if the tumor had metastasized (M). In the context of CRC, the TNM score is applied as indicated in Table 1-3.

Stage	Level of involvement
Tumor	
T1	Limited to mucosa and submucosa
T2	Extension into but not through muscularis of the mucosa
T3	Invasion of perirectal fat
T4	Invasion of adjacent structures
Nodes	
N0	No involved lymph nodes
N1	Fewer than four regional nodes positives for tumor
N2	More than four regional nodes positives for tumor
Metastasis	
M0	No metastasis
M1	Distant metastasis

Table 1-3: Application of the TNM score to colon tumors. Adapted from Oh et. al.²⁸⁴.

Even further, the analysis of the genetic features of tumor lesions allows classifying many patients depending on their outcome and even the possibility to develop chemotherapy resistance. In this context, BRAF and KRAS mutations and microsatellite instability analysis are routinely used as prognostic factors for many tumor types²⁸⁵⁻²⁹¹. Although useful, the multiple possibilities in terms of genetic alterations and phenotypical tumor characteristics opened a scenario where is difficult to develop a correct and useful cancer stratification protocol. Addressing this problem, some works proposed multiple-feature stratification methods to classify CRC patients as shown in Table 1-4.

MSI immune	Canonical	Metabolic	Mesenchimal
14%	37%	13%	23%
MSI, high CIMP, hypermutation	SCNA high	Mixed MSI status, SCNA low, CIMP low	SCNA high
<i>BRAF</i> mutations		<i>KRAS</i> mutations	
Immune infiltration and activation	WNT and MYC activation	Metabolic deregulation	Stromal infiltration, TGF- β activation, angiogenesis
Worse survival after relapse			Worse relapse-free and overall survival

Table 1-4: Proposed molecular CRC stratification. Adapted from Ginney et. al.²⁹². CIMP, CpG island methylator phenotype; MSI, microsatellite instability; SCNA, somatic copy number alterations

The study of the multiple cell signals necessary for the colonocytes proliferation and differentiation processes revealed important colon pathophysiological mechanisms candidates as future cancer biomarkers or as therapeutic targets. During the last years analysis of genetic mutations identified multiple genes involved in cancer development. This knowledge led to propose a multistep genetic model necessary to develop sporadic CRC^{293,294}. Many mutations related to the sequence of developing tumors are mainly related to β -catenin/APC pathway, p53, BRAF, KRAS, and DNA mismatch repairing genes²⁹⁴.

1.7 Introduction to colon signaling

The seemingly simple functions of the large intestine need in fact of the coordination of multiple tissues and cell types different as neurons, inflammatory cells, fibroblasts, and epithelial cells. In this context, the metabolism of colonocytes and lamina propria is complex, requiring intercommunication between both tissues. The latter involves the secretion by supporting epithelial cells (ckit⁺ cells) and lamina propria cells of a large number of growth factors as Wnt3a²⁹⁵⁻²⁹⁷, R-spondin1^{298,299}, EGF³⁰⁰, Notch³⁰¹, and BMP³⁰².

Wnt signaling:

Wnt signaling is related to control growth and patterning during animal development either by secretion and action in adjacent cells³⁰³⁻³⁰⁵ or by long-range activity by gradients³⁰⁶⁻³¹⁰. In the colon, the lamina propria secretes Wnt3a in a gradient, being more expressed near the crypt base. Therefore, the epithelial cells express the Wnt target genes gradually³¹¹, with higher expression at the crypt bottom where the stem cells (Lgr5⁺) reside and lower at the luminal site²⁵⁶. In the small intestine, Wnt3a is secreted by Paneth and mesenchymal cells³¹², while in the large intestine, besides the lamina propria there are Paneth-like cells, which express the cKit protein, with similar properties^{259,313}. The stem cells differentiation into this supporting cKit⁺ cells requires Wnt3a signaling activation and Notch inhibition³¹⁴.

Wnt3a signaling is the main driving force for colon proliferation and differentiation through the nuclear translocation of β -catenin in the named β -catenin canonical pathway (Figure 1-16). β -catenin is a membrane-associated protein, essential for colonocytes intercellular adhesion³¹⁵⁻³²⁴. In physiological conditions, the excess of cytoplasmic β -catenin is degraded by the destruction complex³²⁵. If cytoplasmic β -catenin is not degraded, its translocation to the nucleus is favored, enhancing proliferation once bound to TCF protein³²⁶⁻³³³. Although this signaling can activate other non-canonical pathways, colon organoid studies have demonstrated that the main contribution in colon proliferation is done by the Wnt canonical pathway²⁶⁹.

The union of Wnt3a to the Frizzled/LRP6 receptor complex induces the abduction of Dsh and Axin proteins through the cytoplasmic tail of LRP6^{334,335}, preventing the functional association of the destruction complex³³⁶. The latter is a multiprotein association which phosphorylates proteins like β -catenin, marking them for ubiquitination and subsequent degradation^{337,338}. The genetic program started with this pathway also promotes the expression of proliferation restrictive proteins like Ephrins³³⁹⁻³⁴¹. Ephrin receptors inhibit proliferation when contact cells expressing its ligands, as happen in the stem cell neighbourhood^{340,342}. Consistently, inhibition of the Ephrin B2 receptor increases tumor growth and invasivity³⁴⁰. Thus, loss of this receptor is related to poorer overall survival in CRC patients despite increasing nuclear β -catenin presence inherent of these lesions^{340,343,344}.

Pathological outcomes of this pathway led to tumors and cancer development. Being APC malfunction the usual cause, in fact, mutations in this protein are detected in 75.5% of patients with colorectal tumors and around 59.7% of patients with familial adenomatous polyposis²⁶⁶⁻²⁶⁸.

R-spondin1 signaling:

R-spondin1 is a protein with expression is Wnt-dependent³⁴⁵ and like Wnt3a, it is necessary for the correct colonocyte proliferation profile²⁹⁹. R-spondin1 induces phosphorylation of its receptor which is necessary for the LRP6/Frizzled activation^{346,347}. This ligand binds specifically to LRP6 and has no affinity for the Frizzled receptor³⁴⁶. The simultaneous stimulation of both R-spondin1 and Wnt3a is necessary to activate colonocyte β -catenin signaling^{299,348} (Figure 1-16).

BMP and Noggin signaling:

Bone Morphogenic Protein (BMP) signaling enhances differentiation and inhibits intestinal stem cell proliferative profile^{349,350} (Figure 1-16). Indeed, inactivating mutations of

this protein leads to the massive adenoma formation of the familial adenomatous polyposis disease³⁵¹. Conversely, the Noggin ligand is antagonist of the BMP receptors³⁵² and is secreted by the lamina propria surrounding the crypt bases³⁵⁰. Once activated, BMP receptor heterodimerize and autophosphorylates, then is able to phosphorylate SMAD proteins, a well-known transducer protein family³⁵³⁻³⁵⁵. Despite Wnt signaling is the main proliferative intestinal pathway, the inhibition of BMP through Noggin is necessary for a proper intestinal stem cell proliferative profile³⁵⁰.

EGF signaling:

EGF participates actively in multiple signaling pathways and is a ligand for specific tyrosine kinase receptors named EGFRs³⁵⁶(Figure 1-16). The active role of this receptor in proliferation is highlighted by its overexpression in many cancers^{357,358} which has led to the development of chemotherapy drugs targeting these receptors³⁵⁹⁻³⁶². Many ligands of these receptors are synthesized as precursors and only become active after partial proteolysis³⁵⁶, an activation mechanism particularly relevant in EGFR indirect activation through GPCRs^{356,363}.

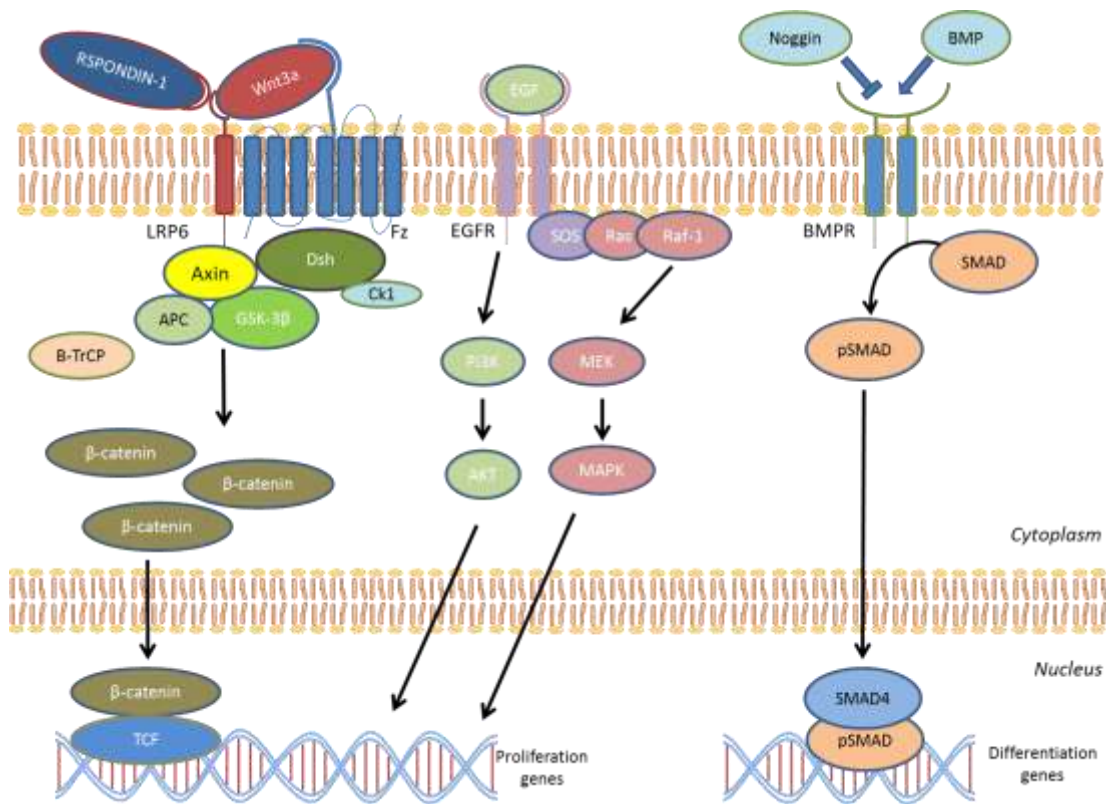


Figure 1-16: Colon main phenotype driving signaling pathways. Adapted from Komiya et. al.³⁶⁴ and Herbst et. al.³⁶⁵. **Wnt3a signaling:**The destruction complex is a multiprotein association composed by Axin, Dvl, Ck1, GSK-3β, APC and β-TrCP proteins which phosphorylates proteins like β-catenin, marking them for ubiquitination and subsequent degradation^{337,338}. While Axin and APC anchors β-catenin to the destruction complex, Ck1 and GSK-3β proteins phosphorylates it³⁶⁶. Initially, CK1^{367,368} phosphorylates β-catenin prior the subsequent three phosphorylations by GSK-3β^{369,370}. β-TrCP is the E3-ubiquitin ligase which bonds the GSK-3β phosphorylated β-catenin to the proteasome³⁷¹⁻³⁷⁷. **BMP signaling:** Phosphorylated SMAD proteins are able to recruit the SMAD4 protein, then the complex translocate to the nucleus where transcribe differentiation genes, mainly PTEN^{378,379}. PTEN is a negative regulator of PI3K³⁷⁸, which in turn stimulates cell-cycle progression and suppress apoptosis through Akt activity³⁵⁰. PTEN inactivation allows Akt activity favouring downstream pathways^{378,380} like nuclear β-catenin signaling. **EGF signaling:** Once activated, this receptors activate the Ras-Raf mitogen-activated protein kinase pathway³⁸¹ and the PI3K-Akt pathway³⁸²⁻³⁸⁴.

Within the variety of colonocytes, all populations can be stratified into four major cell types: stem cells, Paneth-like cells, TA cells and differentiated cells (Figure 1-14, B). Those cell populations can be discriminated by different cell markers: **1)** stem cells express the Lgr5 receptor. Lgr5 is a Wnt target gene²⁹⁸ and marks the stem cells at the small intestine and the colon²⁵⁶. Despite being a rhodopsin-like seven transmembrane G-protein-coupled receptor (GPCR)³⁸⁵⁻³⁸⁷, Lgr5 does not act through the classical GPCR nor β -arrestin signaling³⁸⁸. RSOs proteins bind to this receptor potentiating the Wnt signaling³⁸⁸. This receptor is necessary for the LRP6 phosphorylation and the subsequent accumulation of cytoplasmic β -catenin despite enhancing also its rapid turnover³⁸⁸. **2)** Paneth-like cells can be identified by the cKit protein. c-kit protein is the receptor for the Stem Cell Factor (SCT) also named as mast cell growth factor^{257,258}. It is a marker for colon Paneth-like cells²⁵⁹, the named cKit⁺ cells that express factors necessary for stem cell maintenance like Dll1, Dll4 (Notch ligands) and EGF²⁵⁹. The cKit⁺ cells are goblet cells expressing also Muc2 and are present at the bottom third region of the crypts²⁵⁹. While doing the same function as Paneth cells of the small intestine and sharing the same markers^{259,389}, ckit⁺ cells had not been comprehensively studied and their complete relation with stem cells is not completely understood. **3)** TA cells possess the Wdr43 protein. Wdr43 (WD repeat-containing 43 protein) is involved in nuclear processing of pre-18S ribosomal RNA, while in gastrointestinal track marks for the TA cells. TA cells reside above the cKit-stem cell niche and give the final cell differentiated cell types (enterocytes, goblet cells, and enteroendocrine cells) by rapid divisions²⁵⁶. Finally, most differentiated colonocytes express the Krt20 keratin. Krt20 is a type I keratin and an epithelial differentiation marker as this protein make up the intermediate filaments of epithelial cells³⁹⁰.

Despite the comprehensive knowledge about colon metabolism and CRC, there is still insufficient information to have effective pharmacological therapies and diagnostic and prognostic biomarkers. In fact, there are still no markers for early states of sporadic tumor lesions development. The study of membrane lipids in colon tumor development could be a promising approach to develop new therapies and biomarkers. Unfortunately, the close relationship of multiple cell types in colon compels to the use of tissue visualization techniques like microscopy. MALDI-IMS lipidomic revealed not only the potential of lipids to discriminate between healthy and pathological epithelium, beyond that, a profound analysis revealed subtle but relevant changes along the colon crypts.

1.8 Arachidonic acid derivatives and prostaglandin signaling

As will be described in section 3.2.1., the results revealed a gradual and tight regulation along colon crypts of AA-containing phospholipids and of the enzymes related to AA metabolism, specially PLA₂ and COX enzymes. For these reasons, in the last part of this study, we focused our attention on the role of the AA derived metabolites, in particular, PGs could have on colonocyte fate. The coordinated action of PLA₂ and COX enzymes is derived into the production of highly bioactive molecules like eicosanoids and cannabinoids. These AA-derived molecules are involved in multiple cell processes like cell proliferation or cell fate regulation^{363,391-413}. In terms of colon physiology, eicosanoids, and especially PGs, have been related to mucin secretion, EGF release and more importantly, to the canonical β -catenin pathway^{402,409,414,415}.

PGs are the most studied eicosanoids. Historically, PGs have been related to inflammation and inflammation-related conditions like pain, fever, cancer or Alzheimer's disease. However, their relevance in physiological processes like ovulation, bone formation or gastric mucosa homeostasis highlights PGs as key participants in cell proper development⁴¹⁶⁻⁴¹⁸. Figure 1-17 summarizes the hallmarks of PG research.

1. Introduction

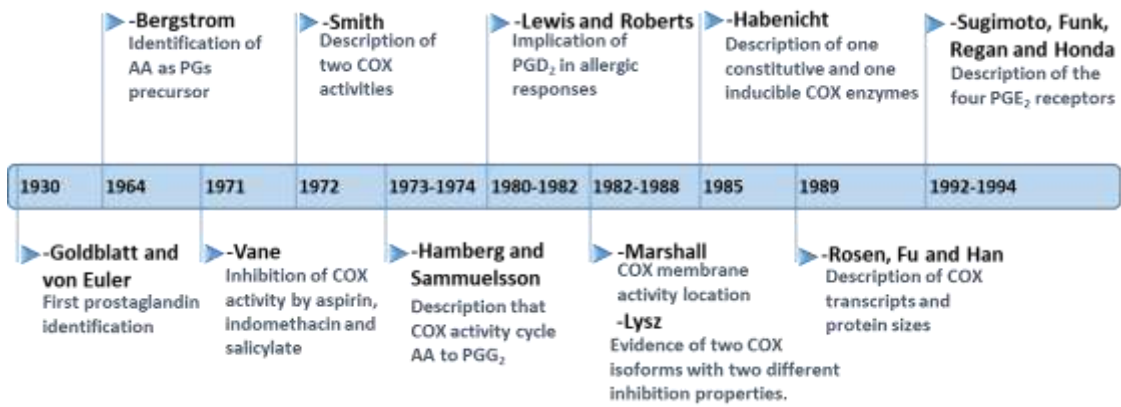


Figure 1-17: Timeline of relevant milestone in prostaglandin research field. PGs were first identified in the 1930s by Goldblatt and von Euler⁴¹⁹⁻⁴²² but was Van Dorp et. al. and Bergstrom et. al. who identified in 1964 the AA as their precursor. In 1971 it was proved that aspirin, indomethacin and salicylate (nonsteroidal anti-inflammatory drugs (NSAIDs)) inhibit the COX activity⁴²³, while in 1972 two distinct PG synthase activities⁴²⁴ were described. It was not until 1988 when it was suggested the COX membrane location and its activity site⁴²⁵. Thus, different studies proposed in 1982 and 1988 the first evidences of two COX isoforms with different autoinactivation rates, sensitivity to NSAIDs and time courses for PGE₂ and PGF_{2α} synthesis^{426,427}. The characterization of the two COX protein isoforms were done by the detection of one constitutive and one inducible COX activities⁴²⁸ and the description of two different transcripts and protein sizes⁴²⁹⁻⁴³¹. The constitutive COX protein was named as COX1, while the inducible protein, related to inflammatory states, COX2. The description of the four known PGE₂ receptors (EP1, EP2, EP3 and EP4) was done from 1992 to 1994. EP3 was the first PGE₂ receptor described in 1992⁴³², and was followed rapidly by the description in 1993 of EP1 and EP4^{433,434}. One year later, EP2 was pharmacologically characterized⁴³⁵.

PGs are not the only AA-derived bioactive molecules, as multiple molecules can be synthesized not only from PGH₂ but directly from the AA (Figure 1-18).

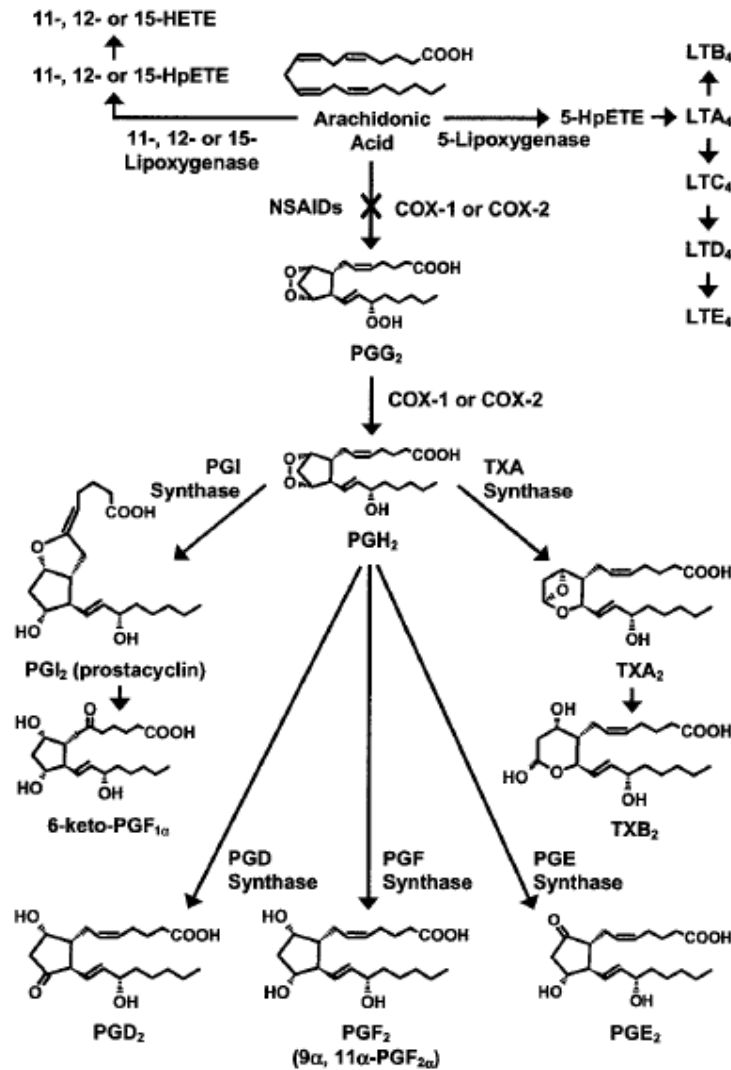


Figure 1-18: Prostaglandins and thromboxanes synthesis scheme. Adapted from Simmons et. al.⁴³⁶. The free AA is cycled by the cyclooxygenase enzymes (COX) to synthesize PGH_2 , a highly unstable eicosanoids precursor. In turn, PGH_2 can be modified by multiple enzymes to provide PGs and thromboxanes

Endocannabinoids are bioactive lipids especially related to nervous system regulation. The main endocannabinoids are the anandamide (AEA) and the 2-arachidonoylglycerol (2-AG); being both compounds inactivated through their hydrolysis to AA by specific lipases^{437,438} (Figure 1-19). Two endocannabinoid receptors have been described so far, CB1 and CB2⁴³⁹⁻⁴⁴¹ both able to inhibit the adenylate cyclase⁴⁴². The central nervous system only expresses the CB1 receptor, responsible for the endocannabinoids analgesic and temperature control effects⁴⁴³. Conversely, the CB2 receptor is mainly present in inflammatory cells modulating inflammatory responses³⁹⁶ by for example repressing the migration of CD8^+ T lymphocytes³⁹³. Both receptors are present in the gastrointestinal tract and inhibit the adenylate cyclase and the cAMP production^{397,442,444}. Also, CB1 has been described as cell migration inhibitor in colon tumor cells³⁹³.

1. Introduction

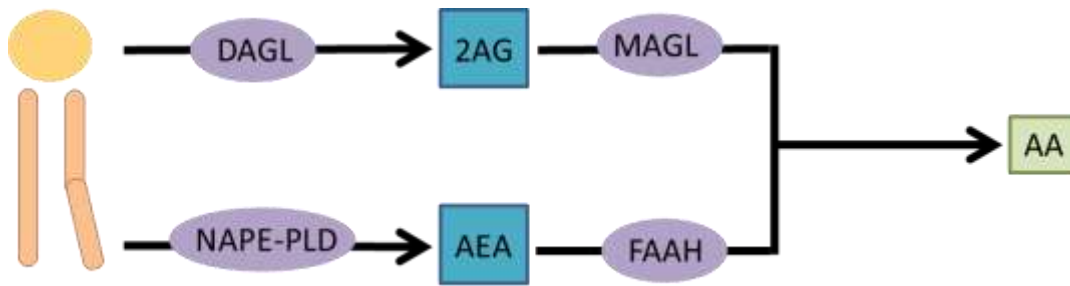


Figure 1-19: Scheme of the endocannabinoids synthesis and degradation. AEA synthesis pathway begins with the transfer of AA from the sn1 position of PC to a PE nitrogen atom by the *N*-acyl transferase (NAT) to form *N*-arachidonyl-phosphatidylethanolamine (NAPE)^{395,445}. The NAPE-specific PLD (NAPE-PLD) converts NAPE to AEA⁴⁴⁶. 2-AG is synthesized from the phosphatidylinositol-4,5-bisphosphate (PIP₂) with AA in the sn2 position by PLC-β. The DAG generated is then hydrolysed by the diacylglycerol lipase (DAGL)^{394,447,448}. 2-AG, 2-arachidonylglycerol; 5-, 12-, 15-LOX, 5-lipoxygenase, 12-lipoxygenase and 15-lipoxygenase respectively; AA, arachidonic acid, AEA, anandamide; COX1-2, cyclooxygenase 1 and 2 respectively; DAGL, diacylglycerol lipase; FAAH, fatty acid amide hydrolase; HETE, hydroxyeicosatetraenoic acid; LT, leukotrienes, MAGL, monoacylglycerol lipase; NAPE-PLD, *N*-arachidonyl-phosphatidylethanolamine specific PLD; PG, prostaglandins; PLA2, phospholipases A2; TX, thromboxanes. Adapted from Chirchiu et. al.⁴⁰¹.

Prostaglandin signaling:

PGs, as well as endocannabinoids, will be described in this section. Figure 1-20 summarizes the current knowledge on the signaling pathways involving the PGs through their interaction with their corresponding GPCR.

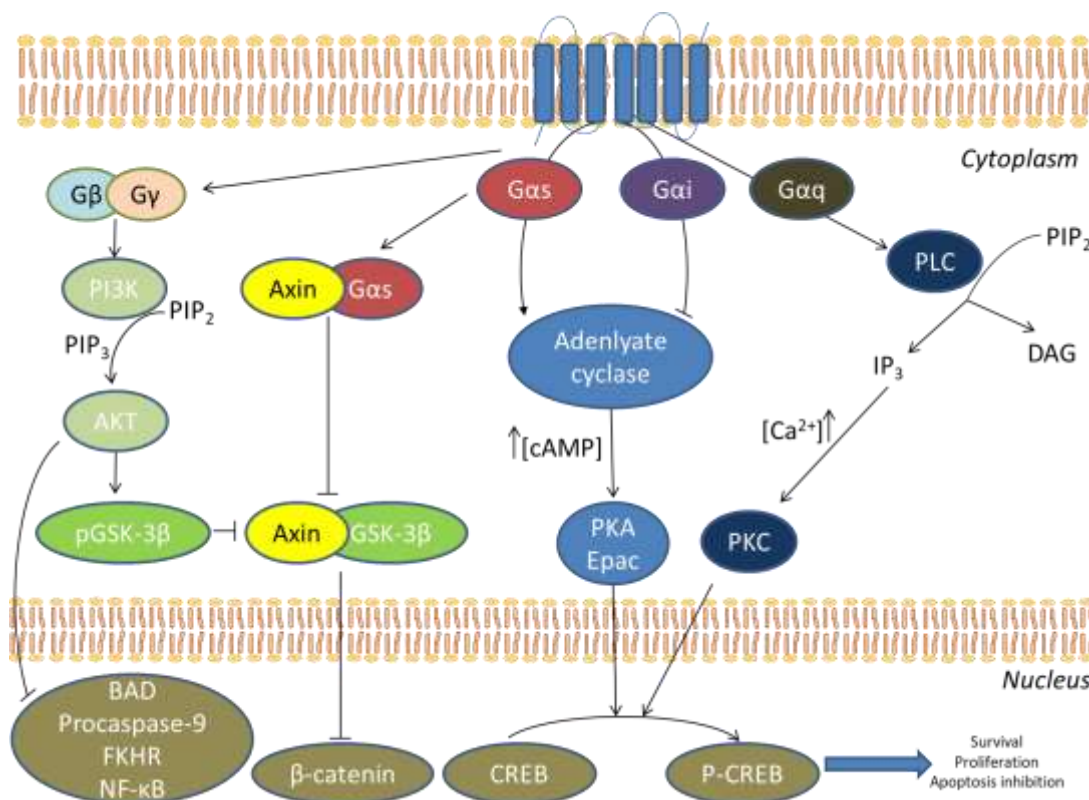


Figure 1-20: Scheme of PGs signaling cascades. The coupling of the G-protein complex to the receptor induces the dissociation of its corresponding G_α subunit from the G_{βγ} complex by substituting GDP for GTP⁴⁴⁹. The dissociated proteins interact with different second messengers participating in multiple pathways like the MAP

kinases, receptor tyrosine kinases, PI3-kinases and c-Jun-N-terminal kinases (JNK)⁴⁵⁰. Of the three types of G_{α} , G_{α_s} activates the adenylate cyclase while G_{α_i} type inhibits the enzyme, stimulating or inhibiting cAMP synthesis respectively^{449,451-457}. The signaling through cAMP can be counteracted by the enzyme phosphodiesterase, which degrades cAMP⁴⁵⁸. G_{α_q} , the third described G_{α} , activates PI-specific PLC β which in turn hydrolyzes PIP₂ to diacylglycerol and inositol 1, 4, 5 triphosphate (IP₃)⁴⁵⁹⁻⁴⁶¹. Union of IP₃ to IP₃ gated calcium channels located at the ER induces a rapid release of ER Ca²⁺^{156,157,433,462,463}. After continuous activation, GPCR and the ligand are internalized through their union to β -arrestin⁴⁶⁴. The increase of cytoplasmic cAMP synthesized from the adenylate cyclase activates the cAMP-dependent protein kinase A (PKA)^{465,466} and other kinases like Epac^{467,468}. Once activated, this protein translocates to the nucleus where phosphorylates transcription factors, being the activation of the Proliferation Cyclic AMP-Responsive Element Binding protein (CREB) the most relevant regarding proliferation⁴⁶⁹. In the nucleus, phospho-CREB induces the expression of survival genes like c-IAP2⁴⁶⁸. Also, the increase of cytoplasmic Ca²⁺ induced by G_{α_q} activated the PKC kinase, which also has CREB as one of its targets¹⁵⁸⁻¹⁶¹. The G_{β} and G_{γ} subunits exert also biological effects by activating the PI3K-AKT axis. This pathway is mostly implicated in regulating apoptosis pathways. When PI3K is activated by the $G_{\beta\gamma}$ complex, phosphorylates PIP₂ to PIP₃. This phosphoinositide activates AKT, a kinase that once activated inhibit pro-apoptotic factors like BAD, procaspase-9, and FKHR¹⁴⁹⁻¹⁵¹. Redundantly also activate factors like CREB and induce NF- κ B nuclear degradation upregulating anti-apoptotic genes. In addition, this pathway inactivates p53 contributing to cancer chromosome instability¹⁵²⁻¹⁵⁴.

PG receptors are named after their main ligand: PGD₂ binds to DP and CRTH2 receptors, PGF₂ has only the FP receptor, and PGE₂ receptors are the EP1, EP2, EP3, and EP4⁴⁷⁰. Next, we briefly summarized the current knowledge existing on these receptors, particularly that relevant for our studies in colon tissue.

PGD₂ and DP receptors:

PGD₂ signaling is mainly associated with allergic responses as is synthesized by activated mast cells and participates in IgE-mediated type I acute allergic responses^{471,472}. Besides its role in inflammatory responses, PGD₂ has been related in platelet aggregation inhibition⁴⁷³, smooth muscle relaxation and contraction⁴⁷⁴, vasodilation and vasoconstriction⁴⁷⁵, mucus secretion⁴⁷⁶ and sleep induction⁴⁷⁷. PGD₂ levels are decreased in colon cancer hepatic metastasis. Thus, treatment with PGD₂ inhibits slightly SW480 and LS174t CRC commercial cell lines proliferation⁴⁷⁸.

Up to now, two PGD₂ receptors have been identified: DP and CRTH2 receptors, both with similar affinity for PGD₂^{479,480}. DP receptor is member of the prostanoid GPCR subfamily being similar to the other PG members while the CRTH2 receptor has little similarity to any of them. DP receptor couples to a G_{α_s} subunit, although some data suggest a cross-activation of the G_{α_q} subunit⁴⁸¹⁻⁴⁸³, while CRTH2 couples to a G_{α_i} ^{479,484}.

PGF_{2 α} and FP receptors:

PGF_{2 α} couples to FP receptor, a G_{α_q} type GPCR⁴⁸⁵. However, PGF_{2 α} can also bind to EP1 and EP3 receptors which complicate the contribution of this molecule to the overall PG signaling^{433,486}. It has been described as a pro-proliferating role of PGF_{2 α} in epidermal tumors⁴⁸⁷. Thus, activation of the FP receptor leads to VEGF expression, increasing angiogenesis in tumors⁴⁰⁰. This signaling pathway stimulates MAPK pathway activation^{398,399}, broadly related to cancer progression^{488,489}. Both PGF_{2 α} and PGE₂ increase motility and invasion of cancer cells, although PGF_{2 α} in an EGFR independent way⁴⁹⁰.

PGE₂ and EP receptors:

Despite the existence of extensive bibliography regarding PG effects and signaling, PGE₂ is, the one most thoroughly described. It is usually considered a pro-inflammatory molecule that regulates vasodilatation⁴⁹¹ and cytokines production^{492,493}. However, PGE₂ participates in other functions, in some cases even contradictory depending on the tissue or the situation. This phenomenon was partly explained with the discovery of the four EP receptors: EP1, EP2, EP3, and EP4. EP3 and EP4 have the highest affinity for PGE₂ while EP1 and EP2 the lowest ($K_d < 1$ nM and $K_d > 10$ nM respectively)⁴⁹⁴. In colon cancer cells, PGE₂ stimulates proliferation in a GPCR-dependent but cAMP-independent way. Upon PGE₂

stimulation, G_s dissociated binds axin protein, uncoupling β -catenin from the destruction complex and stabilizing it. Also, the $G_{\beta\gamma}$ -PI3K-AKT axis activated by PGE_2 phosphorylates GSK-3 β inactivating this protein⁴⁹⁵. The simultaneous presence of more than one PGE_2 receptor in the cells complicates the understanding of its signaling as their signaling pathways are not only different but in some cases completely opposed.

EP1 receptor known mechanism of action is through the G_{α_q} as its activation initiates a PLC-dependent calcium release and PKC activity^{433,462,496}. However, this increase does not correlate with an increase in IP_3 ⁴⁶² and depends on the extracellular calcium suggesting a G_q -independent mechanism⁴⁷⁰. Some studies have related the activity of this receptor with CRC development in mice, however, this effect appeared to be small and not a main factor in the development of CRC⁴⁹⁷.

EP2 and EP4 receptors are coupled to G_s ^{434,435} although EP4 binds PGE_2 with less affinity⁴¹⁵. Pharmacologically these receptors differ in their sensitivity to butaprost (an EP2 agonist): while the EP2 receptor is activated, the EP4 is insensitive to this molecule.

EP2 activation leads to GSK-3 inactivation by phosphorylation in a PKA-dependent PI3K-independent manner⁴¹⁵. Its activation also stimulates EGF receptor transcription, increasing the migration and invasion of colon cancer cells^{363,413}. Due to its shorter C-terminal tail compared to the EP4, EP2 suffers less agonist-induced desensitization through internalization^{498,499}.

EP4 activation induces phosphorylation of extracellular signal-related kinase1/2 (ERK1/2) through PI3K and the subsequent expression of early growth response factor-1^{500,501}. This pathway induces also GSK3 protein phosphorylation, leading to nuclear β -catenin activity⁴¹⁵. Its signaling is not primarily due to an increase in adenylate cyclase activity, as it have been shown that its activation stimulates proliferation in carcinoma cells with almost no increase in cAMP levels⁵⁰². This receptor had a faster internalization rate due to its longer C-terminal tail⁵⁰³. The EP4 receptor have been related to CRC development, as treatment with EP4 antagonist in mouse CRC model decreased the number and size of colon tumors.⁵⁰⁴

EP3 receptor is able to participate in different cell signaling processes due to its multiple described isoforms⁵⁰⁵⁻⁵⁰⁷, although generally couples to G_{α_i} ^{508,509}. For example, the decreased cAMP levels after the EP3A isoform activation results in the MAPK pathway activation⁵¹⁰. Regarding tumorigenesis, some works have related this receptor with tumor development and angiogenesis⁵¹¹, others described just the opposite, suggesting that this receptor could be a tumor suppressor⁵¹². Finally, some studies suggest that EP3 receptor does not play any role in cancer development⁴⁹⁷.

In terms of subcellular localization, EP receptors have been located at both cytoplasmic membrane and nuclei^{410,411,513-515}. Despite this, most studies assume just cytoplasmic membrane stimulation not taking into account the dual location and the potential crosstalk between both locations. Therefore, the role of intracellular PG signaling in cell metabolism is still unknown. A divergent cytoplasmic membrane and intracellular PG signaling is a tempting model to explain the apparent contradictory role of these molecules in cell pathophysiology that some studies reflect.

Finally, in addition to GPCR activation, PGE_2 can activate c-Src which in turn releases EGFR ligands by metalloprotease activation³⁶³. However, some works only observed a minimal increase in EGFR tyrosine phosphorylation upon PGE_2 treatment⁴⁹⁵. In any case, EGFR activation induces ERK2 activation which at the end favors cell proliferation through overexpression of genes like c-fos³⁶³. PGE_2 promotes proliferation at least in one commercial CRC cells, but only in the absence of functional APC, suggesting a late effect of this PG in tumorigenesis. In addition, that work showed that PGE_2 acts at two levels: one dependent on G_{α_s} and one of $G_{\beta\gamma}$ ⁴⁹⁵. The initiated by $G_{\beta\gamma}$ stimulates PI3K and Akt signaling that at the end phosphorylates GSK-3 β . The activation initiated by the G_{α_s} subunit implies its binding to axin

and the subsequent promotion of GSK-3 β release from the destruction complex. Although many works relate PGE₂ to tumor formation and progression^{403,516-521}, the mechanism of action of this PG is still not well understood.

Prostaglandins and cancer treatment

Since the description of inflammation as one of the hallmarks of cancer⁵²², PGs, and especially PGE₂ have been related to several steps of tumorigenesis as increased tumor proliferation^{363,500}, resistance to apoptosis⁴⁰⁷, increased invasiveness⁴¹³, angiogenesis^{406,523}, and immunosuppression^{405,524}. In fact, the participation of both COX enzymes is necessary for tumor development. Thus, in CRC tumors COX1 is more expressed in the epithelial cells while COX-2 is more expressed within the lamina propria⁵²⁵. In this context, the presence of COX1 products at early tumor development stages eases the development of the tumor, while COX2 paracrine signaling would be more implicated in tumor size increase⁵²⁵. The tight involvement of COX activity with cancer was reinforced by epidemiological studies showing a decreased risk of colon (43%), breast (25%), lung (28%), and prostate (27%) cancers when there is a regular intake of NSAIDs⁵²⁶. In addition, there is evidence suggesting that COX inhibitors (mostly NSAIDs) play not only a protective role in cancer development, but also could increase the progression-free and the overall survival in colorectal and breast cancer⁵²⁷⁻⁵²⁹. With this in mind, many studies explored the possibility of inhibiting COX activity to reduce tumor burden and size⁵²⁸⁻⁵⁴². However, the inhibition of both COX produces undesirable side effects^{404,543} especially in the intestinal tract⁵⁴⁴ and cardiovascular tissue^{545,546}. This led to the development of specific COX2 inhibitors, the -oxibs, which unfortunately still present important cardiotoxicity^{404,547-550}. Either way, clinical trials investigating the viability of COX2 inhibition in cancer treatment proved that although reducing the objective response rate, COX2 inhibition does not significantly increase the overall survival while it increases importantly the risk of cardiovascular events⁵⁵¹⁻⁵⁵⁴. In the effort of avoiding undesired side effects and increase effectiveness, some research groups focused on targeting the PG pathway downstream from COX activity. With this approach, some successful studies have been proposed to reduce inflammation through mPGES-1 inhibition, the main enzyme in charge of PGE₂ synthesis^{404,555-558}. While the first results were promising by not producing cardiotoxic effects⁵⁵⁹, this approach is difficult to translate from the murine model to humans due to differences in the enzyme between both species⁴⁰⁴. Besides, the inhibition of this enzyme led to the oversynthesis of other COX derivatives⁴⁰⁴. Being the major product of all PGs, the inhibition of PGE₂ synthesis would lead to the accumulation of PGH₂, the COX product. The accumulation of PGH₂ combined with the blockade of its main derivate synthesis favors the synthesis of other prostanoids, which at the end could lead to other important and undesired side effects^{404,556,559-561}.

The multiple efforts to treat tumor development from a COX inhibition perspective failed due to the exclusive focus on one PG effect over tumorigenesis, ignoring the effects that other PGs exert over the whole biological system. In this context, the understanding of how PG receptors participate in colon pathophysiology could derive into more specific more effective treatments and with fewer side effects. This thesis has contributed to enlarging the knowledge on this aspect (Seccion 3.2.2).

1.9 Lipid biomarkers

A biomarker can be defined as a clinical indicator that reflects a disease diagnosis, progression, prognosis or treatment effects over a patient. Usually used as a diagnostic tool, biomarkers can range from visual clinical symptoms to components of different biological fluids and tissues. Biomarkers can be divided as invasive or non-invasive, depending if is or is not required surgery to evaluate them. The detection of early biomarkers to diagnose and stratify diseases has become a priority in the biomedical field to apply early disease

treatments. Patients stratification is of special relevance in oncology because an early surgical resection can avoid further tumor development, and also because the development of new oncologic drugs is expensive and difficult. Therefore, the development of tools able to detect tumors before becoming invasive would save many lives and significant would reduce the economic burden associated with the chemotherapy treatments.

While most patients stratification tools are based on genetic features, many works have been addressed to identify lipid biomarkers for cancer, where altered lipid levels in both cancer tissue and biological fluids have been described. For example, plasma lipidome from ovarian cancer patients showed differences in LPA, LPC, LPI, and S1P compared to healthy patients^{562,563}. Similarly, plasma and urine of prostate cancer patients present alterations in diacyl, vinyl- and alkenyl PE species and PS, LacCer and HexCer^{564,565}. Even further, the lipidome is sensitive enough to discriminate between breast benign tumors and cancer biopsies by their levels of PI, GluCer, LPC, and PC^{566,567}. Regarding CRC, altered levels of LPC, PC SM and sphingolipids can discriminate between plasma of healthy and patients with CRC^{568,569}. However, the application of lipid biomarkers as routine biomarkers still seems far to be a reality.

1.9.1 Extracellular vesicles as non-invasive biomarkers

To date, the only non-invasive screening tool broadly applied for CRC detection is the fecal occult blood test (FOBT). FOBT relies on the higher bleeding probability of tumor lesions compared to the healthy mucosa. Actual antibody-based detection kits for FOBT detect from 32 to 53% of patients with advanced neoplasia⁵⁷⁰⁻⁵⁷³ and reduce the population screened overall CRC mortality in a 22%⁵⁷⁴. In any case, once a patient presents positive FOBT must undergo a colonoscopy to surgically remove the possible tumor lesion. Unfortunately, FOBT yields those much false negative and positive results that the inefficiency in the process usually overtakes digestive endoscopy departments. Therefore, the development of cheap, feasible and non-invasive biomarkers and stratification tools for this disease is still a pending subject. Among the different approaches to obtain new and complementary to FOBT non-invasive biomarkers, the analysis of EV experienced considerable attention.

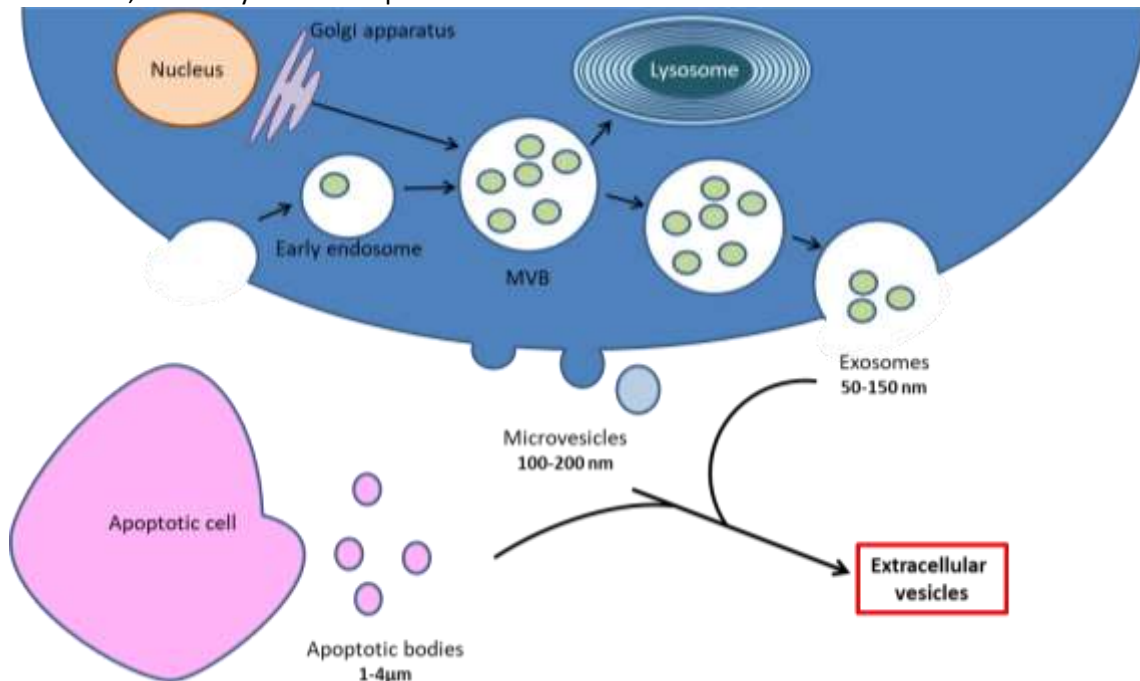


Figure 1-21: Scheme of different known vesicles generated by cells. The endosomal system is the combination

of primary endocytic vesicles, early endosomes, late endosomes, and lysosomes⁵⁷⁵. During their maturation, endosomes accumulate vesicles, while the early endosomes contain almost no internal vesicles; the bigger late endosomes (also known as multivesicular bodies or MBV) can contain hundreds of them^{576,577}. These MVBs sort their content to different and specific destinations^{578,579}. One of the first acknowledged functions of MVBs was the targeting of membrane proteins and lipids to their degradation in lysosomes⁵⁸⁰⁻⁵⁸², although also have been described their function as temporal storage compartments⁵⁸³. The third possible fate of the MVB is the secretion of cellular components to the cell exterior. To accomplish this last possibility, MVBs fuse with the membrane and release their vesicles, known as exosomes. Adapted from Fujita et. al.⁵⁸⁴.

Cells shed different types of vesicles that can be classified according to their origin: blebbing of the plasma membrane (membrane vesicles and apoptotic bodies) or secreted from internal membranes through the endosomal system (exosomes)⁵⁸⁵. The vesicles can be grouped into the term EV (Figure 1-21)⁵⁸⁶. EVs were first studied during the early '80s when it was described that maturing erythrocytes secrete multiple small molecules from fused MVBs⁵⁸⁷⁻⁵⁸⁹. EVs comprise the three main vesicles present in blood: apoptotic bodies, microvesicles, and exosomes. At first, EVs were described as cellular tools to discard cell debris⁵⁸⁸⁻⁵⁹¹. However, later works described cell receptors interaction with EVs lipid and proteins⁵⁹²⁻⁵⁹⁶, which propose them as intercellular messengers. Thus, was revealed their importance in intracellular mechanisms^{597,598} suggesting their possible therapeutic application as anticancer tools⁵⁹⁹. However, the main focus was on the search of fluid biomarkers after the discovery of mRNA and miRNA inside EVs and the possible use of this genetic material by the recipient cells⁶⁰⁰. Using differential centrifugations and filtering processes it is possible to obtain enriched fractions of each one⁶⁰¹. The comprehensive characterization of EVs revealed that their content is highly regulated and comes mainly from the plasma membrane, the endocytic pathway and the cytosol of the parental cell⁶⁰²⁻⁶⁰⁸.

This focus in the field yield to the description of increased circulating EVs in ovarian and pancreatic cancer^{609,610} and their decrease in urine for prostate cancer patients compared with the healthy controls⁶¹¹. Some studies went even further by describing the EVs composition sensitive enough to identify different tumors^{609,611,612} and as treatment monitoring tool^{613,614}. In terms of lipid composition, several studies have described the lipidome of EVs obtained from a diversity of biological sources^{605-607,615-619}. Further, lipid-related enzymatic activities have been described in these vesicles, revealing a complex intercellular lipid metabolism with EVs as central players⁶¹⁹. Surprisingly, only a few explored how EVs lipid molecular species could be used as biomarkers^{565,620-623}.

HYPOTHESIS AND AIM OF THE STUDY

2 Hypothesis and aim of the study

There are multiple pieces of evidence that the lipid composition is highly sensitive to any change in cell status, therefore, we hypothesize that the lipidome can be a good CRC biomarker and the lipid metabolism a promising and unexplored pharmacological target.

The main aim of this thesis was to investigate the role of membrane lipids in colon physiology while identifying lipid biomarkers of CRC. Hence, the objectives of this thesis were:

1. To characterize the lipidome of the colon in cell models and patients and explore how can be used as invasive and/or non-invasive biomarker of CRC.
2. In base of the lipid characterization of the colon and the CRC, exploring the role of specific lipids and lipid-related enzymes in the process of differentiation within colon mucosa.

The results of this study will be divided into two main chapters:

- In the first chapter we characterized the lipidome of commercial cancer cell lines and their derived EV with the objective of detect lipid tumor changes. Also, we used the MALDI-IMS technique to reveal the lipidome of the different components of colon tissue and how they are deregulated in adenomatous polyps. To assess the clinical relevance of these results, we also analyzed EV from CRC patient-derived plasma. This part reveals that exist multiple changes in colon tumor processes reflected in lipid composition that can be potentially used as clinical biomarkers.
- In the second chapter of the thesis, we examined how the changes in colon tissue are regulated. To do this, we analyzed thoughtfully the MALDI-IMS results, revealing strict and subtle lipid and lipid-related enzymes changes parallel to colon differentiation processes. Those changes were mainly related to AA-containing phospholipids and their related enzymes. The final part of this work explores the role of PGs in colonocytes physiology, exposing a complex role of these molecules on cell fate.

RESULTS

3 Results: Chapter 1: Exploring the cell membrane lipidome as colorectal cancer biomarker

3.1.1 Lipid biomarkers for cellular malignization in cell culture model

Taking into account the lipidome sensitivity to cellular changes, this study explored whether the lipid fingerprint could be used to assess the metastatic capacity of colon cancer cells. Metastasis is a complex cellular process that requires changes in cell adhesion and morphology, as cells must detach from and neighboring environment, processes profoundly associated with lipid composition and metabolism⁶²⁴⁻⁶³¹. As a first approach, we analyzed by HPLC-MS the lipid profile of four human CRC cell lines and one human colon primary cell line. We choose cancer-derived cell lines isolated at different stages to have a better knowledge about different grades of invasive cancer (Table 3-1). Thus, HT29, SW480, and LS174t cell lines were isolated from primary tumors, while Colo 201 cell line was isolated from a CRC metastatic site. Finally, healthy primary colonocyte cells were isolated from healthy donors.

Table 3-1: Table describing relevant pathological characteristics of the CRC cell lines used. The second and third columns of the table refer to the cancer types where these cells were isolated.

Cell line name	CRC grade ⁶³²	Tumor characteristics
HT29	Duke's type B colorectal adenocarcinoma	The tumor grew through the muscle layer of the bowel.
SW480	Duke's type B colorectal adenocarcinoma	
LS174t	Duke's type B colorectal adenocarcinoma	
Colo 201	Duke's type D colorectal adenocarcinoma	The tumor was isolated from other body parts after metastasis

In addition to the origin, these cell lines differ in their behavior in culture. Primary, HT29, SW480, and LS174t cells are adherent, while around half Colo 201 population grow in suspension, in addition, Colo 201 divide at a much higher rate than the other cell lines. We know that cell division and confluence rates influence lipid composition and metabolism⁵⁻¹¹. Therefore, to be able to evaluate the cell lipid differences at equivalent conditions we seeded the Colo 201 at a lower concentration to obtain a similar number of cells and confluence at 48h. Cells were cultured with exosome free media, adherent cells were seeded at 1,200 cells/cm² and Colo 201 at 800 cells/cm². More details are provided at the Experimental procedures section.

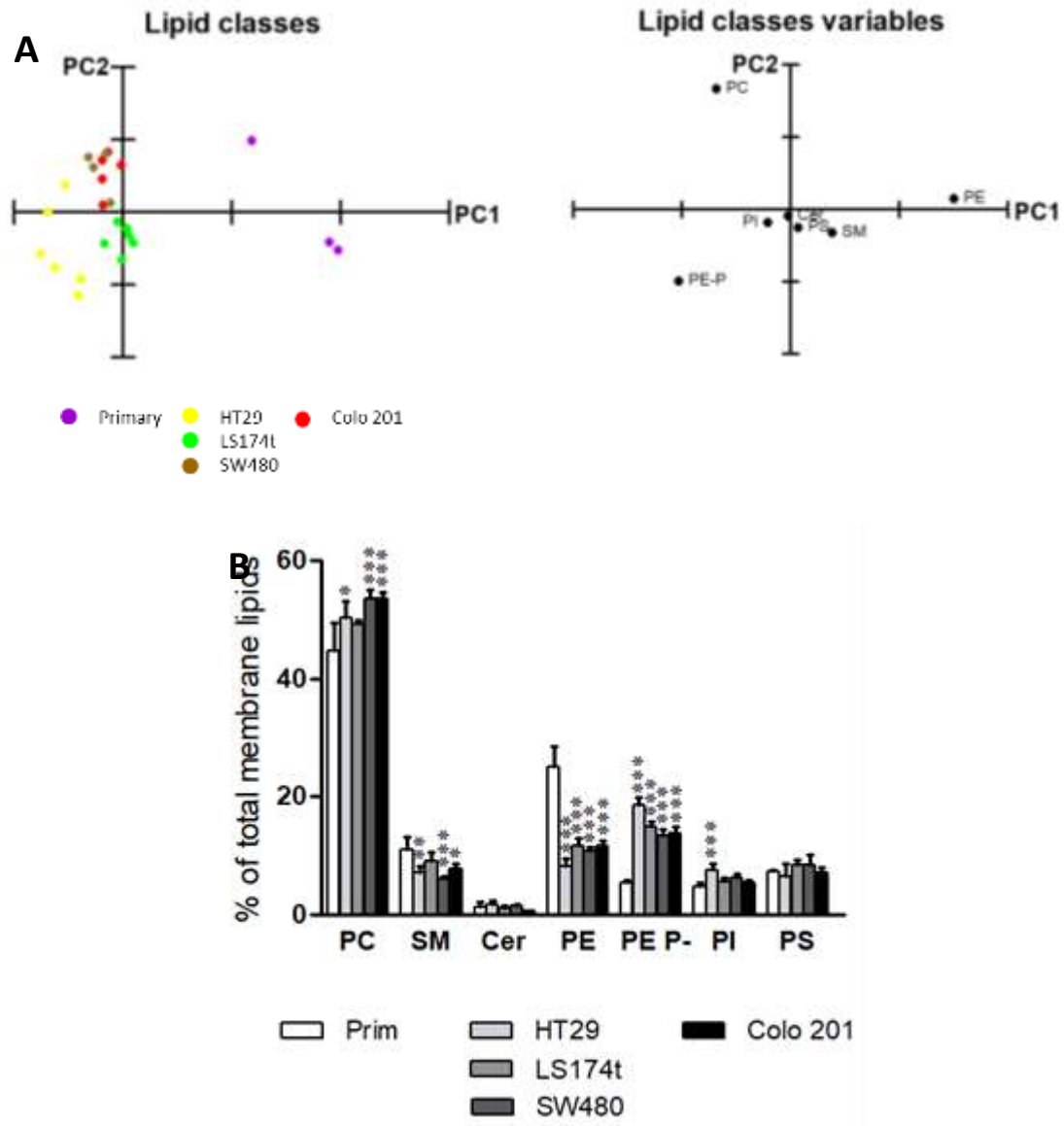


Figure 3-1: Analysis of major membrane lipid classes of the cells analyzed. A) PCA of major membrane lipid classes in the cells analyzed. Explained Variance= 83,42%. PC, phosphatidylcholine; SM, sphingomyelin; Cer, ceramide; PE, phosphatidylethanolamine; PE P-, ethanolamine plasmalogens; PI, phosphatidylinositol; PS, phosphatidylserine. Primary, HT29, LS174t, SW480 and Colo 201 cell lines. **B)** Variance analysis of major membrane lipid classes. Values are expressed as % of total lipids (mean \pm SD), n=3-6. Statistical significance was assessed using one-way ANOVA followed by Bonferroni post-test. Only statistical differences between primary and cancer cells are represented. Comprehensive results were presented in Supplemental table 1. The asterisk (*) indicates a significant difference between a cancer and the primary cell line. * P<0.05; ** P<0.01; *** P<0.001.

Lipidomic analysis provided vast information about the cell lines, which was first represented using Principal Component Analysis (PCA), which helps to visualize the relative proportions between the variables studied. We have included a thorough PCA explanation in the Experimental procedures section. PCA of the lipid classes was able to clearly separate primary from cancer cells basically because of the changes in the relative levels of PE, and to a lesser degree, because of PE plasmalogens and PC levels (Figure 3-1, A). Consistently, the ANOVA showed profound alterations in the lipid class composition between cell lines (Figure 3-1, B and Supplemental table 1). The most abundant lipids in all cells were PC (44.8-53.6%) and PE (11.5-25.1%). Diacyl and vinyl ether ethanolamine species showed the most consistent

differences between primary and all cancer cells. In primary cells, PE and PE-P levels were 25.1% and 5.4% respectively, while in tumor cells, PE and PE-P mean levels were 10.6% and 15.2% respectively. Finally, all cancer cell lines increased PC (44.9% vs. 51.7% primary vs. mean tumor cell value) and decreased SM (11.1% vs. 7.5%) in three of the four tumor cells (all but LS174t). The decrease in tumor SM levels was consistent with previous works⁶³³.

In order to delve into these differences, we performed a PCA using all molecular species detected (Figure 3-2). The results confirmed the capacity of the whole lipidome to separate cells in three groups according to their malignancy, that is, primary cells (Prim) from *in situ* (HT29, SW480, and LS174t) and from highly metastatic cancer cells (Colo 201). Primary cells were mostly separated from the other cells because of the higher amounts in PI 38:3, SM d18:1/24:1 and Cer d18:1/24:1, and lower amounts of PE plasmalogens 16:0/22:6 and SM d18:1/16:0. Colo 201 were separated from the *in situ* cells thanks to the higher content in PS and PE 36:1, SM d18:1/16:0 and Cer 18:1/24:0 and lower content in Cer 18:1/16:0 and 18:1/24:1 and PE plasmalogens 16:0/20:4.

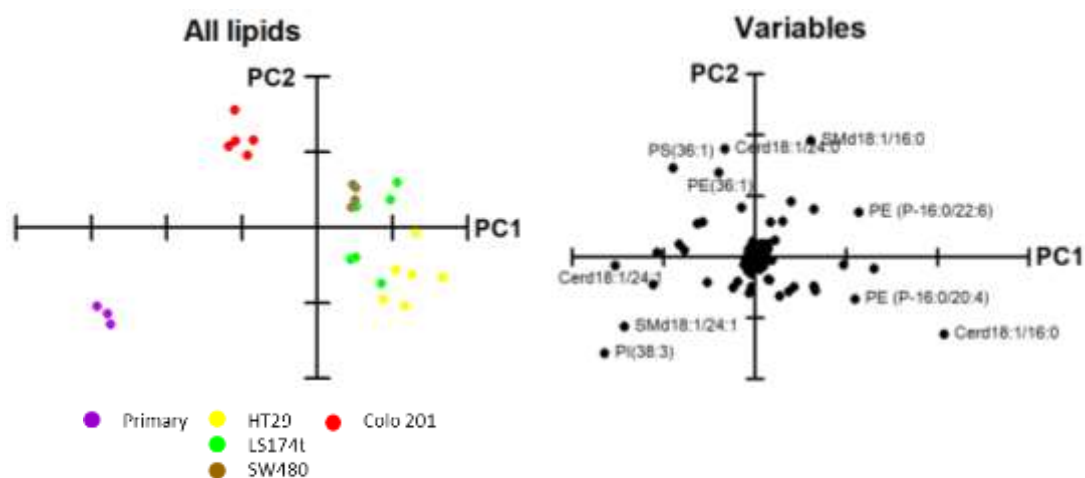


Figure 3-2: PCA analysis of the contribution of each lipid species analyzed in % of the total lipid class. Explained variability 54.55%. Only the most influential species are indicated at each variables PCA analysis. ● Primary, ● HT29, ● LS174t, ● SW480 and ● Colo 201 cell lines.

Despite separating clearly the different cell types, PCA using all lipid species barely explained 50% of samples variance. The low explained variability could indicate that there are minor molecular species different enough to discriminate between cell lines. To identify these minor lipids, each lipid class was analyzed separately by PCA and variance analysis. All lipid classes were able to separate, to a greater or lesser extent, primary cells from the cancer cells (Figure 3-3 and Supplemental figure 1). However, only PC, PE plasmalogens and PS molecular species were able to clearly separate Colo 201 from the rest of the cell lines. The variance analysis of the molecular species of each lipid class confirmed that cell malignization impacted profoundly on lipid composition.

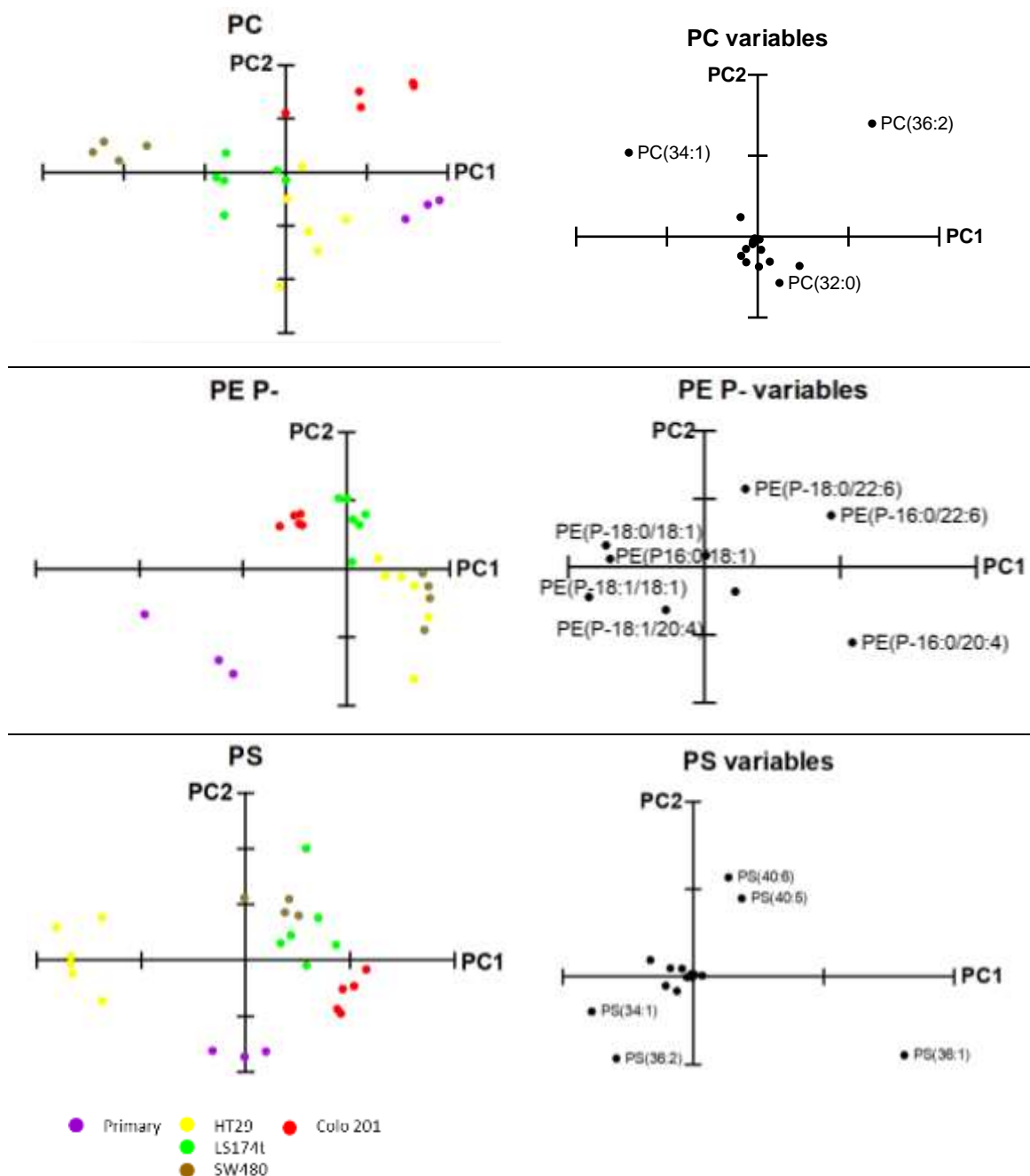


Figure 3-3: PCA of each lipid class separates the primary from the cancer cells. The analysis was made with the contribution in percentage of each molecule to the total amount of the lipid class. Explained variances: PC 82.4%, PE plasmalogens 65.9%, PS 87.5%. Only the most influential variables are indicated at each PCA variables graph. ● Primary, ● HT29, ● LS174t, ● SW480 and ● Colo 201 cell lines.

Consistent with data in human colon epithelium²¹⁷ (expressed in section 3.1.2. of this work), the most abundant PC species in all cell lines was 34:1 (34.6-50.9%) (lowest and highest value throughout the five cell lines analyzed respectively), followed by 36:2 (13.9-27.3%), 34:2 (6.8-13.1%) and 36:1 (7.4-9.2%). Within this lipid class, we detected an increase in 34:1 (34.6% vs. 43.97%, primary vs. the average value in cancer cells), a decrease in 36:3 (5.4% vs. 3.3%) and 36:2 (21.8% vs. 11.9%, except for Colo 201 that was an increase of 27.3%) (Figure 3-4 and Supplemental table 2).

In PE, 36:2 (17.9-34.4%) was the most abundant species, followed by 36:1 (9.9-25.5%), 34:1 (13.0-15.9%), and 38:4 (4.7-14.3%). The increase in 40:7 and 40:6 (0.3% and 0.5% in

primary vs 2.9% and 4.7% in tumor cells respectively) and the decrease in 38:3 were the most consistent changes through all cell lines (Figure 3-4 and Supplemental table 2). *In situ* cancer cells were equally affected in 36:2, 38:3 and 38:4 composition, decreasing 36:2 (34.4% vs. 19.1% primary vs. mean value of the *in situ* cancer cells) and 38:3 (10.6% vs. 15.3%) and increasing 38:4 (8.9% vs. 13.1%). Considering that one of the possible assignments for 36:2 could be 18:0/18:2, for 38:3 18:0/20:3 and for 38:4 18:0/20:4; these changes would be consistent with the metabolic relationship of the fatty acids esterified at the sn-2 position. On the contrary, in Colo 201, 38:4 levels were below all the other cells (4.7%), 36:2 levels were similar to the primary cells (32.1%), while 38:3 decreased to similar levels as the *in situ* cancer cells (3.0%). Finally, 36:1 was increased in Colo 201 cells (1.8-fold respect the primary cells). In PE plasmalogens, the most abundant species was 16:0/20:4 (12.9-33.8%), followed by 18:0/20:4 (13.3-21.7%), 16:0/22:6 (0.7-26.9%) and 18:0/18:1 (5.1-18.1%)(Figure 3-4 and Supplemental Table 2). Its most robust result was the decrease in the oleic acid-containing species, either at sn-1 or sn-2 position(16:0/18:1, 18:1/18:1, 18:0/18:1, 18:1/20:4), which was coincident with changes reported in colon tissue²¹⁸ (expressed in section 3.1.2. of this work). In addition, all cancer cells showed a significant increase in most DHA-containing species (16:0/22:6 and 18:0/22:6) which is consistent with previous reports⁶³⁴.

In PS, 36:1 (37.8-60.5%), 36:2 (7.8-16.4%) and 34:1 (6.9-16.7%) were the most abundant molecular species (Figure 3-4 and Supplemental Table 2). The largest and most consistent changes were the robust increase in 40:5 and 40:6 in all cancer cells compared to primary cells. The most abundant PI molecular species were 38:3 (13.2-47.9%), 38:4 (15.9-30.7%) and 36:1 (1.5-23.6%). PI most pronounced changes affected to MUFA species (34:1 and 36:1). While the primary cells have around 1.0% of both MUFA species, the average values in cancer cells were 11.3% (5.1-15.6%) and 16.7% (9.6-23.6%) for 34:1 and 36:1 respectively(Figure 3-4 and Supplemental Table 1). Interestingly, Colo 201 cells differ in their content in 34:1, 36:2 and 36:1 compared to the rest of cancer cells.

Finally, in terms of sphingolipids, the most abundant species were d18:1/24:1 (9.5-36.5% in SM, 10.9-26.7% in Cer) and d18:1/16:0 (36.7-58.2% in SM and 30.3-56.2% in Cer) (Figure 3-4 and Supplemental Table 2). Interestingly, the most profound changes between cancer and primary cells occurred in these species and both sphingolipids analyzed, with the addition of significant increases of d16:1/18:1 in all cancer cells compared with the primary cells. Thus, d18:1/16:0 increased (1.5-fold in SM and 1.2-fold in Cer) while d18:1/24:1 decreased (25.2% in SM and 8.3% in Cer) in cancer cells compared to primary cells although not significantly in all cancer cells.

3. Results: Chapter 1: Exploring the cell membrane lipidome as colorectal cancer biomarker

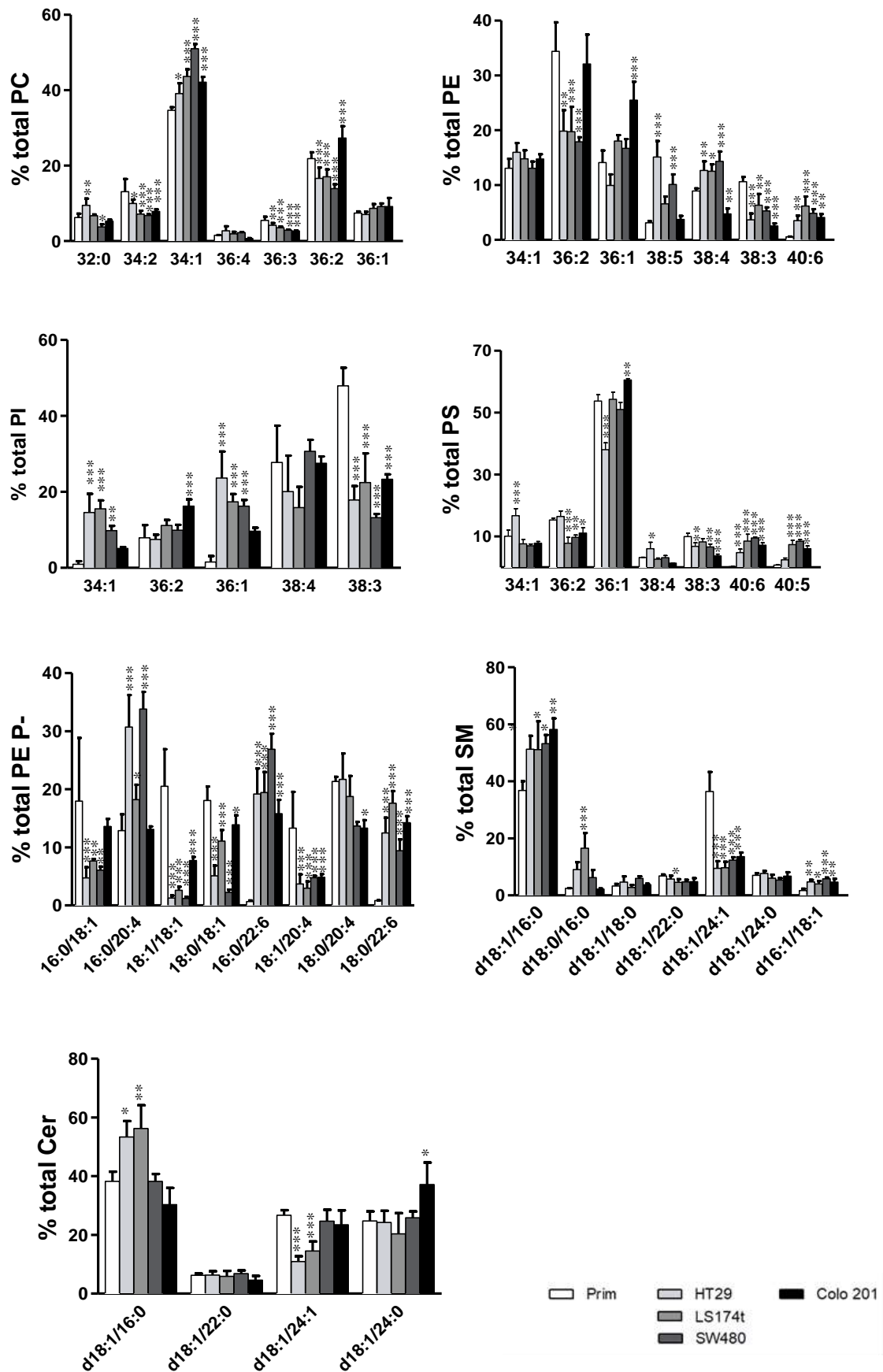


Figure 3-4: Lipid fingerprint in primary, *in situ* and metastatic cancer cells. Bar diagrams comparing the changes in

PC, PE, PS, PI, SM, and Cer lipid composition in primary, HT29, LS174t, SW480, and Colo 201 cells. Values are expressed as a percentage of total fatty acid (mole %) and represent mean \pm SD, n=3-6. Statistical significance was assessed using one way ANOVA followed by Bonferroni post-test. Only significance respect primary cells are expressed. Comprehensive results are presented in Supplemental tables. For clarity, only species account for <5% of total lipid class were included in the graph. * P<0.05; ** P<0.01; *** P<0.001.

Next, we analyzed how specific species, expressed as number of C-atoms:number of double bonds were distributed within phospholipid classes (PC, PE, PE plasmalogens, PS, and PI). This analysis would indicate in which phospholipid class the cells store a particular combination of fatty acids.

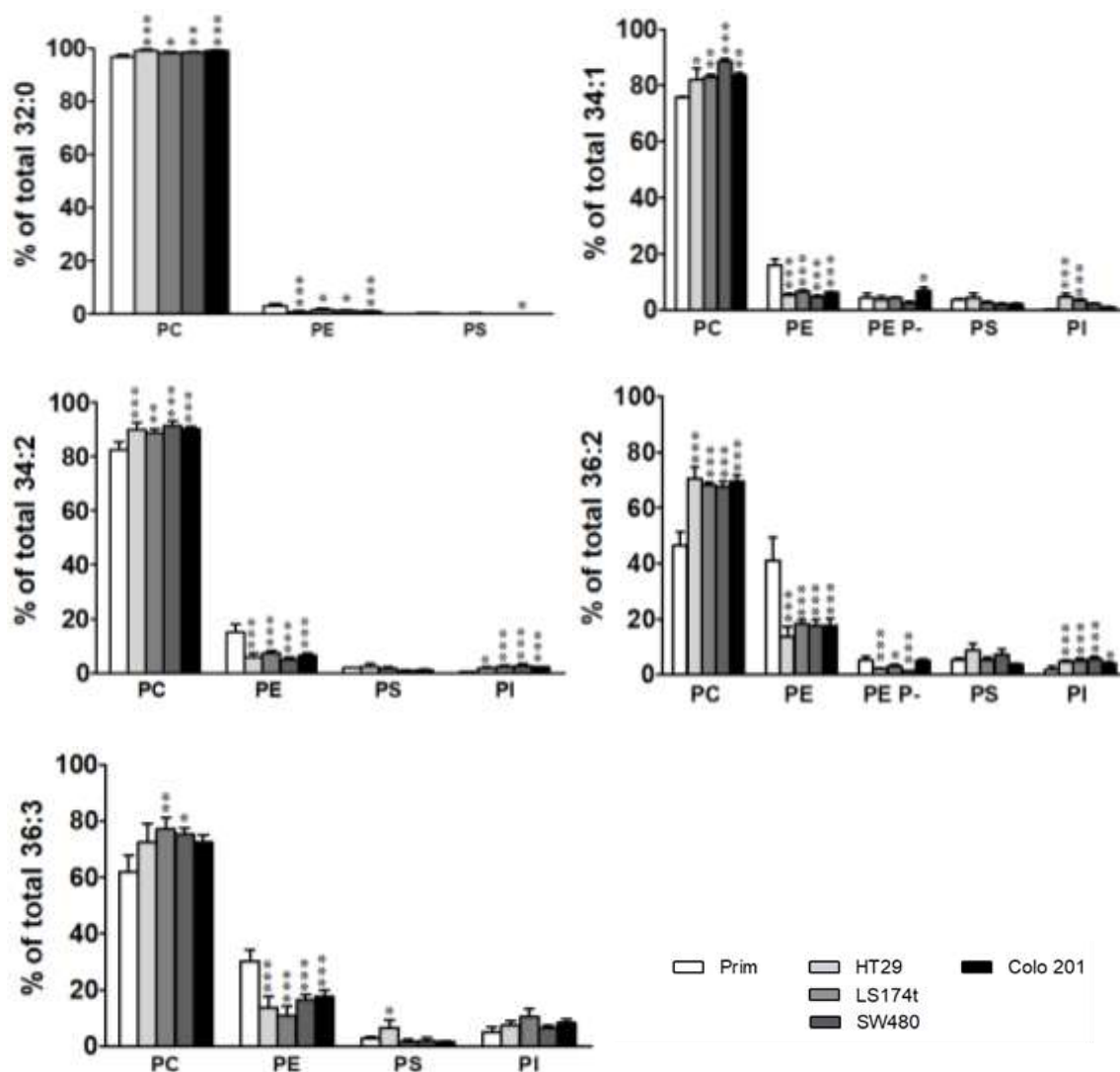


Figure 3-5: Lipid distribution of species accumulated in PC. The total percentage of each fatty acid combination detected was calculated. The contribution of each lipid class to the total amount of fatty acid combination was calculated to evaluate how much is accumulated in each lipid class compared to the others. Values are expressed as a percentage of total fatty acid (mole %) and represent mean \pm SD, n=3-6. Statistical significance was assessed using one way ANOVA followed by Bonferroni post-test. Only significance respect primary cells are expressed. * P<0.05; ** P<0.01; *** P<0.001.

The species showed in Figure 3-5 are mainly accumulated in the PC moiety. Primary cells have relatively similar values of PC and PE species, but cancer cells accumulate these

lipids in PC to the detriment of the rest of species, including PE. The species with the most pronounced changes were 36:2 and 36:3, whose distribution shifted from a PC:PE ratio of 50:40 and 60:30, respectively in primary cells, to 70:10 in cancer cells.

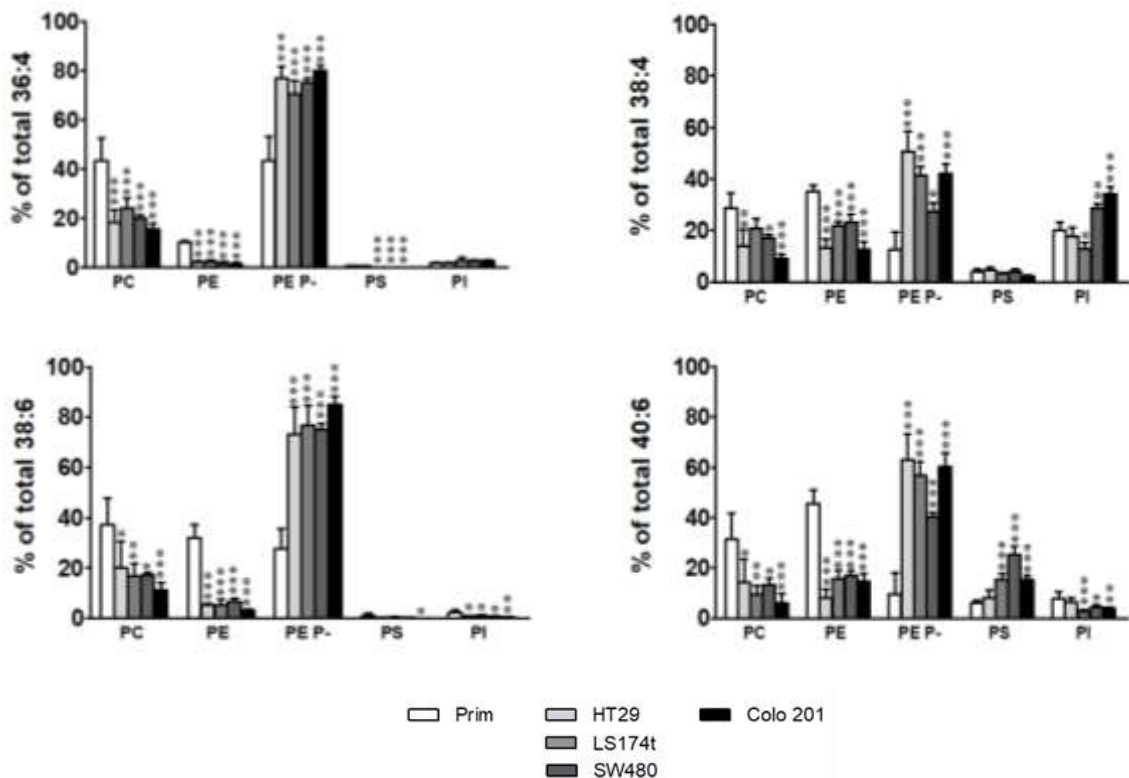


Figure 3-6: Lipid distribution of species shifting from PC and PE to PE plasmalogens in tumor cells compared to the primary cells. The total percentage of each fatty acid combination detected was calculated. The contribution of each lipid class to the total amount of fatty acid combination was calculated to evaluate how much is accumulated in each lipid class compared to the others. Values are expressed as a percentage of total fatty acid (mole %) and represent mean \pm SD, n=3-6. Statistical significance was assessed using one way ANOVA followed by Bonferroni post-test. Only significance respect primary cells are expressed. * P<0.05; ** P<0.01; *** P<0.001.

Figure 3-6 shows species which in primary cells present similar distribution, being the main reservoirs PC, PE and PE plasmalogens. Conversely, tumor cells accumulate these species in PE plasmalogens with a parallel reduction in the other lipid classes hubs, being PC and PE the classes showing a more spectacular decrease. Comparing to the primary cells, tumor cells accumulate 30% more of these molecular species in plasmalogens.

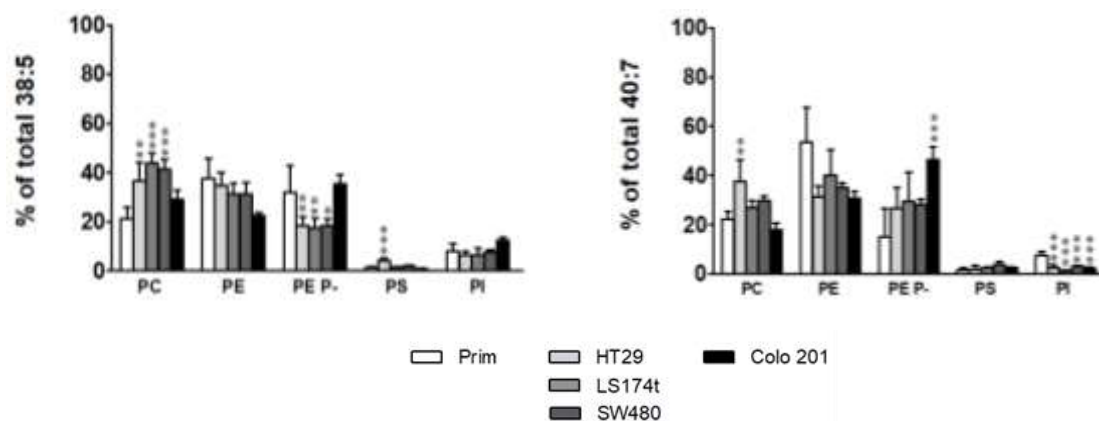


Figure 3-7: Lipid distribution of species shifting to plasmalogens in the *in situ* tumor cells. The total percentage of each fatty acid combination detected was calculated. The contribution of each lipid class to the total amount of fatty acid combination was calculated to evaluate how much is accumulated in each lipid class compared to the others. Values are expressed as a percentage of total fatty acid (mole %) and represent mean \pm SD, n=3-6. Statistical significance was assessed using one way ANOVA followed by Bonferroni post-test. Only significance respect primary cells are expressed. * P<0.05; ** P<0.01; *** P<0.001.

The tumor lipid species showed in Figure 3-7 accumulate AA and DHA species in plasmalogens with saturated fatty acids at the sn-1 position. The probable assignment of 40:7 and 38:5 includes DHA and AA respectively, but with an 18:1 fatty acid at the sn-1 position. Therefore, Figure 3-6 and 3-7 present lipids with an opposite metabolism, as tumor cells did not accumulate more PUFAs in plasmalogens with 18:1 at sn-1 position compared to primary cells.

One last group of lipid species (which include 36:1, 38:3, 40:4 and 40:5) showed a rather miscellaneous behavior and a slight decrease in the species accumulated in PE comparing tumor with primary cells (Supplemental figure 2).

Levels of plasmalogen are coordinated with enzyme changes.

We showed a clear plasmalogen synthesis alteration at the sn-1 level in tumor cells, intending to explain this disturbance we analyzed mRNA expression and protein levels of rate-limiting plasmalogen synthesis enzymes. As the sn-1 plasmalogen position is established in the peroxisome steps of plasmalogen synthesis, we investigated whether tumor cells have disturbed expression of these enzymes. Therefore; fatty acyl-CoA reductase (FAR isoforms 1 and 2), glycerine-phosphate O-acyltransferase (GNPAT) and alkylglycerone-phosphate synthase (AGPS) expression were evaluated (Figure 3-8).

Western Blot analysis showed that FAR1, FAR2, and AGPS protein expression was consistently enhanced in all cancer cell lines compared to primary cells while the only protein behaving consistently at all cell lines were FAR1. The larger impact was observed in AGPS with a 30- to 120-fold increase depending on the cancer cell line. In addition, Colo 201 AGPS expression was a 44- to 90-fold higher than in SW480, LS174t, and HT29 cells. FAR1 and FAR2 were 5- to 12-fold and 1.5- to 2-fold overexpressed in cancer cells compared to primary cells. GNPAT protein expression changes were only detected by SW480 cells overexpression significantly different compared to the other cells (Figure 3-8, A-D).

Next, we evaluated mRNA levels of these enzymes in all cell lines. FAR1 mRNA levels were uniformly overexpressed by 5.6-fold (on average) in all cancer cell lines. AGPS mRNA levels were also overexpressed in all cell lines although values varied considerably among them, being a 4-fold increase in LS174t while the rest of cancer cells present a 1.4-fold change. GNPAT mRNA levels were overexpressed by 3.6-fold in LS174t, while the other cell lines present almost no changes with a change of 0.9-fold in Colo 201, 1.2-fold in HT29 and 0.9-fold

in SW480. Finally, the FAR2 mRNA expression pattern was quite different among cells, being 7.0- and 2.1-fold overexpressed in LS174t and HT29 cells, respectively, but downregulated by 0.3-fold in Colo 201 and SW480 cells (Figure 3-8, E-H).

Altogether these results were consistent with data on plasmalogen levels, indicating that plasmalogen metabolism is profoundly affected at protein and mRNA levels (being the latter highly dependent on the cell line).

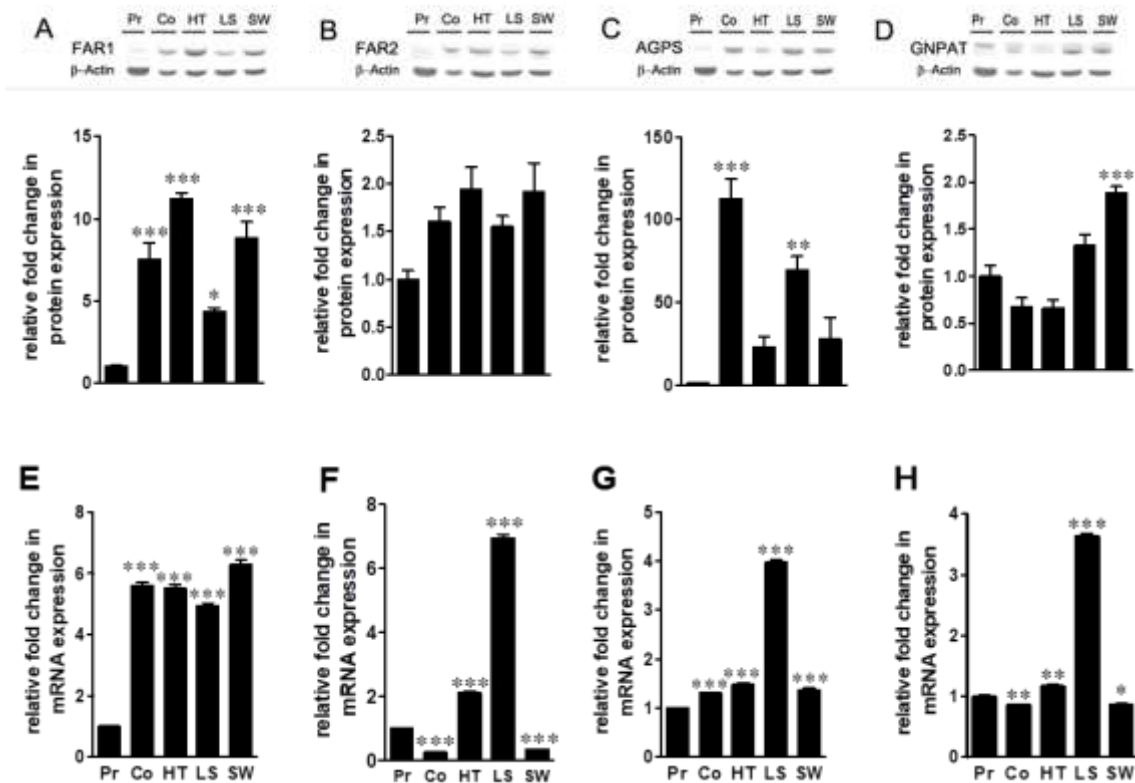


Figure 3-8: A-D) Protein expression of ether lipids synthesis enzymes: FAR1 and FAR2 (fatty acyl-CoA reductases 1 and 2), AGPS (alkyl-glycerone-3-phosphate synthase), and GNPAT (glyceronephosphate O-acyltransferase) in primary (Pr) and cancer colon cell lines (Co, Colo-201; HT, HT29; LS, LS174T; SW, SW480). Values are expressed as a percentage of control and represent the mean \pm SEM, n=3-5; **E-H) Gene expression of ether lipids synthesis enzymes** in primary (Pr) and cancer colon cell lines (Co, Colo-201; HT, HT29; LS, LS174T; SW, SW480). Values are expressed as a percentage of control and represent the mean \pm SEM, n=5. To assess statistical differences one-way ANOVA and Bonferroni post-test was applied. *, cancer vs. primary cell line. * P < 0.05; ** P < 0.01; *** P < 0.001.

Discussion:

Lipidomic data of tumor cells revealed a complex scenario where hundreds of lipids change in a highly orchestrated manner by mechanisms yet to be defined. The lipidome was sensitive enough to not only discriminate between the primary and the tumor cells lipidome but also between cancer cell origin (primary tumor or metastatic site).

Among the multiple changes described, there were two clearly consistent results: the profound shift of PC and PE to PE plasmalogens in tumor cells and the drastic shift of AA- and DHA- containing diacyl species to PE plasmalogens. Besides, the thorough analysis of the cells lipidome is in agreement with previous reports showing lower SM⁶³⁵⁻⁶³⁷ and higher PE plasmalogens content⁶³⁸⁻⁶⁴⁴ in cancer cells, although the causes of these alterations remain unknown. SM changes are in agreement with the works relating SM content to the regulation of cell adhesion^{645,646} and the cleavage furrow formation during cytokinesis⁶⁴⁷, both critical processes in cell division and tumor development. Interestingly, the lipidomic analysis showed

a common change at the molecular species level in both sphingolipids analyzed: SM and Cer. Thus, primary cells were highly enriched in d18:1/24:1 species, while cancer cells in d18:1/16:0. Although these are a rather common sphingolipids species, there is still no clear evidence on their specific role that could certainly depend on the cell type. It is also remarkable the increased amount of SM d18:1/16:0, a molecular species able to distinguish between usual tumor necrosis from infarct-like necrosis in response to treatment⁶⁴⁸. Unlike in phospholipids, fatty acid turnover is not a common way to modify this lipid class molecular species, so the impact must be happening at the species *de novo* synthesis or degradation level.

Regarding plasmalogens, while present in any tissue, they are in higher concentrations in the central nervous system with significant increases during the first years of life⁶⁴⁹⁻⁶⁵¹. In addition, ethanolamine plasmalogens are the main phospholipid in neutrophils⁶⁵²⁻⁶⁵⁶ in skeletal and cardiac muscle⁶⁵⁷⁻⁶⁵⁹ and are the source of PAF in endothelial cells⁶⁶⁰, while in colon account for approximately 10% of total phospholipids⁶⁶¹. Deficiencies in plasmalogen synthesis are associated with cataract formation, mental retardation, craniofacial dysmorphism, rhizomelic shortening of the limbs and lack of muscle tone⁶⁶². Those severe pathological consequences of plasmalogen deficiencies stand out the physiological importance of this lipid class. Also, since the 1960's exist reports indicating enhanced plasmalogen levels in cancer⁶³⁹. Since then, many studies have shown higher levels of plasmalogens in cancer cell lines^{638,640,641}, in xenograft models⁶⁴⁴ or human tumor samples⁶³⁹⁻⁶⁴⁴. In addition, ether lipid content has been positively associated with cell tumor metastatic capacities^{640,643}. The striking PE plasmalogens shift described here, proved to be highly selective for those presenting a saturated fatty acid at the sn-1 position and AA or DHA at the sn-2 position. Importantly, these changes in lipid composition were explained by the overexpression of plasmalogen synthesis enzymes in all cancer cell lines: FAR1, FAR2, and AGPS. Despite the solid evidence of the relevance of these lipids, little is known about the impact on tumorigenesis of the specific ether lipid synthesis enzymes. Although at mRNA levels the effect was less straightforward, we show that all enzymes involved in the rate-limiting steps of ether lipids biosynthesis, except for GNPAT, were overexpressed at the protein level in cancer cells.

The initial reaction in ether lipid synthesis requires the formation of a complex between two AGPS and one GNPAT molecules that will acylate dihydroxyacetone phosphate at the sn-1 position¹²⁶. Recently, AGPS overexpression was associated with cancer cell aggressiveness and invasiveness in primary breast, melanoma, and prostate cell lines⁶⁴⁰. Consistently, we showed that AGPS not only was overexpressed in all cancer cell lines tested but also that there were significant differences between cell lines isolated from the primary tumors or the metastatic sites (Figure 3-8). This result consolidates AGPS expression as a good biomarker for cancer cell metastatic capacity. Conversely, GNPAT mRNA was only overexpressed in LS174t while in the rest of cells was either unaffected or slightly downregulated. A similar observation was reported in a study on murine microglia exposed to inflammatory stimuli⁶⁶³. Therefore, it cannot be ruled out that the tumor inflammatory component could account for the GNPAT mRNA levels observed in this study.

Fatty acyl-CoA reductases catalyze the reduction of a fatty acyl-CoA substrate to the fatty alcohol that will be linked at the sn-1 position of the plasmalogens⁶⁶⁴. Of both FAR enzymes described, FAR1 presents the broadest distribution, while FAR2 is largely restricted to meibomian glands, skin, brain and, importantly for this study, in the small intestine (no data were reported for colon)¹²⁵. Importantly, FAR1 and FAR2 also differ in their activity and substrate preference. FAR1, which seems to be more active, accounts for C16:0, C18:0, and C18:1 fatty alcohols synthesis, while FAR2 prefers C16:0 and C18:0 saturated fatty acids¹²⁵. Furthermore, FAR1 stability (but not FAR2) is post-translationally regulated by a mechanism that senses plasmalogens levels, in which the adequate localization of plasmalogens in the inner leaflet may be fundamental^{665,666}. It is known that apoptosis or exposure to noxious cues

induces translocation to the outer leaflet of both diacyl and ether ethanolamine glycerophospholipids⁶⁶⁶⁻⁶⁶⁹. Therefore, it is possible that in cancer cells, PE plasmalogens translocation could wrongly convey “a low plasmalogen level” signal to the plasmalogen, which could lead to the overexpressed FAR1 levels, as it was observed in this study (Figure 3-8).

In addition, to corroborate the already described increase in PE plasmalogens in cancer, the results also describe a specific shift of certain molecular species (36:4, 38:4, 38:6, 40:6) from PC and PE into PE plasmalogens (Figure 3-6). Thus, while primary cells accumulate these species mainly in PC and PE, cancer cells do it in PE plasmalogens; being 38:4 the species showing smaller changes as also was accumulated in PI. This observation is specific to those species containing a saturated fatty acid at the sn-1 position and AA or DHA at the sn-2 position. FAR1 and FAR2 overexpression could account for the specificity regarding the sn-1 position. It has been proposed that differences between both enzymes expression, activity and substrate preference could be related to cell strategies to differentially channel fatty alcohols either to ether lipid or wax ester synthesis⁶⁷⁰. Conversely, in a context of exacerbated plasmalogen synthesis, FAR2 could also contribute to the total PE plasmalogens pool as has been described early where mRNA levels of this enzyme were overexpressed in intestinal cancer¹²⁵. Despite the differences between cancer cells, when compared to primary cells, these lipid and protein changes were strikingly homogeneous in the four cancer lines, pointing to what could be a common feature of the tumorigenic process.

Figure 3-9 includes recent data linking plasmalogen levels with the adequate recruitment and activation of Akt, a key regulator of cell proliferation^{54,671}. In healthy cells, phosphatidylinositol-3-kinase (PI3K) phosphorylates PIP2 to PIP3, which recruits Akt directly via a PH-pleckstrin domain. Despite the lack of direct pieces of evidence indicating the preference of PI3K enzymatic for AA-containing PIP2, this specificity was shown for PI4K^{54,672}, besides, both PIP2 and PIP3 are enriched in AA⁶⁷³. Altogether, it could be speculated that PI3K, may prefer AA-containing substrates. Thus, other works show that plasmalogens are needed to maintain Akt linked to the membrane^{671,674}, which is crucial for its activation via phosphorylation by PDK1 and PDK2 (among others). Once phosphorylated, Akt shuttles back to the cytosol where phosphorylates a myriad of targets, activating downstream pathways that culminate in cell proliferation. In cancer cells, including CRC cells, PI3K and Akt are overexpressed at protein level⁶⁷⁵⁻⁶⁷⁷. Therefore, the presence of high levels of AA-containing phospholipid^{217,218,634,640} and plasmalogen⁶³⁸⁻⁶⁴⁴ in cancer cells would provide the substrate and the needed environment to sustain the enhanced and uncontrolled cell division.

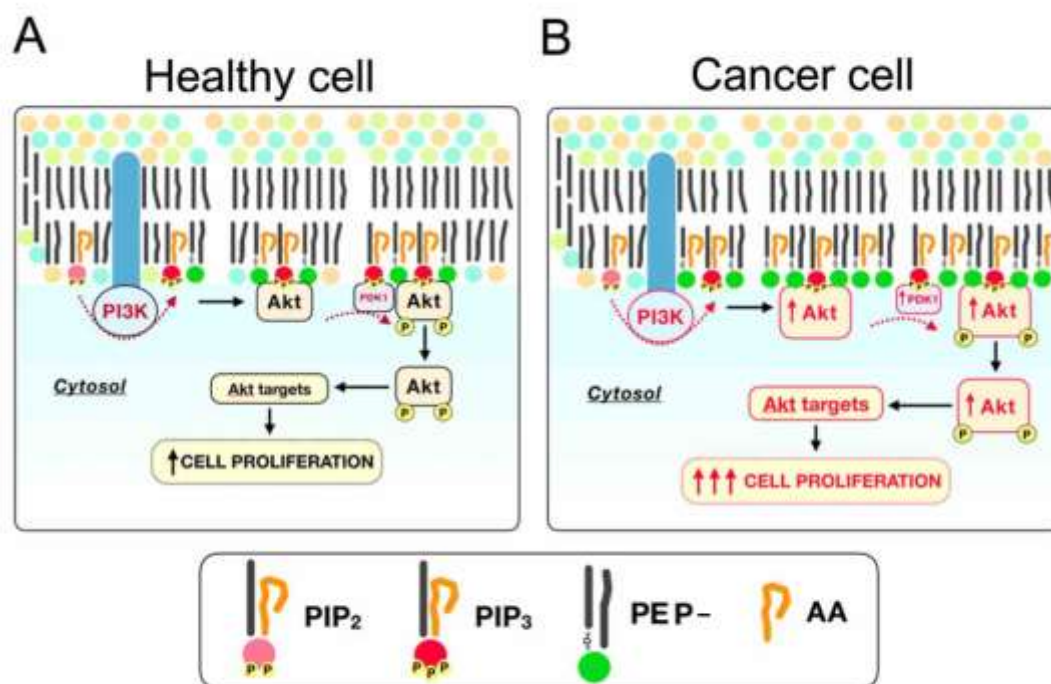


Figure 3-9: A model describing the impact that the most consistent lipid changes observed in cancer cells, the increase in PE plasmalogens and AA-containing phospholipids (in particular PI) on the Akt signaling pathway, a canonical regulating cell differentiation, and proliferation pathway. A) The model in healthy cells. B) Exacerbated Akt signaling stimulated by the increase in PE plasmalogens and AA-containing species in cancer cells.

The cell lipidome is heterogeneous and plastic enough to participate in complex processes like tumorigenesis. While different cell types and pathophysiological conditions present specific changes in lipids, there are broad processes like proliferation, sharing similar lipid characteristics. Our lipidome results show that changes in lipid composition coincide with the optimal scenario in which cancer cells can sustain uncontrolled cell division. This colon cancer cells characterization consolidates lipidome analysis as a powerful tool for establishing accurately the cell pathophysiological state.

3.1.2 Lipid biomarkers for cellular malignization in human tissue

While the knowledge acquired by traditional MS has helped in understanding the relevance of lipids in health and disease, the basic functions of lipids in each cell type is a question still to be answered. Traditional MS requires the homogenization of the tissues to analyze, losing the valuable information about the distribution of their molecular components within the different tissue cells. IMS overcame this limitation by discriminating between tissue different components²¹⁷. There is no doubt that the visualization of the lipids distribution throughout a tissue will help to understand their regulation and physiological functions. MALDI-IMS lipid images of colon slices showed that each tissue present in colon mucosa (epithelium, lamina propria and muscularis of the mucosa) possesses a unique lipidome that reflects precisely the colon anatomy. The analysis of colon tissue slices at 25 μm^2 pixel resolution was able to discriminate between the epithelium, lamina propria and muscularis of the mucosa. However, a higher spatial resolution (10 and 5 μm^2 pixel resolution images) provided further physiological information. Images at 10 μm^2 allowed the visualization of the crypt lumen, but 5 μm^2 ones clearly define the lumen and mirror the colonocytes intracellular

structure. We choose to use $10\ \mu\text{m}^2$ pixel resolution analysis as a compromise between the image size and the biological information obtained (Figure 3-10).

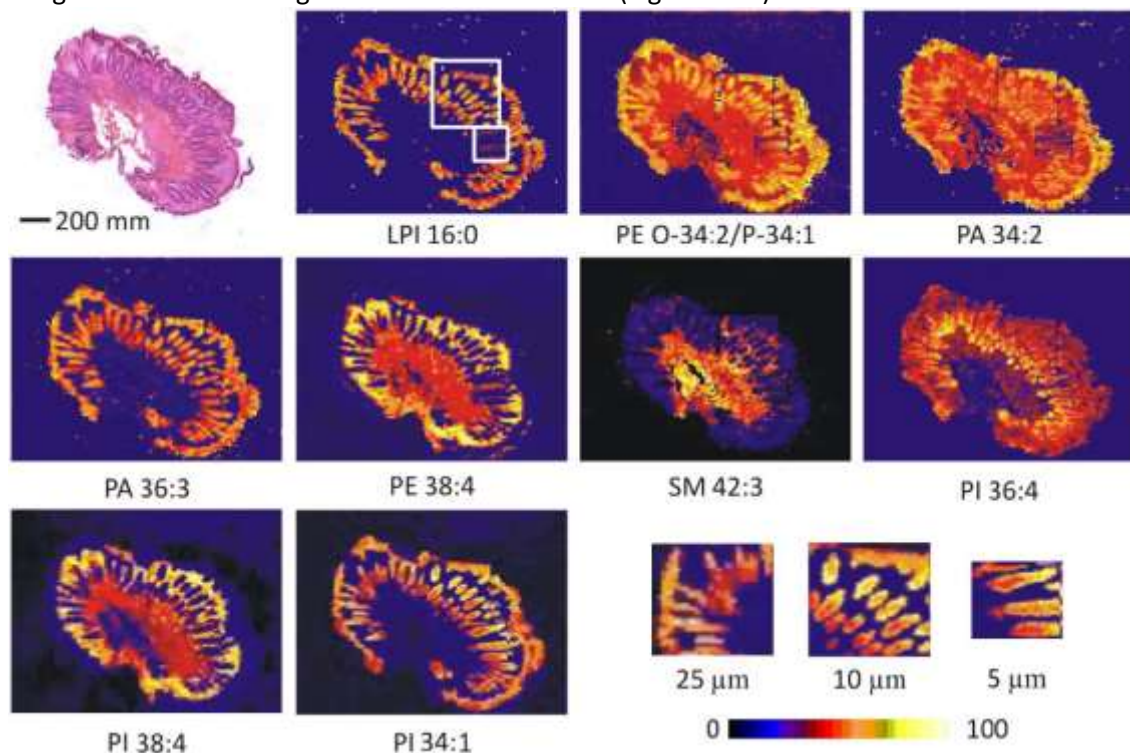


Figure 3-10: Comparison of a colon tissue slice stained with hematoxylin and eosin and representative distributions of lipid species. The large and small squares highlight the areas scanned at 10 and $5\ \mu\text{m}$, respectively. The last three images at the bottom right are a detail of the distribution of PI 34:1 recorded at 25, 10 and $5\ \mu\text{m}$.

The massive amount of information provided by MALDI-IMS images was first analyzed using k-means clustering analysis. The clustering analysis gives general non-guided information of the lipid distribution along with the sample. This approach allows identifying the general behavior of the lipids and more importantly gives the representative composition of each tissue. The k-means analysis group n observations into k clusters where each observation belongs to the cluster with the more similar mean. Applied to lipid IMS, the clusters are made from the pixels with similar lipid composition. This approach in healthy colon tissue determines that the composition of the different tissues of the colon (epithelium and lamina propria) and components like the mucin are different enough to be separated by their lipidome. Also, one additional cluster adjacent to the crypts could be compatible with epithelial nuclei (Figure 3-11).

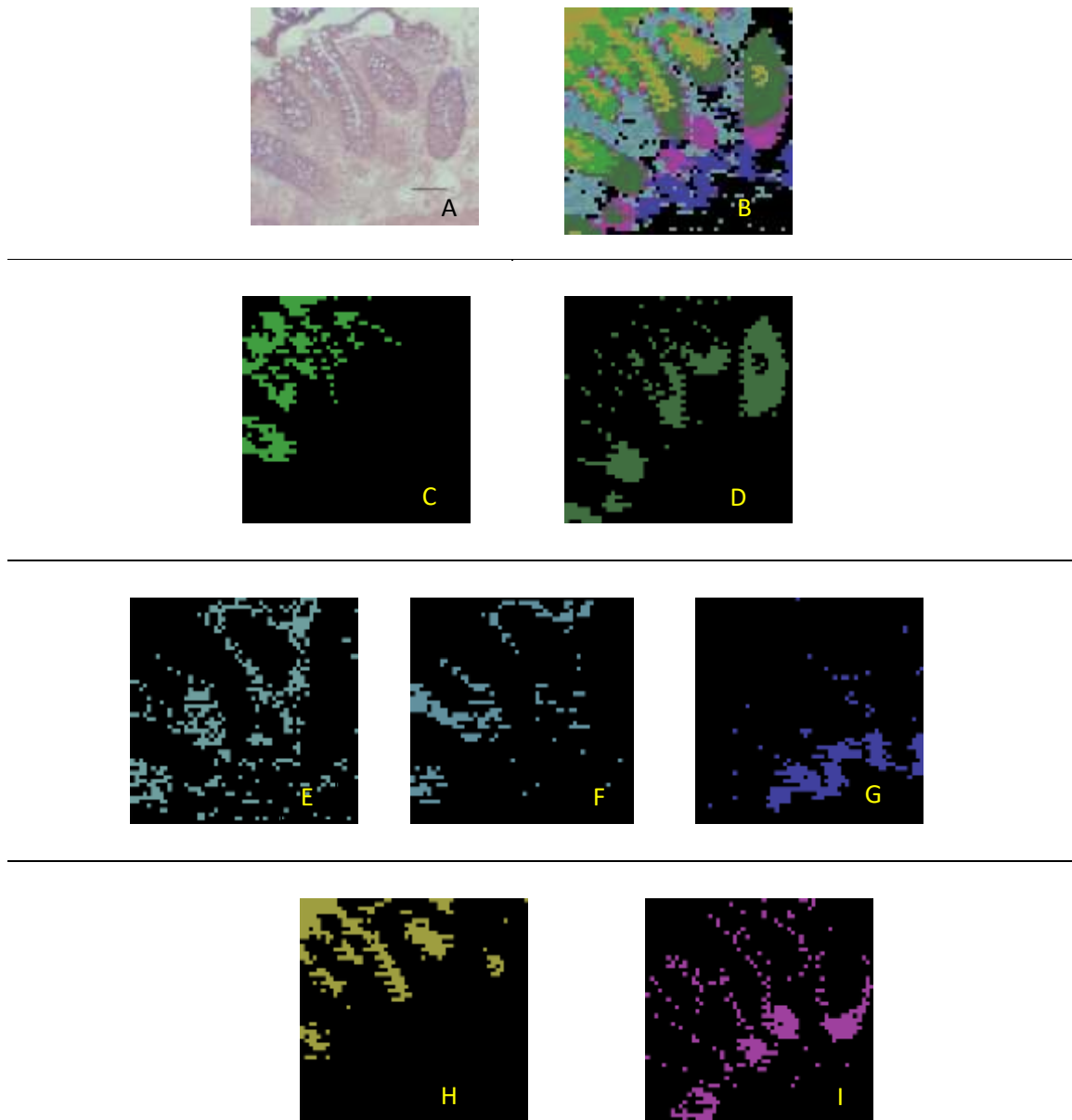


Figure 3-11: Clustering analysis of healthy colon mucosa. This analysis was driven to give 9 clusters and 7 understandable clusters are represented: A) Hematoxylin-Eosin staining of the consecutive slice analyzed by MALDI-IMS. Scale bar= 100 μ m. B) Representation of 7 clusters generated from the k-means analysis. C-D) Clusters corresponding to epithelial cells. C) Epithelial base section of the tissue. D) Epithelial luminal site of the tissue. E-G) Clusters corresponding to lamina propria. E) Apical part of the lamina propria. F) Mid part of the lamina propria. G) Lamina propria surrounding the base of the crypts. H) Cluster corresponding to the tissue mucus. I) Cluster surrounding the epithelial cells that could correspond to the epithelial cells nuclei.

The analysis divides healthy epithelium into two lipid clusters located at the upper (luminal) and lower (basal) parts of the crypt (Figure 3-11, C and D). This distribution is in accordance with the presence of different epithelial cell types with different functions along colon crypts.

To assess the relevance of lipidome as colon cancer biomarker we compared the healthy mucosa clusters to the clusters generated in adenomatous (AD) polyps. The use of AD instead of neoplastic lesions allows still identifying crypts, although with enlargement and divisions, with a clear base and luminal site. MALDI-IMS clustering analysis showed that the

controlled distribution of lipid species was indeed highly disturbed in AD. In fact, unlike healthy epithelium, adenomatous tissue presents only one coherent epithelial cluster, which is consistent with the dedifferentiation process that occurred during the adenoma polyp development (Figure 3-12).

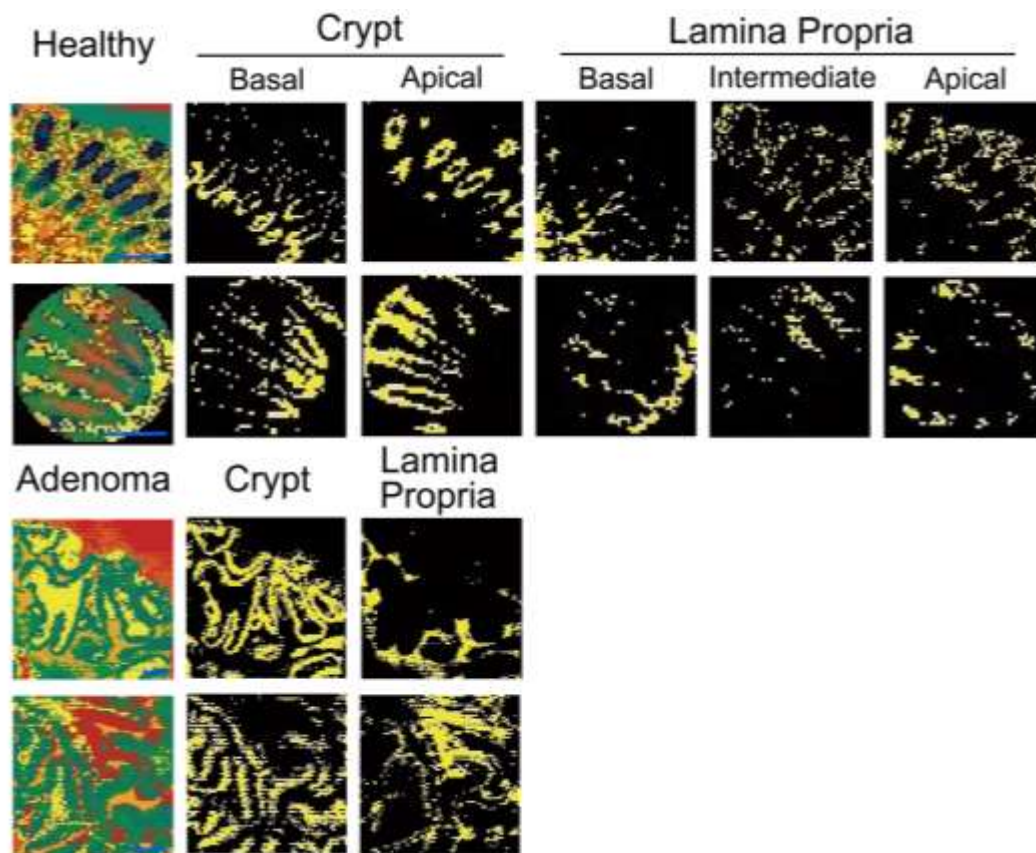
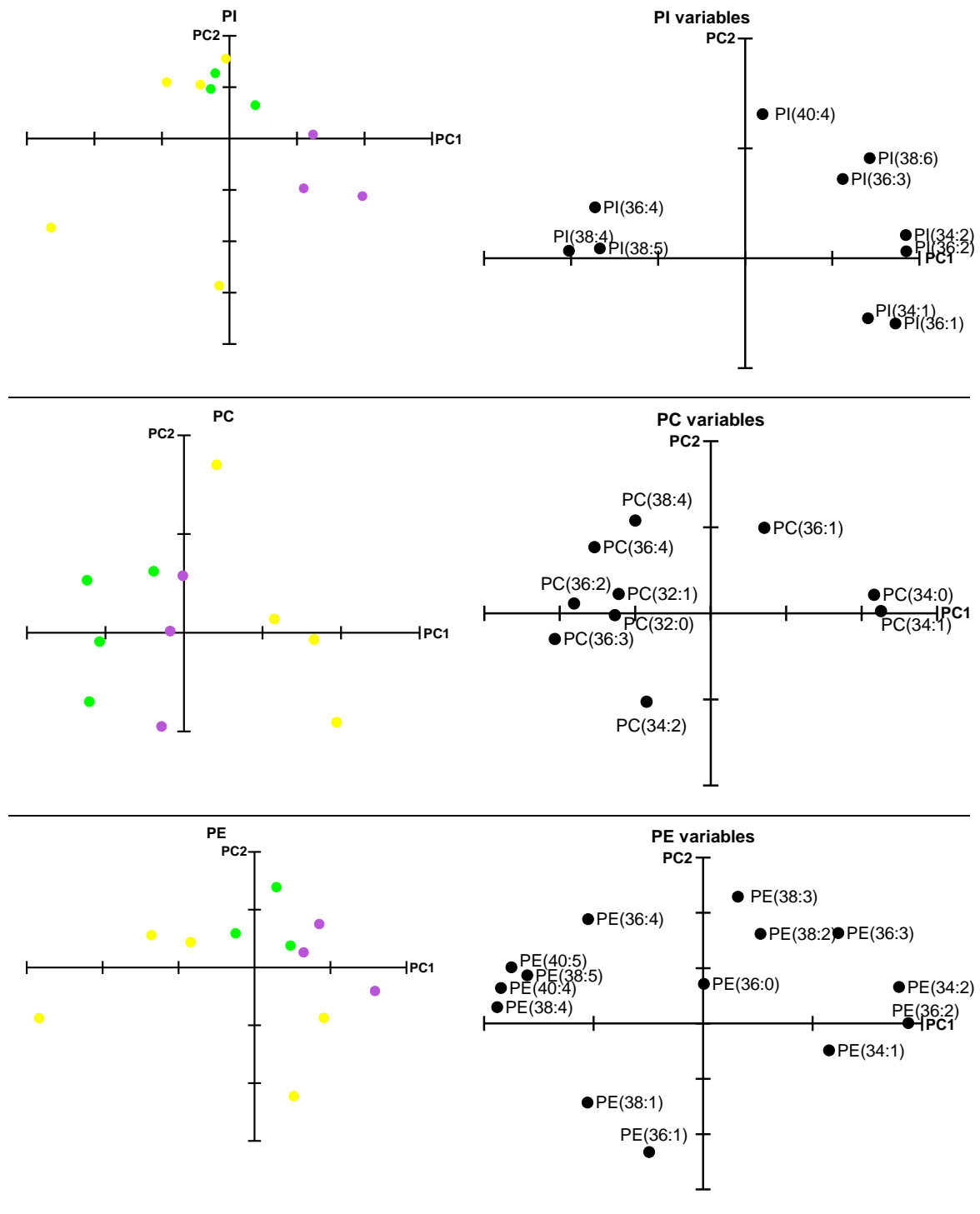


Figure 3-12: Representative examples of cluster formation. In order to compare healthy mucosa and adenomatous polyp samples, MSI results were analyzed by k-means to establish those clusters corresponding to the same cell type. In healthy tissue, the k-means analysis consistently established the apical and basal clusters for the epithelium layer and the basal, intermediate and apical clusters for lamina propria. However, in adenomatous polyps, only one cluster corresponding to the epithelium, as well as one for the lamina propria, were consistently formed. Scale bar = 200 μm .

Epithelium:

To assess statistical differences between samples, the clusters generated corresponding to the equivalent same zone between different samples (for example crypt base) were compared. The statistical comparison of the epithelial clusters (healthy basal, healthy apical and AD epithelial cluster) showed that the AD cluster resembled somehow that of the basal healthy basal cluster (Figure 3-13).



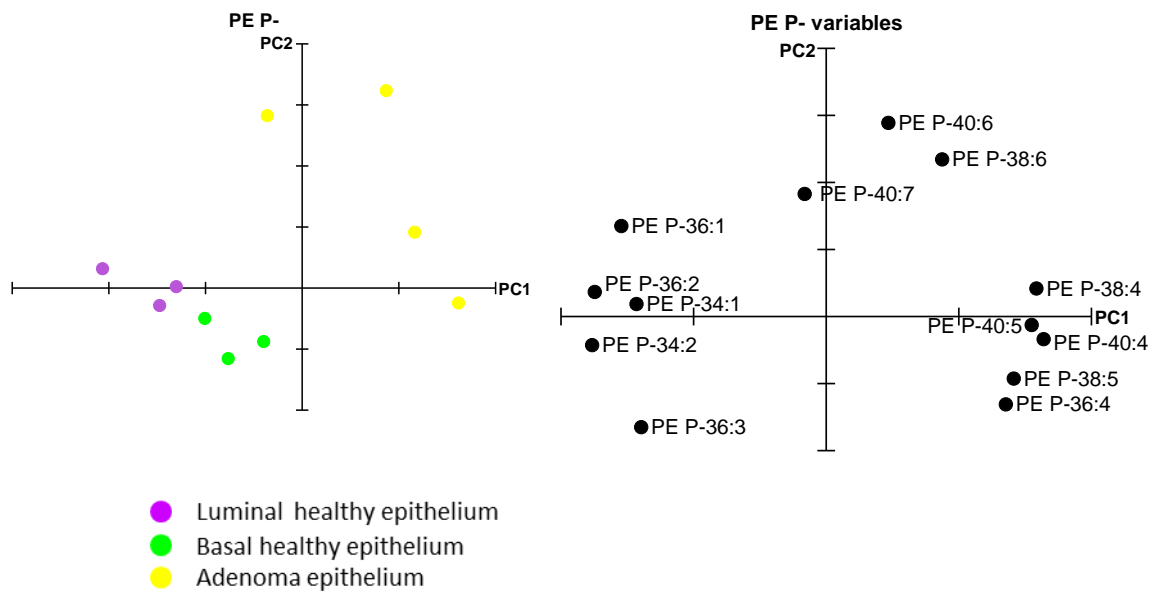
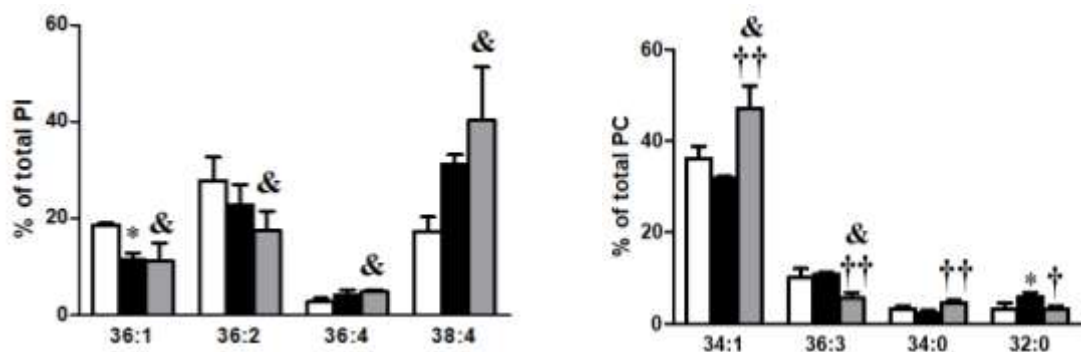


Figure 3-13: PCA of PI, PE, PC and PE plasmalogen species using the clusters of the epithelial layer obtained by k-means. ● Luminal healthy epithelial, ● basal healthy epithelial, ● adenoma epithelial cluster. Here, we represent the scores and loadings plots of PC 1 vs. PC 2. **In PI** the first principal component explains the separation between adenomatous epithelium (yellow) and apical crypt epithelium (purple), being basal crypts (green) located in the middle. This separation can be explained by the grouping of some AA-containing PI species on one side (right) and M/DUFA PI species on the other (left). Explained variance: 60.0% **In PC**, PC1 explains the grouping between adenomatous crypts (blue) on one side and healthy crypts (apical (purple) and basal (green)) on the other. The variation of the percentage of PC 34:1, PC 34:0 and PC 36:1 is responsible for this separation. Explained variance: 40.0%. **PE** species are not as suitable as other species for discrimination between adenomatous groups and healthy mucosa. Explained variance: 45.0% **PE plasmalogens** separates clearly between healthy and adenomatous epithelium due to the relative amounts of PUFA- and MUFA/DUFA-containing species. Having much more PUFA the diseased tissue. On the other hand, the basal epithelia present higher content of AA and DUFA species compared to the luminal epithelium. Explained variance: 54.0% n=3-5. AA: arachidonic acid, DUFA: diunsaturated fatty acids, MUFA: monounsaturated fatty acids, PC: phosphatidylcholine, PE: phosphatidylethanolamine, PI: phosphatidylinositol.



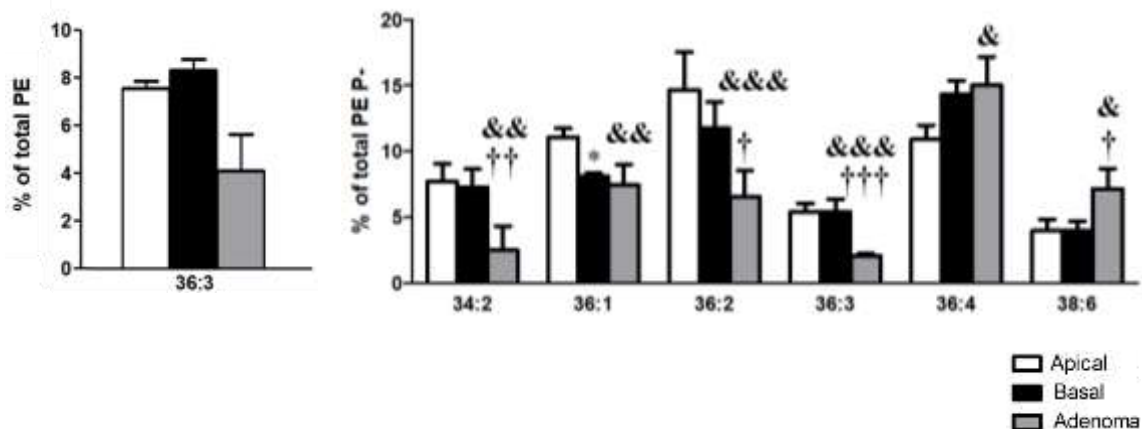


Figure 3-14: Lipid composition is highly regulated along the colon crypt. Bar diagrams showing the comparison of the average lipid composition of healthy apical (white bars) and basal clusters (black bars), and AD cluster (grey bars), previously established by k-means. Values are expressed as mean \pm SD, n=3-5. Statistical significance was assessed using ANOVA followed by Bonferroni post-test analysis. * P < 0.05, ** P < 0.01, apical vs. basal, & P < 0.05, && P < 0.01 apical vs. AD, and † P < 0.05, †† P < 0.001 basal vs. AD. For simplicity, only species showing statistical differences and accounting for more than 3% of total lipid classes appeared, a comprehensive list may be found in Supplemental table 2.

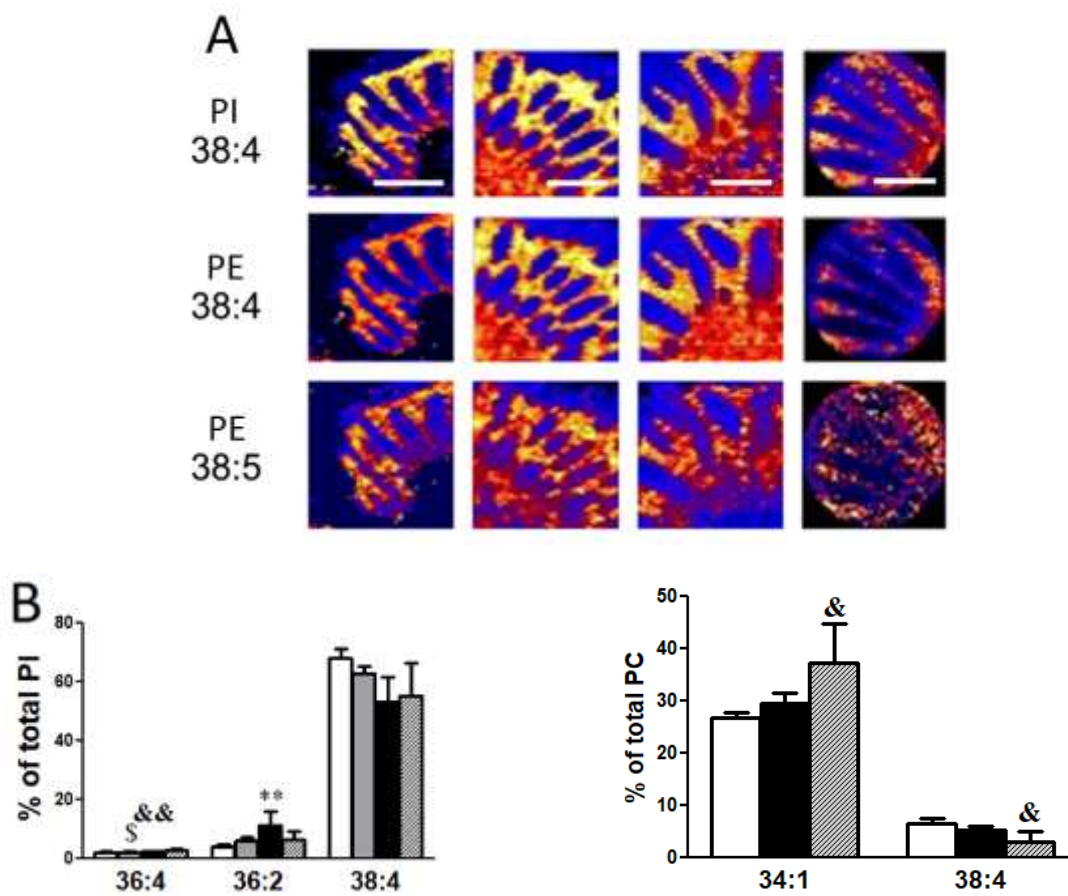
PCA of each phospholipid separated the three types of clusters proving that each one possesses a unique lipid fingerprint. PC, PE, PE plasmalogens, and PI were able to separate between the apical and basal healthy epithelium clusters. The relative amount of AA-containing and MUFA-containing lipids would account for this subtle separation as the basal crypt cells contained more AA-containing species compared to the luminal ones. In addition, the uncontrolled proliferation in adenomatous tissue was reflected in the tissue lipid composition. Contrary to PI, the rest main lipid classes analyzed (PC, PE, and PE plasmalogens) were able to separate the healthy epithelium from the adenomatous one. PE and PE plasmalogens separated the adenomatous epithelium mostly due to its higher amount of AA-containing species (mainly 38:4, 38:5, 40:4 and 40:5). Conversely, PC 34:0 and 34:1 species were more concentrated in AD epithelium being the PC species more relevant for AD and healthy epithelium separation.

Similarities in lipid composition between AD and healthy basal epithelium could be due to the increased proliferative properties over differentiated colonocytes, nevertheless, the pathological status is still reflected in their composition. Interestingly 36:3-containing phospholipids (PI, PE, PE plasmalogens and PC) were the only species decreasing when AD was compared to both apical and basal clusters (although not significantly in PI) (Figure 3-14 and Supplemental table 3). When the apical cluster was compared to AD the decrease in 36:1 and 36:2 parallel to the increase in 36:4 and 38:4 was observed in PI. Also, is remarkable the 15% increase in PC 34:1 and the 3% increase in PE plasmalogens 38:6 in the AD cluster. PE plasmalogen species showed profound differences in lipid composition, which were larger than observed for PI, PE, and PC. Thus, using values of healthy apical segments, the comparison with AD segments showed a robust increase from approximately 50% to 72% in long-chain PUFA-containing species (36:4, 38:4, 38:6, 40:6), and a decrease from 50% to 28% in no-PUFA containing species (34:2, 36:1, 36:2, 36:3).

Lamina propria:

Unlike crypts, the lamina propria is composed of a complex mixture of cells which can be broadly classified into hematopoietic and non-hematopoietic mesenchymal cells. The comprehensive analysis of the lipidome along the lamina propria evidenced an additional level of complexity in understanding the specific function of membrane lipids. Lamina propria and epithelium lipidome stated profound differences between how both tissues handle the same

lipid species. Following a similar approach than the presented for the epithelium, the three clusters established in healthy tissue (basal, intermediate and apical) and the segment found in AD were compared.



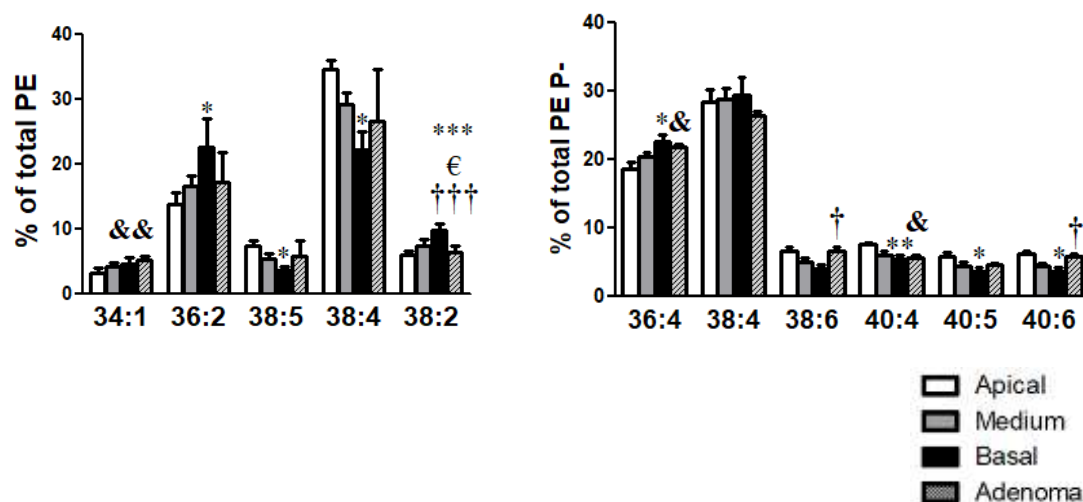


Figure 3-15: A) The lipid analysis by MALDI-IMS surfaced the immunological commitment of the lamina propria. Scale bar = 200 μ m. **B)** Bar diagrams showing the comparison of the average lipid composition of healthy apical (white bars), intermediate (light grey bars) and basal clusters (black bars), and adenomatous cluster (AD) (striped grey bars) for PI, PC, PE, and PE plasmalogen classes. Values are expressed as mean \pm SD, n=3-5. Statistical significance was assessed using ANOVA followed by Bonferroni post-test analysis. * P < 0.05, ** P < 0.01, *** P < 0.001, apical vs. basal; & P < 0.05, && P < 0.01 apical vs. AD; † P < 0.05, †† P < 0.001 basal vs. AD; ‡ P < 0.05 intermediate vs. AD, and € P < 0.05 basal vs. intermediate. For simplicity, except for PI 38:4 species, only species showing statistical differences and accounting for more than 3% of total lipid classes appeared, a comprehensive list may be found in Suppl. Table 3.

First of all, AA-containing species were 5.6-fold more concentrated in the lamina propria compared to the epithelium (Figure 3-15, A), which could be due to the AA proinflammatory capacity and the physiological inflammatory level associated to a healthy colon⁶⁷⁸. On the other hand, the cluster composition analysis showed the inverse pattern seen in the epithelium. Luminal lamina propria compared to the basal site presented a clear tendency to increase in AA-containing species (36:4, 38:4, 38:5, 40:4 and 40:5) and a decrease in 36:2 species (Figure 3-15, B and Supplemental table 4).

While in healthy lamina propria, three clusters in negative mode and two in positive were formed, conversely, adenomatous consistently generated only one cluster. To assess the impact of tumorigenesis over lamina propria lipidome we compared the three healthy clusters to the adenoma. As happens in the epithelium, the adenomatous lamina propria lipidome resembles the basal healthy epithelium. Hence, there is a general decrease in AA-containing species in AD compared to luminal lamina propria. Except for PI 36:4, 38:5 and 40:5, and PE plasmalogen 36:4 which were increased in AD and PE plasmalogen 34:5 that did not change, the rest of AA-containing species decreased in AD compared to healthy luminal lamina propria. This change was compensated by a higher content of MUFA-containing species in AD lamina propria compared to the healthy one (Figure 3-15, B and Supplementary table 3). The opposite changes in tumorigenesis in epithelium and lamina propria states profound differences in how different cell types handle the same lipid species in pathological conditions.

Discussion:

Despite the multiple studies pointing to membrane lipids as central players during cellular processes like cell division, there is still an important information gap about their role and regulation in proliferation and differentiation. The non-guided analysis of lipidome images generated by MALDI-IMS presented here aimed to address this question and showed three consistent conclusions. First, that the lipid composition is specific of each tissue conforming the colon. Second, the lipid composition is sensitive to the cell physiological state, as it can be inferred from the fact that epithelium and lamina propria possess differentiated lipid composition when comparing their basal and luminal sections. Finally, the regulation of the

epithelial and stromal cells lipidome is significantly disturbed in the pathological context of adenomatous polyps.

In the colon, the differential distribution of many lipids defined clearly the histological features of the tissue distinguishing between the epithelial layer, the lamina propria and the muscularis of the mucosa²⁴⁸. The examples shown in the Figure 3-16, where two similar lipids presented an opposite distribution, clearly illustrates how specific lipid composition is for each colon tissue. While PI 38:4 was in higher amounts in lamina propria, PI 36:2 was more present in epithelial cells.

The implications of such divergent lipid composition between different parts of the same tissue evidence the probable inexact results when whole tissue homogenates are analyzed. This phenomenon highlights the limitations of traditional MS setups and the necessity of using MS-imaging to ascertain the real impact of lipids in whole tissue physiology.

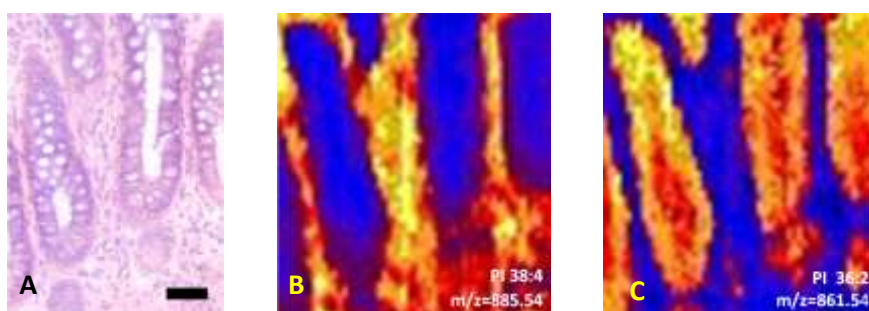


Figure 3-16: A) Healthy colonic mucosa Hematoxylin-Eosin stained. Scale barr=50µm. B-C) PI 38:4 and PI 36:2 respective distribution obtained by MALDI-IMS. The images are a representative example of how different lipids distribute differently along the epithelium and the connective tissue of the colon, presenting each one their own specific lipid composition. It is appreciable that these two lipids, differing only in two carbons and one double bond show a reciprocally exclusive distribution being the PI 38:4 more abundant in the connective and PI 36:2 in the epithelial tissue.

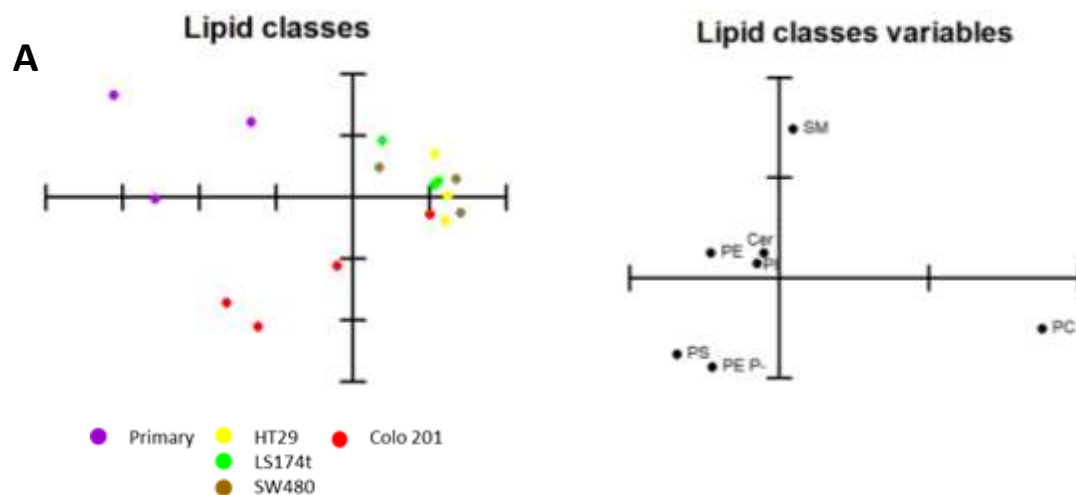
The setting of the colon crypts, with a base of proliferating cells that differentiate along the crypt axis, makes MALDI-IMS perfectly suited to understand the role of lipids in proliferation and differentiation processes. MALDI-IMS lipidome provided insightful information about the colonocytes and the lamina propria physiologic state. The colon is an interesting scenario where both epithelium and lamina propria possess different characteristics depending on the proximity of the cells to the colon lumen. This process was reflected in the lipid composition, as MALDI-IMS images non-guided analysis generated two epithelial clusters with specific lipid composition clearly located at the crypt base and the luminal sites. These epithelial clusters fit with the proliferative profile of the colonocytes, as colonocytes at crypt base (mainly stem cells and TA cells) possess higher proliferative capabilities than the luminal colonocytes. These basal epithelial clusters differed in their higher content in AA-containing and lower MUFA-containing phospholipids at the crypt base compared to the luminal ones. On the other hand, the same analysis was able to reflect a similar but inverse behavior within the lamina propria. Due to the presence of antigens in the stool and the own microbiota, the luminal side of the lamina propria recruits higher immune cells and shows higher immune activation rates near the lumen than near the mucosa base^{678,679}. In the case of the lamina propria, the higher amounts of AA-containing phospholipids were at the luminal side of the colon.

In agreement with the loss in controlling the cell cycle, adenomatous polyps showed a lipidome altered compared to the healthy mucosa. The main consistent lipid change in the adenomatous epithelium was the decrease in all 36:3 species. Thus, it was remarkable the similar AA profile of the adenomatous epithelium compared to the crypt base colonocytes, which could be associated to the high proliferative capabilities of these cells in particular.

In summary, MALDI-IMS lipidome revealed profound regulation of lipid species within colon tissue. The lipid specific profile showed clear differences between the lamina propria and the epithelial cells of the colon. But even further, the lipid composition was able to convey the proliferative status of the colonocytes and the inflammatory state inherent of a healthy lamina propria. While many articles described relevant lipid changes in cancer, opening the opportunity to use lipids as biomarkers^{628,680-682} lipid image analysis of colon tissue may be able to reveal subtler ones. These results clearly proved the great potential of IMS in the clinical field in identifying new and highly specific biomarkers.

3.1.3 Extracellular vesicles lipids as biomarkers of malignization in cell culture model

In this section, we analyzed the lipidome of EVs derived from the cell lines described in section 3.1.1 by HPLC-MS to investigate EVs lipidome as a potential CRC biomarker. The EVs fraction was obtained by differential centrifugation and successive filtrations as described previously⁶⁰¹ and the lipid extract analyzed by HPLC-MS⁶⁸³. The methodology is explained in detail in the Experimental procedures section.



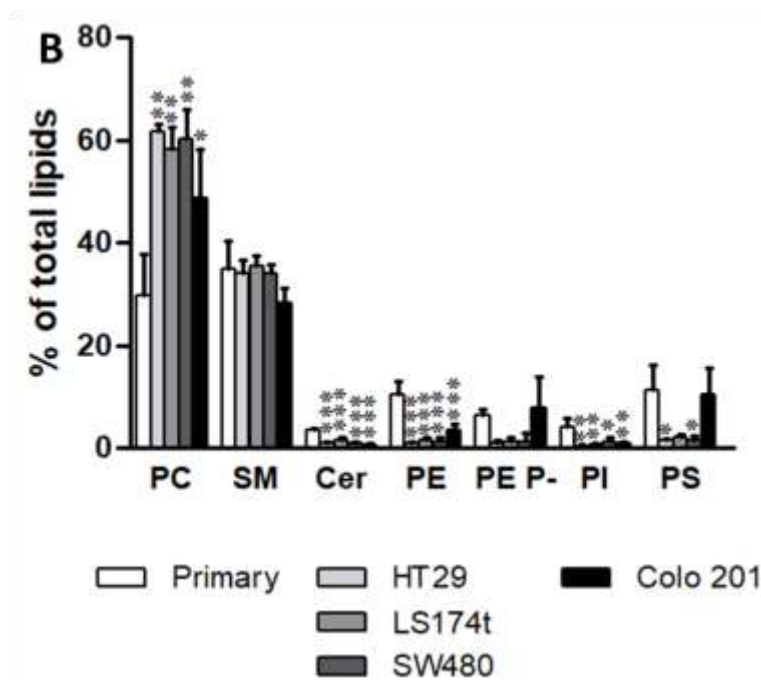


Figure 3-17: Lipid classes content analysis of colon cancer cells-derived EVs. A) Lipid classes content analyzed by PCA. Explained variance: 93.06%. **B)** Representation of all lipid classes values. Mean and SD represented. Only statistical differences with primary cells are represented. Statistical differences were assessed by one-way ANOVA followed by a Bonferroni post-test. * $P < 0.05$; ** $P < 0.01$; *** $P < 0.001$.

PCA of lipid classes was able to separate between primary and cancer cell-derived EVs (Figure 3-17, A). However, and unlike for cells, PCA was not able to discriminate between the *in situ* and Colo 201 cancer cells. In any case, lipid classes influencing the most in the PCA were PC, SM, PE plasmalogens, and PS. Primary cells were clearly separated from the rest due to the PE plasmalogens and PC ratio (high amounts of PE plasmalogens and low amounts of PC). *In situ* cell lines had a profile with high content in PC combined with low levels in PE plasmalogens. Finally, the most malignant cells were characterized by the low PC level compared to the *in situ* cancer cells.

The means representation showed first that, in terms of composition, and consistent with the literature, the most abundant lipids in EVs were PC (29.84-61.6%) and SM (28.4-35.4%)^{620,621,623} (Figure 3-17, B and Supplemental table 5). The most relevant differences between primary and cancer cells were the increase in PC (29.8% vs. 57.2% primary cells vs. tumor cells), and the decrease in Cer (3.4% vs. 0.89%), PE (10.3% vs. 1.7%) and PI (4.1% vs. 0.73%). Despite not being significant, it is worth mentioning how *in situ* cancer cells EVs differed from Colo 201 in their PE plasmalogens (1.0% vs. 7.8% *in situ* cancer cells vs. Colo 201 cells) and PS (1.5% vs. 10.3%) content. In general, *in situ* cancer cells EVs have less lipid variety than the primary and Colo 201 cells.

To better understand EVs regulation and function we compared the lipidome of EVs with the cell of origin (Figure 3-18). In this context, the most robust result was the increase in SM levels in EVs (8.2% vs. 33.3%, cellular content vs. EVs content) a result consistently demonstrated in literature^{589,684}. The opposite pattern was observed in PE and PE plasmalogens content, as EVs of all cells present impoverishment respect their origin cell, although primary derived EVs PE levels are closer to the cell compared to the cancer cells. On the other hand, while primary and Colo 201 maintained a similar ratio of PE plasmalogens and PS, the *in situ* cells showed a drastic decrease in their EVs content for these lipids. Interestingly cancer cells showed enrichment in their PE plasmalogens content compared to the primary

cells that contrast with the drastic decrease in PE plasmalogens of their EVs. PS and Cer showed a similar profile, where *in situ* cancer cells had higher levels in cells, Primary cells showed a slight enrichment in their exosomes and Colo 201 presented similar levels in cells and EVs for both lipid classes. Primary EVs and cells had similar PI levels, however, EVs derived from cancer cells decrease their content in this lipid compared to their origin cell. It is worth mentioning, however, how a minor lipid class as Cer was highly enriched in EVs (almost 3 higher levels in EVs compared to cell lipid content) but was barely affected in the cancer cells.

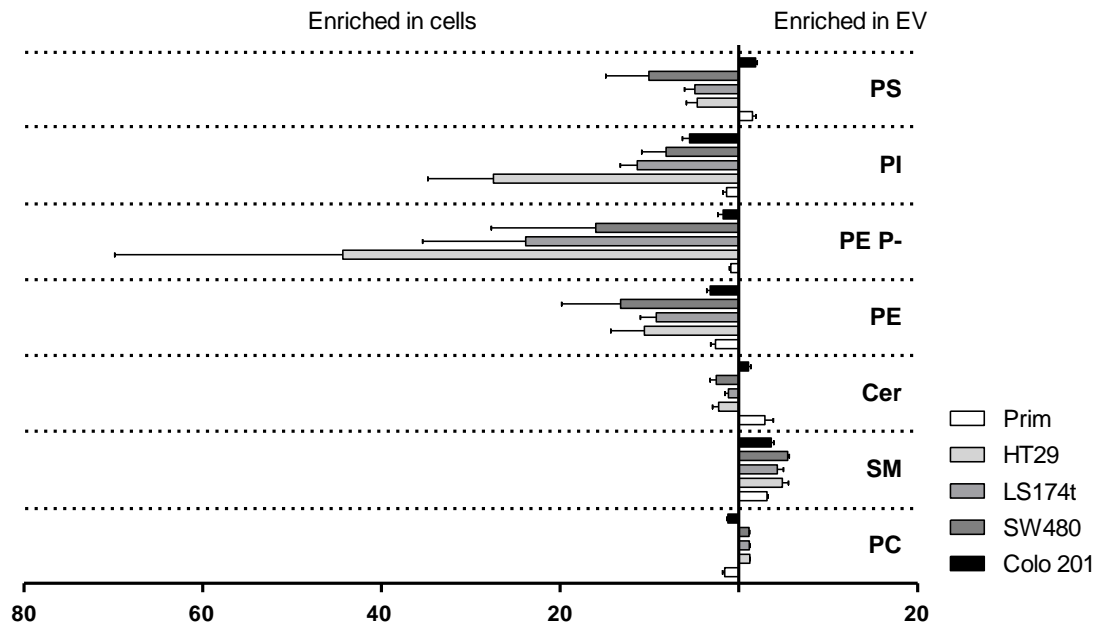
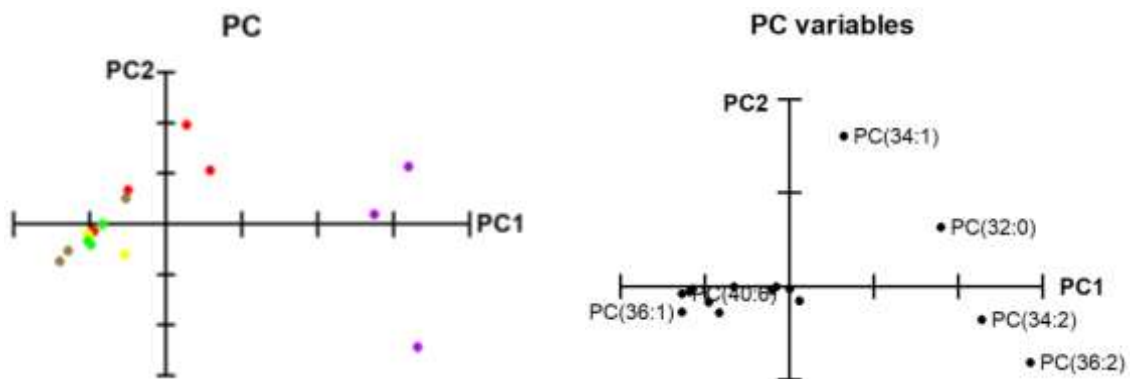


Figure 3-18: Lipid enrichment in cells and cells derived EVs. The ratios were made dividing the cellular composition between the EVs composition on the left side of the graph and inversely on the right side of the graph.

Globally, primary EVs were more similar to parental cells than cancer EVs. To delve into the EVs lipid composition, next, we analyzed their lipid molecular species content.



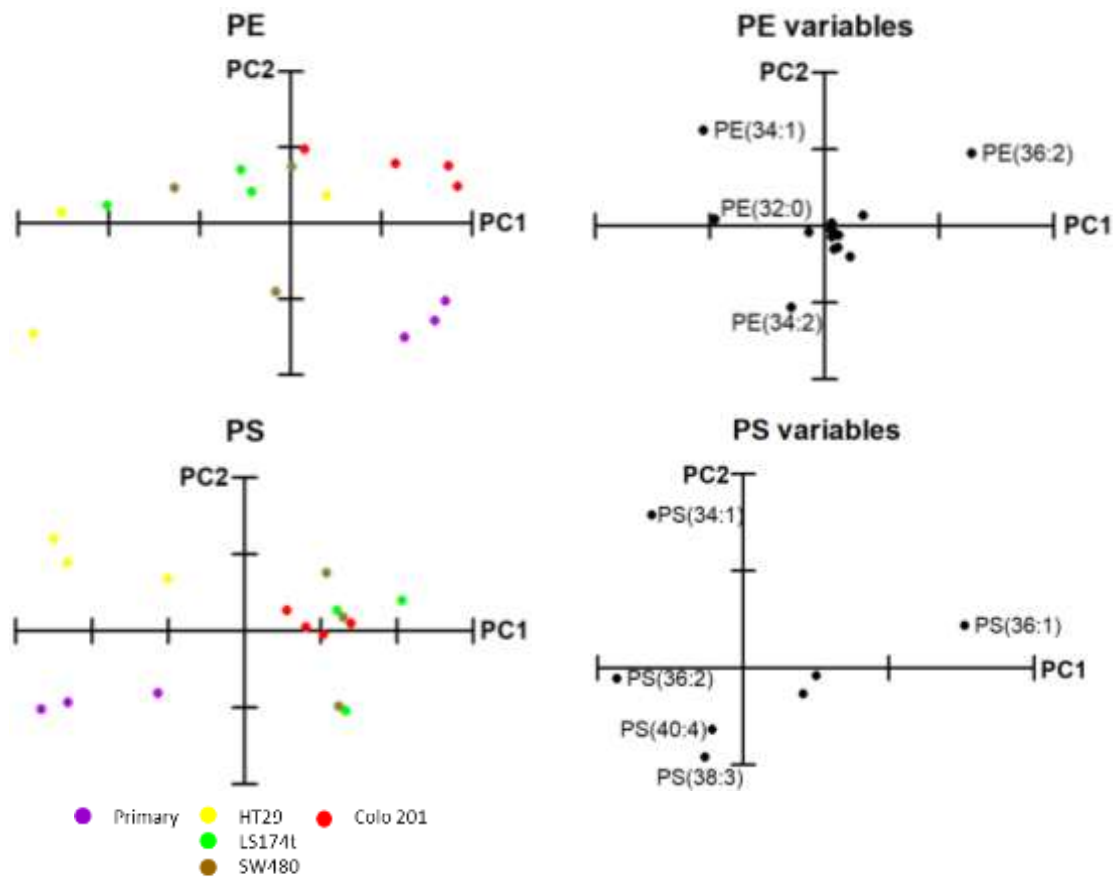
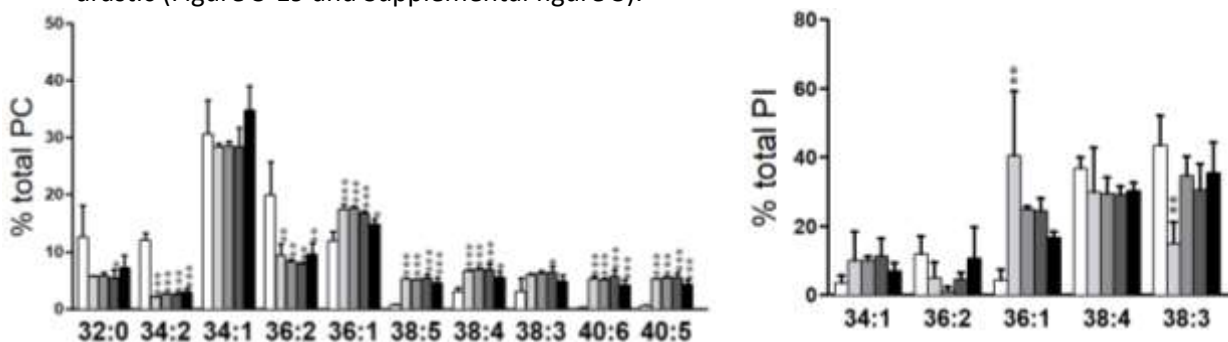


Figure 3-19: PCA of lipid species analyzed in cell culture-derived EVs. Only the most influential variables are indicated at each variables PCA analysis. Explained variances: PC 82.0%, PE 61.2% and PS 71.1%. ● Primary, ● HT29, ● LS174t, ● SW480 and ● Colo 201 cell lines. We only presented here the lipid classes separating clearly between the different EVs origin. The remaining classes are represented in Supplemental figure 3.

The analysis of EVs lipid molecular species revealed profound changes in the acyl chain composition of their lipids. PCA showed that PC (high content of 32:0, 34:2 and 36:2), PE (low content of 34:1 and 32:0), PI (high 38:3 and low 36:1 content) and PS (high 36:2 and 34:1 and low 36:1 content) could separate between primary and cancer cells. Although PC 34:1, PE 36:2 and PI 38:3 are increased in Colo 201 cells respect *in situ* cancer cells, the separation is not drastic (Figure 3-19 and Supplemental figure 3).



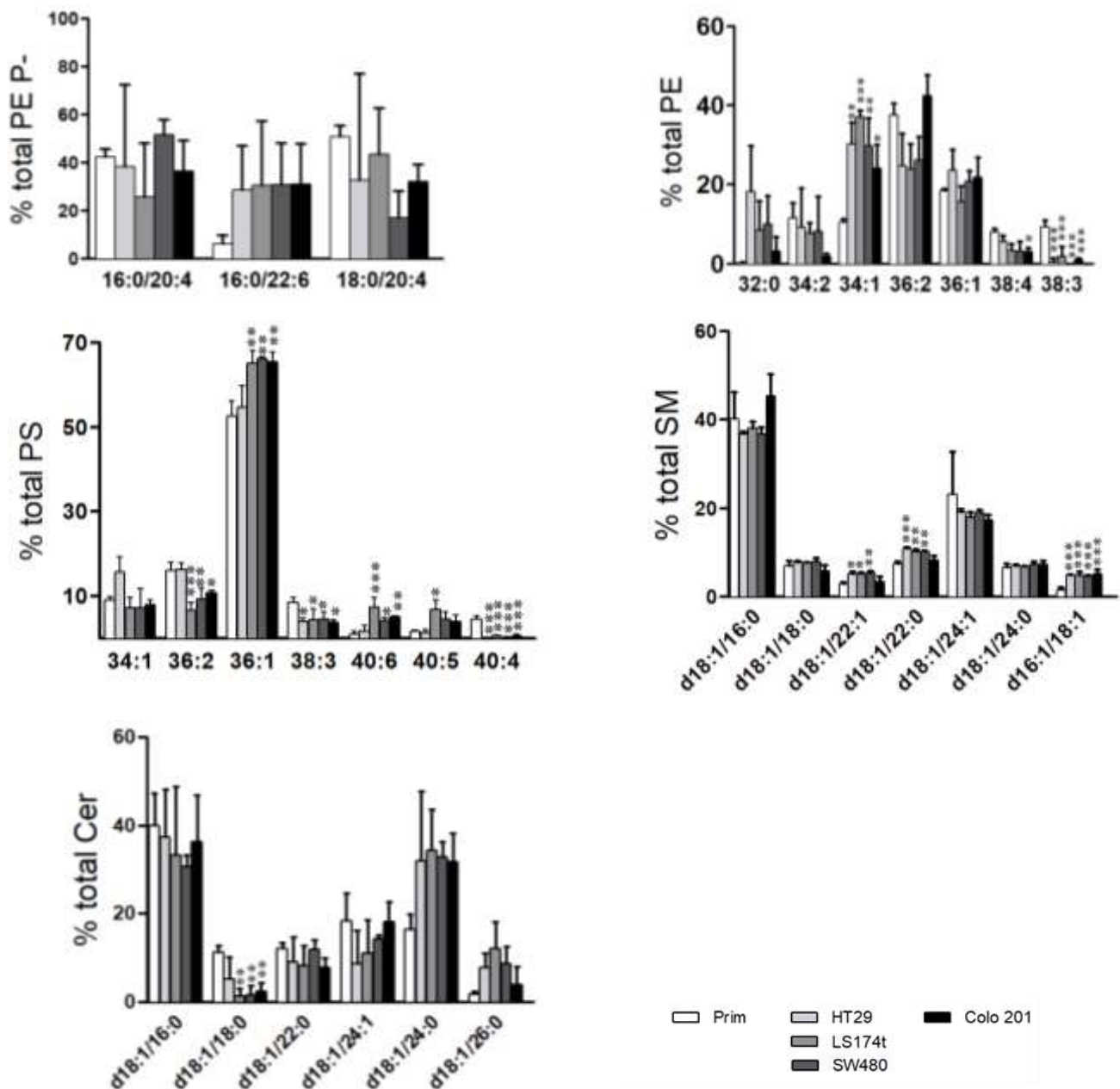


Figure 3-20: Lipid fingerprint in primary, *in situ* and metastatic cancer cells extracellular vesicles. Bar diagrams comparing the levels in PC, PE and PS lipid composition at molecular species levels in primary, HT29, LS174t, SW480, and Colo 201 cells. Values are expressed as a percentage of total fatty acid (mole %) and represent mean \pm SD, n=3-6. Statistical significance was assessed using one way ANOVA comparing primary to cancer cells. For clarity, only species accounting for <5% of total lipid class are included in the graphs. * P<0.05; ** P<0.01; *** P<0.001.

The most abundant PC species were 34:1 (28.3-34.7%) followed by 36:2 (7.8-19.9%) and 36:1 (11.8-17.5%) (Figure 3-20 and Supplemental table 6). The main difference between primary and tumor cells was the drastic increase in PUFA species. Regarding AA-containing species, the most remarkable increases were in 38:5 and 38:4 (5-fold and 2-fold increase respectively) while in DHA-containing species were 40:6 and 40:5 (20-fold increase). Interestingly, 36:1, a MUFA-containing species, was also increased in cancer cells compared to primary cells (11.0% vs. 16.6% primary vs. mean cancer cell content). On the other hand, primary cells were enriched in the diunsaturated species 34:2 (12.0% vs. 2.5% primary vs. mean of all tumor cells) and 36:2 (19.9% vs. 8.8%) compared to all cancer cells (Figure 3-20 and Supplemental table 6). In PE, the most abundant species were 34:1 (10.5-37.1%), 36:2 (24.0-

42.4%) and 36:1 (15.7-23.7%) species (Figure 3-20 and Supplemental table 6). The most relevant differences were the increase in 34:1 (10.5% vs. 30.3% primary vs. mean of all tumor cells) and 32:0 (0.4% vs. 10.0%) and decrease in 38:3 (9.4% vs. 0.85%) occurred in cancer cells derived EVs. In PI, the most abundant species were 38:4 (29.1-36.7%) and 38:3 (14.9-43.5%). However, no significant differences were detected in PI species among the studied cell line-derived EVs (Supplemental table 6). Finally, the most abundant PS species was by far 36:1 (52.6-66.1%) followed by 36:2 (6.5-16.3%). The most consistent changes throughout the cell lines were the decrease in 38:3 (8.5% vs. 4% primary vs. mean of all tumor cells) and 40:4 (4.5% vs. 0.3%) (Figure 3-20 and Supplemental table 6).

Regarding sphingolipids, the most abundant EVs SM species were d18:1/16:0 and d18:1/24:1 in SM (36.8-45.4% and 17.4-23.2% respectively) while in Cer species were d18:1/16:0 and d18:1/24:0 (19.9-30.6% and 16.5-34.3% respectively). Interestingly, most SM species remained rather constant throughout the different cell lines. This and previous works describing high levels of SM in EVs^{620,621,623} suggest a constant SM composition for EVs formation regardless of their origin. Taking into account these constant SM levels is remarkable the higher concentration of sphingolipids d16:1/18:1 in tumor cells (1.6% vs. 4.9%) (Supplemental table 6).

Discussion:

The use of EVs composition as biomarker could pose new approaches to treat diseases like cancer, where early detection is a critical factor for the patient survival. Despite the general interest generated in this field, and the potential of lipids as biomarkers, there are only a few works describing complete lipidome of EVs^{620,621}. Our EVs analyzes are in agreement with previous works showing a drastic enrichment of EVs in SM respect the source of origin^{620,685}. Besides, we described a general impoverishment in *in situ* tumor cell lipidome compared to the primary and the Colo 201 cells. Therefore, the *in situ* cancer cells EVs present high levels of PC and SM, and very low levels of the rest phospholipids, which would lead to more rigid membranes.

In addition, using the comprehensive result of specific lipid molecular species we were able to segregate EVs depending on their origin, being the PC, PE, PI, and PS molecular species the ones able to clearly separate between primary and the rest of cells. On the other hand, Colo 201 derived EVs differentiate from the *in situ* cancer cell by their relatively low levels in PC. In general, the separation between primary and cancer cells was mainly due to their content in MUFA and DUFA species content. Specifically, the most consistent segregation between primary and cancer cells was due to higher PC and PS 36:2 and lower PE 34:1 and 32:0 and PI and PS 36:1 content in the primary EVs. Thus, PC 34:1, PE 36:2 and PI 38:3 molecular species were increased enough in Colo 201 cells, to segregate them from the *in situ* cancer cells.

Here we provide a comprehensive lipidomic analysis of EVs derived from three *in situ*-isolated cancer cells and one metastatic-isolated cancer cell. The results showed that the EVs lipidome is dependent on the cell origin and therefore has the potential of becoming a good biomarker. These changes could help in future works to understand the role and regulation of EVs, but more importantly, could set the base to use the EVs lipidome as a cancer non-invasive biomarker tool.

3.1.4 Extracellular vesicles lipidome as clinical colorectal cancer biomarker

The analysis of commercial cell lines-derived EVs showed that the lipid composition of these vesicles is very sensitive to their origin. These results support the approach of using the lipidome of EVs derived from biological fluids as non-invasive biomarkers for cancer. Unfortunately, all tissues and cells secrete multiple types of vesicles that could mask EVs secreted from tumors, especially at early stages. To assess the viability and sensitivity of using

patient-derived EVs lipidome, this section explores the feasibility of plasma-derived EVs lipidome as clinical biomarkers in patients with different colon tumor types. To this, we classified the patients into four groups. 1) Healthy group, including patients with no clinical discoveries during the colonoscopy; 2) Patients with hyperplastic polyps (HP); 3) patients with adenomatous polyps (AD); 4) patients with invasive neoplasia (Neo). Supplemental table 8 showed relevant clinical characteristics of the patients participating in the study.

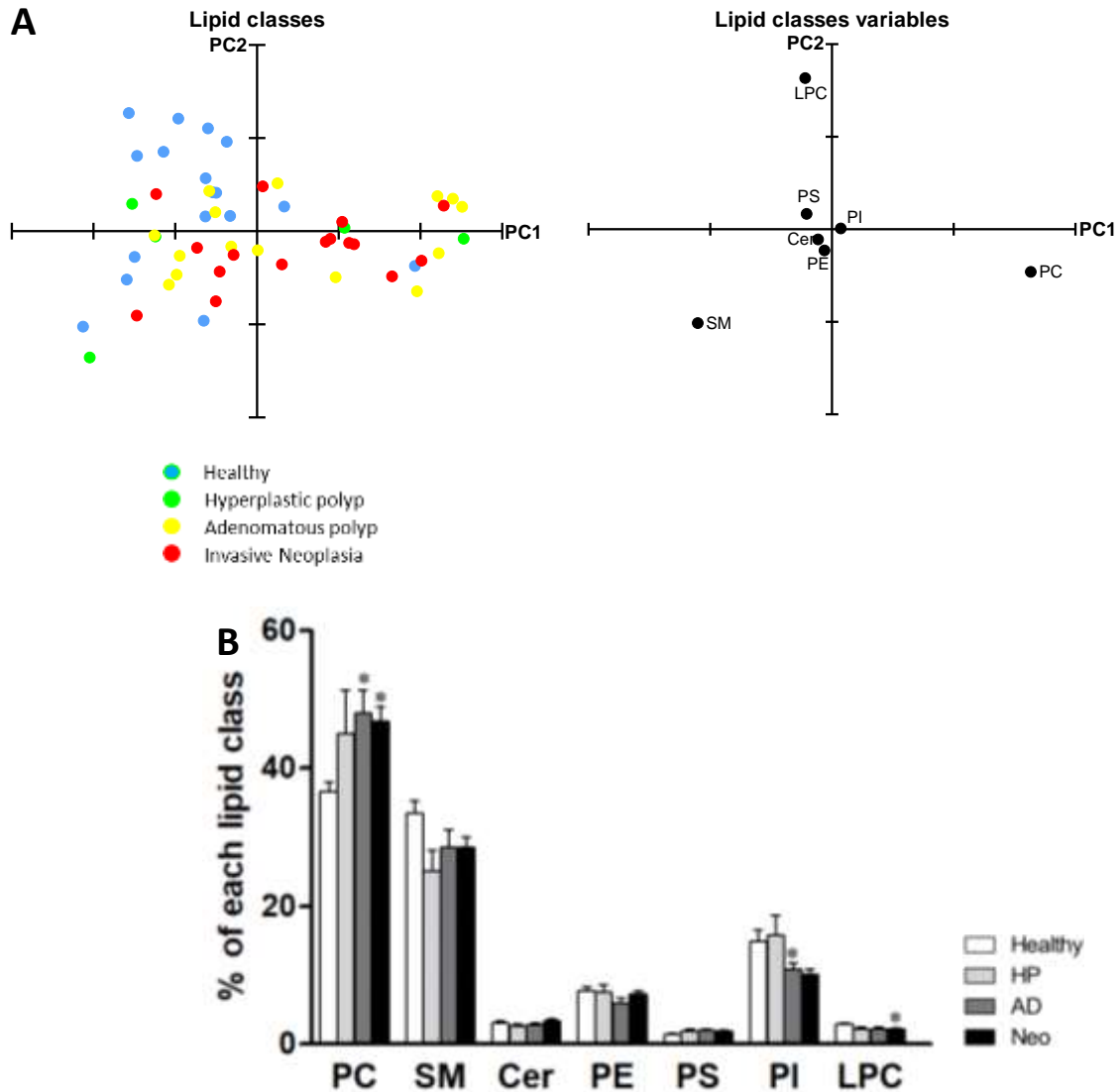


Figure 3-21: Lipid classes content analysis of patients plasma-derived EVs. A) Lipid classes content analyzed by PCA. Explained variance 92.57%. ● Healthy, ● HP, ● AD, and ● Neo patients. **B)** Representation of all lipid classes values. The bars represent healthy (n=13) (white bars), HP (n=5) (light grey bars), AD (n=16) (striped grey bars) and carcinoma patients (n=19) (black bars). Mean and SD represented n=. Only statistical differences between healthy patients are represented. Statistical differences were assessed by one-way ANOVA followed by a Bonferroni post-test. * P<0.05; ** P<0.01; *** P<0.001.

PCA of all lipid classes showed a tendency of grouping EVs according to their clinical classification. The PC1 was the one responsible for stratifying the patients, with almost no participation of the PC2. The most influential lipids classes in PC1 formation were PC and SM. Healthy patients EVs showed higher and levels of SM and lower levels of PC than in AD and in Neo patients. Despite LysoPC is a major contributor to PC2, it mainly explains Healthy EVs

variability, showing no effect of this lipid class in the patients segregation (Figure 3-21, A and Supplemental table 7).

The analysis of the variance confirms the tendencies illustrated by PCA (Figure 3-21, B). As expected and mimicking the cell culture EVs results, the most abundant lipid classes were PC (36.7-48.0%) and SM (25.1-33.5%). The most remarkable result was the PC increase in AD and Neo patients compared to the healthy group (36.7 vs. 47.5% Healthy vs. mean value of AD and Neo patients). In addition, there is a clear tendency in PI decreasing in AD and Neo patients compared to the healthy ones (14.9% vs. 10.5%). The analysis of the lipid molecular species would reveal subtle lipid changes between the patients groups.

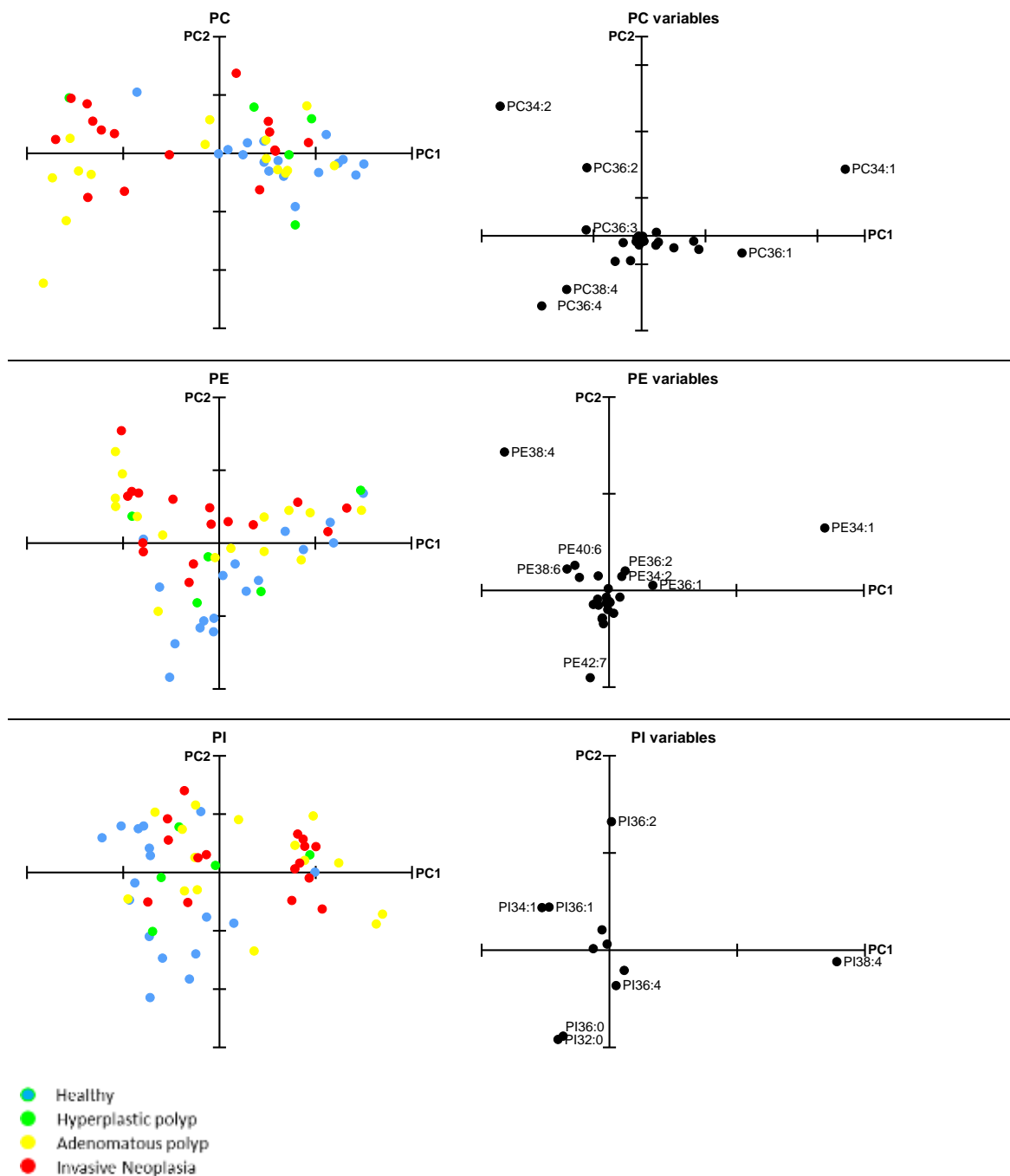
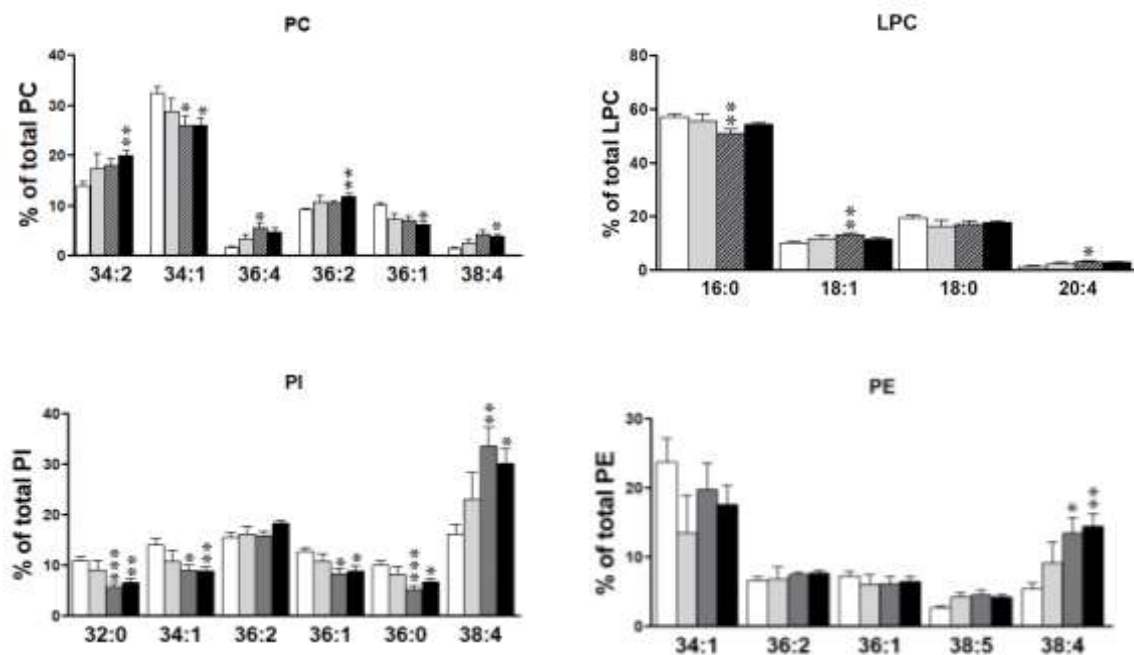


Figure 3-22: PCA of % of each species lipid class in EVs derived from patients plasma. Explained variances: PC 88.1%, PE 92.1%, PI 89.1%. Lipid classes content analyzed by PCA. Explained variance 92.57%. ● Healthy, ● HP, ● AD, and ● Neo patients.

Although PC, PE, and PI showed a clear tendency in separating the different patients groups, the great variability in the EVs lipidome precluded the stratification of all patients according to their EVs lipidome. In any case, PC showed a clear tendency in separating healthy, AD and Neo patients mostly by the influence of PC1. Indeed, healthy patients showed higher levels of PC 36:1 and lower PC 34:2, 36:8 and 38:4 compared to most AD and Neo patients (Figure 3-22). In a similar way, healthy patients derived EVs present higher amounts of PE 34:1 and 42:7 but relatively lower levels of PE 38:4 compared to most AD and Neo patients. Finally, some PI species presented a quite regular composition within each group of patients. PI 38:4 is more present in AD and Neo patients compared to healthy ones; in addition, those patients present lower levels of MUFA-containing species, being PI 34:1, 36:1, 32:0 and 36:0 the less present at AD and Neo patients compared to healthy ones. In general, patients with malignant lesions present higher amounts of AA-containing species (especially 34:8 species) in their EVs. It is worth mentioning the global behavior of HP patients, with a disperse distribution within all phospholipid classes (Figure 3-22 and Supplemental figure 4). The analysis of the variance reinforces the PCA results in identifying further potential lipid biomarkers.



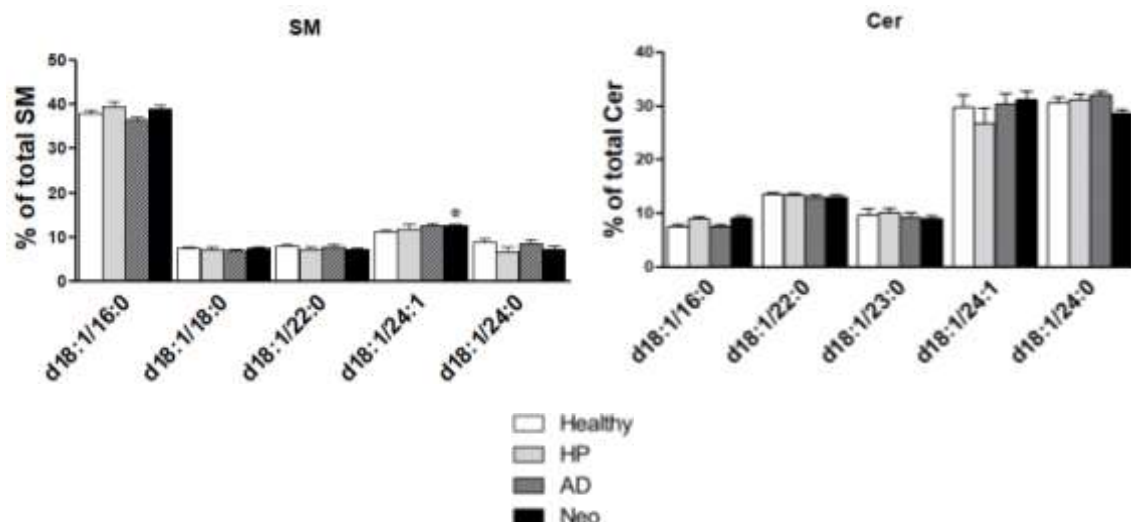


Figure 3-23: Molecular species composition of EVs isolated from patients plasma. For simplicity only represented the species accounting for more than 5% and the major AA-containing species are represented. The bars represent healthy (n=13) (white bars), HP (n=5) (light grey bars), AD (n=16) (striped grey bars) and carcinoma patients (n=19) (black bars). Mean and SD represented n=. Only statistical differences between healthy patients are represented. Statistical differences were assessed by one-way ANOVA followed by a Bonferroni post-test. * P<0.05; ** P<0.01; *** P<0.001. As a major sphingoid base, we assumed that all SM backbones were 18:1 carbon chains, although this was not checked and other minor sphingoid bases could be present at SM molecular species. The comprehensive lipid composition may be found at Supplemental Table 9.

PC most abundant species were 34:1 (26-32.5%), 34:2 (14-20%) and 36:2 (9.2-11.9%). The most consistent composition changes were the decrease in 34:1 (32.5% vs. 26% Healthy vs. mean AD and Neo values) and the increase in 38:3 (1.3% vs. 2%). However there are multiple tendencies of differences between healthy and AD and Neo patients such as: increases in 34:2 (14% vs. 19.1%), 36:4 (1.8% vs. 5.2%), 36:3 (2.6% vs. 4.4%), 36:2 (9.2% vs. 11.9%) and 38:4 (1.5% vs. 4.1%) and decreases in 36:1 (10.1% vs. 6.7%) and 38:1 (3.1% vs. 1.8%) species. On the other hand LPC main species were 16:0 (51-57.2%), 18:0 (16.3-19.4%) and 18:1 (10-13.2%).

The main PE species were 34:1 (13.5-23.7%), 38:4 (5.5-14.5%) and 42:7 (5.1-10.2%). The most consistent change between healthy and AD and Neo patients was the significant increase in 38:4 (5.5% vs. 14%). While not significant there was also a slight increase in 38:5 (2.7% vs. 4.4%) and a decrease in 38:2 (4.4% vs. 3.3%), 38:1 (3% vs. 2.2%), and 42:7 (7.8% vs. 5.4%) species.

The PI class was mainly composed by 38:4 (16.1-33.6%), 36:2 (15.5-18.3%) and 34:1 (8.9-14%) species. Despite being the third most abundant class lipid (mean value of all groups 9.2%), PI was the class showing most species changes. The most notable change was the increase in 38:4 (16.1% vs. 31.8%), but there were also decreases in 32:0 (10.9% vs. 6.1%), 34:2 (6.8% vs. 5.2%), 34:1 (14% vs. 8.9%), 36:1 (12.7% vs. 8.7%) and 36:0 (10% vs. 5.9%) species.

Regarding sphingolipids, the most abundant SM species were SPM 16:0 (36.5-39.4%), SPM 24:1 (11.2-12.7%) and SPM 24:0 (6.7-8.8%). Despite their high relative abundance respect the other lipids, there were almost no difference between SM species, being the only one significant the slight decrease in 16:1-OH (1.3% vs. 1.05% Healthy vs. mean value of AD and Neo) and a slight increase in 24:1 in Neo patients (11.2% vs. 12.7% Healthy vs. Neo patients). Cer most abundant species were 24:0 (28.4-31.9%), 24:1 (26.7-31%) and 22:0 (12.8-13.5%) but no changes or tendencies were detected in their species distribution between healthy and the pathological situations.

The comprehensive analysis of the cell lipid composition showed how, AA- and MUFA-containing phospholipids are markers for proliferation, cells derived EVs and plasma-derived

EVs. Despite this clear tendency, neither MUFA- nor AA-containing species were able to classify correctly all patients analyzed by themselves. Taking advantage of these general AA-MUFA relations we further investigated if the ratio between these species could be used as clinical biomarkers.

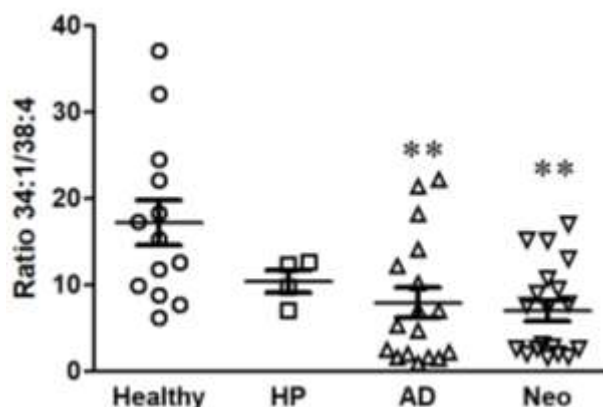


Figure 3-23: The ratio between the 34:1 and 38:4 species discriminate between healthy patients and patients with adenoma and invasive neoplasia. The ratio was calculated by dividing the total content in 34:1 and 38:4 of PC, PE, and PI. Statistical differences were assessed by one-way ANOVA followed by a Bonferroni post-test. ** $P < 0.01$.

The ratio between 34:1 and 38:4 molecular species was sensitive enough to separate significantly between the healthy patients and AD and Neo patients (Figure 3-23). However, this ratio did not apply to each patient as there were false negative results for 62.5% in AD and 52.5% in Neo groups. It is remarkable, the patients presenting very low 34:1/38:4 ratio, suggesting the presence of a subgroup of patients particularly sensitive to this ratio. Finally, although HP patients showed a similar ratio than AD and Neo patients, they did not reach significant differences with healthy patients.

Discussion:

The discovery of reliable, easy and cheap to analyze non-invasive biomarkers for cancer, with minimum inconvenience to patients and clinicians, is a main concern in healthcare. With this in mind, many signs of progresses to identify protein and/or genetic biomarkers in biological fluids occurred, especially within the field of EV^{593,595,600,602,605,609-614,621,623,686}, in the past years. All these works led us with one clear conclusion; despite we still not know the role of EVs in pathophysiology, their potential use as biomarkers is undeniable.

Surprisingly, not many studies focusing on EVs lipidome have been done to date^{620,623}. With the idea of providing further knowledge to this topic, we analyzed the lipidome of plasma-isolated EV from a cohort of patients undergoing colonoscopy. Our results point to an evident shift of some specific molecular species throughout the phospholipids classes in healthy patients and patients who had already developed some kind of tumor lesion in the colon. This shift is sensitive enough to stratify correctly about 37% of AD and 47% of Neo patients. This stratification was associated with the clear tendency in increasing PUFA and decreasing MUFA containing species in patients with adenomatous tumors or invasive neoplasias. More specifically, there was a general increase in 38:4 and a decrease in 34:1 species. It is rather remarkable the sensitivity of the lipidome of EVs particularly in the adenoma condition, as these tumors did not trespass the connective tissue and they are not connected directly to the bloodstream.

The main limitation of the results is the relatively high presence of false positive and negative results. Increasing the number of analyzes and describing exhaustively the patients clinical status could bring light to these results. Although the healthy patients analyzed did not

present any tumor lesion, most of them underwent a colonoscopy trying to detect the cause of some symptomatology, usually unexplained diarrheas or anemias. With this in mind, it would not be surprising that the high variability in EVs “healthy” group would be due to pathological conditions unrelated or partially related to colon tumor development. Unfortunately, to date, we were unable to detect specific symptoms patterns that would explain the false positive patients. In a similar way, it is possible that the AD and Neo patients present variables unrelated to their disease which could interfere with their EVs lipidome. Anyhow, the presence of a subgroup of AD and Neo patients with very low 34:1/38:4 ratio suggest the presence of a subgroup clearly identifiable by this method. Future works should be addressed to understand the factors influencing EVs lipidome to try to understand all the variables influencing EVs lipidome that could influence the final patient diagnostic. The characterization of the lipidome of other blood fractions and diseases could give even more information about the health state of the patient. Maybe the combination of lipidome analysis combined with other parameters like an analysis of circulating RNA could provide information specific enough to stratify correctly patients with colorectal tumors.

This work set the base not just to identify an EV lipid profile for CRC, but proved that the lipidome is a reliable, and relatively easy and economical way to stratify patients according to their necessity to be submitted to other diagnostic tests. This approach to diagnosing diseases seems to be completely viable as most hospitals present the clinical analysis department with mass spectrometers. Thus, unlike happens with MS proteins, the fragments generated in lipidome analysis are easier to analyze once the protocol is established. In any case, EVs lipidome could become a massively used parameter to stratify patients susceptible for more invasive diagnostic techniques than a simple blood analysis.

3.2 Chapter 2: Lipid metabolism in the colonocytes proliferation and differentiation process

3.2.1 Lipidome as biomarker of the physiopathological state of the cell

To date, multiple works have clearly demonstrated that the lipidome is affected by the pathophysiological state of the cells^{23,628,687-690}, a fact consistent with the results showed in chapter 1. Furthermore, our MALDI-IMS clustering analysis was sensitive enough to discriminate between the base and the luminal site of the crypts. Observational evaluation of the MALDI-IMS analysis of the colon showed a gradual distribution of some lipids along the mucosa. Therefore, to try to reveal more subtle changes in colonocytes differentiation we analyzed the MALDI-IMS data by statistical guided analysis.

In this thesis section, we evaluated, pixel-by-pixel, the changes occurring along a path depicted from the base to the luminal site of the crypts. The analysis along healthy colon crypts revealed that multiple lipid molecular species changed in a gradual manner. The levels of these lipids changed along the crypt in a linear or logarithmic manner with high correlation coefficients (R^2 from 0.68 to 0.98). Among these species, the lipids showing more consistent gradients were PI, PE plasmalogens and AA-containing phospholipids (Figure 3-24).

Of all lipids classes detected heterogenous as phospholipids, sphingolipids, triacyl- and diacylglycerides, the limited amount of lipids distributed in a gradient indicates a rather lipid class-specific finding. Despite these gradually distributed lipid species, the total amount of each phospholipid class did not change along the crypt, suggesting the necessity of keeping lipid class levels constant regardless of its differentiation state. Altogether, it is clear that colonocytes strictly regulate their lipid composition concomitant to the differentiation process, modifying some species while constraining others within narrow margins.

3. Results: Chapter 2: Lipid metabolism in the colonocytes proliferation and differentiation process

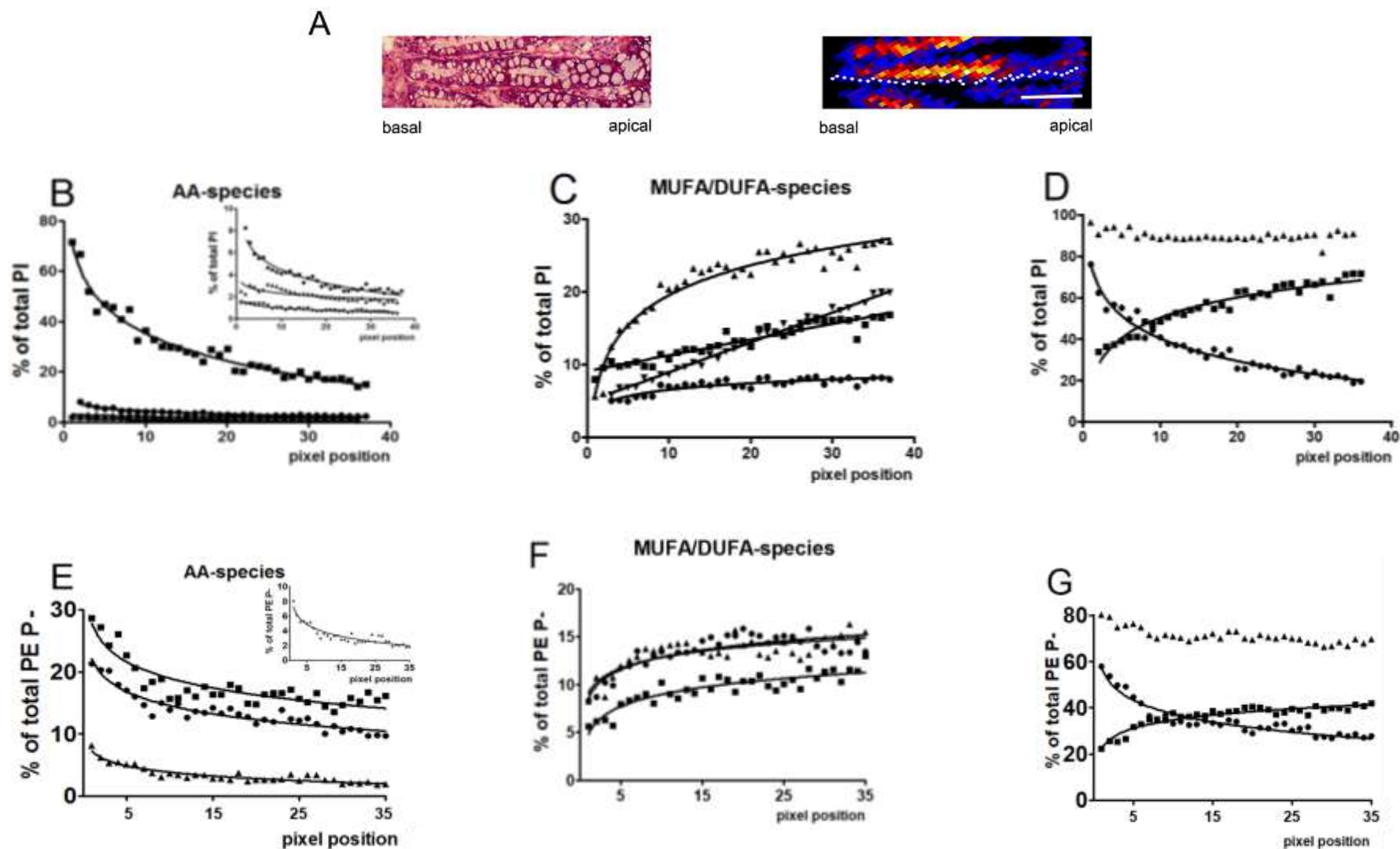


Figure 3-24: Highly coordinated PI and PE plasmalogens species distribution depending on cell healthy crypt position. A) Selected MALDI-IMS image showing the path depicted to analyze, pixel by pixel, the changes in the lipidome along the crypt. **B-D)** Fitted curve showing changes in PI lipid species relative intensity (RI) according to the distance of the pixel to the crypt base; **B)** AA-containing species: 36:4 (●), 38:4 (■), 38:5 (▲), 40:4 (▼); **C)** MUFA/DUFA-containing species: 34:2 (●), 34:1 (■), 36:2 (▲), 36:1 (▼); and **D)** sum of AA-containing species(●), sum of

3. Results: Chapter 2: Lipid metabolism in the colonocytes proliferation and differentiation process

MUFA/DUFA (■) and sum of AA+MUFA/DUFA-containing species (▲). **F-G** Fitted curve showing changes in PE plasmalogens lipid species RI according to the distance of the pixel to the base of the crypt; **E** AA-containing species: 36:4 (●), 38:4 (■), 40:4 (▲); **F** MUFA/DUFA-containing species: 34:1 (●), 36:2 (▲) and 36:1 (■); and **G** sum of AA containing species (●), sum of MUFA/DUFA (■), and sum of AA+MUFA/DUFA-containing species (▲). Values represent the mean of the RI values for each lipid species of 5 different crypts in 4 independent measurements. Scale bar = 100µm.

3. Results: Chapter 2: Lipid metabolism in the colonocytes proliferation and differentiation process

The gradual decrease in AA-containing species was compensated by an increase in MUFA and DUFA species. Although all phospholipid classes analyzed showed this behavior, the most consistent classes were the PI and PE plasmalogens. Within the PI class, all AA-species followed a logarithmic decrease (PI 38:4, 36:4, 38:5 and 40:4; $R^2 = 0.96, 0.94, 0.64$ and 0.89 respectively (Figure 3-24, B). On the contrary, species containing MUFA and or DUFA fatty acids increased compensating the AA gradual decrease, (PI 34:1, 34:2, 36:1 and 36:2, $R^2 = 0.89, 0.76, 0.98$ and 0.94 , respectively) (Figure 3-24, C and Supplemental table 10). Similarly, three of the four AA-containing PE plasmalogens species (36:4, 38:4 and 40:4) decreased in a logarithmic manner with high correlation coefficients $R^2 = 0.91, 0.77$ and 0.84 respectively (Figure 3-24, E and Supplemental table 10). Thus, three MUFA and DUFA species (34:1, 36:1 and 36:2) increased towards the luminal site ($R^2 = 0.70, 0.82$ and 0.63) (Figure 3-24, F and Supplemental table 10). The mirroring changes of the MUFA/DUFA- respect the AA-containing PI and PE plasmalogens indicate a highly synchronized turnover of these species during colonocyte differentiation. These results were consistent with previous literature showing that compared to diacyl species, ether species are highly enriched in PUFA, particularly in AA (approximately 4-fold)^{39,40}. Conversely, PE species were enriched in mono- di and triunsaturated fatty acids (MUFA, DUFA and TrUFA, approximately 1.5-, 1.8- and 3-fold increase respectively). In any case, the progressive distribution of these species was also observed in AA-containing diacyl PE and PC showing a logarithmic decrease (Supplemental table 10). Thus, changes in PE 38:4 and 36:1, and of PC 32:0 could also be mathematically adjusted ($R^2 = 0.79, 0.80, 0.69$, respectively) and, although with lower R^2 values, some additional AA-containing species also showed a logarithmic decrease (PE 38:5, 36:4, and PC 38:4 with an $R^2 = 0.46, 0.46$ and 0.42 respectively). Nevertheless, the most shocking result was the stable values obtained for the 80% of PC species and 60% of PE species (Supplemental table 10). Considering that diacyl PC and PE are the major phospholipid classes in mammalian cells, the results would suggest that these lipid classes could be playing an important role in cell integrity as the cell maintains constant their values regardless of its differentiation stage. Altogether, it is clear that colonocytes strictly regulate their lipid composition species while constraining others within narrow margins.

We analyzed the images obtained in adenomatous polyps following the same approach. The pixel by pixel analysis was consistent with the loss of differentiation in these premalignant lesions. In fact, PI 38:4 and 34:1, two of the PI species showing the most gradual distribution in healthy mucosa, were rather stable along AD crypts, exhibiting variations along AD epithelium of $\pm 15\%$ of their average value. Consistently, PE plasmalogen lipid species present a disturbed distribution in adenomatous epithelium as well. Hence, the regular changes previously observed in healthy epithelium for 36:1, 36:2, 36:4, 38:4 and 40:4 PE plasmalogens species were absent in adenomatous polyps.

The regular changes in lipid composition along colon crypts could only be possible through the coordinated action of enzymes involved in membrane lipid metabolism. As a first approach to investigate the underlying mechanisms, we tested whether or not changes in lipidome were accompanied by changes in protein expression by using immunofluorescence (IF) techniques. Taking into account the general lipid enzyme promiscuity in terms of substrate affinity, we analyzed those enzymes that, according to literature, exhibit most specificity either for the fatty acid moiety (AA/MUFA) or for the phospholipid class, in this case, PI and PE plasmalogens. The comprehensive list of the enzymes studied is listed in Table 3-2. We quantified the IF signal at the top (lumen), center and lower (basal) part of the crypts and the IF values of these areas were statistically analyzed.

Enzyme	Function
Lipid biosynthesis-related proteins	
SCD1	Unsaturates 16:0 or 18:0 to 16:1 and 18:1 respectively ^{691,692} .
ACS4	Bonds Co-A to 20:4 fatty acid. Expressed through PPAR δ ⁶⁹³ .
CDS2	Synthesizes CDP-diacylglycerol for the synthesis of PI ⁶⁹⁴ .
FAD2	Unsaturates 18:2 to 20:4 ⁶⁹⁵ .
Phospholipid plasticity	
MBOAT7	Acyltransferase with preference for AA and PI ^{121,207} .
AGPAT2	Acyltransferase with preference for AA and PA ^{165,696} .
Eicosanoid metabolism-related proteins	
PLA₂G4	Ca ²⁺ dependent PLA2. Preference for AA-containing phospholipids ^{182,697} .
iPLA₂G6	Calcium-independent PLA2. Preference for AA-containing phospholipids ⁶⁹⁸ .
mPGE₂S	Microsomal PGE2 synthase enzyme ^{699,700} .
COX1	Constitutive COX isoform. Rate-limiting step for PGE2 synthesis ^{701,702} .
COX2	Inducible COX isoform. Rate-limiting step for PG synthesis ^{701,703,704} .
Cannabinoid receptors	
CB1	Cannabinoid receptor 1 ⁷⁰⁵ .
CB2	Isoform 2 of cannabinoid receptor ³⁹⁶ .
Phosphoinositides metabolism	
PI3K	Phosphorilates PIP2 to PIP3 ^{706,707} .
PIP2	Important intracellular mediator for the release of intracellular calcium.
Plasmalogen metabolism	
FAR1	Bonds at sn1 position a fatty alcohol. Have preference for saturated and MUFAs ¹²⁵ .
FAR2	Bonds at sn1 position a fatty alcohol. Have preference only for saturated fatty acids ¹²⁵ .
AGPS	Rate limiting enzyme for the plasmalogen synthesis ¹²⁴ .
GNPAT	Rate limiting enzyme for the plasmalogen synthesis ¹²⁴ .

Table 3-2: Comprehensive list of enzymes tested in colon sections.

Figure 3-25 shows the enzymes presenting a significant gradual distribution along colon crypts. The analysis of all the enzymes tested is shown in Supplemental table 11. As explained in section 1.2.2, the main mechanism to modify phospholipid species is by transacylation. During transacylation, the fatty acid at the sn-2 position is hydrolyzed by a PLA₂ and subsequently esterified into a lysophospholipid by an acyltransferase. Therefore we interrogate the human colon for the distribution of two acyltransferase enzymes (Figure 3-25 and Supplemental table 11): MBOAT7, with a high preference for AA and PI; and AGPAT2, with lower affinity for AA^{121,165,207,696}. Unexpectedly, despite the intense AA and MUFA species shift, there were not any gradient in these enzymes (with p-values of 0.191 and 0.838 for the MBOAT7 and AGPAT2 respectively). Taking into account the absence of gradients for these enzymes, we evaluate next the distribution of enzymes involved in AA mobilization instead.

In relation to AA metabolism, we evaluated the expression of acyl-CoA synthase 4 (ACS4), fatty acid desaturase 2 (FAD2), cytosolic Ca²⁺-dependent PLA₂ Group IV (cPLA₂), Ca²⁺-independent PLA₂ Group VI (iPLA₂), COX1 and COX2 and prostaglandin E₂ synthase (PGE₂S) (Figure 3-25 and Supplemental table 11). The analysis showed that the enzymes coordinately engaged in the AA conversion into PGE₂: cPLA₂ (but not iPLA₂), COX1 and PGE₂S, displayed a neat gradient in expression, being the signal significantly more intense at the luminal side than at the base of the crypts ($P \leq 0.003-0.0001$, $\eta^2 \approx 0.3-0.5$). FAD2 followed by ACS4 and COX2, although with much higher P-values, also showed a gradual distribution ($P \leq 0.008, 0.02$ and

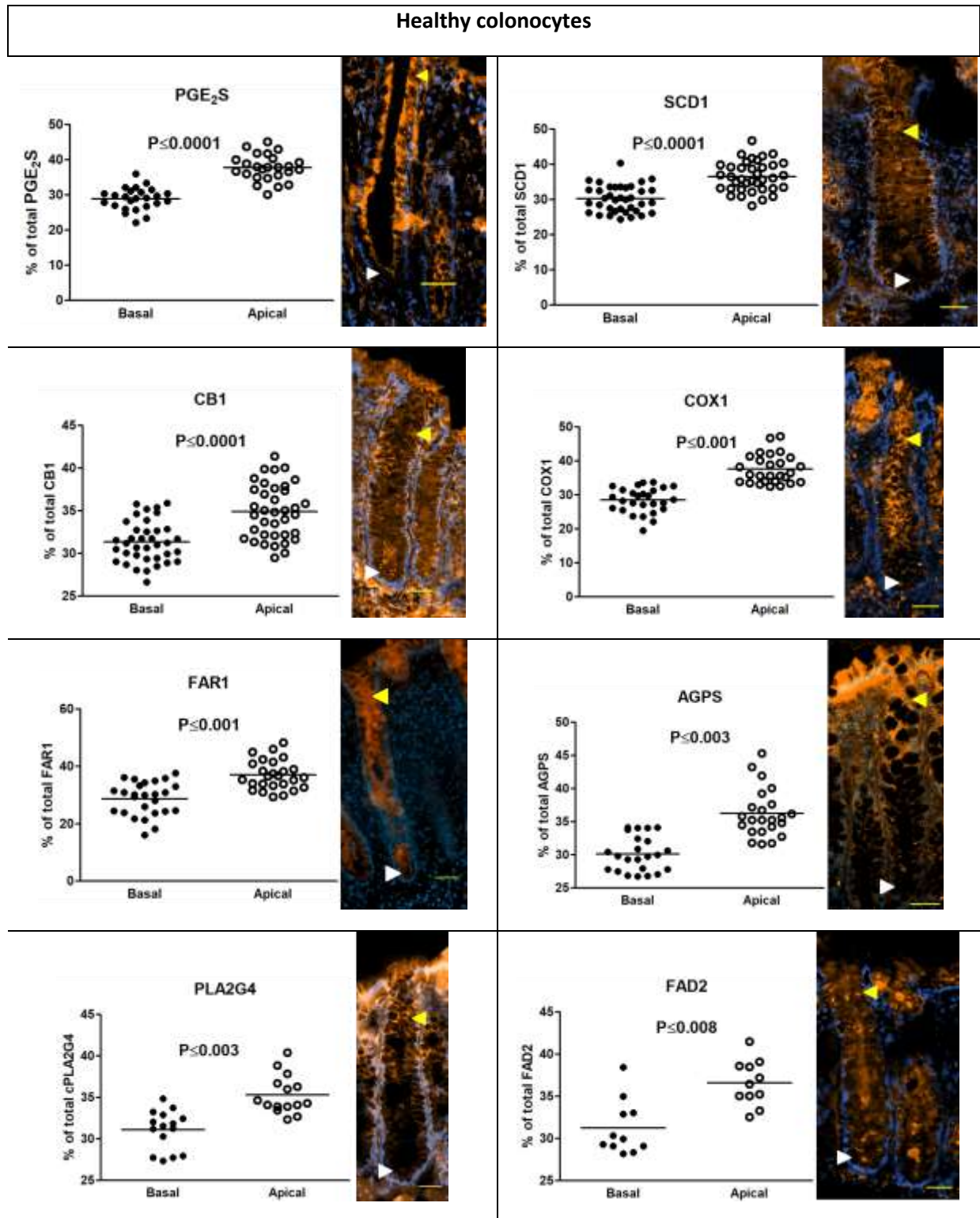
0.04, respectively). In all cases, the magnitude of the change, represented by the η^2 value, was rather similar ($\eta^2 \approx 0.3-0.4$).

While eicosanoids are the most studied AA-related molecules, other families like endocannabinoids also play important roles in cell metabolism. The distribution of CB1 and CB2 was studied along colon crypts as a possible pathway affected during colonocyte differentiation. While CB2 did not show any gradual distribution (Supplemental table 11), CB1 was more present at the luminal crypt side compared to the crypt base ($P \leq 0.0001$ and $\eta^2 = 0.3$) (Figure 3-25).

PI, like AA, plays important roles as highly bioactive molecules precursor, the phosphoinositides. Phosphoinositides are phosphorylated PI derivatives essentials for important metabolic pathways like Akt signaling⁷⁰⁸⁻⁷¹⁰. The first reaction in this pathway is the phosphorylation of PI, catalyzed by PI3K which generates PIP. When its distribution was analyzed in the colon, PI3K showed higher concentration at the luminal site than near the crypt base ($P \leq 0.0011$ and $\eta^2 = 0.3$) (Figure 3-25). However, we did not detect a PIP gradient using a specific antibody (Supplemental table 11).

Regarding PE plasmalogen species we analyzed whether the distribution of plasmalogen species could be explained by the distribution of their rate-limiting synthesis enzymes (AGPS, GNPAT, FAR1, and FAR2). The plasmalogen species showing clearest gradient were the species with saturated fatty acids at the sn-1 position and AA at sn-2. Given the different affinity of FAR1 and 2 enzymes to saturated and unsaturated fatty acids respectively it could be expected a differential enzyme expression. Indeed, AGPS and FAR1 signals were significantly more intense at the luminal side than at the base of the crypt ($P \leq 0.003$ and 0.001 , $\eta^2 = 0.3$ and 0.4 respectively) (Figure 3-25). On the contrary, expression of FAR2 and GNPAT show no variations along colon crypts (Supplemental table 11).

Finally, we investigated if the gradual increase of MUFA-containing species (PI and PE 36:1 mainly) drive us to interrogate about stearoyl-CoA desaturase (SCD1) colon distribution. SCD1 is involved in the conversion of saturated FA into MUFA, especially in the saturation of 16:0 and 18:0 into 16:1 and 18:1 respectively^{691,692}. IF analysis showed that the SCD1 signal increased firmly along the crypt, parallel to the increase of MUFA-containing phospholipids ($P \leq 0.0001$ and $\eta^2 = 0.4$) (Figure 3-25). In addition, we tested CDP-diacylglycerol synthase 2 (CDS2), a rate-limiting enzyme involved in the *de novo* synthesis of PI, which show no variations in its expression (Supplemental table 11).



3. Results: Chapter 2: Lipid metabolism in the colonocytes proliferation and differentiation process

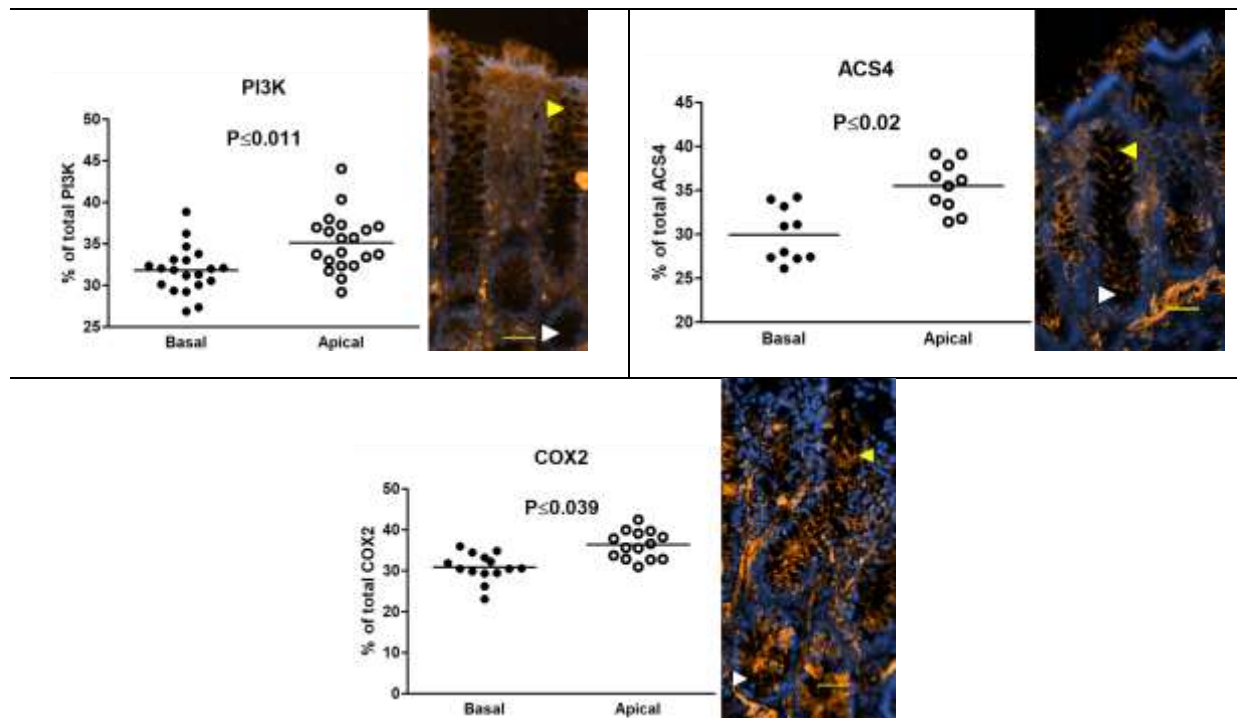


Figure 3-25: Statistical analysis showing a gradual distribution of lipid enzymes along the crypt. Once obtained the IF images, complete crypts were divided into three areas: basal, central and apical as it is described in Experimental procedures. The white arrow points the base of the crypt, while the yellow the luminal site of the crypt. IF values were obtained in at least 12 different sections of 3-4 different patients. Statistical differences were assessed by repeated measurement ANOVAs were computed for IF values using IBM SPSS Statistics 22. Results are reported using a significance level (P-value) of 0.05. ACS4: Acyl-CoA synthase 4; CDS2: CDP-Diacylglycerol Synthase 2; COX1/2: cyclooxygenase 1/2; PLA2G4: Ca²⁺ dependent phospholipase A2; iPLA2: Ca²⁺-independent phospholipase A2; FAD2: fatty acid desaturase 2; PGE₂S: prostaglandin E2 synthase; SCD1: stearoyl-CoA desaturase 1; CB1/2: cannabinoid receptor 1/2; Pi3K: phosphatidylinositol 3-kinase; PIP2: phosphatidylinositol 3 phosphate; MBOAT7: acyltransferase AA specific; AGPAT2: acyltransferase; FAR 1 and FAR2, fatty acid reductase 1 and 2; GNPAT: glycerone-phosphate O-acyltransferase; AGPS: alkylglycerone-phosphate synthase. Scale bar= 50µm.

In order to delve into the role of lipids in colon physiology, we also analyzed the lipids and the same lipid-related enzymes in the pathological context of adenomatous polyps. The gradual distribution of multiple species mirroring the healthy epithelium differentiation process was completely lost in the adenomatous polyps. Species like the PI 38:4 and 34:1, two of the PI with the most accentuated gradient along the healthy crypts, were stable along the AD crypts with variations of $\pm 15\%$ of the average value (being the change in the healthy enterocytes up to 60% in the case of the PI 38:4). Consistent with the lipidome results, the enzyme gradual distribution was lost also in AD polyps (Supplemental table 12). The only protein establishing some kind of gradient was PI3K ($P \leq 0.011$, $\eta^2 = 0.224$), but presenting an inverse gradient compared to healthy enterocytes, being the center of the tumor the region with higher PI3K expression (Figure 3-26 and Supplemental table 12). This protein distribution would be in line with multiple studies showing an increase in PI3K/Akt/mTOR signaling multiple types of cancer stem cells⁷¹¹⁻⁷¹⁵.

Regarding the rest of lipid enzymes tested, their altered expression in adenomatous polyps and CRC agrees with previous literature (ACS4⁷¹⁶, cPLA2⁷¹⁷, COX2^{701,718,719}, FAD2⁷²⁰, CB1³⁹¹, microsomal PGE₂S⁷²¹, SCD1⁷²²). However, to our knowledge, this is the first work describing changes in COX1 expression and lipid composition in a context of tumor development. The massive loss of gradual enzyme distribution reinforces the concept that lipidome is tightly regulated at the protein expression level during the colonocytes differentiation process.

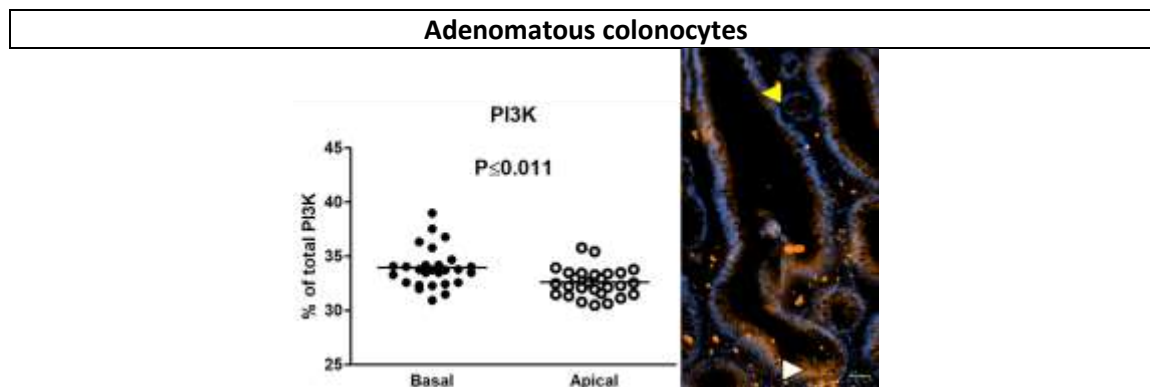


Figure 3-26: Statistical analysis showing a gradual distribution of lipid enzymes along the adenomatous crypt. Once obtained the IF images, complete crypts were divided into three areas: basal, central and apical as it is described in Experimental procedures. The white arrow points the base of the crypt, while the yellow the luminal site of the crypt. IF values were obtained in at least 12 different sections of 3-4 different patients. Statistical differences were assessed by repeated measurement ANOVAs were computed for IF values using IBM SPSS Statistics 22. Results are reported using a significance level (P-value) of 0.05. PI3K: phosphatidylinositol 3-kinase. Scale bar = 50 μ m.

Colon physiology cannot be understood without the lamina propria; which not only keeps the colon protected from infections but also provides the metabolic niche necessary for correct colonocyte development.

Taking into account the consistent generation of three specific clusters along the lamina propria, we decided to examine carefully how the lipidome changed from the base to the lumen of the lamina propria. Following the same approach as in the epithelium, we assessed the changes in a path depicted from the basal to the luminal side of the lamina propria. The results showed that AA-containing species established an opposite gradient to the observed in the colon crypt (Figure 3-27 and Supplemental table 13). Thus, PE species containing AA increased towards the lumen (36:4, 38:4, 38:5 and 40:5, $R_2 = 0.55, 0.55, 0.70$ and 0.49 , respectively), whereas PE 36:1 decreased ($R_2 = 0.55$). In PC, the content of up to five lipid species changed linearly to the distance, being the increase in PC 38:4 and 38:5 and the decrease in PC 34:2 the most relevant changes ($R^2 = 0.47, 0.65$ and 0.63 , respectively). Unlike in the epithelium, all PI species showed a rather scattered distribution, being PI 38:4 ($R_2 = 0.45$) the noticeable exception (Supplemental table 13). A similar scenario was found for plasmalogens, unlike the gradual distribution of AA-containing PE and PC species, only two stromal PE plasmalogens species, accounting for 10% of the total (40:5 and 40:6), showed this type of distribution (with an $R^2 = 0.60$). That is, despite the high AA-content in PE plasmalogens, 90% remained constant regardless of the physiological inflammatory gradient. Particularly interesting were the cases of 36:4 and 38:4, the most abundant species, whose intensity values varied <10% along the lamina propria, 21.1 ± 1.6 and $28.2 \pm 2.6\%$ respectively.

3. Results: Chapter 2: Lipid metabolism in the colonocytes proliferation and differentiation process

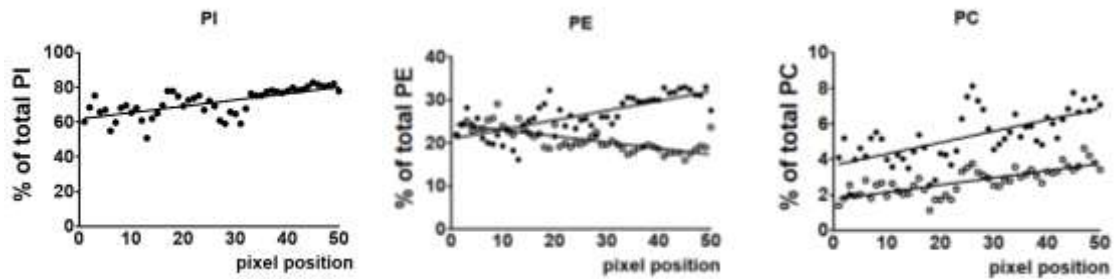


Figure 3-27: The lipid analysis by MALDI-IMS surfaced the immunological commitment of the lamina propria.

A) MALDI-IMS images of AA-containing lipid species in healthy mucosa in negative-ion mode and at 10 μ m of spatial resolution; scale bar = 200 μ m. B) The fitted curve showing changes in PI: 38:44 (●), PE: 38:4 (●) and 36:1 (○) and PC: 38:4 (●) and 38:5 (○) according to the distance of the pixel to the base of the crypt.

We also studied the distribution of the lipid-related enzymes by depicting three regions: the stromal tissue near the base of the crypt, the mid part of the crypt and the luminal part. Consistently, the increase in AA-containing species (mainly 38:4 and 38:5) coincided with a robust gradient in cPLA₂ and COX2 expression, two enzymes strongly involved in the inflammatory response ($P \leq 0.0001$ and 0.007 and $\eta^2 = 0.4$ and 0.2 , respectively) (Figure 3-28 and Supplemental table 14). Surprisingly, COX1 showed a significant but opposite gradient, being more present near crypt base reinforcing its already known role of physiologic maintenance of PG levels ($P \leq 0.025$ and $\eta^2 = 0.1$) (Figure 3-28). In addition to COX1, there is more concentration of MBOAT7 and CB2 in the lamina propria near the crypt base ($P \leq 0.005$ and 0.005 , $\eta^2 = 0.2$ and 0.2 respectively) (Figure 3-28). The presence of more MBOAT7 at the crypt base reinforces the idea of specific traffic of AA and a gradient concomitant to the inflammatory state of the connective tissue. As an immunomodulatory receptor, it is not a surprise that the CB2 receptor showed a strict regulation along the lamina propria. Consistent with the general scattered distribution of plasmalogen species, their synthetic enzymes showed minimal changes along the lamina propria. Thus, AGPS ($P \leq 0.540$), GNPAT ($P \leq 0.392$) and FAR1 ($P \leq 0.177$) presented equal distribution, and only FAR2 was distributed in a gradient ($P \leq 0.047$, $\eta^2 = 0.3$) (Figure 3-28 and Supplemental table 14). Altogether these results suggest that stromal plasmalogens were barely modified during tissue dedifferentiation.

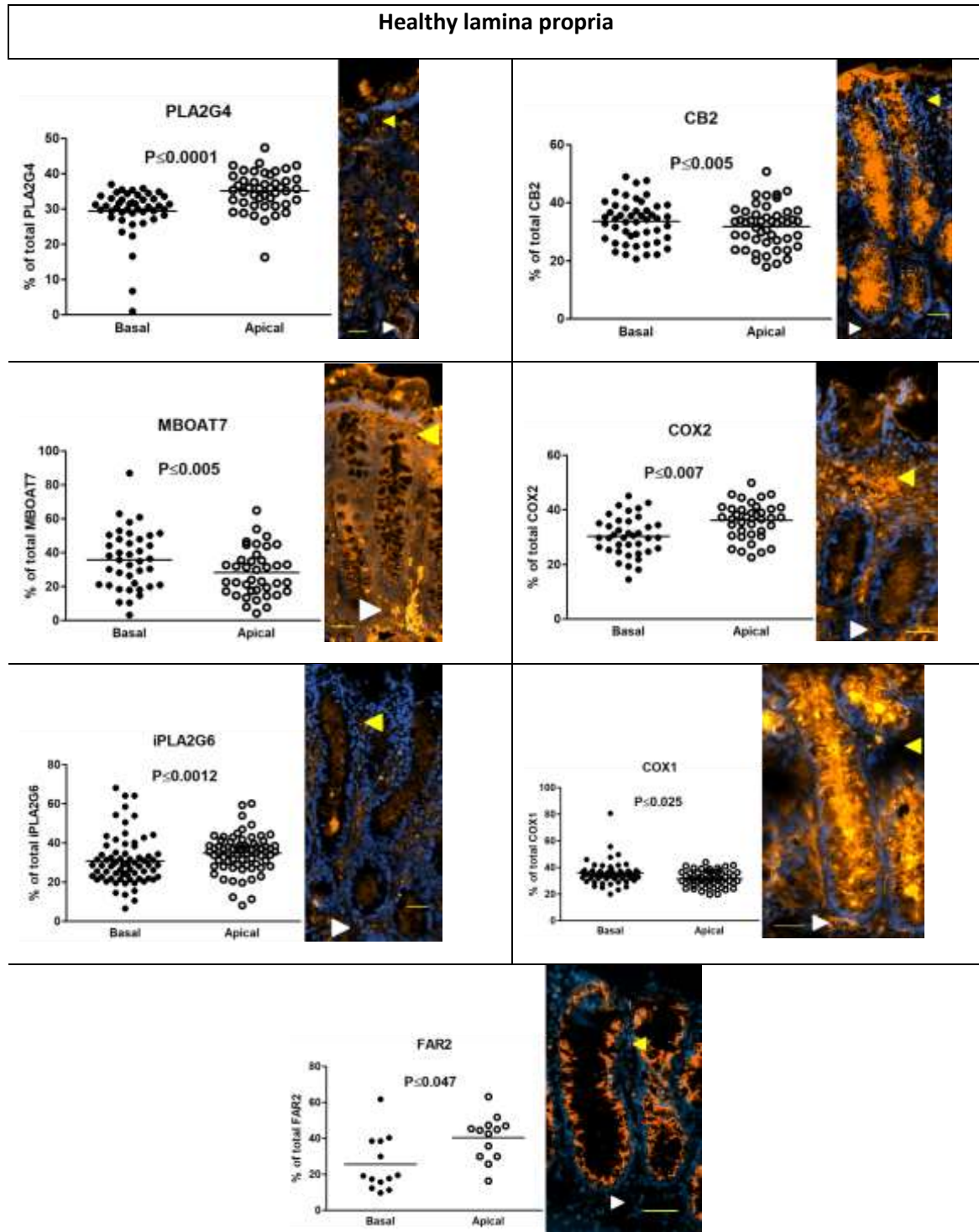


Figure 3-28: Statistical analysis showing a gradual distribution of lipid enzymes along the lamina propria surrounding healthy colon crypts. Once obtained the IF images, complete crypts were divided into three areas: basal, central and apical as it is described in Experimental procedures. The white arrow points the base of the crypt, while the yellow site of the crypt. IF values were obtained in at least 12 different sections of 3-4 different patients. Statistical differences were assessed by repeated measurement ANOVAs were computed for IF values using IBM SPSS Statistics 22. Results were reported using a significance level (P-value) of 0.05. COX1/2: cyclooxygenase 1/2; PLA2G4: Ca²⁺ dependent phospholipase A2; CB2: cannabinoid receptor 2; MBOAT7: acyltransferase AA specific; FAR2, fatty acid reductase 2. Scale bar= 50µm.

Adenomatous lamina propria:

The impaired differentiation process also affected the distribution of lipid enzymes in the adenoma tumor lamina propria. Regarding AA metabolism, PGE₂S and AGPAT2 were more present at the luminal side of the lamina propria ($P \leq 0.0001$ and $P \leq 0.002$ and $\eta^2 = 0.6$ and 0.2 respectively) (Figure 3-29). This distribution could suggest an involvement of PG synthesis at the tumor periphery. On the other hand, there is also a luminal significant increase in FAR1 and FAR2 enzymes ($P \leq 0.019$ and 0.006 , $\eta^2 = 0.3$ and 0.4 respectively) (Figure 3-29). Because AA-containing plasmalogens are the main species inside this lipid class, it is possible that the coordination of plasmalogen and PGE₂ synthesis would be related. Conversely, PLA₂ and COX enzymes did not show any gradual distribution along the adenoma tumor lamina propria (Supplemental table 15). The PLA and COX enzymes (especially COX2)⁷²³⁻⁷²⁷ overexpression in cancer could made unnecessary for the tumor a gradual distribution to enhance its growth as its activity could supply PGH₂ along the whole tumor mucosa. As in the adenomatous epithelium, PI3K is more concentrated at the center of the tumor, decreasing its presence while approaching the luminal site ($P \leq 0.007$, $\eta^2 = 0.2$) (Figure 3-29). Conversely, PiP2 showed an inverse distribution, being more concentrated at the luminal site of the adenoma lamina propria ($P \leq 0.007$, $\eta^2 = 0.2$) (Figure 3-29).

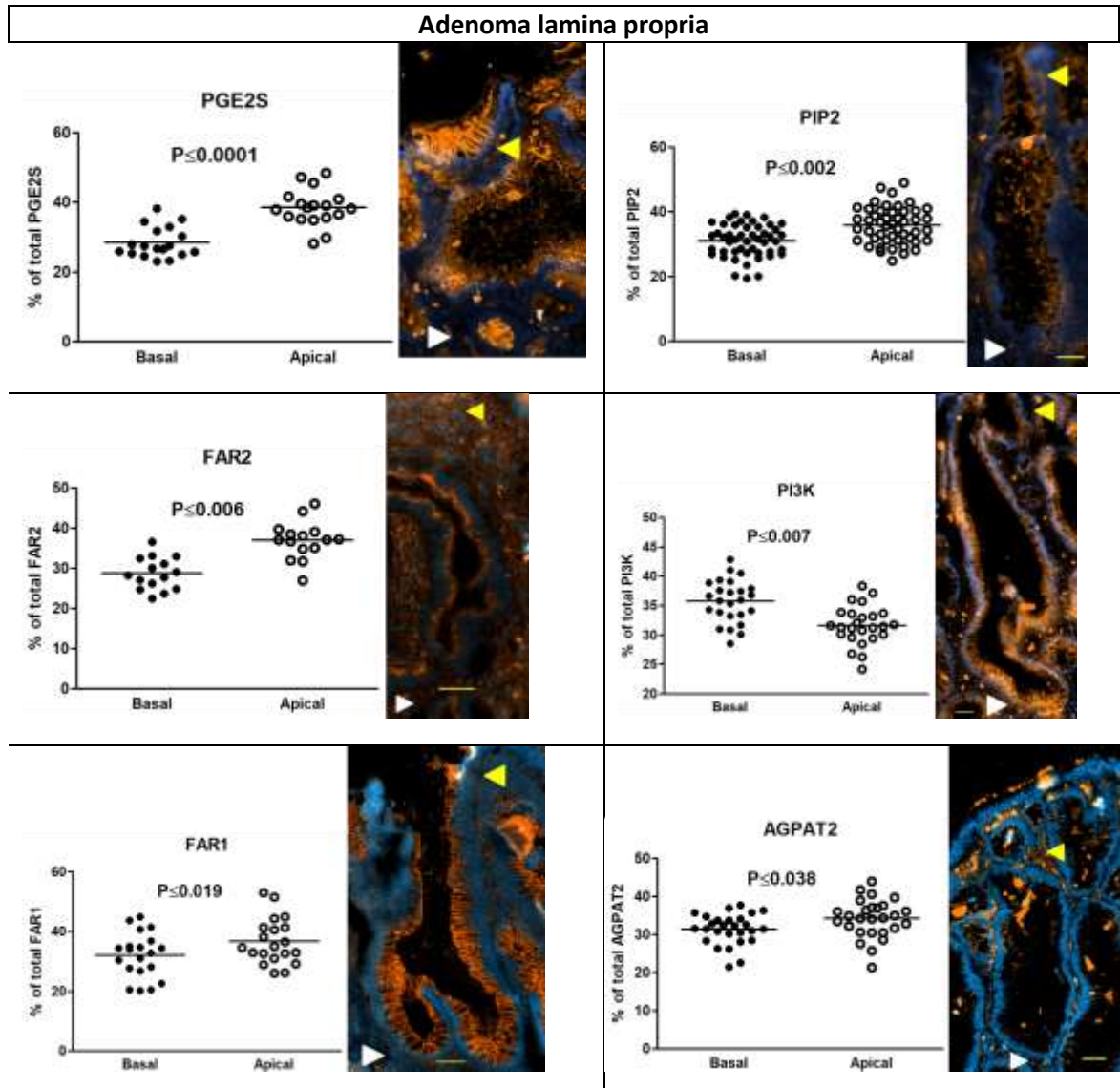


Figure 3-29: Statistical analysis showing a gradual distribution of lipid enzymes along the lamina propria surrounding adenoma colon crypts. Once obtained the IF images, complete crypts were divided into three areas: basal, central and apical as it is described in Experimental procedures. The white arrow points the base of the crypt, while the yellow the luminal site of the crypt. IF values were obtained in at least 12 different sections of 3-4 different patients. Statistical differences were assessed by repeated measurement ANOVAs were computed for IF values using IBM SPSS Statistics 22. Results are reported using a significance level (P-value) of 0.05. PGE₂S: prostaglandin E₂ synthase; Pi3K: phosphatidylinositol 3-kinase; PIP₂: phosphatidylinositol 3 phosphate; AGPAT₂: acyltransferase; FAR 1 and FAR₂, fatty acid reductase 1 and 2. Scale bar= 50μm.

Discussion:

The systematic analysis of the lipidome along specific paths colon tissue depicted in images generated using MALDI-IMS spectra revealed the strict organization of lipid species in both epithelium and lamina propria. Strikingly, AA-containing phospholipids were the species following the most regular distribution patterns along the basal-luminal axis. In the epithelium, lipid composition changed in an orchestrated manner depending on the cell differentiation state, while in lamina propria, it concurred with its characteristic gradient in inflammation^{678,679}. Therefore, these species established an inverse gradient in both tissues, clearly indicating the distinctive role that the same species could play according to the cell type

and, more importantly, to cell context. A previous study in mice described a differential lipid composition along colon crypts using TOF-SIMS⁷²⁸. Unfortunately, the high fragmentation inherent of this technique made impossible the whole molecule reconstruction giving limited lipid information. This definitively hampers the interpretation of the data in the context of the complex lipid metabolism. Other IMS studies on colon lipidome did not achieve enough spatial resolution to observe any gradient^{222,729,730} as they were not able to differentiate between epithelial and stromal cells. Consequently, the present study not only provides a comprehensive description of colon epithelium in terms of phospholipid composition but also identifies regular patterns in lipid distribution implying an organization level that has not been previously described. It is worth mentioning that despite the expected inter-individual variability, the lipid compositional values were very similar between patients. The high reproducibility highlights the robustness of the technique towards experimental variables, such as the amount of matrix deposited and changes in the laser power during the MSI analytical process or differences between sample histological dispositions. Altogether the results presented here, agree with a regulatory mechanism that finely defines the functional distribution of the lipid species. This concept was reinforced by three facts: the gradual variation in the intensity of certain lipid species, the gradient described by enzymes committed to lipid metabolism and the loss of both lipid and protein gradients in a pathological context.

We established that the variation of a defined number of lipid species along crypts could be described using a rather simple mathematical equation ($R^2 \geq 0.7$ – 1.0 for epithelium, $R^2 \geq 0.4$ – 0.7 for lamina propria). All these species were AA-containing phospholipids, PI or PE plasmalogens. We found that 98.5% of PI and 66% of PE plasmalogen species displayed gradual changes in the epithelium, implying that these species are particularly sensitive to the developmental state of the cell. Interestingly, the AA-containing species decrease was compensated by an increase of mono/diunsaturated species.

Consistent with a highly regulated process, gradual expression patterns of lipid enzymes were also found along the crypts, indicating that colonocyte lipid composition is regulated at least at the protein expression level. Despite the current information about multiple enzymes isoforms¹²², is the understanding of how lipid enzymes couple their activity that should reveal lipid regulation processes still not well understood. In this context, we hypothesized that this specificity in phospholipid remodeling could be achieved through the coordinated regulation of PLA₂ and acyltransferase activity. Indeed, in the epithelium, the most prominent gradient was established by the cPLA₂-COX1-PGE₂S axis, which coordinately synthesizes PGE₂. Thus, the robust gradient in SCD1 could explain the gradient of MUFA-containing phospholipids. Interestingly, the distribution of Ca²⁺-dependent PLA₂ coincides with the gradient in calcium ion previously described along the crypt^{731,732}. This would support a gradient in PLA₂ activity along the crypt as the Ca²⁺-independent PLA₂ expression does not change. This activity would hydrolyze AA from the phospholipids participating, together with SCD1, in the fatty acid remodeling process previously described (Figure 1-10). The AA hydrolyzed would be driven to COX1 and PGE₂S for PGE₂ synthesis, which regulates the synthesis and secretion of mucin in mature colonocytes⁴⁰².

These results enlarge the number of proteins that, as nuclear β -catenin⁷³³ or ephrin B2 receptor³⁴⁰, its expression is tightly associated with the colonocytes differentiation process. The gradual changes in lipid enzymes fit with their relatively low substrate specificity. Almost all lipid enzymes do not act over one specific substrate with an on/off mechanism; instead, their action over specific molecular species could be done mainly through the enzyme availability of substrates. Therefore, their regulation occurs mainly through cellular location and presentation of lipids by coupling to other lipid-related proteins. In fact, the coupling of lipid enzymes like ACS4 is a main regulation mechanism for this enzyme activity⁷³⁴. With this in

mind, the gradual differentiation process along colon crypts would be parallel to a gradual supplying of different lipid molecular species to different enzymes along the crypt axis.

Two cell signaling coordinated events may help link the changes in epithelial phospholipid composition and the Wnt signaling pathway, the main regulator of colonocyte proliferation and differentiation program (Figure 3-30). On one hand, upon Frizzled receptor activation, Dvl stimulates both PI4K and PI4P5K by direct interactions, leading to the synthesis of PI-4-phosphate and PI (4,5) biphosphate, respectively^{735,736}. In turn, PI-4,5-P2 is required for Wnt-induced LRP6 phosphorylation, which maintains the Wnt pathway activated, and consequently, stimulating cell proliferation³⁶⁶. On the other hand, PI4K activity was demonstrated to depend on PI fatty acid composition⁶⁷², being higher in the presence of AA and lower in the presence of oleic acid. This activity profile would be in agreement with the attenuation of the Wnt pathway occurring as colonocytes differentiations advances. Thus, it is known that, as differentiation proceeds, Wnt3a becomes less available to colonocytes, while a highly coordinated and yet-to define mechanism, replaces PI 38:4 for MUFA/DUFA-containing PI, poorer PI kinases substrates⁶⁷². All these changes would contribute altogether to the Wnt-proliferative signal attenuation.

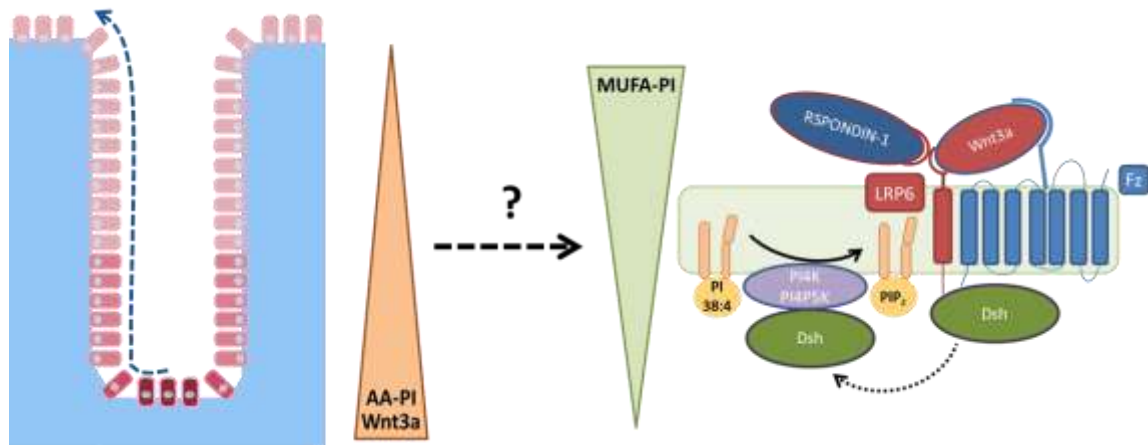


Figure 3-30: A model describing the potential role of PI species turnover in colonocyte differentiation. Wnt3a activates PI(4,5)-P2 synthesis by activating PI-4-K (PI4K) and PI-4-P-5-K (PIP5KI) via Frizzled and Dishevelled^{735,736}. In turn, PI(4,5)-P2 is required for Wnt-induced LRP6 phosphorylation that maintains the Wnt pathway activated. We hypothesize that during differentiation, PLA₂ and acyltransferases act coordinately to replace PI 38:4 for MUFA/DUFA-containing PI, poorer PI kinases substrates⁶⁷² and therefore, decreasing the production of PI (4,5)-P2. The latter, in addition to the gradient in Wnt3a, would contribute to the Wnt-proliferative signal attenuation. Adapted from Qin et. al.⁷³⁵.

Concerning to the lamina propria, the first noticeable result was the high content in AA-containing phospholipids compared to the epithelium (5.6-fold higher), which could be due to the AA proinflammatory capacity and the physiological inflammatory level associated to a healthy colon⁶⁷⁸. Furthermore, we could establish a gradual distribution in lipid species which were almost exclusively associated with AA-containing phospholipids, particularly PE and PC species. Importantly, the AA gradient fully coincided with the gradual distribution of immune cells in healthy colon mucosa, which are frequently found beneath the luminal epithelium, extending down up to a quarter of the way to muscularis mucosae^{678,679}. Hence, we propose that the AA accumulation in PE and PC, the major phospholipid classes in the plasma membrane, is intimately related to the immune response, providing larger AA reservoirs. Consistently, two enzymes strongly involved in the inflammatory response, cPLA₂ and COX2 expression, showed the most robust gradient ($P \leq 0.0001$ and 0.007 , respectively). In line with the gradient in inflammation along the lamina propria, the immunomodulator CB2 receptor showed also a clear gradient ($P \leq 0.005$) with a higher presence surrounding the crypt base. The

presence of an immunomodulatory receptor near the crypt base led to propose a control of immune response at the crypt base to avoid stem cell insults from the immune cells. Conversely, the higher levels of COX1 enzyme in the lamina propria near the crypt base would be consistent with a PG supplementation from stromal cells to the proliferative segment of colon crypts. This would be in agreement with previous reports showing increased intestinal growth with PGE₂ supplementation of intestinal organoids⁷³⁷. These results open the door to investigate thoroughly the changes occurring in lamina propria in the context of the tumorigenic transformation, which may provide new insights besides the already known roles that this tissue has in the appearance and progression of CRC⁷³⁸.

The study of lipid dynamics during colonocyte proliferation and differentiation could shed some light over not only on how the lipid gradual changes are regulated but their function in colonocyte health and disease. With this in mind, the final chapter of this thesis will explore the role of PGs, AA-derived molecules, during colonocyte differentiation. To this, we used mice-derived colon organoids and evaluate the effects of inhibiting their PLA₂ and COX activity simultaneously to PG stimulation.

3.2.2 Prostaglandin signaling in colon proliferation

3.2.2.1 Organoid growth and lipid metabolism.

Using MALDI-IMS and IF assays we revealed the lipid tight regulation in human colon physiology. While colonocytes regulate their lipid composition according to their differentiation state, lamina propria lipids are distributed in agreement to its homeostatic inflammatory tone^{678,679}. In both tissues, the AA-containing lipid and AA related enzymes showed the most regular distribution patterns along the basal-luminal axis. The results showed a fine lipid regulation parallel to lipid-related protein changes and also the loss of both gradients in adenoma context. Altogether these results are in agreement with the subtle regulation of colonocyte cell fate necessary for colon homeostasis²⁹⁵⁻²⁹⁹.

Of the multiple changes observed in colonocytes, highlights the lower expression of AA-PLA₂ and COX enzymes at the crypt base compared to the differentiated colonocytes. Among the COX derivative products involved in colon physiology, PGs participate in intestinal peristalsis and cell survival^{737,739-742}. Unfortunately, there is no knowledge about how PGs distribute and are regulated along the colonocytes crypt axis. In fact, the consistent evidence that PGs are an important stem cell proliferative force^{737,739-742} seems initially contrary to our finding that crypt-base colonocytes present more esterified AA and less COXs and AA-PLA₂ enzymes levels. Therefore, why stem cells would require less mobilization of AA and how this is regulated is an incognita. To study if the protein changes observed in AA-related enzymes participate in the colonocytes proliferation and differentiation process, we study the effects of inhibiting the PLA₂ and COX activities in mouse colon organoids. The use of commercial cell cultures, is unable to reflect the different colonocytes populations present in colon crypts, while colon organoids allow observing the development of crypts with all the colonocytes types present in healthy tissue. Colonocytes organoids are *ex vivo* structures derived from colonic stem cells or colon crypt fragments seeded inside an artificial extracellular matrix. Under certain conditions (especially when stimulated by Wnt3a), the crypt fragments growth to spheroids with the capacity to form new crypts. This model allows evaluating the effects of treatments over colon crypts in a highly reliable way. Once grown for 24h, crypts were treated with cPLA₂GIV, iPLA₂CVI, COX1 and COX2 inhibitors: (arachidonyltrifluoromethyl ketone (ATK), bromoenol lactone (BEL), valeroyl salicylate (VS) and celecoxib (Cel) respectively). The non-toxic effect of each inhibitor at the concentration used was evaluated by visualization of viability (Supplemental figure 5) and by MTT assay at 72h.

The effects of the inhibitors were tested by using commercial kits for PLA₂ and COX activities on isolated mice colon crypts. PLA₂ kit measures the capacity of the sample to hydrolyze labeled PC. The results showed a decrease in the PLA₂ activity of approximately 50% when treatments with ATK (5 μM) and BEL (20 μM) alone or combined were used (Supplemental figure 6, A). The COX activity kit used detects the capacity of the sample to produce a fluorescent product as result of the processing of a labeled COX probe. The COX1 and COX2 inhibitors, VS (0.1 mM) and Cel (4 μM), inhibited around 80% of the total COX activity, either by separate or combined (Supplemental figure 6, B). Higher doses of the inhibitors impaired cellular viability, suggesting that the minimum activity levels for the organoid survival are 50% for the PLA₂ and 80% for the COX respect to the control.

The increase in the organoid size is a reflection of their proliferative capacity; therefore, cultured organoids size was first evaluated by measuring their main area upon 48h.

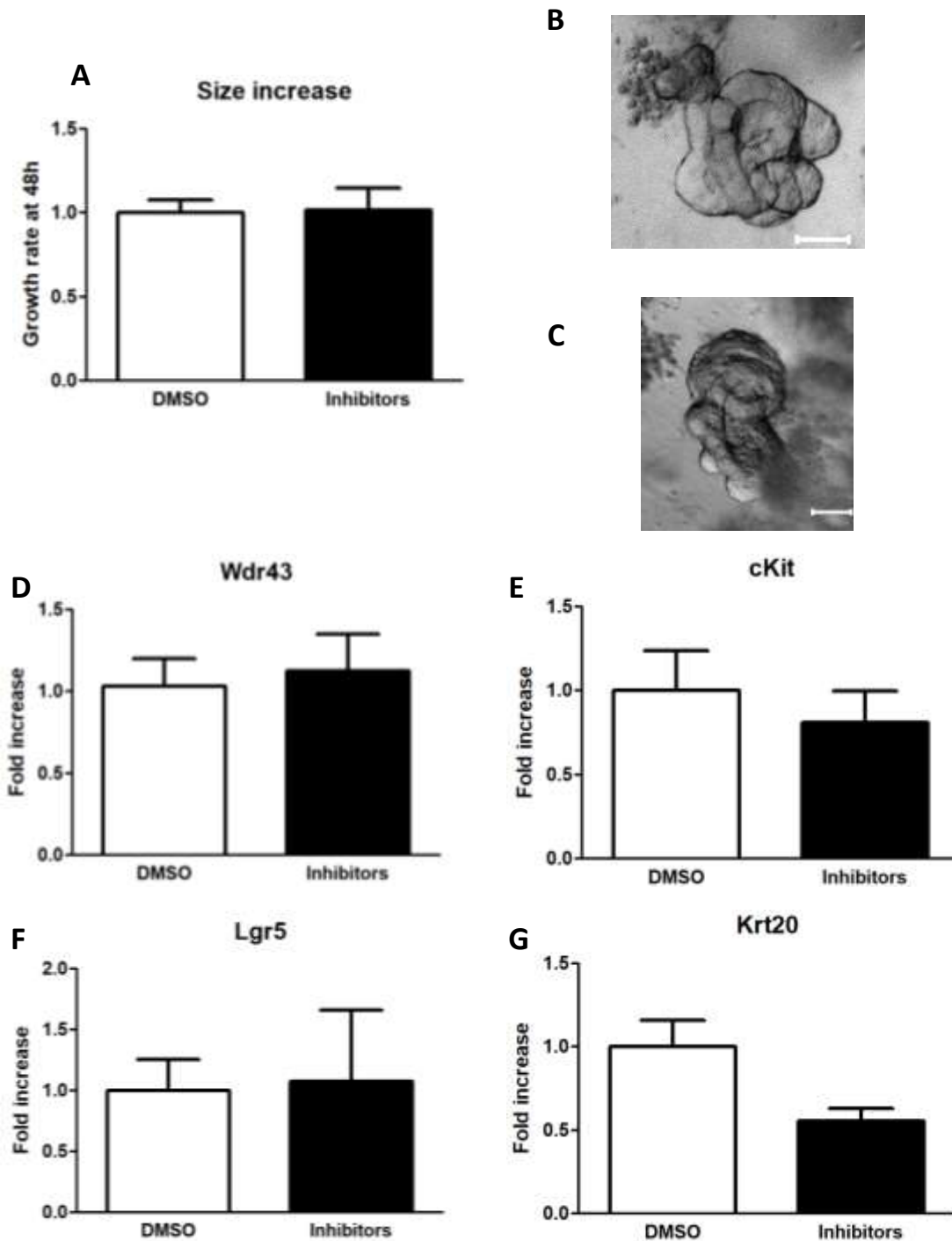


Figure 3-31: Effects of PLA₂ and COX inhibition over mice colon organoid proliferation and differentiation. A) Colon organoid growth. The growth ratio was calculated by dividing the well value at 48h by the mean value at 0h. The experiment was carried out in 8 different animals. Statistical differences were established using one-way ANOVA followed by Bonferroni post-test. **B-C)** Representative images of organoids for each treatment **B)** organoids treated with vehicle, **C)** organoids treated with PLA₂ and COX inhibitors, scale bar= 50 μm. **D-G)** Colon organoid populations assessed by ddPCR. **D)** Wdr43 expression, **E)** cKit expression, **F)** Lgr5 expression **G)** Krt20 expression. ddPCR values are referred to control and represent the mean ± SEM, n=7-3. To assess statistical differences t-test analysis was applied.

At 48h, the vehicle-treated organoids double their size compared to 0h (data not shown). The treatment with PLA₂ and COX inhibitors did not exert any visible effect over the organoid growth rate compared to the control condition (Figure 3-31, A). In addition, taking into account that the differentiation process into multiple cell types keeps the homeostasis of colon crypts, We assessed the effects of the treatments with inhibitors over the colonocytes differentiation process. In this sense, we evaluate four different colonocytes populations by digital droplet PCR (ddPCR). To cover most colonocytes types we quantified the expression of four genes: Lgr5, cKit, Wdr43 and Krt20 (for stem cells, cKit⁺ cells, TA cells, and differentiated colonocytes respectively).

The analysis of the colonocytes populations by ddPCR showed that the PLA₂ and COX inhibition did not exert any visible effect over the cell differentiation process (Figure 3-31 D-G). These results point to another source of COX derivatives able to enhance stem cell proliferation. In fact, the proper proliferation and differentiation of colonocytes require the coordinated secretion of multiple growth factors by the lamina propria (explained in section 1.5). In this context, the higher presence of COX1 in the lamina propria surrounding the crypt base could provide a paracrine eicosanoid supplementation required for a correct colonocyte development. This hypothesis would be in agreement with the COX2 lamina propria gradient focused on the inflammatory role while COX1 would synthesize the PGs necessary for the colon stem cell proper development. This model would mimic the scenario observed in the IF experiments where the colonocytes at the crypt base present less PLA₂ and COX proteins while they are surrounded by a higher presence of COX1 in the lamina propria. With this in mind, next experiments were performed by treating mouse colon organoids with PGF_{2α}, PGD₂, and PGE₂ with or without PLA₂ and COX inhibitors. As in the case of the inhibitors, previous MTT assays proved non-toxic effect of the three PGs tested.

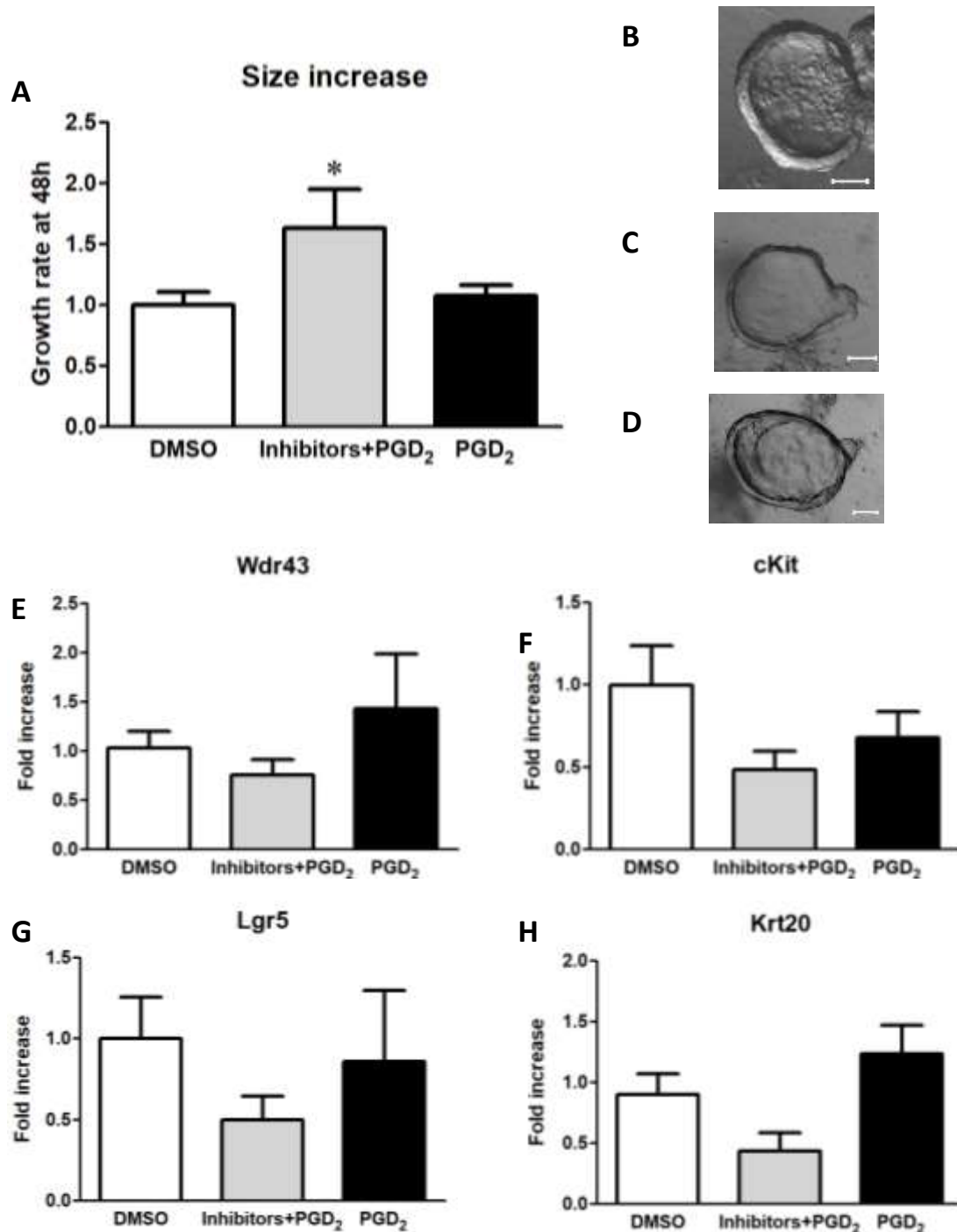


Figure 3-32: Effects of PGD₂ over mice colon organoid proliferation and differentiation. **A)** Colon organoid growth ratio. The growth ratio was calculated by dividing the mean organoid area value at 48h by the mean value at 0h. The experiment was carried out in 8 different animals. Statistical differences were established using one-way ANOVA followed by Bonferroni post-test. Asterisks indicate a significant change: * P<0.05. **B-D)** Representative images of organoids for each treatment **B)** organoids treated with vehicle; **C)** organoids treated with PLA₂, COX inhibitors, and PGD₂; **D)** organoids treated with PGD₂; scale bar= 50 μ m. **E-H) Colonocytes cell phenotypes are not dependent on PGD₂ signaling.** Four different colon epithelial markers were evaluated by ddPCR after treatment with PGD₂ and PLA₂ and COX inhibitors. **E)** Wdr43 expression, **F)** cKit expression, **G)** Lgr5 expression **H)** Krt20 expression. Values are referred to control and represent the mean \pm SEM, n=8-3. Statistical analysis was assessed by One way ANOVA followed by Bonferroni post-test.

The PGD₂ treatment did not increase the organoids size, however, PGD₂ treatment simultaneous to a PLA₂ and COX2 inhibition increased organoids size 1.6-fold respect to control (Figure 3-32, A). Surprisingly, the size increase induced by PGD₂ and PLA₂ and COX inhibition was not reflected by colonocytes markers expression (Figure 3-32, E-H). No PGD₂ treatment or its combination with inhibitors exerted any detectable effect over the possible colonocytes populations.

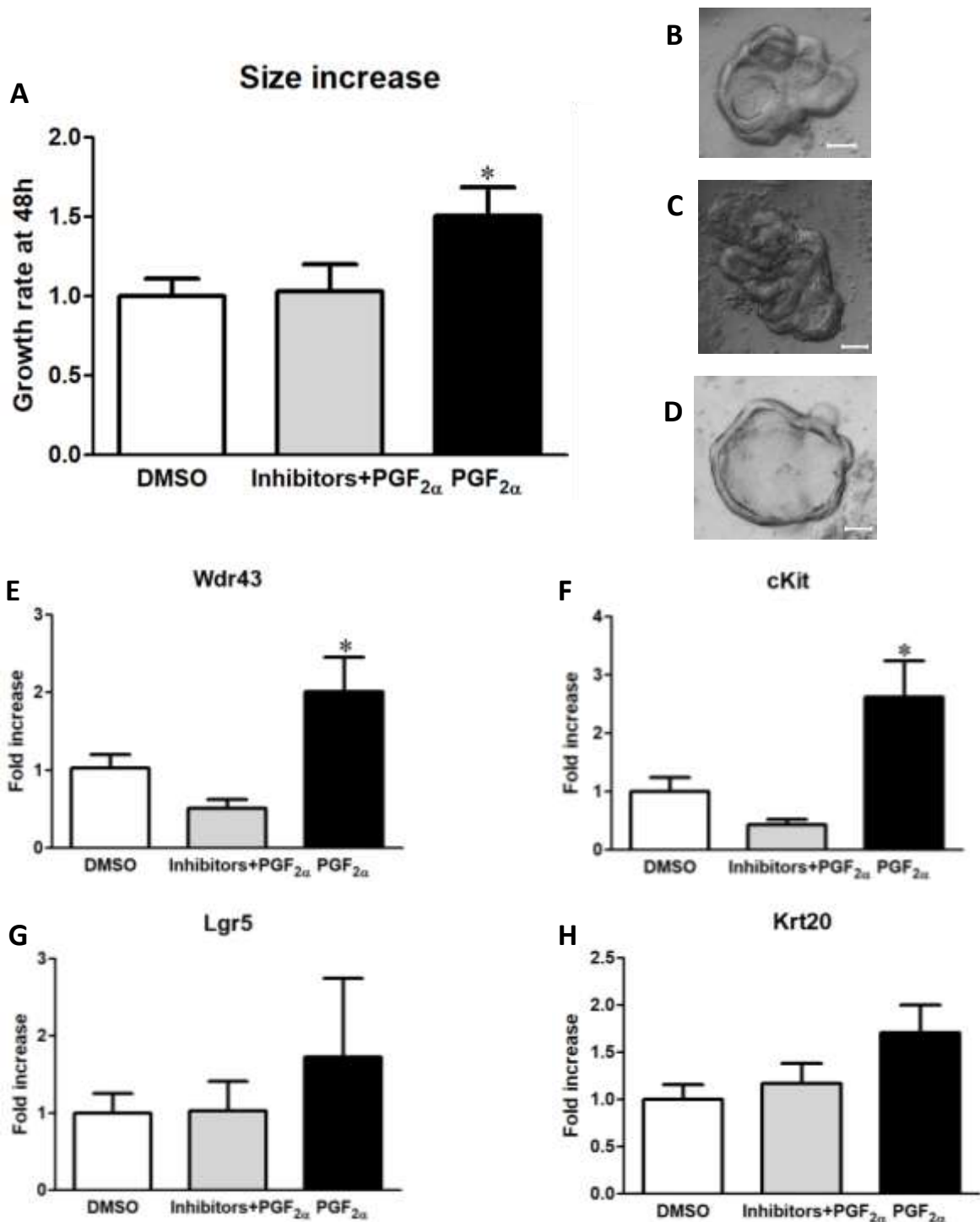


Figure 3-33: Effects of PGF_{2α} over mice colon organoid proliferation and differentiation. **A)** Colon organoid growth ratio. The growth ratio was calculated by dividing mean organoid area value at 48h by the mean value at 0h. The experiment was carried out in 8 different animals. Statistical differences were established using one-way ANOVA followed by Bonferroni post-test. Asterisks indicate a significant change: * P<0.05. **B-D)** Representative images of organoids for each treatment **B)** organoids treated with vehicle; **C)** organoids treated with PLA₂, COX inhibitors, and PGF_{2α}; **D)** organoids treated with PGF_{2α}; scale bar= 50 μm. **E-H) PGF_{2α} is able to modify the colonocytes phenotype.** Four different colon epithelial markers were evaluated by ddPCR after treatment with PGF_{2α} and PLA₂ and COX inhibitors. **E)** Wdr43 expression, **F)** cKit expression, **G)** Lgr5 expression **H)** Krt20 expression. Values are referred to control and represent the mean ± SEM, n=8-3. Statistical analysis was assessed by One way ANOVA followed by Bonferroni post-test.

$\text{PGF}_{2\alpha}$ increased the organoid size 1.75-fold compared to control conditions, however, this effect was reverted when simultaneously are inhibited PLA_2 and COX activities (Figure 3-33, A). The increase in organoid size was not reflected in an increase expression in Lgr5 (Figure 3-33, G). The lack of Lgr5 overexpression simultaneous to a 2.62-fold increase in cKit expression (Figure 3-33, F) suggests a limitation of the cKit cells to secrete functional Wnt3a. In any case, the size increase seems to be mostly due to the increase in TA cells proliferation, reflected by a 2-fold overexpression of Wdr43 marker (Figure 3-33, E). The regression to normal phenotypes upon PLA_2 and COX inhibition could reflect a complex signaling pathway that requires intracellular and extracellular production of PGs.

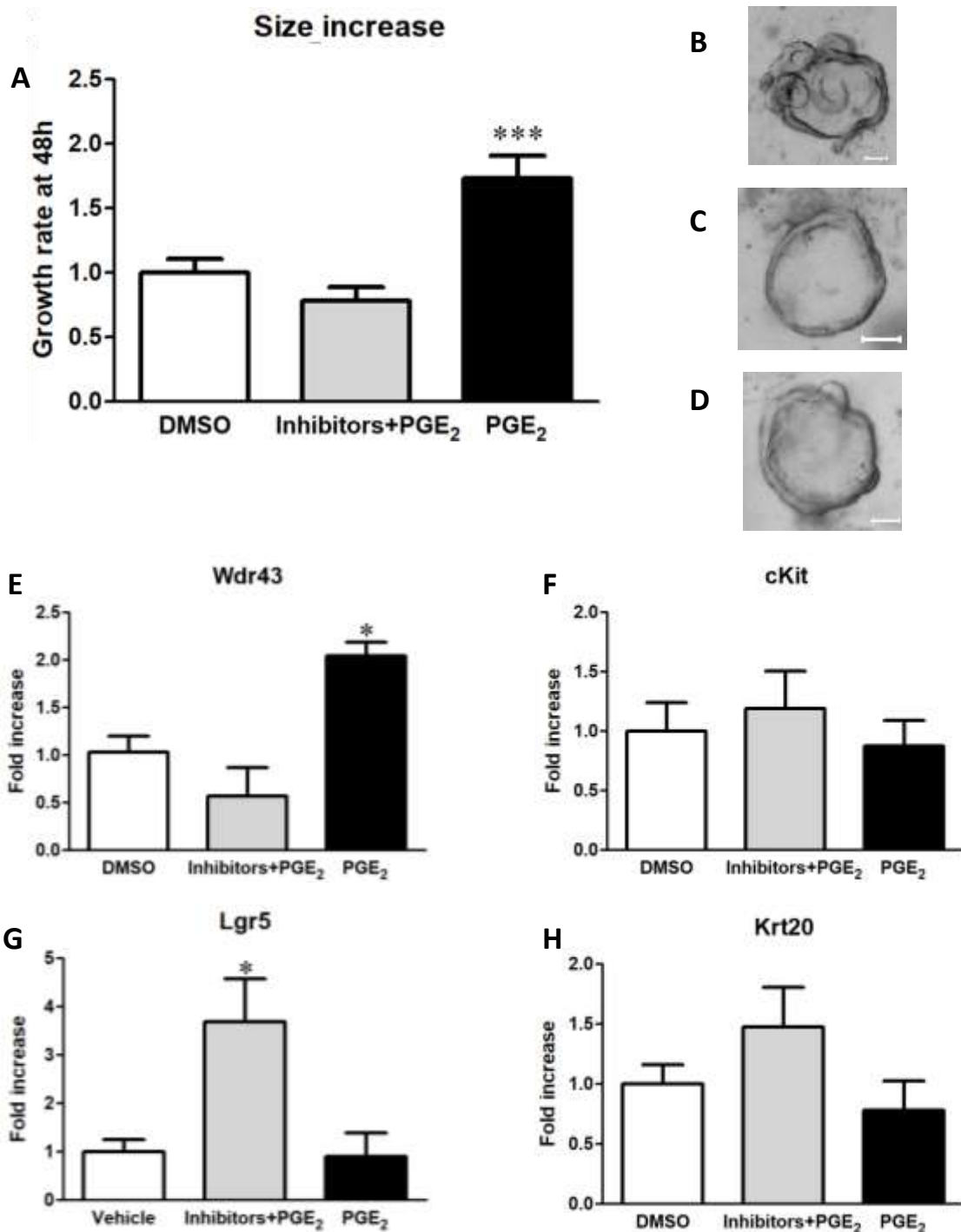


Figure 3-34: Effects of PGE₂ over mice colon organoid proliferation and differentiation. **A)** Colon organoid growth ratio. The growth ratio was calculated by dividing the mean organoid area value at 48h by the mean value at 0h. The experiment was carried out in 8 different animals. Statistical differences were established using one-way ANOVA followed by Bonferroni post-test. Asterisks indicate a significant change: * P<0.05. **B-D)** Representative images of organoids for each treatment **B)** organoids treated with vehicle; **C)** organoids treated with PLA₂, COX inhibitors, and PGE₂; **D)** organoids treated with PGE₂; scale bar= 50 μm. **E-H) PGE₂ signaling is able to modify the colonocytes phenotype.** Four different colon epithelial markers were evaluated by ddPCR after treatment with PGE₂ and PLA₂ and COX inhibitors. **E)** Wdr43 expression, **F)** cKit expression, **G)** Lgr5 expression **H)** Krt20 expression. Values are referred to control and represent the mean ± SEM, n=8-3. Statistical analysis was assessed by One way ANOVA followed by Bonferroni post-test.

PGE_2 did increase the size of the organoids by 1.7-fold respect to the control condition however that increase was counteracted with PLA_2 and COX enzymes inhibition (Figure 3-34, A). In agreement with the organoid size results, PGE_2 did increase the Wdr43 marker by 2-fold (Figure 3-34, E). Surprisingly, PGE_2 alone did not increase any of the other colonocyte populations; however, if it is combined with PLA_2 and COX inhibitors; the markers for Lgr5 were increased, by 3.7-fold. Conversely, cKit^+ cells were not upregulated (Figure 3-34, G and F respectively). This result suggests that PGE_2 not only favors proliferation, but its regulation modulates colonocytes phenotypes.

Figure 3-35 summarizes the outcomes of PGD_2 , $\text{PGF}_{2\alpha}$ and PGE_2 treatments over mouse colon organoids. In summary, the three PGs tested exerted completely different effects over mouse colon organoids.

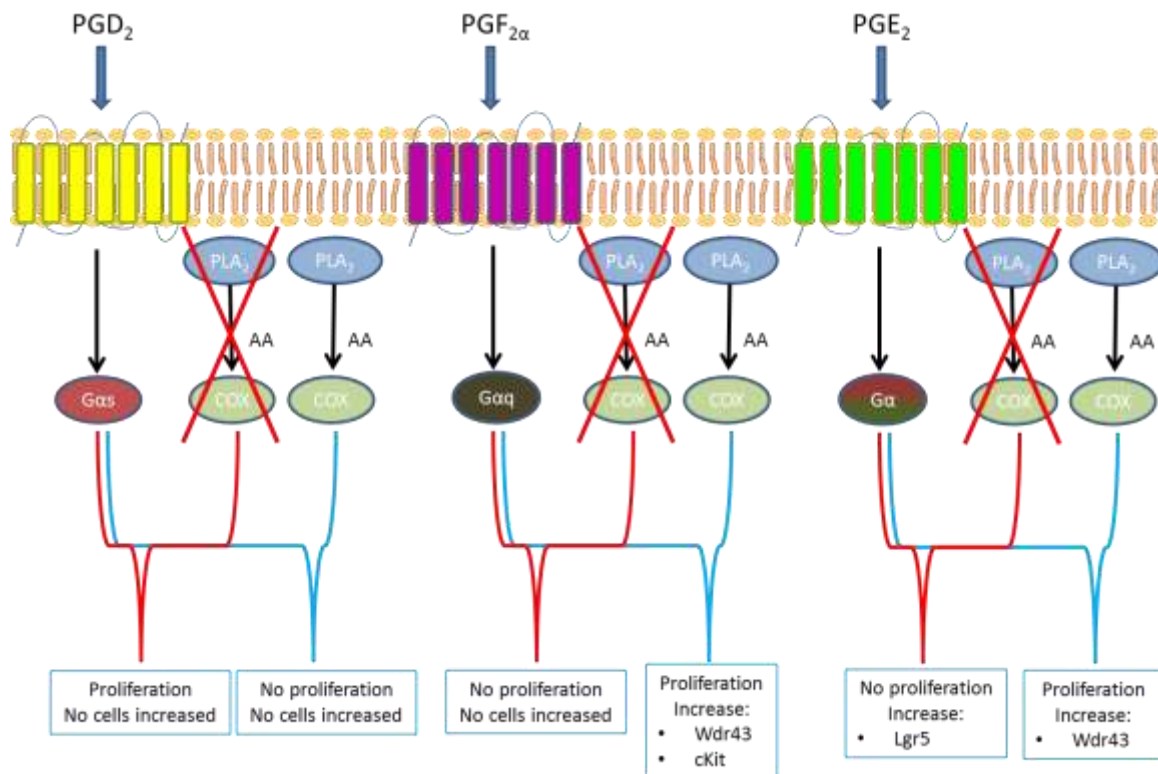


Figure 3-35: Graphical abstract of the effects over proliferation and cell phenotype depending on the prostaglandin supplied and if there is PLA_2 and COX inhibition.

The organoid inhibition of PLA_2 and COX activities did not modulate the colonocytes phenotype. On the other hand, the supplementation of the organoids by different PGs shows a complex scenario where different PGs exert diverse effects upon colonocytes cell fate. These results aware of the use of COX inhibitors to treat colon inflammatory-related diseases. Thus, PGE_2 results showed a complex metabolism where the colonocyte cell populations are heavily dependent on their own PG synthesis capacities. In fact, additionally to PGE_2 supplementation, the inhibition of PLA_2 and COX activities was the only treatment favoring the proliferation of stem cells.

3.2.2.2 Prostaglandin receptors localization in murine colon epithelial cells.

The previous results showed that PGs, depending on if are externally supplemented or generated by the colonocytes, exert different effects on colonocytes proliferation and differentiation processes. This different outcome would fit with a model where the PG

3. Results: Chapter 2: Lipid metabolism in the colonocytes proliferation and differentiation process

signaling triggered from the plasma membrane differs from the intracellular triggered signaling. In agreement with the previous statement, some studies described both COX enzymes at the nuclei and the perinuclear region⁷⁴³⁻⁷⁴⁸. In fact, COX enzymes structures predict their possible location at the lumen of the nuclear envelope and the endoplasmic reticulum⁴³⁶. The particular AA and AA-related enzymes crypt spatial distribution and the differential PG-treated organoids outcome drive us to investigate if intracellular PG signaling could differ from the plasma membrane canonical signaling. First, we investigated the possible presence of PG receptors at colonocytes nuclei. Specifically, we studied the nuclear presence of EP1, EP2, EP3 and EP4, DP and FP receptors in mice colon histological sections. The presence of each receptor was assessed by IF and calculating its colocalization coefficient with the nuclei. In addition, each receptor nuclear presence was assessed by western blot of whole crypt homogenate and nucleus enriched fraction from colon crypts (Figure 3-36).

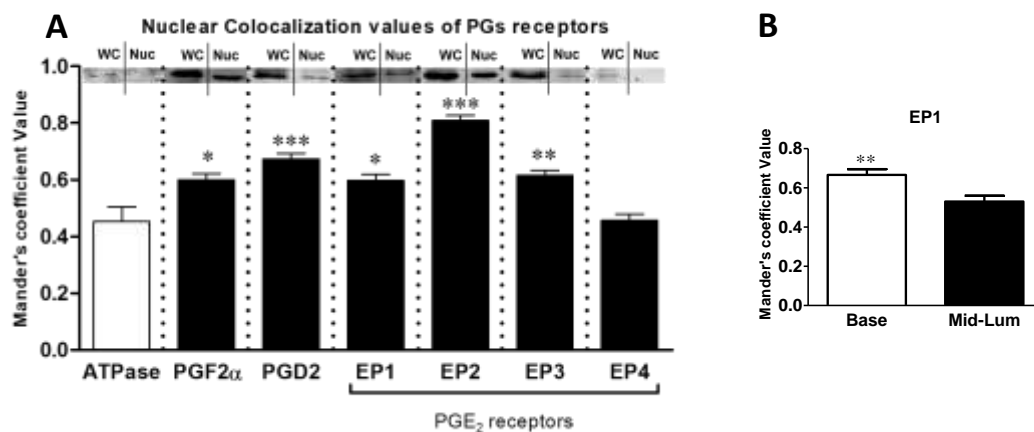


Figure 3-36: A) Mander's coefficient value of different PGs receptors and representative Western Blot of each receptor in whole crypts (WC) and nucleus enriched fraction (Nuc). **B)** Gradual distribution of EP1 receptor along with crypt colonocytes nuclei. Immunofluorescence (IF) experiments were made on NMRI mouse colon. Tissue sections were incubated with primary antibodies for PG receptors (EP1, EP2, EP3 and EP4 (Abcam) for PGE₂, DP (Enzo) for PGD2, and FP (Enzo) for PGF2 α), for ATPase Na⁺/K⁺ as a negative control (Abcam) and with DAPI for nuclei. The images were obtained using a Zeiss confocal microscope and the Mander's colocalization coefficients were calculated using Zen software. Briefly, ROI were manually drawn around the nuclei (10nuclei/crypt, 5 crypts section) in three consecutive sections. The experiment was carried out in 3 different animals. Statistical differences were established using one-way ANOVA followed by Bonferroni post-test. Asterisks indicate a significant change: * P<0.05, ** P<0.001, ***P<0.0001.

IF and western blot analysis showed that all the PG receptors checked except for the EP4 presented colocalization values above the negative control protein (the Na⁺/K⁺ ATPase) (Figure 3-36, A and Supplemental figure 7). Interestingly, the absence of the EP4 receptor in colonocytes nucleus suggests a relevant participation of the membrane EP4 signaling in colonocyte physiology. Thus, the presence of multiple PG receptors at colonocytes nuclei presents a more complex PG pathway than thought before. Furthermore, we assessed if some of these nuclear receptors showed a gradual distribution along the crypts. We found that only the EP1 receptor presents a significantly higher presence at the crypt base nuclei compared with the nuclei at the middle or luminal parts.

The organoid treatment with PGE₂ simultaneous to PLA₂ and COX inhibition was the only treatment overexpressing the stem cell marker Lgr5. On the other hand, the analysis of the PG receptors showed that the only PGE₂ receptor absent at colonocytes nuclei was the EP4. Both results point to the membrane activation of the EP4 receptor as responsible for the stem cell marker overexpression in colon organoids. To asses if the effects of the PGE₂ are mainly due to

effects over this receptor or there is also the participation of other PGE₂ receptors we treated mice colon organoids with the EP4 agonist L-902,688. Thus, we treated the organoids with the EP4 antagonist L-161,982. The toxicity of these compounds was assessed by MTT observing no effects over the colonocytes survival.

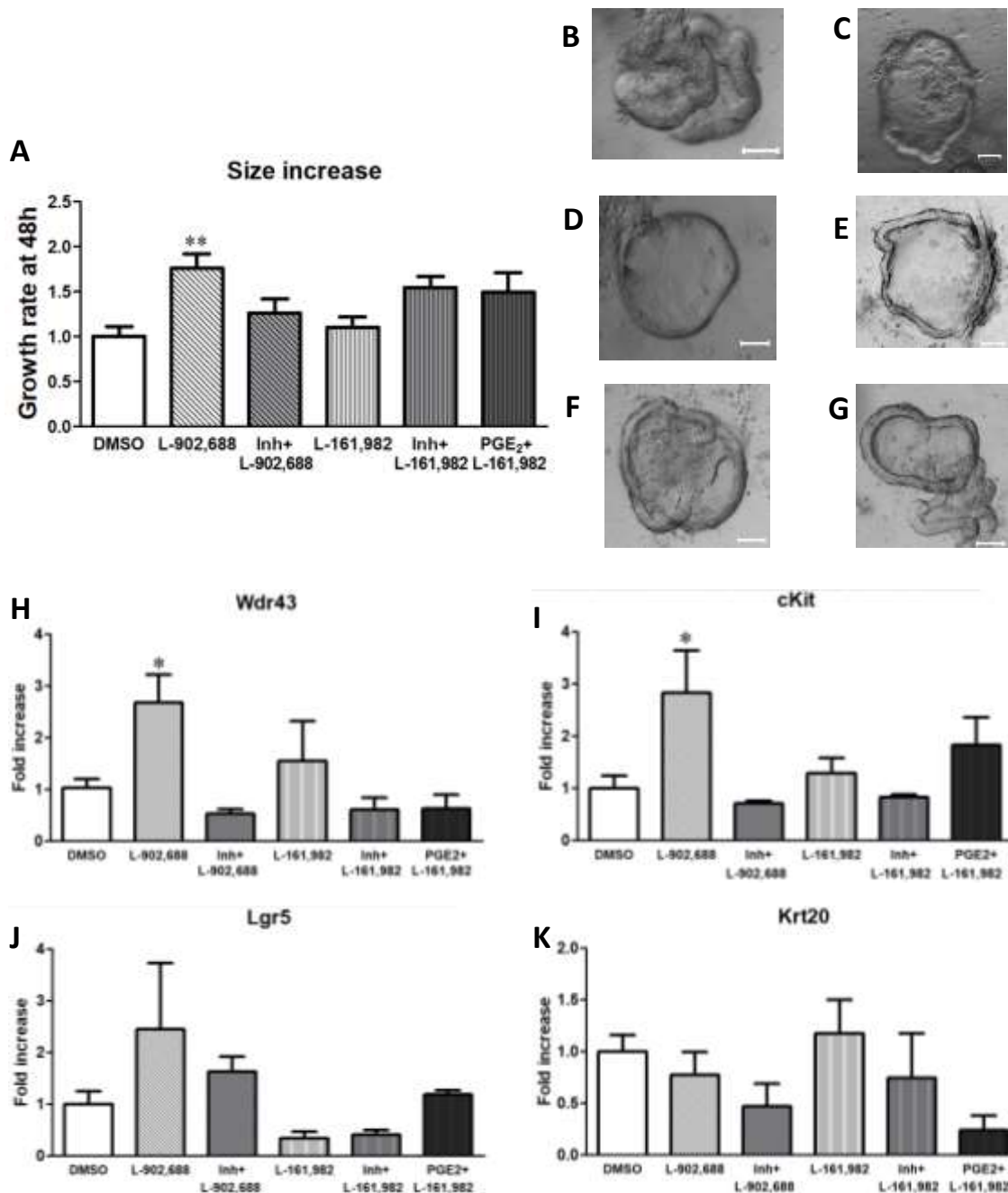


Figure 3-37: Effects of EP4 over mice colon organoid proliferation and differentiation. **A)** Colon organoid growth ratio. The growth ratio was calculated by dividing the mean organoid area value at 48h by the mean value at 0h. The experiment was carried out in 8 different animals. Statistical differences were established using one-way ANOVA followed by Bonferroni post-test. Asterisks indicate a significant change: * $P < 0.05$. **B-G)** Representative images of organoids for each treatment **B)** organoids treated with vehicle; **C)** organoids treated with the EP4 agonist L-902,688; **D)** organoids treated with L-902,688 and PLA₂, COX inhibitors; **E)** organoids treated with the EP4 antagonist L-161,982; **F)** organoids treated with L-161,982 and PLA₂, COX inhibitors; **G)** organoids treated with PGE₂ and L-161,982; scale bar= 50 μ m. **H-K) Modification of the colonocytes phenotype when the EP4 signaling is altered.** Four different colon epithelial markers were evaluated by ddPCR after treatment with PGE₂ and PLA₂ and COX inhibitors. **H)** Wdr43 expression, **I)** cKit expression, **J)** Lgr5 expression **K)** Krt20 expression. Values are referred to control and represent the mean \pm SEM, n=8-3. Statistical analysis was assessed by One way ANOVA followed by Bonferroni post-test.

The EP4 agonist L-902,688 increased the organoid size by 1.7-fold, a similar increase exerted by PGE₂ (Figures 50, A and 53, A). In a similar instance, the inhibition of PLA₂ and COX activities reverse the size increase (Figure 53, A). Treatment with the EP4 antagonist L-161,982 did not change the organoid growth rate. This result shows that EP4 activation is not necessary for epithelial proliferation in the colon, but in any case, increase the proliferation rate upon activation. Besides, the treatment with PLA₂, COX, and L-161.982; and the one with PGE₂ and L-161,982 did increase the size 1.5-fold although not significantly (Figure 53, A). In summary, these results suggest that the size increase effects of PGE₂ are dependent on the cellular membrane EP4 receptor activation. The EP4 agonist not only increased the organoid size at a similar rate than PGE₂ but also increased Wdr43 and cKit expression (Figure 3-37, H and I). These results would strongly suggest that the size increase effects observed when organoids were treated with PGE₂ would be mainly due to its action over the EP4 receptor. For that matter, the stimulation of the EP4 receptor elicits colonocytes proliferation by stimulating the TA cells without affecting the stem cell population. Figure 3-38 summarizes the results of the PGE₂ and EP4 treatments outcomes.

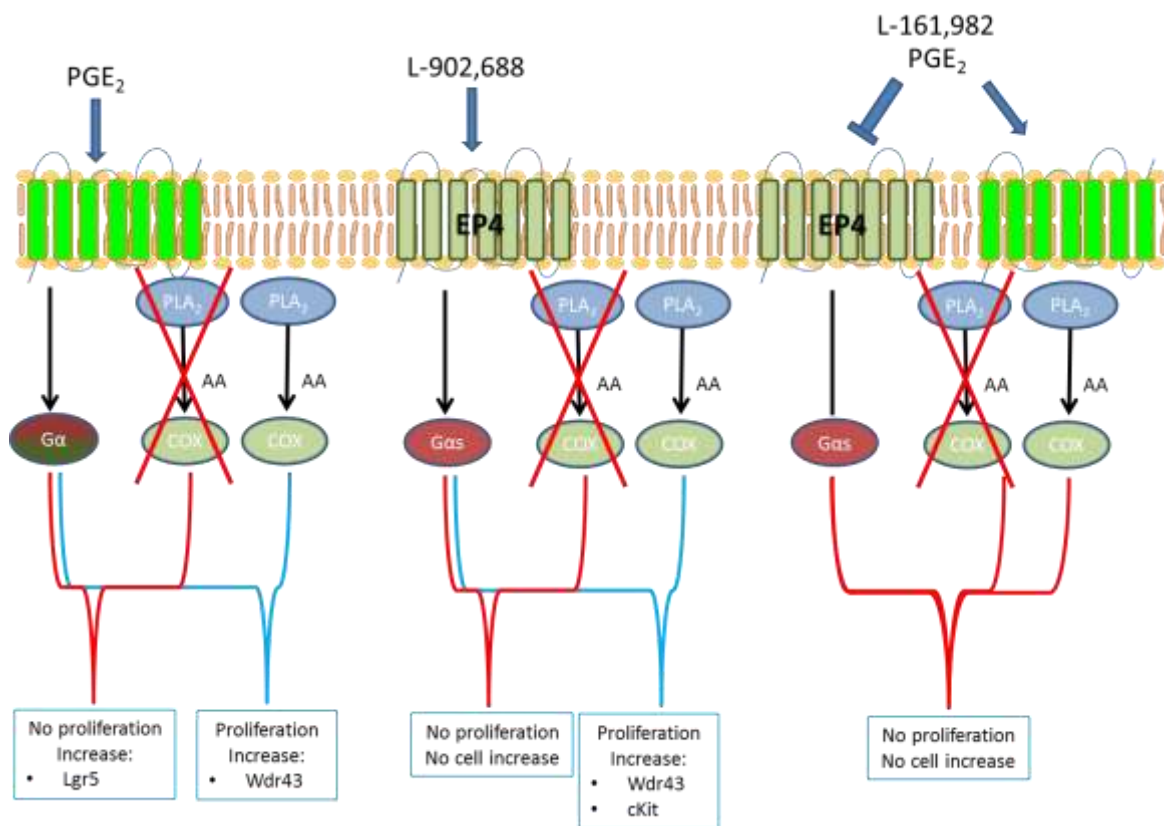


Figure 3-38: Scheme of the effects of the different treatments involving EP4 agonist and antagonists.

Therefore, the stem cell phenotype observed in epithelial cells of the colon seems to be due thanks to the stimulation of other EP receptors concomitant with intracellular PLA₂ and COX activity inhibition.

Discussion:

The colonocytes differentiation process requires the coordinated activity of multiple signaling pathways allowing a controlled proliferation rate of colonocytes. These pathways are mainly controlled by the lamina propria; which secretes multiple growth factors in a gradual manner along the crypt axis²⁹⁵⁻³⁰². The MALDI-IMS and IF results showed in section 3.2.1

suggested that besides the already described growth factor communication, lipid mediators secretion could participate in this differentiation process. In this scenario, the crypt basal cells (stem and cKit⁺ cells) would generate relatively low amounts of eicosanoids reflected on their lower levels of PLA₂ and COX enzymes, regardless of their higher amount of AA-containing phospholipids. Thus, the eicosanoids produced through COX1 expressed at the lamina propria surrounding these cells would provide the eicosanoids necessary for a proper crypt development. Therefore, the modification of the PG signaling in colon organoid model would be able to stimulate the stem cells, located at the crypt base niche. The assessment that five of the six PG receptors tested were present at the colonocytes nuclei already suggest a differential function of these receptors depending on their location. In addition, the treatment of organoids with different PGs with or without PLA₂ and COX inhibition exerted completely different effects depending on the PG tested.

The study of the location of six different PG receptors revealed the presence of most of them in various cell locations. The redundant presence of these receptors could imply different PG effects depending on the site of action. Interestingly, most lipid-related enzymes, due to their low enzymatic specificity, regulate their activity through functional coupling to substrates and locations^{131,208,209}; a mechanism that seems to be shared for the PG synthesis and signaling inside the cell. However, how this coupling is regulated and which specific mechanisms activate are questions to be answered. In addition, we still ignore the possible interactions between the different PG signaling pathways and between the PGs and the other colonocyte proliferation and differentiation pathways like the driven by Wnt3a. In this context, determining the role of the intracellular PG receptors would probably share light over the multiple effects of these COX derived molecules.

Despite being described the participation of PGE₂ in the mature colonocytes mucin secretion⁴⁰², any the organoid treatments increased the colonocyte differentiation marker Krt20. These results suggest that the PG signaling is not implicated in the development of a differentiated colonocyte phenotype. On the other hand, we described that the supplementation of the organoids with PGF_{2α}, PGE₂ or the EP4 agonist L-902,688 increased the organoid proliferation rate, reflected in the organoid size increase. In addition, the bulk of proliferation was parallel to significant overexpression in the TA cells marker Wdr43. The proliferation of these cells is done in an Lgr5 independent activation way²⁵⁶. Interestingly, any of the size increasing treatments increased also the stem cell marker Lgr5. This reflects that while stem cells proliferate steadily renewing the epithelium, the rapid proliferating TA cells are the ones in charge to derive into the different phenotypes of the colon (enterocytes, goblet cells, and enteroendocrine cells)²⁵⁶.

PGD₂ is able to bind two receptors, DP and CRTH. Despite both receptors are GPCR, DP is G_{αs} while CRTH is a G_{αi} type. Therefore, PGD₂ is a puzzling signaling pathway with two opposite receptors described so far. However, to our knowledge there is no study describing the presence of the CRTH receptor within colon mucosa, therefore, the effects of PGD₂ over colon organoids were attempted to be understood assuming its signaling through the DP receptor. DP activation should lead to proliferation through the increase in cAMP, although some works addressed an opposed effect in CRC cell lines⁴⁷⁸. Our treatment of organoids with this molecule led indeed to some puzzling results. PGD₂ alone did not increase the organoid size and did not change any cell marker tested. Nevertheless, in the presence of PLA₂ and COX inhibitors, the PGD₂ treatment increased the organoid size without changing any cell population.

It is difficult to explain how the organoids increased their size without affecting any of the cell populations, especially when the condition necessary implies inhibiting the endogenous PLA₂ and COX activities. This result suggests that the exogenous PGD₂ stimulation simultaneous to PLA₂ and COX inhibition stimulates colonocytes proliferation regardless of

their differentiation state. How this receptor is able to stimulate proliferation without affecting the cell fate in the colon is still an incognita to be answered.

PGF_{2α} receptor is G_{αq} type, which should increase proliferation through PKC phosphorylation of CREB. Indeed, organoid treatment with this molecule led to organoid size increase and overexpression of the TA cells marker, a result in agreement with previous reports where PGF_{2α} increased proliferation in epithelial tumors⁴⁸⁷. Interestingly, this PG also increased the cKit⁺ cell population. Given the necessity of Notch inhibition for a correct cKit⁺ cell population development³¹⁴ is tempting to suggest a regulation of PGF_{2α} over this signaling pathway. Upon activation, Notch receptors are proteolyzed, the free cytoplasmic fragment is a transcription factor^{749,750} able to enhance enterocytes differentiation³⁰¹. EGF is able to antagonize Notch signaling⁷⁵¹, thus, knowing that EGF can be released indirectly by GPCRs is possible that the cKit overexpression would be due thanks to an indirect EGF release. Paradoxically, the increase in cKit⁺ cells did not increase the stem cell population questioning the capacity of these accompanying cells to secrete functional Wnt3a in intestinal physiology, an idea already explored by other authors^{314,752}.

In any case, the inhibition of the epithelial PG synthesis by PLA₂ and COX inhibition reversed any detectable effect over the organoid growth and cell differentiation. This latter result reinforces the idea that endogenous PG synthesis and signaling are necessary for a correct PGF_{2α} stimulation.

To complicate even further the scenario, PGF_{2α} is able to stimulate also EP1 and EP3. EP1 and EP are G_{αq} receptors and therefore a cross-activation should not have in principle divergent effects. Conversely, EP3 is G_{αi}, therefore its activation should inhibit the adenylate cyclase and its subsequent effects over stimulation. Anyhow, the clear increase in proliferation suggests a small effect of the EP3 receptor upon colon organoid PGF_{2α} stimulation.

PGE₂ receptors comprise all three GPCR types, being the EP2 and EP4 receptors stimulators of the adenylate cyclase, the EP3 receptor an inhibitor, and the EP1 a PKC activator. These even contradictory pathways complicate the understanding of how this PG acts, especially in cells like colonocytes which express all receptors. That level of complexity escalated with the description of the presence of EP1, EP2, and EP3 at colonocyte nuclei. As happens with PGF_{2α} conditions, treatment of the organoids with PGE₂ increased their size, an effect counteracted if PLA₂ and COX activities are, in addition, inhibited. However, the cell phenotypic outcome is completely different, as PGE₂ did not overexpress cKit, and simultaneous inhibition of PLA₂ and COX increased colon stem cell marker. Interestingly, PGE₂ treatment simultaneous to PLA₂ and COX inhibition mimics the conditions already described by MALDI-IMS and IF, where the crypt base cells present less PLA₂ and COX but are accompanied by a higher presence of COX1 in the lamina propria nearby.

EP2 and EP4 are G_{αs}, a GPCR type directly related to nuclear β-catenin signaling through destruction complex disengaging⁴⁹⁵, and therefore are the most likable candidates to overexpress Lgr5. EP4 activation through its antagonist L-902,688 increased not only the organoid size but also TA and cKit⁺ cell markers. Like the situation with PGF_{2α}, the simplest explanation for the organoid size increase was the parallel overexpression of Wdr43. However, is intriguing again why the increase in cKit⁺ cells did not stimulate the stem cell phenotype and question the effectiveness of these cells to secrete Wnt3a as previously described^{314,752}. As EP4 stimulation simultaneous to PG synthesis inhibition was unable to stimulate Lgr5 expression, therefore PGE₂ stem cell proliferation seems to be a consequence of EP2 exogenous supplementation. However, the implication of PGE₂, and more specifically, EP2 signaling in the Wnt3a colonocytes stimulation requires further investigations.

An alternative explanation of these results could imply the β-catenin stabilization through GSK3b phosphorylation produced by the βγ heterodimer⁴⁹⁵. However, as all GPCR are able to stimulate the βγ signaling, is unlikely that this is the leading pathway in Lgr5

overexpression upon PGE₂ stimulation. Other explanations could include a synergistic inhibition of intracellular EP1, EP2, and EP3, although such complex interaction seems less probable that the participation of just one receptor. In any case, it is still an incognita if the mechanism of the stem cell increase is related to their direct proliferation of instead just favors the secretion by the cKit⁺ cells of other growth factors like Wnt3a. Figure 3-39 summarizes the model proposed for stem cell stimulation in colon crypts.

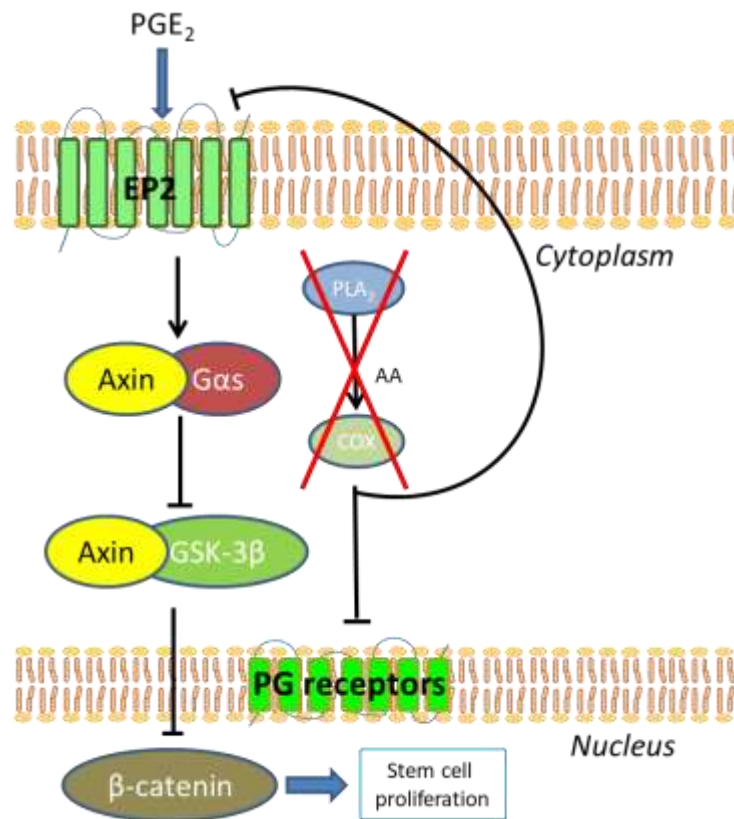


Figure 3-39: Scheme of the effects of the proposed model different treatments involving EP4 agonist and antagonists.

The treatment of mice colon organoids with different PGs led us with the conclusion that each one tested exerted divergent effects over proliferation and differentiation. Previous studies in colon cancer already showed different effects of the three PGs regarding cell proliferation. PGD₂, despite being considered pro-inflammatory inhibits slightly the proliferation of CRC cell lines⁴⁷⁸. Conversely, many works had related PGF_{2α} as a factor increasing angiogenesis, proliferation, migration, and invasion in various tumor types^{400,487,490}. The PGE₂ signaling is more complicated due to the existence of four different EP receptors, each one participating differently in colon cancer progression. EP1 and EP3 showed small effects over CRC proliferation, while some studies exposed their pro-proliferative properties^{497,511} others showed anti-proliferative capacities of these receptors^{497,512}. The role of EP2 and EP4 seems more consistent as stimulators of tumor progression^{363,413,415,500,501,504}. In addition to these shreds of evidence, this work suggests a scenario where endogenous PG synthesis could also regulate cell fate and proliferation capacities by complementing the exogenous PG supplementation.

Unfortunately, the limitations of the study make unable the presentation of solid conclusions about the specific roles of each PG in the context of colonocytes proliferation and

differentiation. One of the most capital obstacles was that the inhibition of PLA₂ and COX enzymatic activity was not complete, and therefore we cannot discard the participation of endogenous PGs in the signaling. In order to overcome this specific limitation, we should first ascertain where each endogenous and exogenous PG mainly acts.

Regardless of the multiple works addressing the role of PG receptors over tumor progression, there is little knowledge about their roles in cell metabolism. The results showed here reveal the importance of knowing the roles of the different PGs in different contexts. In fact, the results showed here present a model where the use of COX inhibitors to treat pathological conditions with an inflammatory component is an oversimplification of the PG signaling as ignores their diverse consequences over healthy cell physiology. Thus, despite being a promising approach to treat tumor development, COX inhibitors like the NSAIDs presented too many relevant side effects to be a viable antitumor tool^{404,543-550,556,559-561}. Perhaps, future treatments over specific COX products and their receptors could treat the noxious components of diseases with inflammatory components minimizing the undesired side effects of inhibiting COX activity.

GENERAL DISCUSSION

4 General discussion

With nucleic acids, sugars, and proteins, lipids are one of the basic molecules for life. Their hydrophobic or amphipatic properties give them multiple functions essential for life as bioactive molecules, energy reservoir, and membrane components. Their participation in main cellular processes could set the base for therapeutic targets and sensitive biomarkers. This work uses the colon context to study differentiation processes and tumor detection in the context of CRC.

The chapter 1 of this thesis explores the capacity of the lipidome of being used as a CRC biomarker.

The subtle lipid regulation during the epithelium differentiation process showed in this study reveals new dimensions in the role of lipid species in cell physiology. The outcome of this work breaks with the general belief that the membrane lipids are roughly regulated with the only role of separating the different cell compartments. Instead, we showed that the presence of many lipid, regardless of its relative amount and its known function, is exquisitely defined according to the cell type and to cell physiological state. Thus, the lipid composition is highly sensitive to the metastatic state of cells to the point that the lipids in their derived EVs are able to be stratified according to their origin. This latter fact was translated to the clinical field, where we proved that the lipidome of plasma-derived EVs stratifies a relevant population of patients with dangerous tumors.

In the last years, EV content had received more attention. These vesicles are relatively easy to isolate and do not require invasive techniques in order to isolate them. In line with this strategy, we analyzed the lipid content of these vesicles in order to reveal their possible use as non-invasive biomarkers.

In a first approach, we analyzed EVs isolated from CRC cell lines and compared their lipidome with primary colon cell culture from healthy tissue. Lipid analysis of these vesicles revealed that their lipid content is specific enough to separate them according to their cell of origin. The comprehensive lipid analysis showed a clear impoverishment on the EVs lipidome of the tumor cells, especially the *in situ* tumor cells, compared to the primary cells-derived EVs. The lipid classes analysis showed a clear increase in PC and decreases in PE, PI and Cer lipid classes in tumor cells. Further analysis of the molecular species revealed a general shift from PUFA-containing species to MUFA- and DUFA-containing ones. This general behavior was kept in plasma-derived EVs from patients submitted to colonoscopy. In the patients derived EVs, there were no differences between patients groups using just the lipid class composition. However, a comprehensive analysis of lipid plasma-derived EVs showed that lipid species composition was unable to discriminate between the different patient groups. However, as in cell-derived EVs, there was a clear tendency to increase PUFA-containing species in patients with adenomas and neoplasias compared to the healthy ones. Specifically, the major changes were in AA-containing species in detriment of MUFA-containing ones. The further exploration of this phenomenon showed that the relative amounts of 34:1 and 38:4 species as a promising lipid measurement for patients stratification. Although not discriminating between all the patients analyzed, most of them were correctly classified by their 34:1/38:4 ratio and a subgroup of adenoma and invasive neoplasia patients with a very low ratio was revealed. In summary, the EVs lipidome seems a future useful tool to stratify patients wich would require further diagnostic tests like a colonoscopy.

In addition to non-invasive biomarkers, this work explored the lipid changes that occurred in colon cancer cells isolated from different stages of the disease and in tissue biopsies by MALDI-IMS. Indeed, lipid composition was sensitive enough to discriminate between healthy primary cells and CRC cell lines. Clear differences were perceived within lipid

classes, especially by PE and PE plasmalogen relative abundance, with a clear shift to PE plasmalogens class seemingly coming from PE in the cancer cells. Further analysis of lipid molecular species revealed a general increase in PUFA-containing phospholipids to the detriment of MUFA and DUFA in tumor cells compared to the primary ones. Thus, lipid class changes were highlighted when lipid molecular species distribution between lipid classes was studied. Distribution of PUFA-containing lipids showed a pronounced shift from PE and PC species to PE plasmalogen species in tumor cells compared to primary cells. That shift was specific of molecular species with saturated fatty acids at the sn-1 position while species with 18:1 at sn-1 position (18:1/22:6 and 18:1/20:4) did not show that shift. Further analysis showed that indeed, the rate-limiting enzymes in charge of synthesizing the fatty alcohols required for plasmalogen synthesis were disturbed in colon cancer cell lines.

Cell results from comprehensive lipidome come up with new clues of how metastatic processes could require specific lipid changes that we could exploit as biomarkers and/or therapeutic targets. To assess the applicability of those results we also analyzed colon healthy and adenomatous mucosa by MALDI-IMS. The lipid distribution provided by MALDI-IMS discriminates clearly between the different tissues present in colon mucosa: epithelium, lamina propria and muscularis of the mucosa. Additionally to the mean lipid composition, the application of k-means clustering to the images separated the epithelium in two segments and the lamina propria in three. The two epithelial segments correspond in fact to the base and the luminal site of the crypts, mirroring the differentiation process present in colon crypts. Furthermore, the segments generated in the lamina propria could correspond to the physiological inflammatory state of this tissue. To understand better how the lipidome reflects proliferative pathologies we verified whether the lipid composition reflects the pathological disarrangement produced in colon adenomatous polyps (AD), the most common colon lesions leading to CRC⁷⁵³. Despite being estimated that only 5 to 10% of adenomas undergo invasive lesions⁷⁵⁴, AD are considered to be the precursor lesion for approximately 60-70% of carcinomas that arise via the “adenoma-carcinoma” pathway described in 1990^{293,755}. The MALDI analysis over adenomatous mucosa showed the inability of the k-means analysis of separating different compartments, reflecting the undifferentiated state of the tumor epithelial cells. In addition, when the adenomatous epithelial lipid composition was compared to the healthy clusters, the analysis showed a similar lipid composition between the healthy basal epithelial cells and the adenomatous epithelium. As the healthy colon stem cells reside at the bottom of the crypt, this similar lipid composition is in agreement with the dedifferentiated state of both healthy and adenoma cells.

By taking advantage of the sensitivity of the lipidome to the physiological state of the cells, the first chapter of the thesis showed multiple changes in the tumor transformation of the colon. Among the changes detected, highlights the increase in PUFA content by the tumor cells compared to the healthy ones. On the other hand, the analysis of EVs revealed the possibility of using its lipid analysis as a non-invasive diagnosis tool. In this context, the ratio between the 38:4 and 34:1 species stand out as a stratification tool for at least a population of patients with adenoma or invasive neoplasia.

The second chapter of this thesis explores the fine distribution of the lipids along with the colon tissue and the possible lipid mechanisms implicated in the colonocytes proliferation and differentiation processes.

In the second chapter of the thesis, we explored thoroughly the MALDI-IMS results presented already in section 3.1.3. The description using a mathematical equation of the gradual distribution of lipid species implies that based merely on its lipid signature, it is possible to predict and assess the pathophysiological status of a single cell within a tissue. Taking into account that this was demonstrated in human tissue, the translational impact that lipid image fingerprint may have in the clinical field is clearly reinforced. In addition to those

results, the IF characterization of the lipid-related enzymes presented a complex scenario where AA-derived molecules would play important roles in colon physiology. The results showed in section 3.2.1 set the base for the experiments where we revealed the divergent effects of the endogenous and exogenous supplementation of three different PGs.

The analysis of the images pixel by pixel along the colon mucosa axis revealed a gradual distribution of the AA-containing phospholipids at the epithelium and within the lamina propria. The lipids presenting the most gradual distribution were the PE plasmalogen and the PI species. In the epithelium, the gradient was in agreement with the differentiation state of the cells, being the cells present at the base of the crypt (stem and cKit cells) the ones presenting higher levels of these lipids. The gradual decrease in AA-containing phospholipids was compensated by MUFA- and DUFA- containing phospholipids according to the proximity to the colon lumen. Both AA and MUFA/DUFA gradients fitted into lineal or logarithmic equations, reflecting the tight regulation of the lipids to the differentiation state of the colonocytes. In a similar way but inversely, the lamina propria presented also an AA gradient, although in this case, the lower concentration of these species was found at the basal side of the mucosa. Also, the MUFA/DUFA species compensate for the increase of AA-containing species towards the lumen. In addition, the enzymes related to the metabolism of these lipids showed also a coordinated distribution along the colon epithelium and lamina propria. Conversely, the lipid and enzyme gradients were completely lost in the context of adenoma tumors. These analyses showed the fine lipid regulation parallel to the colonocytes differentiation state and to the inflammatory state of the healthy colon.

The MALDI and IF analysis of the colon mucosa showed a colon stem cell lipid profile with high levels of esterified AA species and relatively low levels of enzymes able to metabolize them. In order to understand better the regulation of the AA in colon crypts, we modified its metabolism by using chemical inhibitors with or without exogenous supplementation of PGs. The analysis of the proliferation and differentiation of the colonocytes showed diverse effects for each of the three PGs tested (PGD₂, PGF_{2α}, and PGE₂). Among the effects visualized, the only treatment increasing the population of stem cells was the treatment of PGE₂ simultaneous to PLA₂ and COX inhibition. To further explore the mechanism of this stimulation we checked the possibility that colonocytes present PG receptors in the nuclei besides the plasma membrane. Of all the receptors checked, the only one not present in colonocytes nuclei was the EP4. Therefore, we studied if was the activation of the EP4 simultaneous to the PLA₂ and COX inhibition the responsible for the increase in the stem cell marker. As both EP2 and EP4 are the only receptors which signaling could be related directly to the nuclear location of β-catenin, the main proliferation and differentiation factor in colonocytes we proposed a model compatible with our results able to explain the stem cell increase. In this model, would be the exogenous stimulation of EP2 coincident with the inhibition of the endogenous PG signaling, the stimulus which could favor the stem cell proliferation. Unfortunately, the lack of inhibiting completely the PLA₂ and the COX activities limit the extent of the conclusions. The remaining PG synthesis capacity of the organoids was probably stimulating the colonocytes receptors to a different extent. Next experiments should be addressed in order to know the specific roles of each plasma membrane and intracellular PG receptor. In addition, there is still the question of the possible interaction between the different PG signaling pathways and the other differentiation driving pathways like the Wnt in the colon. In any case, the demonstration that the modification of the PG metabolism can affect the colonocytes proliferation and differentiation capacities opens the gate to study these receptors as more specific targets for inflammatory-related diseases.

The thorough characterization of the colon in healthy and tumor conditions set the base to study important cell processes like proliferation and differentiation. The understanding of the mechanisms underlying the membrane lipid composition will be able to delve into the

cellular processes that lead to cancer. This thesis is a clear example of how the lipid composition study is a powerful research tool with high potential to detect useful biomarkers and effective therapeutic targets.

CONCLUSIONS

5 Conclusions

1. The lipidome is clearly affected during the cell malignant transformation. The changes described herein depend on the model of study (commercial cell lines vs. human tissue samples). However, in both a global increase in esterified arachidonic species was described, as well as an increase in plasmalogen species.
2. The thorough characterization of EV lipidome leads us to conclude that lipid species are clearly segregated during the shedding process, leading to an increase in SM and an impoverishment in PI, PE and PE plasmalogens. However, EV still conserves part of the parental lipid fingerprint, and consequently, this can be used to stratify EV according to the cell type origin in model systems as well as in human samples (healthy vs patients with adenomatous polyps or invasive neoplasia).
3. IMS is a very powerful technique to identify lipid biomarkers, particularly at spatial resolutions below the average cell size. Hence, the IMS analysis of human colon mucosa clearly demonstrated that base merely on the lipidome, the two main tissues presenting the mucosa, i.e. epithelium, stroma, as well as the presence of tissue a malignant transformation are clearly distinguishable.
4. IMS analysis of human colon mucosa was able to establish that the lipid composition in colonocytes is sensitive to their differentiation state, identifying PI, PE plasmalogens and AA-containing phospholipids as the species most affected during the process. Consistently, this tight regulation of the lipidome was clearly disturbed in tumor epithelium.
5. IMS analysis of human colon mucosa was able to establish gradual changes along with the stroma, particularly in AA-containing phospholipids, that fully coincides with the distribution of immune cells within the tissue.
6. The role of PGs in colon pathophysiology is still not well understood, as PGE₂, PGD₂, and PGF_{2α} exert different effects (even opposite) on colon epithelium proliferation. Therefore, more specific therapies specifically targeting PG receptors signaling could avoid some undesired secondary effects associated with COX inhibition treatments.

EXPERIMENTAL PROCEDURES

6 Experimental procedures

6.1 Chapter 1

6.1.1 Commercial cell lines culture conditions

CRC cell lines, Colo-201, HT29, LS174T, and SW480 were purchased from the European Collection of Authenticated Cell Cultures (ECACC, Salisbury, UK). The primary colon epithelial cell line was purchased from Innoprot (Ref. P10768, Derio, Spain). Depending on the cell line, $2\text{-}3 \times 10^4$ cells were plated and grown for 72h in the appropriated medium completed with exosome-free FBS (10% v/v) (Labclinics, Barcelona, Spain. Ref. S181B-500), 1% non-essential aminoacids (Labclinics, Barcelona, Spain. Ref. NEAA-B), 2mM glutamine (Labclinics, Barcelona, Spain. Ref. P1012-500GR). Cells were plated as follows: primary cell line, 30.000 cells/cm², 48h in Colonic Epithelial Cell Medium (Innoprot, Bizkaia, Spain. Ref. P60165) without FBS; SW480, 20.000 cells/cm², 48h in DMEM (Labclinics, Barcelona, Spain. Ref. L0106-500); HT29, 30.000 cells/cm², 48h, in MEM (Labclinics, Barcelona, Spain. Ref. MEMA-RXA); LS174t, 30.000 cells/cm², 48h, in MEM (Labclinics, Barcelona, Spain. Ref. MEMA-RXA); and Colo 201 20.000 cells/cm², 72h, in RPMI (Labclinics, Barcelona, Spain. Ref. L0490-500). The additional 24h for the Colo 201 cells were added to assure that these cells, which half of the population grow in suspensión, adhered well.

For the collection of the EV, after 48 hours after being plated (72 for the Colo 201) the medium was collected and kept at -80°C until processing.

6.1.2 Extracellular vesicles isolation

The EV isolation protocol from cell culture was performed adapting the protocol described in Crescitelli et. al.⁶⁰¹. Briefly, the medium was centrifuged for 10 minutes at 300g to remove suspended cells. A second centrifugation at 2000 for 20 minutes precipitate big cellular debris and dead cells. To discard the apoptotic bodies, the supernatant was filtered by gravity through a 0.8 µm pore size filter. Then, the volume was centrifugated at 12200g for 40 minutes using an ultracentrifuge (Optima L-100 XP Ultracentrifuge, Beckman Coulter, Barcelona, Spain) using a 70Ti rotor and 26.9 ml tubes (Izasa, Barcelona, Spain). The supernatant was filtered by pressure through a 0.2 µm filter. The final centrifugation to precipitate the EVs was done at 120000g for 70 min with the same ultracentrifuge, rotor, and tubes than the previous step. All the processes were done at 4°C. The assessment of the EVs correct size was done by electronic transmission microscopy and the presence of exosomes by the expression of CD40 antigen evaluated with western blot.

The plasma-derived EVs protocol was the same but with a dilution of the plasma in PBS at least at a 1:1 ratio before the first centrifugation.

6.1.3 Cells and cell-derived EVs lipid composition

The lipids were extracted according to Ogiso et.al. protocol⁶⁸³. Internal standard solutions were prepared as described previously⁶⁸³ were added to the internal standard solution. For measurements of plasmalogen PE (PE plasmalogens), an external standard solution containing 50 pmol each of PE(28:0) and PE plasmalogens18:0/18:1 was prepared. Pretreatment and measurement of the external standard solution were performed simultaneously with the samples and derived [peak area of PE plasmalogens18:0/18:1/peak area of PE(28:0)] values were used as the corrective coefficients for the quantitation of PE plasmalogens, respectively.

Lipid extractions were performed as described previously⁶⁸³, with several modifications. Briefly, cell pellets were sonicated for 10 s with 0.1 ml methanol/butanol (1:1) to inactivate the associated enzymes using an ultrasonic bath. After the addition of 0.05 ml standard lipid mixture, 0.05 ml of 0.5 M phosphate buffer (pH 6.0), and 0.2 ml of water, the samples were shaken with 0.7 ml of butanol and sonicated for 3 min in an ultrasonic bath. After centrifugation, the upper layer was collected. The original suspension was re-extracted by the addition of 0.35 ml each of ethyl acetate and hexane, followed by centrifugation. The resulting extract was combined with the first butanol extract. After the addition of 0.7 ml methanol, 10% (0.21 ml) of this solution was dried under reduced pressure at 40°C, and dissolved in 20 µl of LC mobile phase B and 30 µl of mobile phase A. This sample was used to analyze Cer, SM, PE and PC levels. The remaining 90% (1.8 ml) of the extract was fractionated on a DEAE-cellulose column (500 µl bed volume packed in a 1 ml polypropylene pipette tip), previously activated by acetic acid. After washing with 2 ml of methanol, the column-bound lipids were eluted with 1 ml methanol/28% aqueous ammonia/formic acid (1,000:33:22). The organic solvent was evaporated from the eluate under reduced pressure at 50°C, after which dried materials were dissolved with 50 µl of mobile phase A. The resulting sample was used for the analyses of acidic lipids (i.e. PS, PG, PI, and PA).

Sphingolipids			
Molecular species	Final concentration	Dilution	Supplier/ Reference
SM(d18:1/12:0)	1µM	MeOH	Instruchemie/ 860583
Cer(d18:1/12:0)	1µM	MeOH	Instruchemie/ 860502
GlcCer(d18:1/12:0)	1µM	MeOH	Instruchemie/ 860543
LacCer(d18:1/12:0)	1µM	MeOH	Instruchemie/ 860545
GM3(d18:1/12:0)	1µM	MeOH	Avanti/860058P
Cer-1-P(d18:1/12:0)	1µM	MeOH	Instruchemie/ 860531
Sph(d17:1)	1µM	MeOH	Instruchemie/ 860640
Sph-1-P(d17:1)	1µM	MeOH	Instruchemie/ 860641
Phospholipids			
Molecular species	Final concentration	Dilution	Supplier/ Reference
PC(14:0/14:0)	10µM	MeOH	Avanti/830345P

PE(14:0/14:0)	10 μ M	M:C (2:1)	Avanti/850745P
PS(14:0/14:0)	1 μ M	M:C:W (2:1:1)	Avanti/840033P
PA(14:0/14:0)	1 μ M	MeOH	Avanti/830345P
PG(14:0/14:0)	1 μ M	M:C (2:1)	Avanti/840445P
PI(16:0/16:0)	1 μ M	M:C (2:1)	Avanti/850141
DAG(14:0/14:0)	1 μ M	M:C (2:1)	Avanti/800814P

-LC-MS analysis

Lipids were measured using LC-MS/MS as described previously⁶⁸³, except that the collision energy was set to 30 V for Cer, SM, PE, and PC. The mass transitions were additionally set to 702.5/364.2, 724.5/364.2, 728.6/390.2, 730.6/392.2, 748.5/364.2, 750.5/390.2, 752.6/392.2, 774.5/390.2, and 776.6/392.2 for PE plasmalogens in the positive ion mode. Each molecular species was identified based on the MS/MS spectrum and the LC retention times, and quantities present were calculated from the peak areas of the measured lipids, compared with those of the internal standards. Each level of measured lipids was normalized to the total protein content.

6.1.4 Principal component analysis

The Principal Component Analysis (PCA) is a very useful tool to reveal sample tendencies and the variables that make able to discriminate between them. PCA reduces the dimensionality of the dataset while retaining most of its variance⁷⁵⁶. To achieve that, the analysis projects a first vector with the direction that explains the maximum variability, named PC1. Then, a second component (PC2) uncorrelated to the PC1 and able to explain the most remaining variance is projected. Principal components are generated until all the variance can be explained. The variables presenting higher differences between samples have more impact on the first PCs as explain most variability. Thus, the representation of only a few PCs is able to explain the distribution of multiple samples along with a cloud of variables. PCA simplifies multiple variables experiments easing the identification of the relevant variables of a dataset.

The PCA calculates scores for each sample and variable at each principal component. The sample scores describe which samples are different and which are similar. As more separated are represented two samples, more different in their variables will be. In the same way, the variables score plot show how each variable participate in the samples separation and what is the relation between variables within a sample (e.g. if the variable X is higher but the Y is lower in the controls respect a treatment). This analysis gives a lot of information about the samples and variables distribution useful to clarify a large amount of data, however, is not able to give information about the significance of the differences.

To interpret the PCA we must focus on the distance between the variable and the axis center in the spatial representation of the PCA scores. As more close are the variables to the axis, less participates this particular variable to the samples separation, and inversely, when the variables are far from the axis, more separate the samples along this PC.

An in deep review of what is Principal Component Analysis can be found was explained by Ringner⁷⁵⁶.

6.1.5 Protein quantification

Protein concentration in the samples was measured using a protein assay based on the Bradford dye-binding method, according to manufacturer's instructions (Bio-Rad Laboratories, Madrid, Spain). The assay is based on the reaction of protein with an alkaline copper tartrate solution and Folin reagent. The color development is due mainly to the amino acids tyrosine and tryptophan. Proteins effect a reduction of the Folin reagent by loss of 1, 2 or 3 oxygen atoms thereby producing one or more of several possible reduced species which have a characteristic blue color with maximum absorbance at 750 nm. The protein concentration was calculated extrapolating the values into a standard curve.

6.1.6 Western Blot

The samples were mixed with 10X electrophoresis loading buffer (120 mM Tris-HCl, pH 6.8, 4% SDS, 50% glycerol, 0.1% bromphenol blue, and 10% mM β -mercaptoethanol) and then boiled for 3 minutes. For the immunoblotting, the equal protein content extracts were resolved in SDS-polyacrylamide gel and transferred to nitrocellulose membranes (Whatman). After transference, the membranes were blocked with blocking solution (PBS containing 5% non-fat dry milk and 0.1% Tween) for 1h at room temperature. Then the membranes were incubated overnight at 4°C with the specific antibodies: rabbit anti-GNPAT (1:600, Atlas antibodies, Ref. HPA060059), rabbit anti-AGPS (1:600, Atlas antibodies, Ref. HPA030209), rabbit anti-FAR1 (1:6000, Antibodies-online, Ref. ABIN2174097), rabbit anti-FAR2 (1:6000, Antibodies-online, Ref. ABIN709091), rabbit anti-EP1 receptor (1:500, Bioss Antibodies, Woburn, Massachusetts, Ref. bs-6316R), rabbit anti-EP2 receptor (1:1500, Antibodies-online, Ref. ABIN3184492), rabbit anti-EP3 receptor (1:500, Bioss Antibodies, Woburn, Massachusetts, Ref. bs-1876R), rabbit anti-EP4 receptor (1:500, Bioss Antibodies, Woburn, Massachusetts, Ref. bs-8538R), rabbit anti-DP receptor (5 μ g/ml, Enzo Life Sciences, Barcelona, Spain, Ref. ADI-905-800-100), rabbit anti-FP receptor (5 μ g/ml, Enzo Life Sciences, Barcelona, Spain, Ref. ADI-905-901-100) rabbit anti Na⁺/K⁺ ATPase (1:10000, Abcam, Cambridge, UK, Ref. ab124677) and β -actin (1:10000, LI-COR Biosciences Ref. 926–42,212). After incubation, membranes were washed with PBS containing 0.1% Tween 20 (Sigma-Aldrich), and with 0.1% Tween 20 PBS containing 5% BSA (Sigma-Aldrich) for polyclonal antibodies. Then they were incubated with goat anti-rabbit IRDye 800CW (1:5000, LI-COR, Ref. 926–32,211) or Alexa 680 donkey anti-mouse IgG (1:2500, Abcam, Ref. ab175774) secondary antibodies at room temperature for 1 h. Membranes were visualized using an Odyssey CLx Imaging System (LI-COR Biosciences, Nebraska, USA); Quantity one software (Bio-Rad) was used to quantify the specific signals. Normalization was performed by the protein/ β -actin content except for the evaluations of the PG receptors at the nuclei.

Antibody	Concentration used	Provider
Primary antibodies		
rabbit anti-GNPAT	1:600	Atlas antibodies
rabbit anti-AGPS	1:600	Atlas antibodies
rabbit anti-FAR1	1:6000	Antibodies-online
rabbit anti-FAR2	1:6000	Antibodies-online

rabbit anti-EP1 receptor	1:500	Bioss Antibodies
rabbit anti-EP2 receptor	1:1500	Antibodies-online
rabbit anti-EP3 receptor	1:500	Bioss Antibodies
rabbit anti-EP4 receptor	1:500	Bioss Antibodies
rabbit anti-DP receptor	5µg/ml	Enzo Life Sciences
rabbit anti-FP receptor	5µg/ml	Enzo Life Sciences
rabbit anti Na ⁺ /K ⁺ ATPase	1:10000	Abcam
β-actin	1:10000	LI-COR Biosciences
Secondary antibodies		
goat anti-rabbit IRDye 800CW	1:5000	LI-COR
Alexa 680 donkey anti-mouse IgG	1:2500	Abcam

6.1.7 RNA isolation protocol

Samples for RNA isolation were lysed in one volume of Tripure reagent (Sigma-Aldrich). After homogenated, 1/3 volume of Chloroform was added. The tube was vigorously shaken and left on ice for 10 minutes. Then the tube was centrifuged at 12000g at 4°C for 15 minutes. The superior phase was transferred to a new tube with one volume of isopropanol and then placed ON at -20°C. To precipitate the RNA, the tube was centrifuged at 12000g at 4°C for 10 minutes. The RNA was then resuspended with an adequate volume of DNA/RNase free water.

The purity of the RNA was assessed by a Nanodrop (Nanodrop 2000, Thermo Fisher, Barcelona, Spain). In any case, the 260/280 ratio was between 1.7 and 2 to be acceptable for analysis.

6.1.8 Quantitative Reverse Transcription-Polymerase Chain Reaction (qRT-PCR)

Total RNA was isolated from samples using Tripure reagent (Sigma-Aldrich) and the following transcription to cDNA (up to 1µg RNA) with SensiFAST cDNA Synthesis Kit (Bioline, London, UK). Quantitative real-time PCR was performed in CFX96 Touch™ Real-Time PCR Detection System (Bio-Rad), with Hard-Shell® 96-Well PCR Plates, low profile, thin wall, skirted, white/clear (Bio-Rad), using Sensi Fast™ SYBR® No-Rox Kit (Bioline), PCR Water Ultra Pure 18.2MΩ, DNase/RNase-Free (Bioline) and the following primers: Human FAR1: Fw 5'-GTACAACAGGCAGCACTAATCC-3', Rv 5'-TTGGAGGTTAGATTTACATTGGGC-3'; Human FAR2: Fw5'-GCGACTGGGAAAGGGTTTCT-3', Rv5'-CCAATTGCAGGGATTGATGT-3'; Human GNPAT: Fw 5'-GCCAGTTATAGCAGCAGGAATG-3', Rv 5'-GCCAGTAGAGTTTATTGCCAC-3'; Human AGPS: Fw 5'-GTGATACACCTCCTTCTGTTGT-3', Rv 5'-TCGCTCAAACATTCTTCCC-3'; Human 18S Fw 5'-TAAGCAACGAGACTCTGGCAT-3', 18S Rv 5'-CGGACATCTAAGGGCATCACAG-3' (Isogen, Utrecht, Netherlands).

6.1.9 Tissue samples processing for imaging techniques

The sample collection for this study was specifically approved by the Ethics Research Committee of the Balearic Islands (IB 2118/13 PI). Informed consent was obtained in written form from each patient before performing each endoscopy. Human colon biopsies were obtained in the Endoscopic Room of the Hospital Universitari Son Espases (Palma, Spain) or of the Hospital Comarcal de Inca (Inca, Spain). Endoscopic biopsies were resected using a Radial Jaw Standard Capacity Biopsy Forceps (Radial Jaw™ 4, Boston Scientific, USA) and immediately snapped frozen in liquid nitrogen and saved at $-80\text{ }^{\circ}\text{C}$ until sample preparation.

If the samples were used for imaging techniques sections of $\sim 10\text{ }\mu\text{m}$ thickness were prepared using no cryoprotective substances and no embedding material in a cryostat (Leica CM3050S) at $-20\text{ }^{\circ}\text{C}$ and placed on plain glass microscope slides. A consecutive section was stained with hematoxylin and eosin (H&E) for structure identification and 9 consecutive slices were placed in adherent glass slides for IF imaging.

6.1.10 MALDI-IMS analysis

2-Mercaptobenzothiazole (MBT) and 1,5-diaminonaphtalene (DAN) matrices, as well as hematoxylin and eosin for histological staining were purchased from Sigma-Aldrich. Water, methanol, acetonitrile, 2-propanol and formic acid (Fisher Scientific, Fair Lawn, NJ, USA) were of Optima® LC/MS grade. Leucine enkephalin acetate hydrate, ammonium acetate, and sodium hydroxide solution were purchased from Sigma-Aldrich Chemie (Steinheim, Germany). Detailed information regarding the MALDI-imaging and data analysis can be found in Garate et al.²⁴⁸. Briefly four sections of control and four sections of AD colon from different individuals were scanned in negative-ion mode, while four sections of control and another three sections of AD colon were scanned in positive-ion mode, using the orbitrap analyzer of an LTQ-Orbitrap XL (Thermo Fisher, Bilbao, Spain), equipped with an N₂ laser (100 μJ max power, elliptical spot, 60 Hz repetition rate). Mass resolutions of 30,000, 60,000 and 100,000 at $m/z = 400\text{ Da}$ were used to record the data, and the scanning range was 480–1000 Da in positive-ion mode and 550–1200 Da in negative-ion mode.

Lipid assignment was based on the comparison between the experimental m/z and the species in the software's database (33000 lipid species plus adducts) and in lipid maps database (www.lipidmaps.org). Mass accuracy was always better than 9 ppm and it was typically better than 3 ppm. In this type of analyzers, the mass accuracy depends somehow in the intensity of the peaks, and thus, those m/z with higher intensity present better mass accuracy. In those cases where no univocal assignment was found, a comparison with the data from UHPLC–MS/MS was performed. If any of the candidates was not detected by UHPLC–MS, and it was not detected as another adduct in the MALDI-IMS experiment, this candidate was not considered for the assignment.

MBT (2-mercaptobenzothiazole)²³⁰ and DAN (1,5-diaminonaphtalene)⁷⁵⁷ were used as matrices for positive and negative ion detection respectively and were deposited with the aid of a glass sublimator (Ace Glass 8023)²⁴⁸. Spectra were analyzed using dedicated software (MSIAnalyst, NorayBioinformatics S. L.). A detailed description of data processing may be found in Ref.²⁴⁸, but briefly, the spectra were normalized using a total ion current (TIC) algorithm, and aligned using the Xiong method during the parsing stage⁷⁵⁸. All peaks with intensity values lower than the 0.5% of the intensity of the strongest peak were filtered to reduce the number of m/z and to speed up the analysis.

Recently, we have demonstrated that variations in the adduct ratio may hide other physiologically relevant changes in lipid concentration^{644,759}. Therefore, data on the relative abundance of species detected in positive-ion mode were generated adding all adducts of each species in a single mass channel. Thus, the values reported for, for example, PC 34:1 contain the data from PC 34:1 + H⁺, PC 34:1 + Na⁺, PC 34:1 + K⁺ and PC 34:1 + MBT⁺. In those cases in which a mass channel contains contribution from more than one species, the percentage due

to each species was determined using the H⁺/Na⁺/K⁺ ratio found for each^{644,759} lipid class and assumed constant for all the species of a given class. This ratio was calculated for each individual spectrum with the aid of a home-built program. The correction cannot be performed just by deconvolution of the average spectrum, as it may change for each type of tissue^{644,759}. The spectra in each experiment were grouped using k-means for comparison. Changes between healthy and adenomatous cluster lipid composition were assessed using ANOVA followed by Bonferroni post-test.

6.1.11 Plasma-derived EVs lipid composition

Lipid extraction of plasma-derived EVs was performed according to the method of Bligh and Dyer²¹³ in the presence of not naturally occurring lipid species as internal standards. The following lipid species were added as internal standards: PC 14:0/14:0, PC 22:0/22:0, PE 14:0/14:0, PE 20:0/20:0 (di-phytanoyl), PS 14:0/14:0, PS 20:0/20:0 (di-phytanoyl), PI 17:0/17:0, LPC 13:0, LPC 19:0, LPE 13:0, Cer d18:1/14:0, Cer 17:0, D7-FC, CE 17:0 and CE 22:0. A total of 120 µg of EVs pellet resuspended in PBS were extracted. Chloroform phase was recovered by a pipetting robot (Tecan Genesis RSP 150) and vacuum dried. The residues were dissolved in either in 10 mM ammonium acetate in methanol/chloroform (3:1, v/v) (for low mass resolution tandem MS) or chloroform/methanol/2-propanol (1:2:4 v/v/v) with 7.5 mM ammonium formate (for high resolution MS).

The analysis of lipids was performed by direct flow injection analysis (FIA) using either a triple quadrupole mass spectrometer (FIA-MS/MS; QQQ triple quadrupole) or a hybrid quadrupole-Orbitrap mass spectrometer (FIA-FTMS; high mass resolution).

FIA-MS/MS (QQQ) was performed in positive ion mode using the analytical setup and strategy described previously^{760,761}. A fragment ion of m/z 184 was used for PC, SM⁷⁶⁰ and lysophosphatidylcholine (LPC)⁷⁶². The following neutral losses were applied: PE 141, PS 185, phosphatidylglycerol (PG) 189 and PI 277⁷⁶³. PE plasmalogens were analyzed according to the principles described by Zemski-Berry⁷⁶⁴. Sphingosine based Cer and hexosylceramides (HexCer) were analyzed using a fragment ion of m/z 264⁷⁶⁵. Lipid species were annotated according to the recently published proposal for shorthand notation of lipid structures that are derived from MS⁸⁴. For these data glycerophospholipid species annotation was based on the assumption of even-numbered carbon chains only. SM species annotation is based on the assumption that a sphingoid base with two hydroxyl groups is present.

The Fourier Transform Mass Spectrometry (FIA-FTMS) setup is described in detail in Höring et. al.⁷⁶⁶. Triacylglycerol (TG), diacylglycerol (DG) and cholesteryl ester (CE) were recorded in positive ion mode FTMS in m/z range 500 - 1000 for 1 min with a maximum injection time (IT) of 200 ms, an automated gain control (AGC) of 1*106, three microscans and a target resolution of 140000 (at 200 m/z). The mass range of negative ion mode was split into two parts. LPC and lysophosphatidylethanolamine (LPE) were analyzed in the range 400 - 650 m/z. PC, PE, PS, SM and Cer were measured in m/z range 520 - 960. Multiplexed acquisition (MSX) was used for, the [M +NH₄]⁺ of free cholesterol (FC) (404.39 m/z) and D7-cholesterol (411.43 m/z) 0.5 min acquisition time, with a normalized collision energy of 10 %, an IT of 100 ms, AGC of 1*105, isolation window of 1 m/z, and a target resolution of 140000. Data processing details were described in Höring et. al. using the ALEX software⁷⁶⁷ which includes peak assignment and intensity picking. The extracted data were exported to Microsoft Excel 2010 and further processed by self-programmed Macros.

6.2 Chapter 2

6.2.1 Immunofluorescence in colon tissue

Sections of 10 μm thickness as described in Section 6.1.9 were placed on positive charged adherent plain glass microscope slides. The fixation of the immunological slides and the retrieval of its antigens were performed using pre-chilled methanol:acetone (Sigma Aldrich, Madrid, Spain and Scharlau, Barcelona, Spain, respectively) at 1:1 dilution. Slides were blocked using BSA at 5% (Sigma Aldrich) for 10 min. The immunostaining was made for 1 h at room temperature (RT) followed by an incubation with a secondary antibody for 45 min at RT in a humidified chamber. Nuclei were stained with 4',6-diamidino-2-phenylindole (DAPI, Dako-Agilent Technologies, Santa Clara, CA, USA) at 1:10,000 dilution for 1 min at RT. Slides were mounted in Dako Fluorescent Mounting Medium (Dako, Agilent Technologies). The following primary antibodies were used: rabbit anti-ACSL4 (PA5-27137, Thermo Scientific, Waltham, MA, USA; 1:1500), rabbit anti-PLA2 Group IV (PA5-29100, Thermo Scientific, 1:1500); rabbit anti-PGE2S (HPA020631, Atlas Antibodies, Stockholm, Sweden, 1:75), rabbit anti-PLA2 group VI (HPA001171, Atlas Antibodies, 1:200), rabbit anti-FADS2 (HPA006741, Atlas antibodies, 1:260), rabbit anti-CDS2 (HPA019698, Atlas antibodies, 1:50); mouse anti-COX1 (SC-19998, Santa Cruz Biotechnology, 1:500), mouse anti-COX2 at dilution (sc-19999, Santa Cruz, 1:525), mouse anti-SCD1 (ab39969, Abcam, Cambridge, UK, 1:500), rabbit anti-CB1 (PA1-743, Thermo Fisher, Barcelona, Spain, 1:1250), mouse anti-CB2 (MAB3655, Fisher Scientific, Madrid, Spain, 1:20), goat anti-MBOAT7 (sc-243245, Santa Cruz, Heidelberg, Germany, 1:500), goat anti-AGPAT2 (sc-68585 Santa Cruz, Heidelberg, Germany, 1:500), mouse anti-PIP2 (Abcam, Cambridge, UK, 1:200), rabbit anti-PI3KR3 (Uniprot, 1:50), rabbit anti AGPS (Atlas antibodies, Bromma, Sweden, 1:500), rabbit anti GNPAT (Atlas antibodies, Bromma, Sweden, 1:200), rabbit anti-FAR1 (Antibodies-online, Aachen, Germany, 1:150), rabbit anti-FAR2 (Antibodies-online, Aachen, Germany, 2 $\mu\text{g}/\text{ml}$). Secondary antibodies used were donkey anti-mouse alexa fluor 555 (ab150106, Abcam, Cambridge, UK, 1:600), chicken anti-rabbit alexa fluor 488 (A-11008, Life Technologies, 1:400), donkey anti-rabbit alexa fluor 555 (A31572, Life Technologies, 1:400), chicken anti-goat alexa fluor 488 (A21467, Life Technologies, 1:400). Images were obtained with Axioscope Cell Observer microscope (Carl Zeiss, Germany). Once IF images were captured, the crypts appearing entire were divided in three areas (upper/luminal, intermediate and down/basal) and the IF intensity values were obtained using the microscope software. To evaluate statistically the differences in protein expression along the crypt, repeated measurement ANOVAs were computed for healthy and for adenomatous tissue in separated analysis using IBMSPSS Statistics 22. Results are reported using a significance level (i.e., alpha) of 0.05 and eta-square to indicate the magnitude of the difference. A similar approach was taken for lamina propria.

Antibody	Concentration used	Provider
Primary antibodies		
rabbit anti-ACSL4	1:1500	Thermo Scientific
rabbit anti-PLA2 Group IV	1:1500	Thermo Scientific
rabbit anti-PGE2S	1:75	Atlas Antibodies
rabbit anti-PLA2 group VI	1:200	Atlas Antibodies
rabbit anti-FADS2	1:260	Atlas Antibodies
rabbit anti-CDS2	1:50	Atlas Antibodies
mouse anti-COX1	1:500	Santa Cruz

mouse anti-COX2	1:525	Santa Cruz
mouse anti-SCD1	1:500	Abcam
rabbit anti-CB1	1:1250	Thermo Fischer
mouse anti-CB2	1:20	Fisher Scientific
goat anti-MBOAT7	1:500	Santa Cruz
goat anti-AGPAT2	1:500	Santa Cruz
mouse anti-PIP2	1:200	Abcam
rabbit anti-PI3KR3	1:50	Uniprot
rabbit anti AGPS	1:500	Atlas Antibodies
rabbit anti GNPAT	1:200	Atlas Antibodies
rabbit anti-FAR1	1:150	Antibodies-online
rabbit anti-FAR2	2µg/ml	Antibodies-online
Secondary antibodies		
donkey anti-mouse alexa fluor 555	1:600	Abcam
chicken anti-rabbit alexa fluor 488	1:400	Life Technologies
donkey anti-rabbit alexa fluor 555	1:400	Life Technologies
chicken anti-goat alexa fluor 488	1:400	Life Technologies

6.2.2 Organoid cell culture

6.2.2.1 Wnt3a and RSPONDIN-1 complemented medium preparation

To allow organoids development is necessary the presence of Wnt3a and RSPONDIN-1 ligands in the medium. To this, we used fibroblasts with a plasmid for Wnt3a or RSPONDIN-1 synthesis coupled to Zeocin gene resistance. The fibroblasts are expanded for at least one week with DMEM/F12, 10% FBS, 1% Penicilyn/Streptomycin, 1% GlutaMax (Labclinics, Barcelona, Spain.) and 1% Zeocin (Invivogen, Toulouse, France). To generate the complemented media the fibroblasts are seeded without Zeocin and after reaching confluence the medium is changed. After one week complementing the medium, the medium is filtered through 20µm mesh, aliquoted and stored at -80°C until use.

6.2.2.2 Crypt isolation and organoid culture

The sample collection for this study was specifically approved by the Animal Ethics Research Committee of the IdISBa (2015/17/AEXP). The organoids were generated from crypt fragments from NMRI mice. The protocol was adapted from⁷⁶⁸. The mice colon was extracted and the distal part (the last 2-3 cm) collected. A biopsy-size fragment (3mm³ approximately) was kept at -80°C for colocalization evaluations. The remaining distal part of the colon is and flushed out with PBS + Primocyn (0.2%). The higher seeding efficiency of the distal colon made it a more suitable part to form organoids⁷³⁷. The tissue is minced into small pieces and washed twice in PBS with Primocyn (0.2%) for 5 min. The shaking must be gentle and the PBS must be removed by decantation. The tissue is suspended in 5ml of DMEM/F12 with 1% FBS (complete DMEM) and 500 U/ml collagenase 1X and incubated at 37°C for 30 minutes in a water bath shaking vigorously every 5 minutes. To finish dissociate the tissue and to stop the collagenase activity 5 ml of complete DMEM were added and the tissue pipetted with a 10ml pipette. The top 5 ml of the crypt suspension is transferred to a new tube, passing through a 100µm cell strainer to remove large materials. The DMEM addition and filtration processes are repeated 3 times. The liberated crypts were combined by centrifuging at 300g for 5 minutes. A final wash is done with 5ml complete DMEM and a centrifugation at 60g for 3 minutes twice (the two centrifugations allows a better precipitation of the crypts). At this speed, the crypts but not the cells precipitate. The viable crypts fragments were seeded in 15µl of cold matrigel in a 96 well plate. The organoids were cultured with WENR culture media described in^{389,737} with some modifications. WENR contained 50% Wnt and 10% RSPONDIN complemented media, 40% DMEM/F12 complete media (10% FBS, 1% Primocin), 1x B27 (which helps in forming cell spheres and sustain their propagation⁷⁶⁹), 1x N2 (used in primary cultures as a supplementation growth factor⁷⁷⁰), 1mM N-acetylcysteine (NaC) (used as antioxidant and as a mucolytic agent⁷⁷¹), 100 ng/ml Noggin, 50 ng/ml EGF.

The concentration of each inhibitor was: 5 µM for Arachidonyl trifluoromethyl ketone, 20 µM for Bromoenol lactone, 0.1 mM for Valeroyl salicylate, 4 µM for Celecoxib. In the case of the PGD₂, PGF_{2α}, and PGE₂ all were used at 0.022 µM. The EP4 agonist L-902,688 was used at 1 µM while its antagonist L-161.982 was used at 10 µM.

Images of the organoids were obtained with Axioscope Cell Observer microscope (Carl Zeiss, Germany) at 0h, 24h, and 48h of treatment. The growth rate was calculated by dividing the mean size of the organoids at 48h between the mean size of the same well at 0h. The area quantification was done using Zen Blue Software (Carl Zeiss, Germany).

6.2.3 Organoid MTT assays

The assessment of the organoids viability after the different treatments was assessed by direct visualization and by MTT assay. We used the Roche MTT assay kit (Sigma-Aldrich, Spain). The assay is based on the cleavage of the yellow tetrazolium salt MTT to purple formazan crystals by metabolic active cells⁷⁷². This cellular reduction involves the pyridine nucleotide cofactors NADH and NADPH⁷⁷³. The formazan crystals formed were solubilized and the cells lysed by using the Solubilization solution (with SDS). The resulting colored solution is quantified using a scanning multiwell spectrophotometer Synergy H1 microplate reader (BioTek, Bad Friedrichshall, Germany). The signal was calculated by substrating the reference absorbance at 690 nm to the 550 nm signal absorbance.

6.2.4 PLA₂ and COX inhibition assessment

The PLA₂ and COX activities capacities after their inhibition were assessed over isolated mice crypts. The crypts were isolated as described in section 6.2.2.2 and then the corresponding assay was performed in the presence of the inhibitors at the working

concentrations. In order to be able to compare all the samples, the protein content of each reaction was assessed as explained in section 6.1.5.

PLA₂ inhibition assessment

The PLA₂ activity was measured with the EnzCheck PLA₂ Assay Kit of Invitrogen (Thermo Fisher, Barcelona, Spain). This assay is based on the different fluorescence of a labeled AA depending if is free or esterified. The excitation of the sample was at 490nm, while the emission was measured at 515 and 575 nm. The value of PLA₂ was calculated by doing the ratio between the emission at 515 and the one at 575.

COX inhibition assessment

The COX activity was measured with the COX Activity Assay Kit of Abcam. This kit measures the fluorescence emitted at 587 nm of a COX probe after its peroxidation.

6.2.5 Digital Droplet PCR

To know the effects of influencing in the PG signaling besides proliferation, we assessed the effects of each treatment over differentiation by quantifying different cell markers using digital droplet PCR (ddPCR). ddPCR is based on the preparation of an emulsion of thousands of droplets. Each droplet should contain only one copy of cDNA, the primers and the polymerase. With more copies of one gene more droplets would amplify their content and therefore would display signal. The main advantage of this technique over conventional qPCR is its higher sensitivity and their quantitative results which can leave aside the evaluation of a housekeeping gene⁷⁷⁴. The markers used were: Krt20 for differentiated cells, ckit for the cKit⁺ cells, Lgr5 for the stem cells and Wdr43 for the TA cells.

Total RNA was isolated from samples using Tripure reagent (Sigma-Aldrich) and following transcription to cDNA (up to 1µg RNA) with SensiFAST cDNA Synthesis Kit (Bioline, London, UK). Droplets were generated using QX200 droplet generator (Biorad) and the PCR reaction in a thermocycler (C1000 TouchTM thermal cycler, Biorad). The positive droplets were quantified using QX200 droplet reader (Biorad). The concentration values were used to assess differences between the different conditions. The PCR reactions were performed using QX200 ddPCR EvaGreen supermix, PCR Water Ultra Pure 18.2MΩ, DNase/RNase-Free (Bioline) and the following primers: Mouse Lgr5: Fw 5'-ACCCGCCAGTCTCCTACATC-3', Rv 5'-GCATCTAGGCGCAGGGATTG-3' (Tm = 57.5°C); cKit: Fw 5'-TGGCTCTGGACCTGGATGAT-3', Rv 5'-ATCTTTGTGATCCGCCGTG3' (Tm = 60.8°C); Krt20: Fw 5'-TAGAGTTGCAGTCCCACCTC-3', Rv 5'-TGTTCTTGTTCTGGCGTTC-3' (Tm = 60.8°C); Wdr43: Fw 5'-AGTCTCCTTACACAGGGCT-3', Rv 5'-CGGTATCCTCAGCACAGTCC-3' (Tm = 60.6°C) (Isogen, Utrecht, Netherlands).

6.2.6 Nuclear colocalization of prostaglandin receptors in colonocytes by IF

To detect the presence of PGs receptors on the nucleus, we labeled each protein and analyze its colocalization with the nuclei labeled with DAPI using the Manders' colocalization coefficient (MCC).

The MCC works as follows: for two probes that can be named R and G, two different MCC are derived, M1 is the fraction of R in compartments containing G, and the M2 would be the fraction of G in compartments containing R. These coefficients are calculated as follows:

$$M_1 = \frac{\sum_i R_{i,colocal}}{\sum_i R_i}$$

Where $R_i \text{ colocal} = R_i$ if $G_i > 0$ and $R_i \text{ colocal} = 0$ if $G_i = 0$ and

$$M_2 = \frac{\sum_i G_{i,colocal}}{\sum_i G_i}$$

where $G_i \text{ colocal} = G_i$ if $R_i > 0$ and $G_i \text{ colocal} = 0$ if $R_i = 0$.

This method for evaluating colocalization measures co-occurrence regardless of the proportionality between the channels. The main con of this method is the great effect that the background exerts over this value.

To overcome the effect of the background over the MCC we chosed the next approach: With the point scatter of the colocalization graph we can determine a good threshold for each channel (DAPI and the antibody). For each protein, a specific threshold was applied for each image. The negative colocalization values were assessed by analyzing tissue areas without nuclei but with antibody signal (like epithelial cell membrane), areas from luminal colon and a negative area apart from the tissue. The threshold was established at the point where the protein channel was just above the negative colocalization areas and the increasing DAPI channel enough to have Mander's colocalization values of 0 on the negative areas.

Despite the decrease in the background signal, there is always some remaining colocalization value. To assess which Mander's coefficient value is a real negative in the colon we also calculate this coefficient for the Na/K ATPase at the nucleus. The values equal or below this exclusive cytoplasmic membrane protein MCC were considered negative.

Tissue slices were fixed and their antigens retrieved by using ice-cold Methanol:Acetone (1:1) for 10 minutes. After that, the slices were blocked with BSA at 5%. Then were incubated using the next antibodies: rabbit anti-EP1 receptor (1:300, Bioss Antibodies, Woburn, Massachusetts, Ref. bs-6316R), rabbit anti-EP2 (1:250, Antibodies-online, Ref. ABIN3184492), rabbit anti-EP3 receptor (1:400, Bioss Antibodies, Woburn, Massachusetts, Ref. bs-1876R), rabbit anti-EP4 receptor (1:300, Bioss Antibodies, Woburn, Massachusetts, Ref. bs-8538R), rabbit anti-DP receptor (1:500, Enzo Life Sciences, Barcelona, Spain, Ref. ADI-905-800-100), rabbit anti-FP receptor (1:500, Enzo Life Sciences, Barcelona, Spain, Ref. ADI-905-901-100) rabbit anti Na^+/K^+ ATPase (1:100 Abcam, Cambridge, UK, Ref. ab124677). The secondary antibody used was donkey anti-rabbit alexa fluor 555 (A31572, Life Technologies, 1:400) and DAPI for nuclei. The images were obtained using Zeiss confocal microscope and the Mander's colocalization coefficients were calculated using Zen software. Briefly, ROI were manually drawn around the nuclei (10nuclei/crypt, 5 crypts section) in three consecutive sections.

6.3 Statistical analysis

Unless specified, all statistical analysis was made using Graphpad Prism Software.

BIBLIOGRAPHY

7 Bibliography

- 1 M. Sud *et al.* LMSD: LIPID MAPS structure database. *Nucleic Acids Res.* **35**, doi:doi:10.1093/nar/gkl838 (2007).
- 2 Spiro, M. J. & McKibbin, J. M. The lipides of rat liver cell fractions. *J Biol Chem* **219**, 643-651 (1956).
- 3 Macfarlane, M. G., Gray, G. M. & Wheeldon, L. W. Fatty acid composition of phospholipids from subcellular particles of rat liver. *Biochem J* **77**, 626-631 (1960).
- 4 Eichberg, J., Whittaker, V. P. & Dawson, R. M. Distribution of lipids in subcellular particles of guinea-pig brain. *Biochem J* **92**, 91-100 (1964).
- 5 Echard, A. Phosphoinositides and cytokinesis: the "PIP" of the iceberg. *Cytoskeleton* **69**, 893-912, doi:10.1002/cm.21067 (2012).
- 6 Echard, A. Membrane traffic and polarization of lipid domains during cytokinesis. *Biochemical Society transactions* **36**, 395-399, doi:10.1042/BST0360395 (2008).
- 7 Ng, M. M., Chang, F. & Burgess, D. R. Movement of membrane domains and requirement of membrane signaling molecules for cytokinesis. *Developmental cell* **9**, 781-790, doi:10.1016/j.devcel.2005.11.002 (2005).
- 8 Dambournet, D. *et al.* Rab35 GTPase and OCRL phosphatase remodel lipids and F-actin for successful cytokinesis. *Nature cell biology* **13**, 981-988, doi:10.1038/ncb2279 (2011).
- 9 Sagona, A. P. *et al.* PtdIns(3)P controls cytokinesis through KIF13A-mediated recruitment of FYVE-CENT to the midbody. *Nature cell biology* **12**, 362-371, doi:10.1038/ncb2036 (2010).
- 10 Field, S. J. *et al.* PtdIns(4,5)P₂ functions at the cleavage furrow during cytokinesis. *Curr Biol* **15**, 1407-1412, doi:10.1016/j.cub.2005.06.059 (2005).
- 11 Atilla-Gokcumen, G. E. *et al.* Dividing cells regulate their lipid composition and localization. *Cell* **156**, 428-439, doi:10.1016/j.cell.2013.12.015 (2014).
- 12 Nikolopoulou, E. *et al.* Arachidonic acid-dependent gene regulation during preadipocyte differentiation controls adipocyte potential. *J Lipid Res* **55**, 2479-2490, doi:10.1194/jlr.M049551 (2014).
- 13 Yoshida, K., Shinohara, H., Haneji, T. & Nagata, T. Arachidonic acid inhibits osteoblast differentiation through cytosolic phospholipase A₂-dependent pathway. *Oral diseases* **13**, 32-39, doi:10.1111/j.1601-0825.2006.01239.x (2007).
- 14 Ponec, M., Weerheim, A., Kempenaar, J., Mommaas, A. M. & Nugteren, D. H. Lipid composition of cultured human keratinocytes in relation to their differentiation. *J Lipid Res* **29**, 949-961 (1988).
- 15 Pena, L. *et al.* Critical role for cytosolic group IVA phospholipase A₂ in early adipocyte differentiation and obesity. *Biochim Biophys Acta* **1861**, 1083-1095, doi:10.1016/j.bbalip.2016.06.004 (2016).
- 16 Gil-de-Gomez, L. *et al.* A phosphatidylinositol species acutely generated by activated macrophages regulates innate immune responses. *Journal of immunology* **190**, 5169-5177, doi:10.4049/jimmunol.1203494 (2013).
- 17 Rubio, J. M. *et al.* Group V secreted phospholipase A₂ is upregulated by IL-4 in human macrophages and mediates phagocytosis via hydrolysis of ethanolamine phospholipids. *Journal of immunology* **194**, 3327-3339, doi:10.4049/jimmunol.1401026 (2015).
- 18 Astudillo, A. M., Balgoma, D., Balboa, M. A. & Balsinde, J. Dynamics of arachidonic acid mobilization by inflammatory cells. *Biochim Biophys Acta* **1821**, 249-256, doi:10.1016/j.bbalip.2011.11.006 (2012).

- 19 Fonteh, A. N. & Chilton, F. H. Rapid remodeling of arachidonate from phosphatidylcholine to phosphatidylethanolamine pools during mast cell activation. *Journal of immunology* **148**, 1784-1791 (1992).
- 20 Reich, M. & Wainio, W. W. Role of phospholipids in cytochrome c oxidase activity. *J Biol Chem* **236**, 3062-3065 (1961).
- 21 Lingwood, D. & Simons, K. Lipid rafts as a membrane-organizing principle. *Science* **327**, 46-50, doi:10.1126/science.1174621 (2010).
- 22 Simons, K. & Gerl, M. J. Revitalizing membrane rafts: new tools and insights. *Nat Rev Mol Cell Biol* **11**, 688-699, doi:10.1038/nrm2977 (2010).
- 23 Lavie, Y. & Liscovitch, M. Changes in lipid and protein constituents of rafts and caveolae in multidrug resistant cancer cells and their functional consequences. *Glycoconjugate journal* **17**, 253-259 (2000).
- 24 Botelho, A. V., Huber, T., Sakmar, T. P. & Brown, M. F. Curvature and hydrophobic forces drive oligomerization and modulate activity of rhodopsin in membranes. *Biophys J* **91**, 4464-4477, doi:10.1529/biophysj.106.082776 (2006).
- 25 McMahan, H. T. & Gallop, J. L. Membrane curvature and mechanisms of dynamic cell membrane remodelling. *Nature* **438**, 590-596, doi:10.1038/nature04396 (2005).
- 26 Simons, K. & Toomre, D. Lipid rafts and signal transduction. *Nat Rev Mol Cell Biol* **1**, 31-39 (2000).
- 27 Gohlke, R. S. & McLafferty, F. W. Early gas chromatography/mass spectrometry. *Journal of the American Society for Mass Spectrometry* **4**, 367-371, doi:10.1016/1044-0305(93)85001-E (1993).
- 28 Contreras, F. X. *et al.* Molecular recognition of a single sphingolipid species by a protein's transmembrane domain. *Nature* **481**, 525-529 (2011).
- 29 Fahy, E. *et al.* A comprehensive classification system for lipids. *J Lipid Res* **46**, 839-861, doi:10.1194/jlr.E400004-JLR200 (2005).
- 30 Brockerhoff, H. & Hoyle, R. J. On the Structure of the Depot Fats of Marine Fish and Mammals. *Archives of biochemistry and biophysics* **102**, 452-455, doi:10.1016/0003-9861(63)90254-6 (1963).
- 31 Brockerhoff, H. Fatty acid distribution patterns of animal depot fats. *Comparative biochemistry and physiology* **19**, 1-12 (1966).
- 32 Rawicz, W., Olbrich, K. C., McIntosh, T., Needham, D. & Evans, E. Effect of chain length and unsaturation on elasticity of lipid bilayers. *Biophys J* **79**, 328-339, doi:10.1016/S0006-3495(00)76295-3 (2000).
- 33 Pinot, M. *et al.* Lipid cell biology. Polyunsaturated phospholipids facilitate membrane deformation and fission by endocytic proteins. *Science* **345**, 693-697, doi:10.1126/science.1255288 (2014).
- 34 Dugave, C. & Demange, L. Cis-trans isomerization of organic molecules and biomolecules: implications and applications. *Chemical reviews* **103**, 2475-2532, doi:10.1021/cr0104375 (2003).
- 35 Ran-Ressler, R. R., Devapatla, S., Lawrence, P. & Brenna, J. T. Branched chain fatty acids are constituents of the normal healthy newborn gastrointestinal tract. *Pediatric research* **64**, 605-609, doi:10.1203/PDR.0b013e318184d2e6 (2008).
- 36 Wanders, R. J., Jansen, G. A. & Skjeldal, O. H. Refsum disease, peroxisomes and phytanic acid oxidation: a review. *Journal of neuropathology and experimental neurology* **60**, 1021-1031 (2001).
- 37 Houtkooper, R. H. & Vaz, F. M. Cardiolipin, the heart of mitochondrial metabolism. *Cellular and molecular life sciences : CMLS* **65**, 2493-2506, doi:10.1007/s00018-008-8030-5 (2008).

- 38 Gallala, H. D. & Sandhoff, K. Biological function of the cellular lipid BMP-BMP as a key activator for cholesterol sorting and membrane digestion. *Neurochemical research* **36**, 1594-1600, doi:10.1007/s11064-010-0337-6 (2011).
- 39 DaTorre, S. D. & Creer, M. H. Differential turnover of polyunsaturated fatty acids in plasmalogen and diacyl glycerophospholipids of isolated cardiac myocytes. *J Lipid Res* **32**, 1159-1172 (1991).
- 40 Ford, D. A. & Gross, R. W. Plasmenylethanolamine is the major storage depot for arachidonic acid in rabbit vascular smooth muscle and is rapidly hydrolyzed after angiotensin II stimulation. *Proc Natl Acad Sci U S A* **86**, 3479-3483 (1989).
- 41 Gaposchkin, D. P. & Zoeller, R. A. Plasmalogen status influences docosahexaenoic acid levels in a macrophage cell line. Insights using ether lipid-deficient variants. *J Lipid Res* **40**, 495-503 (1999).
- 42 Braverman, N. E. & Moser, A. B. Functions of plasmalogen lipids in health and disease. *Biochim Biophys Acta* **1822**, 1442-1452, doi:10.1016/j.bbadis.2012.05.008 (2012).
- 43 Farooqui, A. A. & Horrocks, L. A. Plasmalogens, phospholipase A2, and docosahexaenoic acid turnover in brain tissue. *Journal of molecular neuroscience : MN* **16**, 263-272; discussion 279-284 (2001).
- 44 Chilton, F. H. & Connell, T. R. 1-ether-linked phosphoglycerides. Major endogenous sources of arachidonate in the human neutrophil. *J Biol Chem* **263**, 5260-5265 (1988).
- 45 Broniec, A. *et al.* Interactions of plasmalogens and their diacyl analogs with singlet oxygen in selected model systems. *Free radical biology & medicine* **50**, 892-898, doi:10.1016/j.freeradbiomed.2011.01.002 (2011).
- 46 Morandat, S. *et al.* Plasmalogens protect unsaturated lipids against UV-induced oxidation in monolayer. *Biochim Biophys Acta* **1616**, 137-146 (2003).
- 47 Sindelar, P. J., Guan, Z., Dallner, G. & Ernster, L. The protective role of plasmalogens in iron-induced lipid peroxidation. *Free radical biology & medicine* **26**, 318-324 (1999).
- 48 Glaser, P. E. & Gross, R. W. Plasmenylethanolamine facilitates rapid membrane fusion: a stopped-flow kinetic investigation correlating the propensity of a major plasma membrane constituent to adopt an HII phase with its ability to promote membrane fusion. *Biochemistry* **33**, 5805-5812 (1994).
- 49 Thai, T. P. *et al.* Impaired membrane traffic in defective ether lipid biosynthesis. *Human molecular genetics* **10**, 127-136, doi:10.1093/hmg/10.2.127 (2001).
- 50 Facciotti, F. *et al.* Peroxisome-derived lipids are self antigens that stimulate invariant natural killer T cells in the thymus. *Nature immunology* **13**, 474-480, doi:10.1038/ni.2245 (2012).
- 51 Dorninger, F. *et al.* Homeostasis of phospholipids - The level of phosphatidylethanolamine tightly adapts to changes in ethanolamine plasmalogens. *Biochim Biophys Acta* **1851**, 117-128, doi:10.1016/j.bbalip.2014.11.005 (2015).
- 52 Hoefler, G. *et al.* Biochemical abnormalities in rhizomelic chondrodysplasia punctata. *The Journal of pediatrics* **112**, 726-733 (1988).
- 53 Schutgens, R. B., Bouman, I. W., Nijenhuis, A. A., Wanders, R. J. & Frumau, M. E. Profiles of very-long-chain fatty acids in plasma, fibroblasts, and blood cells in Zellweger syndrome, X-linked adrenoleukodystrophy, and rhizomelic chondrodysplasia punctata. *Clinical chemistry* **39**, 1632-1637 (1993).
- 54 D'Souza, K. & Epand, R. M. Enrichment of phosphatidylinositols with specific acyl chains. *Biochim Biophys Acta* **1838**, 1501-1508, doi:10.1016/j.bbamem.2013.10.003 (2014).
- 55 Snyder, F. *Ether Lipids: Chemistry and Biology*. (Academic Press, 1972).
- 56 Goldstein, J. L. & Brown, M. S. A century of cholesterol and coronaries: from plaques to genes to statins. *Cell* **161**, 161-172, doi:10.1016/j.cell.2015.01.036 (2015).

- 57 Roche, Y. *et al.* Depletion of phytosterols from the plant plasma membrane provides evidence for disruption of lipid rafts. *FASEB journal : official publication of the Federation of American Societies for Experimental Biology* **22**, 3980-3991, doi:10.1096/fj.08-111070 (2008).
- 58 Dietschy, J. M. & Turley, S. D. Thematic review series: brain Lipids. Cholesterol metabolism in the central nervous system during early development and in the mature animal. *J Lipid Res* **45**, 1375-1397, doi:10.1194/jlr.R400004-JLR200 (2004).
- 59 van Blitterswijk, W. J., van der Meer, B. W. & Hilkmann, H. Quantitative contributions of cholesterol and the individual classes of phospholipids and their degree of fatty acyl (un)saturation to membrane fluidity measured by fluorescence polarization. *Biochemistry* **26**, 1746-1756 (1987).
- 60 Song, Y., Kenworthy, A. K. & Sanders, C. R. Cholesterol as a co-solvent and a ligand for membrane proteins. *Protein science : a publication of the Protein Society* **23**, 1-22, doi:10.1002/pro.2385 (2014).
- 61 Martin, M. G., Pfrieger, F. & Dotti, C. G. Cholesterol in brain disease: sometimes determinant and frequently implicated. *EMBO reports* **15**, 1036-1052, doi:10.15252/embr.201439225 (2014).
- 62 Vance, J. E. Lipid imbalance in the neurological disorder, Niemann-Pick C disease. *FEBS letters* **580**, 5518-5524, doi:10.1016/j.febslet.2006.06.008 (2006).
- 63 An, D., Na, C., Bielawski, J., Hannun, Y. A. & Kasper, D. L. Membrane sphingolipids as essential molecular signals for *Bacteroides* survival in the intestine. *Proc Natl Acad Sci U S A* **108 Suppl 1**, 4666-4671, doi:10.1073/pnas.1001501107 (2011).
- 64 Merrill, A. H., Jr. De novo sphingolipid biosynthesis: a necessary, but dangerous, pathway. *J Biol Chem* **277**, 25843-25846, doi:10.1074/jbc.R200009200 (2002).
- 65 Bose, R. *et al.* Ceramide synthase mediates daunorubicin-induced apoptosis: an alternative mechanism for generating death signals. *Cell* **82**, 405-414 (1995).
- 66 Quintans, J., Kilkus, J., McShan, C. L., Gottschalk, A. R. & Dawson, G. Ceramide mediates the apoptotic response of WEHI 231 cells to anti-immunoglobulin, corticosteroids and irradiation. *Biochem Biophys Res Commun* **202**, 710-714, doi:10.1006/bbrc.1994.1988 (1994).
- 67 Verheij, M. *et al.* Requirement for ceramide-initiated SAPK/JNK signalling in stress-induced apoptosis. *Nature* **380**, 75-79, doi:10.1038/380075a0 (1996).
- 68 Cuvillier, O. *et al.* Suppression of ceramide-mediated programmed cell death by sphingosine-1-phosphate. *Nature* **381**, 800-803, doi:10.1038/381800a0 (1996).
- 69 Kanto, T., Kalinski, P., Hunter, O. C., Lotze, M. T. & Amoscato, A. A. Ceramide mediates tumor-induced dendritic cell apoptosis. *Journal of immunology* **167**, 3773-3784 (2001).
- 70 Thudicum, J. L. W. A Treatise on the Chemical Constitution of Brain. (1884).
- 71 O'Brien, J. S. & Sampson, E. L. Lipid composition of the normal human brain: gray matter, white matter, and myelin. *J Lipid Res* **6**, 537-544 (1965).
- 72 Chan, R. B. *et al.* Comparative lipidomic analysis of mouse and human brain with Alzheimer disease. *J Biol Chem* **287**, 2678-2688, doi:10.1074/jbc.M111.274142 (2012).
- 73 Wang, Q. & London, E. Lipid Structure and Composition Control Consequences of Interleaflet Coupling in Asymmetric Vesicles. *Biophys J* **115**, 664-678, doi:10.1016/j.bpj.2018.07.011 (2018).
- 74 Brown, D. A. & London, E. Structure and function of sphingolipid- and cholesterol-rich membrane rafts. *J Biol Chem* **275**, 17221-17224, doi:10.1074/jbc.R000005200 (2000).
- 75 J, C., PB, G. & LF, L. C. The masked lipids of nuclei. *Quart J Microscop Sci* **100**, 325-337 (1959).
- 76 J, C. & PB, G. Lipid components in nucleohistone. *Biochem J* **69** (1958).

- 77 PB, G. Histochemical evidence for the presence of lipids on the chromosomes of animal cells. *Exp Cell Res* **39**, 136–144 (1965).
- 78 Fukasawa, M., Nishijima, M. & Hanada, K. Genetic evidence for ATP-dependent endoplasmic reticulum-to-Golgi apparatus trafficking of ceramide for sphingomyelin synthesis in Chinese hamster ovary cells. *The Journal of cell biology* **144**, 673-685 (1999).
- 79 Huitema, K., van den Dikkenberg, J., Brouwers, J. F. & Holthuis, J. C. Identification of a family of animal sphingomyelin synthases. *Embo J* **23**, 33-44 (2004).
- 80 van Helvoort, A., van't Hof, W., Ritsema, T., Sandra, A. & van Meer, G. Conversion of diacylglycerol to phosphatidylcholine on the basolateral surface of epithelial (Madin-Darby canine kidney) cells. Evidence for the reverse action of a sphingomyelin synthase. *J Biol Chem* **269**, 1763-1769 (1994).
- 81 Bartke, N. & Hannun, Y. A. Bioactive sphingolipids: metabolism and function. *Journal of lipid research* **50 Suppl**, S91-96, doi:10.1194/jlr.R800080-JLR200 (2009).
- 82 Kolter, T., Proia, R. L. & Sandhoff, K. Combinatorial ganglioside biosynthesis. *J Biol Chem* **277**, 25859-25862, doi:10.1074/jbc.R200001200 (2002).
- 83 Hakomori, S. Glycosphingolipids in cellular interaction, differentiation, and oncogenesis. *Annual review of biochemistry* **50**, 733-764, doi:10.1146/annurev.bi.50.070181.003505 (1981).
- 84 Liebisch, G. *et al.* Shorthand notation for lipid structures derived from mass spectrometry. *Journal of lipid research* **54**, 1523-1530, doi:10.1194/jlr.M033506 (2013).
- 85 van Meer, G. & de Kroon, A. I. Lipid map of the mammalian cell. *Journal of cell science* **124**, 5-8, doi:10.1242/jcs.071233 (2011).
- 86 Dougherty, R. M., Galli, C., Ferro-Luzzi, A. & Iacono, J. M. Lipid and phospholipid fatty acid composition of plasma, red blood cells, and platelets and how they are affected by dietary lipids: a study of normal subjects from Italy, Finland, and the USA. *Am J Clin Nutr* **45**, 443-455, doi:10.1093/ajcn/45.2.443 (1987).
- 87 Gray, G. M. & Yardley, H. J. Lipid compositions of cells isolated from pig, human, and rat epidermis. *J Lipid Res* **16**, 434-440 (1975).
- 88 Pradas, I. *et al.* Lipidomics Reveals a Tissue-Specific Fingerprint. *Frontiers in physiology* **9**, 1165, doi:10.3389/fphys.2018.01165 (2018).
- 89 Holthuis, J. C. & Menon, A. K. Lipid landscapes and pipelines in membrane homeostasis. *Nature* **510**, 48-57, doi:10.1038/nature13474 (2014).
- 90 van Meer, G., Voelker, D. R. & Feigenson, G. W. Membrane lipids: where they are and how they behave. *Nat Rev Mol Cell Biol* **9**, 112-124 (2008).
- 91 Barceló-Coblijn, G. & Murphy, E. J. An improved method for separating cardiolipin by HPLC. *Lipids* **43**, 971-976 (2008).
- 92 Marquardt, D., Geier, B. & Pabst, G. Asymmetric lipid membranes: towards more realistic model systems. *Membranes* **5**, 180-196, doi:10.3390/membranes5020180 (2015).
- 93 Nickels, J. D., Smith, J. C. & Cheng, X. Lateral organization, bilayer asymmetry, and inter-leaflet coupling of biological membranes. *Chemistry and physics of lipids* **192**, 87-99, doi:10.1016/j.chemphyslip.2015.07.012 (2015).
- 94 Gennis, R. B. in *Biomembranes* (Springer, 1989).
- 95 Kobayashi, T. & Menon, A. K. Transbilayer lipid asymmetry. *Current biology : CB* **28**, R386-R391, doi:10.1016/j.cub.2018.01.007 (2018).
- 96 Wautier, M. P. *et al.* Red blood cell phosphatidylserine exposure is responsible for increased erythrocyte adhesion to endothelium in central retinal vein occlusion.

- Journal of thrombosis and haemostasis : JTH* **9**, 1049-1055, doi:10.1111/j.1538-7836.2011.04251.x (2011).
- 97 Hankins, H. M., Baldrige, R. D., Xu, P. & Graham, T. R. Role of flippases, scramblases and transfer proteins in phosphatidylserine subcellular distribution. *Traffic* **16**, 35-47, doi:10.1111/tra.12233 (2015).
- 98 Segawa, K. *et al.* Caspase-mediated cleavage of phospholipid flippase for apoptotic phosphatidylserine exposure. *Science* **344**, 1164-1168, doi:10.1126/science.1252809 (2014).
- 99 Riedl, S. *et al.* In search of a novel target - phosphatidylserine exposed by non-apoptotic tumor cells and metastases of malignancies with poor treatment efficacy. *Biochimica et biophysica acta* **1808**, 2638-2645, doi:10.1016/j.bbamem.2011.07.026 (2011).
- 100 Murate, M. *et al.* Transbilayer distribution of lipids at nano scale. *J Cell Sci* **128**, 1627-1638, doi:10.1242/jcs.163105 (2015).
- 101 Kiessling, V., Wan, C. & Tamm, L. K. Domain coupling in asymmetric lipid bilayers. *Biochim Biophys Acta* **1788**, 64-71, doi:10.1016/j.bbamem.2008.09.003 (2009).
- 102 Harayama, T. & Riezman, H. Understanding the diversity of membrane lipid composition. *Nature reviews. Molecular cell biology* **19**, 281-296, doi:10.1038/nrm.2017.138 (2018).
- 103 Contreras, F. X. *et al.* Molecular recognition of a single sphingolipid species by a protein's transmembrane domain. *Nature* **481**, 525-529, doi:10.1038/nature10742 (2012).
- 104 Adolf, F. *et al.* Scission of COPI and COPII vesicles is independent of GTP hydrolysis. *Traffic* **14**, 922-932, doi:10.1111/tra.12084 (2013).
- 105 Behnia, R. & Munro, S. Organelle identity and the signposts for membrane traffic. *Nature* **438**, 597-604, doi:10.1038/nature04397 (2005).
- 106 Lu, S. M. & Fairn, G. D. Mesoscale organization of domains in the plasma membrane - beyond the lipid raft. *Critical reviews in biochemistry and molecular biology* **53**, 192-207, doi:10.1080/10409238.2018.1436515 (2018).
- 107 Quest, A. F., Leyton, L. & Parraga, M. Caveolins, caveolae, and lipid rafts in cellular transport, signaling, and disease. *Biochemistry and cell biology = Biochimie et biologie cellulaire* **82**, 129-144, doi:10.1139/o03-071 (2004).
- 108 Graziani, A., Bricko, V., Carmignani, M., Graier, W. F. & Groschner, K. Cholesterol- and caveolin-rich membrane domains are essential for phospholipase A2-dependent EDHF formation. *Cardiovascular research* **64**, 234-242, doi:10.1016/j.cardiores.2004.06.026 (2004).
- 109 Suetsugu, S., Kurisu, S. & Takenawa, T. Dynamic shaping of cellular membranes by phospholipids and membrane-deforming proteins. *Physiological reviews* **94**, 1219-1248, doi:10.1152/physrev.00040.2013 (2014).
- 110 Stancevic, B. & Kolesnick, R. Ceramide-rich platforms in transmembrane signaling. *FEBS letters* **584**, 1728-1740, doi:10.1016/j.febslet.2010.02.026 (2010).
- 111 Simons, K. & Ikonen, E. Functional rafts in cell membranes. *Nature* **387**, 569-572, doi:10.1038/42408 (1997).
- 112 Marsh, D. Lateral pressure profile, spontaneous curvature frustration, and the incorporation and conformation of proteins in membranes. *Biophysical journal* **93**, 3884-3899, doi:10.1529/biophysj.107.107938 (2007).
- 113 McMahon, H. T. & Boucrot, E. Membrane curvature at a glance. *Journal of cell science* **128**, 1065-1070, doi:10.1242/jcs.114454 (2015).

- 114 Attard, G. S., Templer, R. H., Smith, W. S., Hunt, A. N. & Jackowski, S. Modulation of CTP:phosphocholine cytidyltransferase by membrane curvature elastic stress. *Proc Natl Acad Sci U S A* **97**, 9032-9036, doi:10.1073/pnas.160260697 (2000).
- 115 Lee, J., Taneva, S. G., Holland, B. W., Tieleman, D. P. & Cornell, R. B. Structural basis for autoinhibition of CTP:phosphocholine cytidyltransferase (CCT), the regulatory enzyme in phosphatidylcholine synthesis, by its membrane-binding amphipathic helix. *The Journal of biological chemistry* **289**, 1742-1755, doi:10.1074/jbc.M113.526970 (2014).
- 116 Bigay, J. & Antonny, B. Curvature, lipid packing, and electrostatics of membrane organelles: defining cellular territories in determining specificity. *Developmental cell* **23**, 886-895, doi:10.1016/j.devcel.2012.10.009 (2012).
- 117 Kennedy, E. P. Biosynthesis of complex lipids. *Federation proceedings* **20**, 934-940 (1961).
- 118 Pascual, F. & Carman, G. M. Phosphatidate phosphatase, a key regulator of lipid homeostasis. *Biochim Biophys Acta* **1831**, 514-522, doi:10.1016/j.bbalip.2012.08.006 (2013).
- 119 Vance, J. E. Historical perspective: phosphatidylserine and phosphatidylethanolamine from the 1800s to the present. *J Lipid Res* **59**, 923-944, doi:10.1194/jlr.R084004 (2018).
- 120 Moessinger, C. *et al.* Two different pathways of phosphatidylcholine synthesis, the Kennedy Pathway and the Lands Cycle, differentially regulate cellular triacylglycerol storage. *BMC cell biology* **15**, 43, doi:10.1186/s12860-014-0043-3 (2014).
- 121 Shindou, H., Hishikawa, D., Harayama, T., Eto, M. & Shimizu, T. Generation of membrane diversity by lysophospholipid acyltransferases. *Journal of biochemistry* **154**, 21-28, doi:10.1093/jb/mvt048 (2013).
- 122 Yamashita, A. *et al.* Acyltransferases and transacylases that determine the fatty acid composition of glycerolipids and the metabolism of bioactive lipid mediators in mammalian cells and model organisms. *Prog Lipid Res* **53**, 18-81, doi:10.1016/j.plipres.2013.10.001 (2014).
- 123 Astudillo, A. M., Balboa, M. A. & Balsinde, J. Selectivity of phospholipid hydrolysis by phospholipase A2 enzymes in activated cells leading to polyunsaturated fatty acid mobilization. *Biochimica et biophysica acta. Molecular and cell biology of lipids* **1864**, 772-783, doi:10.1016/j.bbalip.2018.07.002 (2019).
- 124 Velíšek J., C. K. Biosynthesis of Food Constituents: Lipids. 2. Triacylglycerols, Glycerophospholipids, and Glyceroglycolipids – a Review. *Czech J. Food Sci.* **24**, 241–254 (2006).
- 125 Cheng, J. B. & Russell, D. W. Mammalian wax biosynthesis. I. Identification of two fatty acyl-Coenzyme A reductases with different substrate specificities and tissue distributions. *J Biol Chem* **279**, 37789-37797, doi:10.1074/jbc.M406225200 (2004).
- 126 Biermann, J., Just, W. W., Wanders, R. J. & Van Den Bosch, H. Alkyl-dihydroxyacetone phosphate synthase and dihydroxyacetone phosphate acyltransferase form a protein complex in peroxisomes. *European journal of biochemistry* **261**, 492-499 (1999).
- 127 de Vet, E. C. *et al.* Ether lipid biosynthesis: alkyl-dihydroxyacetonephosphate synthase protein deficiency leads to reduced dihydroxyacetonephosphate acyltransferase activities. *J Lipid Res* **40**, 1998-2003 (1999).
- 128 de Vet, E. C., Ijlst, L., Oostheim, W., Wanders, R. J. & van den Bosch, H. Alkyl-dihydroxyacetonephosphate synthase. Fate in peroxisome biogenesis disorders and identification of the point mutation underlying a single enzyme deficiency. *J Biol Chem* **273**, 10296-10301 (1998).
- 129 Kent, C. CTP:phosphocholine cytidyltransferase. *Biochim Biophys Acta* **1348**, 79-90 (1997).

- 130 Polokoff, M. A., Wing, D. C. & Raetz, C. R. Isolation of somatic cell mutants defective in the biosynthesis of phosphatidylethanolamine. *J Biol Chem* **256**, 7687-7690 (1981).
- 131 Vance, D. E. & Vance, J. E. *Biochemistry of Lipids, Lipoproteins and Membranes*. 6th edn, (2016).
- 132 Henry, S. A., Klig, L. S. & Loewy, B. S. The genetic regulation and coordination of biosynthetic pathways in yeast: amino acid and phospholipid synthesis. *Annual review of genetics* **18**, 207-231, doi:10.1146/annurev.ge.18.120184.001231 (1984).
- 133 Imai, A. & Gershengorn, M. C. Regulation by phosphatidylinositol of rat pituitary plasma membrane and endoplasmic reticulum phosphatidylinositol synthase activities. A mechanism for activation of phosphoinositide resynthesis during cell stimulation. *J Biol Chem* **262**, 6457-6459 (1987).
- 134 Barcelo-Coblijn, G. & Murphy, E. J. Alpha-linolenic acid and its conversion to longer chain n-3 fatty acids: benefits for human health and a role in maintaining tissue n-3 fatty acid levels. *Prog Lipid Res* **48**, 355-374, doi:10.1016/j.plipres.2009.07.002 (2009).
- 135 Fadok, V. A., de Cathelineau, A., Daleke, D. L., Henson, P. M. & Bratton, D. L. Loss of phospholipid asymmetry and surface exposure of phosphatidylserine is required for phagocytosis of apoptotic cells by macrophages and fibroblasts. *J Biol Chem* **276**, 1071-1077, doi:10.1074/jbc.M003649200 (2001).
- 136 Fadok, V. A. *et al.* Particle digestibility is required for induction of the phosphatidylserine recognition mechanism used by murine macrophages to phagocytose apoptotic cells. *Journal of immunology* **151**, 4274-4285 (1993).
- 137 Fadok, V. A. *et al.* Exposure of phosphatidylserine on the surface of apoptotic lymphocytes triggers specific recognition and removal by macrophages. *Journal of immunology* **148**, 2207-2216 (1992).
- 138 Epand, R. M. Recognition of polyunsaturated acyl chains by enzymes acting on membrane lipids. *Biochim Biophys Acta* **1818**, 957-962, doi:10.1016/j.bbamem.2011.07.018 (2012).
- 139 Dawson, R. M. The measurement of ³²P labelling of individual cephalins and lecithin in a small sample of tissue. *Biochim Biophys Acta* **14**, 374-379 (1954).
- 140 Hokin, L. E. & Hokin, M. R. Metabolism of phospholipids in vitro. *Can J Biochem Physiol* **34**, 349-360 (1956).
- 141 Kemp, P., Hubscher, G. & Hawthorne, J. N. Phosphoinositides. 3. Enzymic hydrolysis of inositol-containing phospholipids. *Biochem J* **79**, 193-200 (1961).
- 142 Berridge, M. J. & Irvine, R. F. Inositol phosphates and cell signalling. *Nature* **341**, 197-205, doi:10.1038/341197a0 (1989).
- 143 Lassing, I. & Lindberg, U. Specific interaction between phosphatidylinositol 4,5-bisphosphate and profilactin. *Nature* **314**, 472-474 (1985).
- 144 Ma, L., Cantley, L. C., Janmey, P. A. & Kirschner, M. W. Corequirement of specific phosphoinositides and small GTP-binding protein Cdc42 in inducing actin assembly in *Xenopus* egg extracts. *J Cell Biol* **140**, 1125-1136 (1998).
- 145 Yin, H. L. & Janmey, P. A. Phosphoinositide regulation of the actin cytoskeleton. *Annual review of physiology* **65**, 761-789, doi:10.1146/annurev.physiol.65.092101.142517 (2003).
- 146 Whitman, M., Downes, C. P., Keeler, M., Keller, T. & Cantley, L. Type I phosphatidylinositol kinase makes a novel inositol phospholipid, phosphatidylinositol-3-phosphate. *Nature* **332**, 644-646, doi:10.1038/332644a0 (1988).
- 147 Traynor-Kaplan, A. E., Harris, A. L., Thompson, B. L., Taylor, P. & Sklar, L. A. An inositol tetrakisphosphate-containing phospholipid in activated neutrophils. *Nature* **334**, 353-356, doi:10.1038/334353a0 (1988).

- 148 Auger, K. R., Serunian, L. A., Soltoff, S. P., Libby, P. & Cantley, L. C. PDGF-dependent tyrosine phosphorylation stimulates production of novel polyphosphoinositides in intact cells. *Cell* **57**, 167-175 (1989).
- 149 Wang, Q. *et al.* Regulation of TRAIL expression by the phosphatidylinositol 3-kinase/Akt/GSK-3 pathway in human colon cancer cells. *J Biol Chem* **277**, 36602-36610, doi:10.1074/jbc.M206306200 (2002).
- 150 Chen, X. *et al.* Constitutively active Akt is an important regulator of TRAIL sensitivity in prostate cancer. *Oncogene* **20**, 6073-6083, doi:10.1038/sj.onc.1204736 (2001).
- 151 Hennessy, B. T., Smith, D. L., Ram, P. T., Lu, Y. & Mills, G. B. Exploiting the PI3K/AKT pathway for cancer drug discovery. *Nature reviews. Drug discovery* **4**, 988-1004, doi:10.1038/nrd1902 (2005).
- 152 Sherr, C. J. & Weber, J. D. The ARF/p53 pathway. *Current opinion in genetics & development* **10**, 94-99 (2000).
- 153 Toi, M., Saji, S., Suzuki, A., Yamamoto, Y. & Tominaga, T. MDM2 in Breast Cancer. *Breast cancer* **4**, 264-268 (1997).
- 154 Carroll, P. E. *et al.* Centrosome hyperamplification in human cancer: chromosome instability induced by p53 mutation and/or Mdm2 overexpression. *Oncogene* **18**, 1935-1944, doi:10.1038/sj.onc.1202515 (1999).
- 155 Imae, R. *et al.* LYCAT, a homologue of *C. elegans* acl-8, acl-9, and acl-10, determines the fatty acid composition of phosphatidylinositol in mice. *J Lipid Res* **53**, 335-347, doi:10.1194/jlr.M018655 (2012).
- 156 Meyer, T., Wensel, T. & Stryer, L. Kinetics of calcium channel opening by inositol 1,4,5-trisphosphate. *Biochemistry* **29**, 32-37 (1990).
- 157 Mayrleitner, M., Chadwick, C. C., Timerman, A. P., Fleischer, S. & Schindler, H. Purified IP3 receptor from smooth muscle forms an IP3 gated and heparin sensitive Ca²⁺ channel in planar bilayers. *Cell calcium* **12**, 505-514 (1991).
- 158 Qu, X., Xiao, D. & Weber, H. C. Human gastrin-releasing peptide receptor mediates sustained CREB phosphorylation and transactivation in HuTu 80 duodenal cancer cells. *FEBS Lett* **527**, 109-113 (2002).
- 159 Perry, C., Sklan, E. H. & Soreq, H. CREB regulates AChE-R-induced proliferation of human glioblastoma cells. *Neoplasia* **6**, 279-286, doi:10.1593/neo.3424 (2004).
- 160 Corbett, G. T., Roy, A. & Pahan, K. Sodium phenylbutyrate enhances astrocytic neurotrophin synthesis via protein kinase C (PKC)-mediated activation of cAMP-response element-binding protein (CREB): implications for Alzheimer disease therapy. *J Biol Chem* **288**, 8299-8312, doi:10.1074/jbc.M112.426536 (2013).
- 161 Lecureur, V. *et al.* MAPK- and PKC/CREB-dependent induction of interleukin-11 by the environmental contaminant formaldehyde in human bronchial epithelial cells. *Toxicology* **292**, 13-22, doi:10.1016/j.tox.2011.11.011 (2012).
- 162 Frerman, F. E. & White, D. C. Membrane lipid changes during formation of a functional electron transport system in *Staphylococcus aureus*. *Journal of bacteriology* **94**, 1868-1874 (1967).
- 163 Dickens, B. F. & Thompson, G. A., Jr. Rapid membrane response during low-temperature acclimation. Correlation of early changes in the physical properties and lipid composition of *Tetrahymena* microsomal membranes. *Biochim Biophys Acta* **644**, 211-218 (1981).
- 164 Gould, G. W. Animal cell cytokinesis: The role of dynamic changes in the plasma membrane proteome and lipidome. *Seminars in cell & developmental biology* **53**, 64-73, doi:10.1016/j.semcd.2015.12.012 (2016).

- 165 Shindou, H., Hishikawa, D., Harayama, T., Yuki, K. & Shimizu, T. Recent progress on acyl CoA: lysophospholipid acyltransferase research. *J Lipid Res* **50 Suppl**, S46-51, doi:10.1194/jlr.R800035-JLR200 (2009).
- 166 Waku, K. & Nakazawa, Y. Acyltransferase activity to 1-acyl-, 1-O-alkenyl-, and 1-O-alkyl-glycero-3-phosphorylcholine in Ehrlich ascites tumor cells. *Journal of biochemistry* **72**, 495-497 (1972).
- 167 Shindou, H. & Shimizu, T. Acyl-CoA:lysophospholipid acyltransferases. *J Biol Chem* **284**, 1-5, doi:10.1074/jbc.R800046200 (2009).
- 168 Shimizu, T. Lipid mediators in health and disease: enzymes and receptors as therapeutic targets for the regulation of immunity and inflammation. *Annual review of pharmacology and toxicology* **49**, 123-150, doi:10.1146/annurev.pharmtox.011008.145616 (2009).
- 169 Lands, W. E. Stories about acyl chains. *Biochim Biophys Acta* **1483**, 1-14 (2000).
- 170 Lands, W. E. Metabolism of glycerolipides; a comparison of lecithin and triglyceride synthesis. *J Biol Chem* **231**, 883-888 (1958).
- 171 Mosior, M., Six, D. A. & Dennis, E. A. Group IV cytosolic phospholipase A2 binds with high affinity and specificity to phosphatidylinositol 4,5-bisphosphate resulting in dramatic increases in activity. *J Biol Chem* **273**, 2184-2191 (1998).
- 172 Bou Khalil, M. *et al.* Lipidomics era: accomplishments and challenges. *Mass spectrometry reviews* **29**, 877-929, doi:10.1002/mas.20294 (2010).
- 173 Stephens, W. W., Walker, J. L. & Myers, W. The action of cobra poison on the blood: a contribution to the study of passive immunity. *J. Pathol. Bacteriol.* **5**, 279-301 (1898).
- 174 Davidson, F. F. & Dennis, E. A. Evolutionary relationships and implications for the regulation of phospholipase A2 from snake venom to human secreted forms. *Journal of molecular evolution* **31**, 228-238 (1990).
- 175 Kramer, R. M. *et al.* Structure and properties of a human non-pancreatic phospholipase A2. *J Biol Chem* **264**, 5768-5775 (1989).
- 176 Seilhamer, J. J. *et al.* Cloning and recombinant expression of phospholipase A2 present in rheumatoid arthritic synovial fluid. *J Biol Chem* **264**, 5335-5338 (1989).
- 177 Heinrikson, R. L., Krueger, E. T. & Keim, P. S. Amino acid sequence of phospholipase A2-alpha from the venom of *Crotalus adamanteus*. A new classification of phospholipases A2 based upon structural determinants. *J Biol Chem* **252**, 4913-4921 (1977).
- 178 Dufton, M. J. & Hider, R. C. Classification of phospholipases A2 according to sequence. Evolutionary and pharmacological implications. *European journal of biochemistry* **137**, 545-551 (1983).
- 179 Alonso, F., Henson, P. M. & Leslie, C. C. A cytosolic phospholipase in human neutrophils that hydrolyzes arachidonoyl-containing phosphatidylcholine. *Biochim Biophys Acta* **878**, 273-280 (1986).
- 180 Kramer, R. M., Checani, G. C., Deykin, A., Pritzker, C. R. & Deykin, D. Solubilization and properties of Ca²⁺-dependent human platelet phospholipase A2. *Biochim Biophys Acta* **878**, 394-403 (1986).
- 181 Sharp, J. D. *et al.* Molecular cloning and expression of human Ca²⁺-sensitive cytosolic phospholipase A2. *J Biol Chem* **266**, 14850-14853 (1991).
- 182 Clark, J. D. *et al.* A novel arachidonic acid-selective cytosolic PLA2 contains a Ca²⁺-dependent translocation domain with homology to PKC and GAP. *Cell* **65**, 1043-1051 (1991).
- 183 Murakami, M. *et al.* Detection of three distinct phospholipases A2 in cultured mast cells. *Journal of biochemistry* **111**, 175-181 (1992).

- 184 Diez, E., Louis-Flamberg, P., Hall, R. H. & Mayer, R. J. Substrate specificities and properties of human phospholipase A2 in a mixed vesicle model. *J Biol Chem* **267**, 18342-18348 (1992).
- 185 Underwood, K. W. *et al.* A novel calcium-independent phospholipase A2, cPLA2-gamma, that is prenylated and contains homology to cPLA2. *J Biol Chem* **273**, 21926-21932 (1998).
- 186 Channon, J. Y. & Leslie, C. C. A calcium-dependent mechanism for associating a soluble arachidonoyl-hydrolyzing phospholipase A2 with membrane in the macrophage cell line RAW 264.7. *J Biol Chem* **265**, 5409-5413 (1990).
- 187 Gijon, M. A., Spencer, D. M., Kaiser, A. L. & Leslie, C. C. Role of phosphorylation sites and the C2 domain in regulation of cytosolic phospholipase A2. *J Cell Biol* **145**, 1219-1232 (1999).
- 188 Glover, S. *et al.* Translocation of the 85-kDa phospholipase A2 from cytosol to the nuclear envelope in rat basophilic leukemia cells stimulated with calcium ionophore or IgE/antigen. *J Biol Chem* **270**, 15359-15367 (1995).
- 189 Nakatani, Y., Tanioka, T., Sunaga, S., Murakami, M. & Kudo, I. Identification of a cellular protein that functionally interacts with the C2 domain of cytosolic phospholipase A(2)alpha. *J Biol Chem* **275**, 1161-1168 (2000).
- 190 Reynolds, L. J., Hughes, L. L., Louis, A. I., Kramer, R. M. & Dennis, E. A. Metal ion and salt effects on the phospholipase A2, lysophospholipase, and transacylase activities of human cytosolic phospholipase A2. *Biochim Biophys Acta* **1167**, 272-280 (1993).
- 191 Pickard, R. T. *et al.* Identification of essential residues for the catalytic function of 85-kDa cytosolic phospholipase A2. Probing the role of histidine, aspartic acid, cysteine, and arginine. *J Biol Chem* **271**, 19225-19231 (1996).
- 192 Rubin, B. B. *et al.* Cytosolic phospholipase A2-alpha is necessary for platelet-activating factor biosynthesis, efficient neutrophil-mediated bacterial killing, and the innate immune response to pulmonary infection: cPLA2-alpha does not regulate neutrophil NADPH oxidase activity. *J Biol Chem* **280**, 7519-7529, doi:10.1074/jbc.M407438200 (2005).
- 193 Casas, J. *et al.* Requirement of JNK-mediated phosphorylation for translocation of group IVA phospholipase A2 to phagosomes in human macrophages. *Journal of immunology* **183**, 2767-2774, doi:10.4049/jimmunol.0901530 (2009).
- 194 Girotti, M., Evans, J. H., Burke, D. & Leslie, C. C. Cytosolic phospholipase A2 translocates to forming phagosomes during phagocytosis of zymosan in macrophages. *J Biol Chem* **279**, 19113-19121, doi:10.1074/jbc.M313867200 (2004).
- 195 Tang, J. *et al.* A novel cytosolic calcium-independent phospholipase A2 contains eight ankyrin motifs. *J Biol Chem* **272**, 8567-8575 (1997).
- 196 Balsinde, J., Bianco, I. D., Ackermann, E. J., Conde-Frieboes, K. & Dennis, E. A. Inhibition of calcium-independent phospholipase A2 prevents arachidonic acid incorporation and phospholipid remodeling in P388D1 macrophages. *Proc Natl Acad Sci U S A* **92**, 8527-8531 (1995).
- 197 Balsinde, J., Fernandez, B. & Solis-Herruzo, J. A. Increased incorporation of arachidonic acid into phospholipids in zymosan-stimulated mouse peritoneal macrophages. *European journal of biochemistry* **221**, 1013-1018 (1994).
- 198 Conde-Frieboes, K. *et al.* Activated Ketones as Inhibitors of Intracellular Ca²⁺-Dependent and Ca²⁺-Independent Phospholipase A2. *J Am Chem Soc* **118**, 5519-5525 (1996).
- 199 Balsinde, J. & Dennis, E. A. Bromoenol lactone inhibits magnesium-dependent phosphatidate phosphohydrolase and blocks triacylglycerol biosynthesis in mouse P388D1 macrophages. *J Biol Chem* **271**, 31937-31941 (1996).

- 200 Matsuda, S. *et al.* Member of the membrane-bound O-acyltransferase (MBOAT) family encodes a lysophospholipid acyltransferase with broad substrate specificity. *Genes to cells : devoted to molecular & cellular mechanisms* **13**, 879-888, doi:10.1111/j.1365-2443.2008.01212.x (2008).
- 201 Zhao, Y. *et al.* Identification and characterization of a major liver lysophosphatidylcholine acyltransferase. *J Biol Chem* **283**, 8258-8265, doi:10.1074/jbc.M710422200 (2008).
- 202 Hishikawa, D. *et al.* Discovery of a lysophospholipid acyltransferase family essential for membrane asymmetry and diversity. *Proc Natl Acad Sci U S A* **105**, 2830-2835, doi:10.1073/pnas.0712245105 (2008).
- 203 Shindou, H. *et al.* A single enzyme catalyzes both platelet-activating factor production and membrane biogenesis of inflammatory cells. Cloning and characterization of acetyl-CoA:LYSO-PAF acetyltransferase. *J Biol Chem* **282**, 6532-6539, doi:10.1074/jbc.M609641200 (2007).
- 204 Cao, J. *et al.* Molecular identification of a novel mammalian brain isoform of acyl-CoA:lysophospholipid acyltransferase with prominent ethanolamine lysophospholipid acylating activity, LPEAT2. *J Biol Chem* **283**, 19049-19057, doi:10.1074/jbc.M800364200 (2008).
- 205 Chen, X., Hyatt, B. A., Mucenski, M. L., Mason, R. J. & Shannon, J. M. Identification and characterization of a lysophosphatidylcholine acyltransferase in alveolar type II cells. *Proc Natl Acad Sci U S A* **103**, 11724-11729, doi:10.1073/pnas.0604946103 (2006).
- 206 Nakanishi, H. *et al.* Cloning and characterization of mouse lung-type acyl-CoA:lysophosphatidylcholine acyltransferase 1 (LPCAT1). Expression in alveolar type II cells and possible involvement in surfactant production. *J Biol Chem* **281**, 20140-20147, doi:10.1074/jbc.M600225200 (2006).
- 207 Lee, H. C. *et al.* *Caenorhabditis elegans* mboa-7, a member of the MBOAT family, is required for selective incorporation of polyunsaturated fatty acids into phosphatidylinositol. *Molecular biology of the cell* **19**, 1174-1184, doi:10.1091/mbc.E07-09-0893 (2008).
- 208 Digel, M., Eehalt, R., Stremmel, W. & Fullekrug, J. Acyl-CoA synthetases: fatty acid uptake and metabolic channeling. *Mol Cell Biochem* **326**, 23-28, doi:10.1007/s11010-008-0003-3 (2009).
- 209 Kuch, E. M. *et al.* Differentially localized acyl-CoA synthetase 4 isoenzymes mediate the metabolic channeling of fatty acids towards phosphatidylinositol. *Biochim Biophys Acta* **1841**, 227-239, doi:10.1016/j.bbali.2013.10.018 (2014).
- 210 McDonald, J. G., Ivanova, P. T. & Brown, H. A. in *Biochemistry of Lipids, Lipoproteins and Membranes* (eds Ridgway Neale D. & McLeod Roger S.) Ch. Second, (2016).
- 211 Christie, W. W. & Han, X. *Lipid Analysis, Fourth Edition: Isolation, Separation, Identification and Lipidomic Analysis*. Fourth Edition edn, (2010).
- 212 Folch, J., Lees, M. & Sloane Stanley, G. H. A simple method for the isolation and purification of total lipides from animal tissues. *J Biol Chem* **226**, 497-509 (1957).
- 213 Bligh, E. G. & Dyer, W. J. A rapid method of total lipid extraction and purification. *Can J Biochem Physiol* **37**, 911-917 (1959).
- 214 Sparkman, O. D. *Mass spectrometry desk reference*. (Pittsburgh: Global View Pub, 2000).
- 215 Kofeler, H. C., Fauland, A., Rechberger, G. N. & Trotsmuller, M. Mass spectrometry based lipidomics: an overview of technological platforms. *Metabolites* **2**, 19-38, doi:10.3390/metabo2010019 (2012).

- 216 Fahy, E. *et al.* LipidFinder on LIPID MAPS: peak filtering, MS searching and statistical analysis for lipidomics. *Bioinformatics* **35**, 685-687, doi:10.1093/bioinformatics/bty679 (2019).
- 217 Bestard-Escalas, J. *et al.* Lipid fingerprint image accurately conveys human colon cell pathophysiologic state: A solid candidate as biomarker. *Biochim Biophys Acta* **1861**, 1942-1950, doi:10.1016/j.bbaliip.2016.09.013 (2016).
- 218 Lopez, D. H. *et al.* Tissue-selective alteration of ethanolamine plasmalogen metabolism in dedifferentiated colon mucosa. *Biochim Biophys Acta* **1863**, 928-938, doi:10.1016/j.bbaliip.2018.04.017 (2018).
- 219 Fenn, J. B., Mann, M., Meng, C. K., Wong, S. F. & Whitehouse, C. M. Electrospray ionization for mass spectrometry of large biomolecules. *Science* **246**, 64-71 (1989).
- 220 Takats, Z., Wiseman, J. M., Gologan, B. & Cooks, R. G. Mass spectrometry sampling under ambient conditions with desorption electrospray ionization. *Science* **306**, 471-473, doi:10.1126/science.1104404 (2004).
- 221 Cooks, R. G., Ouyang, Z., Takats, Z. & Wiseman, J. M. Detection Technologies. Ambient mass spectrometry. *Science* **311**, 1566-1570, doi:10.1126/science.1119426 (2006).
- 222 Gerbig, S. *et al.* Analysis of colorectal adenocarcinoma tissue by desorption electrospray ionization mass spectrometric imaging. *Analytical and bioanalytical chemistry* **403**, 2315-2325, doi:10.1007/s00216-012-5841-x (2012).
- 223 Wiseman, J. M. *et al.* Desorption electrospray ionization mass spectrometry: Imaging drugs and metabolites in tissues. *Proc Natl Acad Sci U S A* **105**, 18120-18125, doi:10.1073/pnas.0801066105 (2008).
- 224 Vickerman, J. C. Molecular imaging and depth profiling by mass spectrometry--SIMS, MALDI or DESI? *The Analyst* **136**, 2199-2217, doi:10.1039/c1an00008j (2011).
- 225 Watrous, J. D., Alexandrov, T. & Dorrestein, P. C. The evolving field of imaging mass spectrometry and its impact on future biological research. *Journal of mass spectrometry : JMS* **46**, 209-222, doi:10.1002/jms.1876 (2011).
- 226 Braun, R. M. *et al.* Spatially resolved detection of attomole quantities of organic molecules localized in picoliter vials using time-of-flight secondary ion mass spectrometry. *Analytical chemistry* **71**, 3318-3324 (1999).
- 227 McDonnell, L. A. & Heeren, R. M. Imaging mass spectrometry. *Mass spectrometry reviews* **26**, 606-643, doi:10.1002/mas.20124 (2007).
- 228 Karas, M. & Hillenkamp, F. Laser desorption ionization of proteins with molecular masses exceeding 10,000 daltons. *Analytical chemistry* **60**, 2299-2301 (1988).
- 229 Tanaka, K. *et al.* Protein and polymer analyses up to m/z 100000 by laser ionization time-of-flight mass spectrometry. *Rapid Commun. Mass Spectrom.* **2**, 151-153 (1988).
- 230 Astigarraga, E. *et al.* Profiling and imaging of lipids on brain and liver tissue by matrix-assisted laser desorption/ionization mass spectrometry using 2-mercaptobenzothiazole as a matrix. *Analytical chemistry* **80**, 9105-9114, doi:10.1021/ac801662n (2008).
- 231 Peterson, D. S. Matrix-free methods for laser desorption/ionization mass spectrometry. *Mass spectrometry reviews* **26**, 19-34, doi:10.1002/mas.20104 (2007).
- 232 Barcelo-Coblijn, G. & Fernandez, J. A. Mass spectrometry coupled to imaging techniques: the better the view the greater the challenge. *Frontiers in physiology* **6**, 3, doi:10.3389/fphys.2015.00003 (2015).
- 233 Fuchs, B., Suss, R. & Schiller, J. An update of MALDI-TOF mass spectrometry in lipid research. *Prog Lipid Res* **49**, 450-475, doi:10.1016/j.plipres.2010.07.001 (2010).
- 234 Rubakhin, S. S., Jurchen, J. C., Monroe, E. B. & Sweedler, J. V. Imaging mass spectrometry: fundamentals and applications to drug discovery. *Drug Discov. Today* **10**, 823-837 (2005).

- 235 Thomas, A. *et al.* Histology-driven data mining of lipid signatures from multiple imaging mass spectrometry analyses: application to human colorectal cancer liver metastasis biopsies. *Analytical chemistry* **85**, 2860-2866, doi:10.1021/ac3034294 (2013).
- 236 Bestard-Escalas, J. *et al.* Tight regulation of the lipid composition along human colonic crypts according to the cell differentiation state revealed by MALDI-IMS techniques. *En preparación* (2015).
- 237 Belu, A. M., Graham, D. J. & Castner, D. G. Time-of-flight secondary ion mass spectrometry: techniques and applications for the characterization of biomaterial surfaces. *Biomaterials* **24**, 3635-3653 (2003).
- 238 Li, T. *et al.* Simultaneous analysis of microbial identity and function using NanoSIMS. *Environmental microbiology* **10**, 580-588, doi:10.1111/j.1462-2920.2007.01478.x (2008).
- 239 Touboul, D. *et al.* Tissue molecular ion imaging by gold cluster ion bombardment. *Analytical chemistry* **76**, 1550-1559, doi:10.1021/ac035243z (2004).
- 240 Sjovall, P., Lausmaa, J. & Johansson, B. Mass spectrometric imaging of lipids in brain tissue. *Analytical chemistry* **76**, 4271-4278, doi:10.1021/ac049389p (2004).
- 241 Touboul, D., Kollmer, F., Niehuis, E., Brunelle, A. & Laprevote, O. Improvement of biological time-of-flight-secondary ion mass spectrometry imaging with a bismuth cluster ion source. *Journal of the American Society for Mass Spectrometry* **16**, 1608-1618, doi:10.1016/j.jasms.2005.06.005 (2005).
- 242 Weibel, D. *et al.* A C60 primary ion beam system for time of flight secondary ion mass spectrometry: its development and secondary ion yield characteristics. *Analytical chemistry* **75**, 1754-1764 (2003).
- 243 Biddulph, G. X., Piwowar, A. M., Fletcher, J. S., Lockyer, N. P. & Vickerman, J. C. Properties of C84 and C24H12 molecular ion sources for routine TOF-SIMS analysis. *Analytical chemistry* **79**, 7259-7266, doi:10.1021/ac071442x (2007).
- 244 Cheng, J., Kozole, J., Hengstebeck, R. & Winograd, N. Direct comparison of Au(3)(+) and C(60)(+) cluster projectiles in SIMS molecular depth profiling. *Journal of the American Society for Mass Spectrometry* **18**, 406-412, doi:10.1016/j.jasms.2006.10.017 (2007).
- 245 Kettling, H. *et al.* MALDI mass spectrometry imaging of bioactive lipids in mouse brain with a Synapt G2-S mass spectrometer operated at elevated pressure: improving the analytical sensitivity and the lateral resolution to ten micrometers. *Analytical chemistry* **86**, 7798-7805, doi:10.1021/ac5017248 (2014).
- 246 Deeley, J. M. *et al.* Sphingolipid distribution changes with age in the human lens. *J Lipid Res* **51**, 2753-2760, doi:10.1194/jlr.M007716 (2010).
- 247 Murphy, R. C., Hankin, J. A. & Barkley, R. M. Imaging of lipid species by MALDI mass spectrometry. *J Lipid Res* **50 Suppl**, S317-322, doi:10.1194/jlr.R800051-JLR200 (2009).
- 248 Garate, J. *et al.* Imaging Mass Spectrometry Increased Resolution Using 2-mercaptobenzothiazole and 2,5-diaminonaphtalene: Application to Lipid Distribution in Human Colon *Analytical and bioanalytical chemistry* (2015).
- 249 Ifa, D. R., Wiseman, J. M., Song, Q. & Cooks, R. G. Development of capabilities for imaging mass spectrometry under ambient conditions with desorption electrospray ionization (DESI). *International Journal of Mass Spectrometry* **259**, 8-15 (2007).
- 250 Ridell, R., Petras, R., Williams, G. & Sobin, L. *Tumors of the Intestines*. (2002).
- 251 Levine, D. S. & Haggitt, R. C. Normal histology of the colon. *The American journal of surgical pathology* **13**, 966-984 (1989).
- 252 Lord, M. G., Valies, P. & Broughton, A. C. A morphologic study of the submucosa of the large intestine. *Surgery, gynecology & obstetrics* **145**, 55-60 (1977).

- 253 Roediger, W. E. Role of anaerobic bacteria in the metabolic welfare of the colonic mucosa in man. *Gut* **21**, 793-798 (1980).
- 254 Bugaut, M. Occurrence, absorption and metabolism of short chain fatty acids in the digestive tract of mammals. *Comparative biochemistry and physiology. B, Comparative biochemistry* **86**, 439-472 (1987).
- 255 Griffiths, D. F., Davies, S. J., Williams, D., Williams, G. T. & Williams, E. D. Demonstration of somatic mutation and colonic crypt clonality by X-linked enzyme histochemistry. *Nature* **333**, 461-463, doi:10.1038/333461a0 (1988).
- 256 Barker, N. *et al.* Identification of stem cells in small intestine and colon by marker gene Lgr5. *Nature* **449**, 1003-1007, doi:10.1038/nature06196 (2007).
- 257 Zsebo, K. M. *et al.* Stem cell factor is encoded at the Sl locus of the mouse and is the ligand for the c-kit tyrosine kinase receptor. *Cell* **63**, 213-224 (1990).
- 258 Williams, D. E. *et al.* Identification of a ligand for the c-kit proto-oncogene. *Cell* **63**, 167-174 (1990).
- 259 Rothenberg, M. E. *et al.* Identification of a cKit(+) colonic crypt base secretory cell that supports Lgr5(+) stem cells in mice. *Gastroenterology* **142**, 1195-1205 e1196, doi:10.1053/j.gastro.2012.02.006 (2012).
- 260 Andrew, A., Kramer, B. & Rawdon, B. B. The origin of gut and pancreatic neuroendocrine (APUD) cells--the last word? *The Journal of pathology* **186**, 117-118, doi:10.1002/(SICI)1096-9896(1998100)186:2<117::AID-PATH152>3.0.CO;2-J (1998).
- 261 Cheng, H. & Leblond, C. P. Origin, differentiation and renewal of the four main epithelial cell types in the mouse small intestine. V. Unitarian Theory of the origin of the four epithelial cell types. *The American journal of anatomy* **141**, 537-561, doi:10.1002/aja.1001410407 (1974).
- 262 Garcia, S. B., Park, H. S., Novelli, M. & Wright, N. A. Field cancerization, clonality, and epithelial stem cells: the spread of mutated clones in epithelial sheets. *The Journal of pathology* **187**, 61-81, doi:10.1002/(SICI)1096-9896(199901)187:1<61::AID-PATH247>3.0.CO;2-I (1999).
- 263 Grossmann, J. *et al.* New isolation technique to study apoptosis in human intestinal epithelial cells. *The American journal of pathology* **153**, 53-62, doi:10.1016/S0002-9440(10)65545-9 (1998).
- 264 Rak, J. *et al.* Collateral expression of proangiogenic and tumorigenic properties in intestinal epithelial cell variants selected for resistance to anoikis. *Neoplasia* **1**, 23-30 (1999).
- 265 Shanmugathan, M. & Jothy, S. Apoptosis, anoikis and their relevance to the pathobiology of colon cancer. *Pathology international* **50**, 273-279 (2000).
- 266 Powell, S. M. *et al.* APC mutations occur early during colorectal tumorigenesis. *Nature* **359**, 235-237, doi:10.1038/359235a0 (1992).
- 267 Groden, J. *et al.* Identification and characterization of the familial adenomatous polyposis coli gene. *Cell* **66**, 589-600 (1991).
- 268 Friedl, W. *et al.* Can APC mutation analysis contribute to therapeutic decisions in familial adenomatous polyposis? Experience from 680 FAP families. *Gut* **48**, 515-521 (2001).
- 269 Michels, B. E. *et al.* Human colon organoids reveal distinct physiologic and oncogenic Wnt responses. *J Exp Med*, doi:10.1084/jem.20180823 (2019).
- 270 Ferlay J, S. I., Ervik M, Dikshit R, Eser S, Mathers C, Rebelo M, Parkin DM, Forman D, Bray F. GLOBOCAN 2012 v1.0, Cancer Incidence and Mortality Worldwide: IARC Cancer Base V.1.0. (International Agency for Research on Cancer, Lyon, France, 2013).
- 271 Arnold, M. *et al.* Global patterns and trends in colorectal cancer incidence and mortality. *Gut* **66**, 683-691, doi:10.1136/gutjnl-2015-310912 (2017).

- 272 Vogelstein, B. *et al.* Cancer genome landscapes. *Science* **339**, 1546-1558, doi:10.1126/science.1235122 (2013).
- 273 Jones, S. *et al.* Comparative lesion sequencing provides insights into tumor evolution. *Proc Natl Acad Sci U S A* **105**, 4283-4288, doi:10.1073/pnas.0712345105 (2008).
- 274 Yachida, S. *et al.* Clinical significance of the genetic landscape of pancreatic cancer and implications for identification of potential long-term survivors. *Clinical cancer research : an official journal of the American Association for Cancer Research* **18**, 6339-6347, doi:10.1158/1078-0432.CCR-12-1215 (2012).
- 275 Vogelstein, B. & Kinzler, K. W. The Path to Cancer --Three Strikes and You're Out. *The New England journal of medicine* **373**, 1895-1898, doi:10.1056/NEJMp1508811 (2015).
- 276 Bozic, I. *et al.* Evolutionary dynamics of cancer in response to targeted combination therapy. *eLife* **2**, e00747, doi:10.7554/eLife.00747 (2013).
- 277 Semrad, T. J., Fahrni, A. R., Gong, I. Y. & Khatri, V. P. Integrating Chemotherapy into the Management of Oligometastatic Colorectal Cancer: Evidence-Based Approach Using Clinical Trial Findings. *Annals of surgical oncology* **22 Suppl 3**, S855-862, doi:10.1245/s10434-015-4610-4 (2015).
- 278 Moertel, C. G. *et al.* Fluorouracil plus levamisole as effective adjuvant therapy after resection of stage III colon carcinoma: a final report. *Annals of internal medicine* **122**, 321-326 (1995).
- 279 Huang, A. C. *et al.* T-cell invigoration to tumour burden ratio associated with anti-PD-1 response. *Nature* **545**, 60-65, doi:10.1038/nature22079 (2017).
- 280 Tauriello, D. V., Calon, A., Lonardo, E. & Batlle, E. Determinants of metastatic competency in colorectal cancer. *Molecular oncology* **11**, 97-119, doi:10.1002/1878-0261.12018 (2017).
- 281 Chambers, A. F., Groom, A. C. & MacDonald, I. C. Dissemination and growth of cancer cells in metastatic sites. *Nature reviews. Cancer* **2**, 563-572, doi:10.1038/nrc865 (2002).
- 282 Mehlen, P. & Puisieux, A. Metastasis: a question of life or death. *Nature reviews. Cancer* **6**, 449-458, doi:10.1038/nrc1886 (2006).
- 283 van Zijl, F., Krupitza, G. & Mikulits, W. Initial steps of metastasis: cell invasion and endothelial transmigration. *Mutation research* **728**, 23-34, doi:10.1016/j.mrrev.2011.05.002 (2011).
- 284 Oh, Y. T. *et al.* Assessment of the prognostic factors for a local recurrence of rectal cancer: the utility of preoperative MR imaging. *Korean journal of radiology* **6**, 8-16, doi:10.3348/kjr.2005.6.1.8 (2005).
- 285 Lochhead, P. *et al.* Microsatellite instability and BRAF mutation testing in colorectal cancer prognostication. *Journal of the National Cancer Institute* **105**, 1151-1156, doi:10.1093/jnci/djt173 (2013).
- 286 Deng, G. *et al.* BRAF mutation is frequently present in sporadic colorectal cancer with methylated hMLH1, but not in hereditary nonpolyposis colorectal cancer. *Clinical cancer research : an official journal of the American Association for Cancer Research* **10**, 191-195 (2004).
- 287 Douillard, J. Y. *et al.* Panitumumab-FOLFOX4 treatment and RAS mutations in colorectal cancer. *The New England journal of medicine* **369**, 1023-1034, doi:10.1056/NEJMoa1305275 (2013).
- 288 Davies, H. *et al.* Mutations of the BRAF gene in human cancer. *Nature* **417**, 949-954, doi:10.1038/nature00766 (2002).
- 289 Van Cutsem, E. *et al.* Cetuximab plus irinotecan, fluorouracil, and leucovorin as first-line treatment for metastatic colorectal cancer: updated analysis of overall survival according to tumor KRAS and BRAF mutation status. *Journal of clinical oncology :*

- official journal of the American Society of Clinical Oncology **29**, 2011-2019, doi:10.1200/JCO.2010.33.5091 (2011).
- 290 Popat, S., Hubner, R. & Houlston, R. S. Systematic review of microsatellite instability and colorectal cancer prognosis. *Journal of clinical oncology : official journal of the American Society of Clinical Oncology* **23**, 609-618, doi:10.1200/JCO.2005.01.086 (2005).
- 291 Boland, C. R. & Goel, A. Microsatellite instability in colorectal cancer. *Gastroenterology* **138**, 2073-2087 e2073, doi:10.1053/j.gastro.2009.12.064 (2010).
- 292 Guinney, J. *et al.* The consensus molecular subtypes of colorectal cancer. *Nature medicine* **21**, 1350-1356, doi:10.1038/nm.3967 (2015).
- 293 Fearon, E. R. & Vogelstein, B. A genetic model for colorectal tumorigenesis. *Cell* **61**, 759-767 (1990).
- 294 Chung, D. C. The genetic basis of colorectal cancer: insights into critical pathways of tumorigenesis. *Gastroenterology* **119**, 854-865 (2000).
- 295 Kuhnert, F. *et al.* Essential requirement for Wnt signaling in proliferation of adult small intestine and colon revealed by adenoviral expression of Dickkopf-1. *Proc Natl Acad Sci U S A* **101**, 266-271, doi:10.1073/pnas.2536800100 (2004).
- 296 Pinto, D., Gregorieff, A., Begthel, H. & Clevers, H. Canonical Wnt signals are essential for homeostasis of the intestinal epithelium. *Genes & development* **17**, 1709-1713, doi:10.1101/gad.267103 (2003).
- 297 Korinek, V. *et al.* Depletion of epithelial stem-cell compartments in the small intestine of mice lacking Tcf-4. *Nature genetics* **19**, 379-383, doi:10.1038/1270 (1998).
- 298 de Lau, W. *et al.* Lgr5 homologues associate with Wnt receptors and mediate R-spondin signalling. *Nature* **476**, 293-297, doi:10.1038/nature10337 (2011).
- 299 Kim, K. A. *et al.* Mitogenic influence of human R-spondin1 on the intestinal epithelium. *Science* **309**, 1256-1259, doi:10.1126/science.1112521 (2005).
- 300 Dignass, A. U. & Sturm, A. Peptide growth factors in the intestine. *European journal of gastroenterology & hepatology* **13**, 763-770 (2001).
- 301 van Es, J. H. *et al.* Notch/gamma-secretase inhibition turns proliferative cells in intestinal crypts and adenomas into goblet cells. *Nature* **435**, 959-963, doi:10.1038/nature03659 (2005).
- 302 Kosinski, C. *et al.* Gene expression patterns of human colon tops and basal crypts and BMP antagonists as intestinal stem cell niche factors. *Proc Natl Acad Sci U S A* **104**, 15418-15423, doi:10.1073/pnas.0707210104 (2007).
- 303 van den Heuvel, M., Nusse, R., Johnston, P. & Lawrence, P. A. Distribution of the wingless gene product in Drosophila embryos: a protein involved in cell-cell communication. *Cell* **59**, 739-749 (1989).
- 304 Thorpe, C. J., Schlesinger, A., Carter, J. C. & Bowerman, B. Wnt signaling polarizes an early C. elegans blastomere to distinguish endoderm from mesoderm. *Cell* **90**, 695-705 (1997).
- 305 Goldstein, B., Takeshita, H., Mizumoto, K. & Sawa, H. Wnt signals can function as positional cues in establishing cell polarity. *Developmental cell* **10**, 391-396, doi:10.1016/j.devcel.2005.12.016 (2006).
- 306 Strigini, M. & Cohen, S. M. Wingless gradient formation in the Drosophila wing. *Curr Biol* **10**, 293-300 (2000).
- 307 Neumann, C. J. & Cohen, S. M. Long-range action of Wingless organizes the dorsal-ventral axis of the Drosophila wing. *Development* **124**, 871-880 (1997).
- 308 Zecca, M., Basler, K. & Struhl, G. Direct and long-range action of a wingless morphogen gradient. *Cell* **87**, 833-844 (1996).

- 309 Kiecker, C. & Niehrs, C. A morphogen gradient of Wnt/beta-catenin signalling regulates anteroposterior neural patterning in *Xenopus*. *Development* **128**, 4189-4201 (2001).
- 310 Coudreuse, D. Y., Roel, G., Betist, M. C., Destree, O. & Korswagen, H. C. Wnt gradient formation requires retromer function in Wnt-producing cells. *Science* **312**, 921-924, doi:10.1126/science.1124856 (2006).
- 311 Munoz, J. *et al.* The Lgr5 intestinal stem cell signature: robust expression of proposed quiescent '+4' cell markers. *EMBO J* **31**, 3079-3091, doi:10.1038/emboj.2012.166 (2012).
- 312 Farin, H. F., Van Es, J. H. & Clevers, H. Redundant sources of Wnt regulate intestinal stem cells and promote formation of Paneth cells. *Gastroenterology* **143**, 1518-1529 e1517, doi:10.1053/j.gastro.2012.08.031 (2012).
- 313 Kabiri, Z. *et al.* Stroma provides an intestinal stem cell niche in the absence of epithelial Wnts. *Development* **141**, 2206-2215, doi:10.1242/dev.104976 (2014).
- 314 Sasaki, N. *et al.* Reg4+ deep crypt secretory cells function as epithelial niche for Lgr5+ stem cells in colon. *Proc Natl Acad Sci U S A* **113**, E5399-5407, doi:10.1073/pnas.1607327113 (2016).
- 315 Bradley, R. S., Cowin, P. & Brown, A. M. Expression of Wnt-1 in PC12 cells results in modulation of plakoglobin and E-cadherin and increased cellular adhesion. *J Cell Biol* **123**, 1857-1865 (1993).
- 316 Nathke, I. S., Hinck, L., Swedlow, J. R., Papkoff, J. & Nelson, W. J. Defining interactions and distributions of cadherin and catenin complexes in polarized epithelial cells. *J Cell Biol* **125**, 1341-1352 (1994).
- 317 Hinck, L., Nelson, W. J. & Papkoff, J. Wnt-1 modulates cell-cell adhesion in mammalian cells by stabilizing beta-catenin binding to the cell adhesion protein cadherin. *J Cell Biol* **124**, 729-741 (1994).
- 318 Hinck, L., Nathke, I. S., Papkoff, J. & Nelson, W. J. Dynamics of cadherin/catenin complex formation: novel protein interactions and pathways of complex assembly. *J Cell Biol* **125**, 1327-1340 (1994).
- 319 Hinck, L., Nathke, I. S., Papkoff, J. & Nelson, W. J. Beta-catenin: a common target for the regulation of cell adhesion by Wnt-1 and Src signaling pathways. *Trends Biochem Sci* **19**, 538-542 (1994).
- 320 Watabe, M., Nagafuchi, A., Tsukita, S. & Takeichi, M. Induction of polarized cell-cell association and retardation of growth by activation of the E-cadherin-catenin adhesion system in a dispersed carcinoma line. *J Cell Biol* **127**, 247-256 (1994).
- 321 McCrea, P. D. & Gumbiner, B. M. Purification of a 92-kDa cytoplasmic protein tightly associated with the cell-cell adhesion molecule E-cadherin (uvomorulin). Characterization and extractability of the protein complex from the cell cytostructure. *J Biol Chem* **266**, 4514-4520 (1991).
- 322 McCrea, P. D., Turck, C. W. & Gumbiner, B. A homolog of the armadillo protein in *Drosophila* (plakoglobin) associated with E-cadherin. *Science* **254**, 1359-1361 (1991).
- 323 Kemler, R. & Ozawa, M. Uvomorulin-catenin complex: cytoplasmic anchorage of a Ca²⁺-dependent cell adhesion molecule. *Bioessays* **11**, 88-91, doi:10.1002/bies.950110403 (1989).
- 324 Kemler, R., Ozawa, M. & Ringwald, M. Calcium-dependent cell adhesion molecules. *Current opinion in cell biology* **1**, 892-897 (1989).
- 325 Albuquerque, C. *et al.* The 'just-right' signaling model: APC somatic mutations are selected based on a specific level of activation of the beta-catenin signaling cascade. *Human molecular genetics* **11**, 1549-1560 (2002).
- 326 Syed, V., Mak, P., Du, C. & Balaji, K. C. Beta-catenin mediates alteration in cell proliferation, motility and invasion of prostate cancer cells by differential expression of

- E-cadherin and protein kinase D1. *Journal of cellular biochemistry* **104**, 82-95, doi:10.1002/jcb.21603 (2008).
- 327 Giese, K., Kingsley, C., Kirshner, J. R. & Grosschedl, R. Assembly and function of a TCR alpha enhancer complex is dependent on LEF-1-induced DNA bending and multiple protein-protein interactions. *Genes & development* **9**, 995-1008 (1995).
- 328 Molenaar, M. *et al.* XTcf-3 transcription factor mediates beta-catenin-induced axis formation in *Xenopus* embryos. *Cell* **86**, 391-399 (1996).
- 329 Behrens, J. *et al.* Functional interaction of beta-catenin with the transcription factor LEF-1. *Nature* **382**, 638-642, doi:10.1038/382638a0 (1996).
- 330 Clevers, H. C. & Grosschedl, R. Transcriptional control of lymphoid development: lessons from gene targeting. *Immunology today* **17**, 336-343 (1996).
- 331 van de Wetering, M. *et al.* Armadillo coactivates transcription driven by the product of the *Drosophila* segment polarity gene dTCF. *Cell* **88**, 789-799 (1997).
- 332 Tetsu, O. & McCormick, F. Beta-catenin regulates expression of cyclin D1 in colon carcinoma cells. *Nature* **398**, 422-426, doi:10.1038/18884 (1999).
- 333 He, T. C. *et al.* Identification of c-MYC as a target of the APC pathway. *Science* **281**, 1509-1512 (1998).
- 334 Mao, J. *et al.* Low-density lipoprotein receptor-related protein-5 binds to Axin and regulates the canonical Wnt signaling pathway. *Molecular cell* **7**, 801-809 (2001).
- 335 Zeng, X. *et al.* Initiation of Wnt signaling: control of Wnt coreceptor Lrp6 phosphorylation/activation via frizzled, dishevelled and axin functions. *Development* **135**, 367-375, doi:10.1242/dev.013540 (2008).
- 336 Tolwinski, N. S. *et al.* Wg/Wnt signal can be transmitted through arrow/LRP5,6 and Axin independently of Zw3/Gsk3beta activity. *Developmental cell* **4**, 407-418 (2003).
- 337 He, X., Semenov, M., Tamai, K. & Zeng, X. LDL receptor-related proteins 5 and 6 in Wnt/beta-catenin signaling: arrows point the way. *Development* **131**, 1663-1677, doi:10.1242/dev.01117 (2004).
- 338 Gordon, M. D. & Nusse, R. Wnt signaling: multiple pathways, multiple receptors, and multiple transcription factors. *J Biol Chem* **281**, 22429-22433, doi:10.1074/jbc.R600015200 (2006).
- 339 Batlle, E. *et al.* EphB receptor activity suppresses colorectal cancer progression. *Nature* **435**, 1126-1130, doi:10.1038/nature03626 (2005).
- 340 Clevers, H. & Batlle, E. EphB/EphrinB receptors and Wnt signaling in colorectal cancer. *Cancer Res* **66**, 2-5, doi:10.1158/0008-5472.CAN-05-3849 (2006).
- 341 Pasquale, E. B. Eph-ephrin bidirectional signaling in physiology and disease. *Cell* **133**, 38-52, doi:10.1016/j.cell.2008.03.011 (2008).
- 342 Sansom, O. J. *et al.* Loss of Apc in vivo immediately perturbs Wnt signaling, differentiation, and migration. *Genes & development* **18**, 1385-1390, doi:10.1101/gad.287404 (2004).
- 343 Jubb, A. M. *et al.* EphB2 is a prognostic factor in colorectal cancer. *Clinical cancer research : an official journal of the American Association for Cancer Research* **11**, 5181-5187, doi:10.1158/1078-0432.CCR-05-0143 (2005).
- 344 Lugli, A. *et al.* EphB2 expression across 138 human tumor types in a tissue microarray: high levels of expression in gastrointestinal cancers. *Clinical cancer research : an official journal of the American Association for Cancer Research* **11**, 6450-6458, doi:10.1158/1078-0432.CCR-04-2458 (2005).
- 345 Kamata, T. *et al.* R-spondin, a novel gene with thrombospondin type 1 domain, was expressed in the dorsal neural tube and affected in Wnts mutants. *Biochim Biophys Acta* **1676**, 51-62 (2004).

- 346 Wei, Q. *et al.* R-spondin1 is a high affinity ligand for LRP6 and induces LRP6 phosphorylation and beta-catenin signaling. *J Biol Chem* **282**, 15903-15911, doi:10.1074/jbc.M701927200 (2007).
- 347 Tamai, K. *et al.* A mechanism for Wnt coreceptor activation. *Molecular cell* **13**, 149-156 (2004).
- 348 Kim, K. A. *et al.* R-Spondin proteins: a novel link to beta-catenin activation. *Cell cycle (Georgetown, Tex)* **5**, 23-26, doi:10.4161/cc.5.1.2305 (2006).
- 349 He, X. C., Zhang, J. & Li, L. Cellular and molecular regulation of hematopoietic and intestinal stem cell behavior. *Annals of the New York Academy of Sciences* **1049**, 28-38, doi:10.1196/annals.1334.005 (2005).
- 350 He, X. C. *et al.* BMP signaling inhibits intestinal stem cell self-renewal through suppression of Wnt-beta-catenin signaling. *Nature genetics* **36**, 1117-1121, doi:10.1038/ng1430 (2004).
- 351 Hardwick, J. C. *et al.* Bone morphogenetic protein 2 is expressed by, and acts upon, mature epithelial cells in the colon. *Gastroenterology* **126**, 111-121 (2004).
- 352 Haramis, A. P. *et al.* De novo crypt formation and juvenile polyposis on BMP inhibition in mouse intestine. *Science* **303**, 1684-1686, doi:10.1126/science.1093587 (2004).
- 353 Beck, S. E. *et al.* Bone morphogenetic protein signaling and growth suppression in colon cancer. *American journal of physiology. Gastrointestinal and liver physiology* **291**, G135-145, doi:10.1152/ajpgi.00482.2005 (2006).
- 354 Kretzschmar, M., Liu, F., Hata, A., Doody, J. & Massague, J. The TGF-beta family mediator Smad1 is phosphorylated directly and activated functionally by the BMP receptor kinase. *Genes & development* **11**, 984-995 (1997).
- 355 Itoh, S., Itoh, F., Goumans, M. J. & Ten Dijke, P. Signaling of transforming growth factor-beta family members through Smad proteins. *European journal of biochemistry* **267**, 6954-6967 (2000).
- 356 Fischer, O. M., Hart, S., Gschwind, A. & Ullrich, A. EGFR signal transactivation in cancer cells. *Biochemical Society transactions* **31**, 1203-1208, doi:10.1042/ (2003).
- 357 Ciardiello, F. Epidermal growth factor receptor tyrosine kinase inhibitors as anticancer agents. *Drugs* **60 Suppl 1**, 25-32; discussion 41-22 (2000).
- 358 Ciardiello, F. & Tortora, G. A novel approach in the treatment of cancer: targeting the epidermal growth factor receptor. *Clinical cancer research : an official journal of the American Association for Cancer Research* **7**, 2958-2970 (2001).
- 359 Goldstein, N. I., Prewett, M., Zuklys, K., Rockwell, P. & Mendelsohn, J. Biological efficacy of a chimeric antibody to the epidermal growth factor receptor in a human tumor xenograft model. *Clinical cancer research : an official journal of the American Association for Cancer Research* **1**, 1311-1318 (1995).
- 360 Harris, M. Monoclonal antibodies as therapeutic agents for cancer. *The Lancet. Oncology* **5**, 292-302, doi:10.1016/S1470-2045(04)01467-6 (2004).
- 361 Gutmann, D. H., Hunter-Schaedle, K. & Shannon, K. M. Harnessing preclinical mouse models to inform human clinical cancer trials. *The Journal of clinical investigation* **116**, 847-852, doi:10.1172/JCI28271 (2006).
- 362 Ritter, C. A. & Arteaga, C. L. The epidermal growth factor receptor-tyrosine kinase: a promising therapeutic target in solid tumors. *Seminars in oncology* **30**, 3-11, doi:10.1053/sonc.2003.50027 (2003).
- 363 Pai, R. *et al.* Prostaglandin E2 transactivates EGF receptor: a novel mechanism for promoting colon cancer growth and gastrointestinal hypertrophy. *Nature medicine* **8**, 289-293, doi:10.1038/nm0302-289 (2002).
- 364 Komiya, Y. & Habas, R. Wnt signal transduction pathways. *Organogenesis* **4**, 68-75 (2008).

- 365 Herbst, R. S. Review of epidermal growth factor receptor biology. *International journal of radiation oncology, biology, physics* **59**, 21-26, doi:10.1016/j.ijrobp.2003.11.041 (2004).
- 366 Clevers, H. Wnt/beta-catenin signaling in development and disease. *Cell* **127**, 469-480, doi:10.1016/j.cell.2006.10.018 (2006).
- 367 Amit, S. *et al.* Axin-mediated CKI phosphorylation of beta-catenin at Ser 45: a molecular switch for the Wnt pathway. *Genes & development* **16**, 1066-1076, doi:10.1101/gad.230302 (2002).
- 368 Liu, C. *et al.* Control of beta-catenin phosphorylation/degradation by a dual-kinase mechanism. *Cell* **108**, 837-847 (2002).
- 369 Fiol, C. J., Mahrenholz, A. M., Wang, Y., Roeske, R. W. & Roach, P. J. Formation of protein kinase recognition sites by covalent modification of the substrate. Molecular mechanism for the synergistic action of casein kinase II and glycogen synthase kinase 3. *J Biol Chem* **262**, 14042-14048 (1987).
- 370 Frame, S. & Cohen, P. GSK3 takes centre stage more than 20 years after its discovery. *Biochem J* **359**, 1-16 (2001).
- 371 Aberle, H., Bauer, A., Stappert, J., Kispert, A. & Kemler, R. beta-catenin is a target for the ubiquitin-proteasome pathway. *EMBO J* **16**, 3797-3804, doi:10.1093/emboj/16.13.3797 (1997).
- 372 Orford, K., Crockett, C., Jensen, J. P., Weissman, A. M. & Byers, S. W. Serine phosphorylation-regulated ubiquitination and degradation of beta-catenin. *J Biol Chem* **272**, 24735-24738 (1997).
- 373 Hart, M. *et al.* The F-box protein beta-TrCP associates with phosphorylated beta-catenin and regulates its activity in the cell. *Curr Biol* **9**, 207-210 (1999).
- 374 Kitagawa, M. *et al.* An F-box protein, FWD1, mediates ubiquitin-dependent proteolysis of beta-catenin. *EMBO J* **18**, 2401-2410, doi:10.1093/emboj/18.9.2401 (1999).
- 375 Latres, E., Chiaur, D. S. & Pagano, M. The human F box protein beta-Trcp associates with the Cul1/Skp1 complex and regulates the stability of beta-catenin. *Oncogene* **18**, 849-854, doi:10.1038/sj.onc.1202653 (1999).
- 376 Liu, C. *et al.* beta-Trcp couples beta-catenin phosphorylation-degradation and regulates *Xenopus* axis formation. *Proc Natl Acad Sci U S A* **96**, 6273-6278 (1999).
- 377 Winston, J. T. *et al.* The SCFbeta-TRCP-ubiquitin ligase complex associates specifically with phosphorylated destruction motifs in I κ B α and beta-catenin and stimulates I κ B α ubiquitination in vitro. *Genes & development* **13**, 270-283 (1999).
- 378 Stambolic, V. *et al.* Negative regulation of PKB/Akt-dependent cell survival by the tumor suppressor PTEN. *Cell* **95**, 29-39 (1998).
- 379 Balemans, W. & Van Hul, W. Extracellular regulation of BMP signaling in vertebrates: a cocktail of modulators. *Developmental biology* **250**, 231-250 (2002).
- 380 Vazquez, F., Ramaswamy, S., Nakamura, N. & Sellers, W. R. Phosphorylation of the PTEN tail regulates protein stability and function. *Mol Cell Biol* **20**, 5010-5018 (2000).
- 381 Aloy, I. & Yarden, Y. The ErbB signaling network in embryogenesis and oncogenesis: signal diversification through combinatorial ligand-receptor interactions. *FEBS Lett* **410**, 83-86 (1997).
- 382 Muthuswamy, S. K., Gilman, M. & Brugge, J. S. Controlled dimerization of ErbB receptors provides evidence for differential signaling by homo- and heterodimers. *Mol Cell Biol* **19**, 6845-6857 (1999).
- 383 Liu, W., Li, J. & Roth, R. A. Heregulin regulation of Akt/protein kinase B in breast cancer cells. *Biochem Biophys Res Commun* **261**, 897-903, doi:10.1006/bbrc.1999.1144 (1999).

- 384 Burgering, B. M. & Coffey, P. J. Protein kinase B (c-Akt) in phosphatidylinositol-3-OH
kinase signal transduction. *Nature* **376**, 599-602, doi:10.1038/376599a0 (1995).
- 385 McDonald, T. *et al.* Identification and cloning of an orphan G protein-coupled receptor
of the glycoprotein hormone receptor subfamily. *Biochem Biophys Res Commun* **247**,
266-270, doi:10.1006/bbrc.1998.8774 (1998).
- 386 Hsu, S. Y., Liang, S. G. & Hsueh, A. J. Characterization of two LGR genes homologous to
gonadotropin and thyrotropin receptors with extracellular leucine-rich repeats and a G
protein-coupled, seven-transmembrane region. *Molecular endocrinology* **12**, 1830-
1845, doi:10.1210/mend.12.12.0211 (1998).
- 387 Hermey, G., Methner, A., Schaller, H. C. & Hermans-Borgmeyer, I. Identification of a
novel seven-transmembrane receptor with homology to glycoprotein receptors and its
expression in the adult and developing mouse. *Biochem Biophys Res Commun* **254**,
273-279, doi:10.1006/bbrc.1998.9882 (1999).
- 388 Carmon, K. S., Gong, X., Lin, Q., Thomas, A. & Liu, Q. R-spondins function as ligands of
the orphan receptors LGR4 and LGR5 to regulate Wnt/beta-catenin signaling. *Proc Natl
Acad Sci U S A* **108**, 11452-11457, doi:10.1073/pnas.1106083108 (2011).
- 389 Sato, T. *et al.* Paneth cells constitute the niche for Lgr5 stem cells in intestinal crypts.
Nature **469**, 415-418, doi:10.1038/nature09637 (2011).
- 390 Wildi, S. *et al.* Characterization of cytokeratin 20 expression in pancreatic and
colorectal cancer. *Clinical cancer research : an official journal of the American
Association for Cancer Research* **5**, 2840-2847 (1999).
- 391 Wang, D. *et al.* Loss of cannabinoid receptor 1 accelerates intestinal tumor growth.
Cancer Res **68**, 6468-6476, doi:10.1158/0008-5472.CAN-08-0896 (2008).
- 392 Lunn, C. A., Reich, E. P. & Bober, L. Targeting the CB2 receptor for immune modulation.
Expert opinion on therapeutic targets **10**, 653-663, doi:10.1517/14728222.10.5.653
(2006).
- 393 Joseph, J., Niggemann, B., Zaenker, K. S. & Entschladen, F. Anandamide is an
endogenous inhibitor for the migration of tumor cells and T lymphocytes. *Cancer
immunology, immunotherapy : CII* **53**, 723-728, doi:10.1007/s00262-004-0509-9
(2004).
- 394 Stella, N., Schweitzer, P. & Piomelli, D. A second endogenous cannabinoid that
modulates long-term potentiation. *Nature* **388**, 773-778, doi:10.1038/42015 (1997).
- 395 Di Marzo, V. *et al.* Formation and inactivation of endogenous cannabinoid anandamide
in central neurons. *Nature* **372**, 686-691, doi:10.1038/372686a0 (1994).
- 396 Munro, S., Thomas, K. L. & Abu-Shaar, M. Molecular characterization of a peripheral
receptor for cannabinoids. *Nature* **365**, 61-65, doi:10.1038/365061a0 (1993).
- 397 Hermanson, D. J. & Marnett, L. J. Cannabinoids, endocannabinoids, and cancer. *Cancer
metastasis reviews* **30**, 599-612, doi:10.1007/s10555-011-9318-8 (2011).
- 398 Xu, W., Chou, C. L., Israel, D. D., Hutchinson, A. J. & Regan, J. W. PGF(2alpha)
stimulates FP prostanoid receptor mediated crosstalk between Ras/Raf signaling and
Tcf transcriptional activation. *Biochem Biophys Res Commun* **381**, 625-629,
doi:10.1016/j.bbrc.2009.02.102 (2009).
- 399 Xu, W. *et al.* FP prostanoid receptor-mediated induction of the expression of early
growth response factor-1 by activation of a Ras/Raf/mitogen-activated protein kinase
signaling cascade. *Mol Pharmacol* **73**, 111-118, doi:10.1124/mol.107.038778 (2008).
- 400 Sales, K. J. *et al.* A novel angiogenic role for prostaglandin F2alpha-FP receptor
interaction in human endometrial adenocarcinomas. *Cancer Res* **65**, 7707-7716,
doi:10.1158/0008-5472.CAN-05-0101 (2005).

- 401 Chiurchiu, V., Leuti, A. & Maccarrone, M. Bioactive Lipids and Chronic Inflammation: Managing the Fire Within. *Frontiers in immunology* **9**, 38, doi:10.3389/fimmu.2018.00038 (2018).
- 402 Dey, I., Lejeune, M. & Chadee, K. Prostaglandin E2 receptor distribution and function in the gastrointestinal tract. *British journal of pharmacology* **149**, 611-623, doi:10.1038/sj.bjp.0706923 (2006).
- 403 Jain, S., Chakraborty, G., Raja, R., Kale, S. & Kundu, G. C. Prostaglandin E2 regulates tumor angiogenesis in prostate cancer. *Cancer Res* **68**, 7750-7759, doi:10.1158/0008-5472.CAN-07-6689 (2008).
- 404 Larsson, K. & Jakobsson, P. J. Inhibition of microsomal prostaglandin E synthase-1 as targeted therapy in cancer treatment. *Prostaglandins & other lipid mediators* **120**, 161-165, doi:10.1016/j.prostaglandins.2015.06.002 (2015).
- 405 Kalinski, P. Regulation of immune responses by prostaglandin E2. *Journal of immunology* **188**, 21-28, doi:10.4049/jimmunol.1101029 (2012).
- 406 Trompezinski, S., Pernet, I., Schmitt, D. & Viac, J. UV radiation and prostaglandin E2 up-regulate vascular endothelial growth factor (VEGF) in cultured human fibroblasts. *Inflammation research : official journal of the European Histamine Research Society ... [et al.]* **50**, 422-427, doi:10.1007/PL00000265 (2001).
- 407 Sheng, H., Shao, J., Morrow, J. D., Beauchamp, R. D. & DuBois, R. N. Modulation of apoptosis and Bcl-2 expression by prostaglandin E2 in human colon cancer cells. *Cancer Res* **58**, 362-366 (1998).
- 408 Williams, C. S., Mann, M. & DuBois, R. N. The role of cyclooxygenases in inflammation, cancer, and development. *Oncogene* **18**, 7908-7916, doi:10.1038/sj.onc.1203286 (1999).
- 409 Fujino, H., Srinivasan, D. & Regan, J. W. Cellular conditioning and activation of beta-catenin signaling by the FPB prostanoid receptor. *J Biol Chem* **277**, 48786-48795, doi:10.1074/jbc.M209393200 (2002).
- 410 Gobeil, F., Jr. *et al.* Nuclear prostaglandin signaling system: biogenesis and actions via heptahelical receptors. *Canadian journal of physiology and pharmacology* **81**, 196-204 (2003).
- 411 Gobeil, F., Jr. *et al.* Regulation of eNOS expression in brain endothelial cells by perinuclear EP(3) receptors. *Circulation research* **90**, 682-689 (2002).
- 412 Fischer, S. M. Prostaglandins and cancer. *Frontiers in bioscience : a journal and virtual library* **2**, d482-500 (1997).
- 413 Buchanan, F. G., Wang, D., Bargiacchi, F. & DuBois, R. N. Prostaglandin E2 regulates cell migration via the intracellular activation of the epidermal growth factor receptor. *J Biol Chem* **278**, 35451-35457, doi:10.1074/jbc.M302474200 (2003).
- 414 Fujino, H. & Regan, J. W. FP prostanoid receptor activation of a T-cell factor/beta -catenin signaling pathway. *J Biol Chem* **276**, 12489-12492, doi:10.1074/jbc.C100039200 (2001).
- 415 Fujino, H., West, K. A. & Regan, J. W. Phosphorylation of glycogen synthase kinase-3 and stimulation of T-cell factor signaling following activation of EP2 and EP4 prostanoid receptors by prostaglandin E2. *J Biol Chem* **277**, 2614-2619, doi:10.1074/jbc.M109440200 (2002).
- 416 Smith, W. L., DeWitt, D. L. & Garavito, R. M. Cyclooxygenases: structural, cellular, and molecular biology. *Annual review of biochemistry* **69**, 145-182, doi:10.1146/annurev.biochem.69.1.145 (2000).
- 417 Vane, J. R. & Botting, R. M. Mechanism of action of anti-inflammatory drugs. *Scandinavian journal of rheumatology. Supplement* **102**, 9-21 (1996).

- 418 Simon, L. S. Role and regulation of cyclooxygenase-2 during inflammation. *The American journal of medicine* **106**, 37S-42S (1999).
- 419 Goldblatt, M. W. Properties of human seminal plasma. *The Journal of physiology* **84**, 208-218 (1935).
- 420 Goldblatt, M. W. Constituents of human seminal plasma. *Biochem J* **29**, 1346-1357 (1935).
- 421 Von Euler, U. S. [Further studies of prostaglandin, the physically active substance of certain genital glands]. *Skandinavisches Archiv fur Physiologie* **81**, 65-80 (1939).
- 422 von Euler, U. S. On the specific vaso-dilating and plain muscle stimulating substances from accessory genital glands in man and certain animals (prostaglandin and vesiglandin). *The Journal of physiology* **88**, 213-234 (1936).
- 423 Vane, J. R. Inhibition of prostaglandin synthesis as a mechanism of action for aspirin-like drugs. *Nature: New biology* **231**, 232-235 (1971).
- 424 Smith, W. L. & Lands, W. E. Oxygenation of polyunsaturated fatty acids during prostaglandin biosynthesis by sheep vesicular gland. *Biochemistry* **11**, 3276-3285 (1972).
- 425 Marshall, P. J. & Kulmacz, R. J. Prostaglandin H synthase: distinct binding sites for cyclooxygenase and peroxidase substrates. *Arch Biochem Biophys* **266**, 162-170 (1988).
- 426 Lysz, T. W. & Needleman, P. Evidence for two distinct forms of fatty acid cyclooxygenase in brain. *J Neurochem* **38**, 1111-1117 (1982).
- 427 Lysz, T. W., Zweig, A. & Keeting, P. E. Examination of mouse and rat tissues for evidence of dual forms of the fatty acid cyclooxygenase. *Biochemical pharmacology* **37**, 921-927 (1988).
- 428 Habenicht, A. J. *et al.* Human platelet-derived growth factor stimulates prostaglandin synthesis by activation and by rapid de novo synthesis of cyclooxygenase. *The Journal of clinical investigation* **75**, 1381-1387, doi:10.1172/JCI111839 (1985).
- 429 Rosen, G. D., Birkenmeier, T. M., Raz, A. & Holtzman, M. J. Identification of a cyclooxygenase-related gene and its potential role in prostaglandin formation. *Biochem Biophys Res Commun* **164**, 1358-1365 (1989).
- 430 Fu, J. Y., Masferrer, J. L., Seibert, K., Raz, A. & Needleman, P. The induction and suppression of prostaglandin H₂ synthase (cyclooxygenase) in human monocytes. *J Biol Chem* **265**, 16737-16740 (1990).
- 431 Han, J. W., Sadowski, H., Young, D. A. & Macara, I. G. Persistent induction of cyclooxygenase in p60v-src-transformed 3T3 fibroblasts. *Proc Natl Acad Sci U S A* **87**, 3373-3377 (1990).
- 432 Sugimoto, Y. *et al.* Cloning and expression of a cDNA for mouse prostaglandin E receptor EP3 subtype. *J Biol Chem* **267**, 6463-6466 (1992).
- 433 Funk, C. D. *et al.* Cloning and expression of a cDNA for the human prostaglandin E receptor EP1 subtype. *J Biol Chem* **268**, 26767-26772 (1993).
- 434 Honda, A. *et al.* Cloning and expression of a cDNA for mouse prostaglandin E receptor EP2 subtype. *J Biol Chem* **268**, 7759-7762 (1993).
- 435 Regan, J. W. *et al.* Cloning of a novel human prostaglandin receptor with characteristics of the pharmacologically defined EP2 subtype. *Mol Pharmacol* **46**, 213-220 (1994).
- 436 Simmons, D. L., Botting, R. M. & Hla, T. Cyclooxygenase isozymes: the biology of prostaglandin synthesis and inhibition. *Pharmacological reviews* **56**, 387-437, doi:10.1124/pr.56.3.3 (2004).
- 437 Giang, D. K. & Cravatt, B. F. Molecular characterization of human and mouse fatty acid amide hydrolases. *Proc Natl Acad Sci U S A* **94**, 2238-2242 (1997).

- 438 Bisogno, T. *et al.* Biosynthesis, release and degradation of the novel endogenous cannabimimetic metabolite 2-arachidonoylglycerol in mouse neuroblastoma cells. *Biochem J* **322 (Pt 2)**, 671-677 (1997).
- 439 Brown, A. J. Novel cannabinoid receptors. *British journal of pharmacology* **152**, 567-575, doi:10.1038/sj.bjp.0707481 (2007).
- 440 Starowicz, K., Nigam, S. & Di Marzo, V. Biochemistry and pharmacology of endovanilloids. *Pharmacology & therapeutics* **114**, 13-33, doi:10.1016/j.pharmthera.2007.01.005 (2007).
- 441 Pertwee, R. G. Emerging strategies for exploiting cannabinoid receptor agonists as medicines. *British journal of pharmacology* **156**, 397-411, doi:10.1111/j.1476-5381.2008.00048.x (2009).
- 442 Bayewitch, M. *et al.* The peripheral cannabinoid receptor: adenylate cyclase inhibition and G protein coupling. *FEBS Lett* **375**, 143-147 (1995).
- 443 Matsuda, L. A., Lolait, S. J., Brownstein, M. J., Young, A. C. & Bonner, T. I. Structure of a cannabinoid receptor and functional expression of the cloned cDNA. *Nature* **346**, 561-564, doi:10.1038/346561a0 (1990).
- 444 Schatz, A. R., Lee, M., Condie, R. B., Pulaski, J. T. & Kaminski, N. E. Cannabinoid receptors CB1 and CB2: a characterization of expression and adenylate cyclase modulation within the immune system. *Toxicology and applied pharmacology* **142**, 278-287, doi:10.1006/taap.1996.8034 (1997).
- 445 Schmid, H. H. Pathways and mechanisms of N-acylethanolamine biosynthesis: can anandamide be generated selectively? *Chem Phys Lipids* **108**, 71-87 (2000).
- 446 Sugiura, T. *et al.* Transacylase-mediated and phosphodiesterase-mediated synthesis of N-arachidonylethanolamine, an endogenous cannabinoid-receptor ligand, in rat brain microsomes. Comparison with synthesis from free arachidonic acid and ethanolamine. *European journal of biochemistry* **240**, 53-62 (1996).
- 447 Bisogno, T., Melck, D., De Petrocellis, L. & Di Marzo, V. Phosphatidic acid as the biosynthetic precursor of the endocannabinoid 2-arachidonoylglycerol in intact mouse neuroblastoma cells stimulated with ionomycin. *J Neurochem* **72**, 2113-2119 (1999).
- 448 Bisogno, T. *et al.* Cloning of the first sn1-DAG lipases points to the spatial and temporal regulation of endocannabinoid signaling in the brain. *J Cell Biol* **163**, 463-468, doi:10.1083/jcb.200305129 (2003).
- 449 Landry, Y., Niederhoffer, N., Sick, E. & Gies, J. P. Heptahelical and other G-protein-coupled receptors (GPCRs) signaling. *Current medicinal chemistry* **13**, 51-63 (2006).
- 450 Kroeze, W. K., Sheffler, D. J. & Roth, B. L. G-protein-coupled receptors at a glance. *J Cell Sci* **116**, 4867-4869, doi:10.1242/jcs.00902 (2003).
- 451 Sunahara, R. K. & Taussig, R. Isoforms of mammalian adenylyl cyclase: multiplicities of signaling. *Molecular interventions* **2**, 168-184, doi:10.1124/mi.2.3.168 (2002).
- 452 Kamenetsky, M. *et al.* Molecular details of cAMP generation in mammalian cells: a tale of two systems. *J Mol Biol* **362**, 623-639, doi:10.1016/j.jmb.2006.07.045 (2006).
- 453 Reimer, R., Heim, H. K., Muallem, R., Odes, H. S. & Sewing, K. F. Effects of EP-receptor subtype specific agonists and other prostanoids on adenylate cyclase activity of duodenal epithelial cells. *Prostaglandins* **44**, 485-493 (1992).
- 454 Trist, D. G., Collins, B. A., Wood, J., Kelly, M. G. & Robertson, A. D. The antagonism by BW A868C of PGD2 and BW245C activation of human platelet adenylate cyclase. *British journal of pharmacology* **96**, 301-306 (1989).
- 455 Adie, E. J., Mullaney, I., McKenzie, F. R. & Milligan, G. Concurrent down-regulation of IP prostanoid receptors and the alpha-subunit of the stimulatory guanine-nucleotide-binding protein (Gs) during prolonged exposure of neuroblastoma x glioma cells to

- prostanoid agonists. Quantification and functional implications. *Biochem J* **285 (Pt 2)**, 529-536 (1992).
- 456 Ichikawa, A., Sugimoto, Y. & Negishi, M. Molecular aspects of the structures and functions of the prostaglandin E receptors. *Journal of lipid mediators and cell signalling* **14**, 83-87 (1996).
- 457 Fabre, J. E. *et al.* Activation of the murine EP3 receptor for PGE2 inhibits cAMP production and promotes platelet aggregation. *The Journal of clinical investigation* **107**, 603-610, doi:10.1172/JCI10881 (2001).
- 458 Omori, K. & Kotera, J. Overview of PDEs and their regulation. *Circulation research* **100**, 309-327, doi:10.1161/01.RES.0000256354.95791.f1 (2007).
- 459 Berridge, M. J. Inositol trisphosphate and diacylglycerol: two interacting second messengers. *Annual review of biochemistry* **56**, 159-193, doi:10.1146/annurev.bi.56.070187.001111 (1987).
- 460 Wilson, D. B. *et al.* Isolation and characterization of the inositol cyclic phosphate products of polyphosphoinositide cleavage by phospholipase C. Physiological effects in permeabilized platelets and Limulus photoreceptor cells. *J Biol Chem* **260**, 13496-13501 (1985).
- 461 Ishii, H., Connolly, T. M., Bross, T. E. & Majerus, P. W. Inositol cyclic triphosphate [inositol 1,2-(cyclic)-4,5-triphosphate] is formed upon thrombin stimulation of human platelets. *Proc Natl Acad Sci U S A* **83**, 6397-6401 (1986).
- 462 Watabe, A. *et al.* Cloning and expression of cDNA for a mouse EP1 subtype of prostaglandin E receptor. *J Biol Chem* **268**, 20175-20178 (1993).
- 463 Mayeux, P. R., Mais, D. E., Carr, C. & Halushka, P. V. Human erythroleukemia cells express functional thromboxane A2/prostaglandin H2 receptors. *J Pharmacol Exp Ther* **250**, 923-927 (1989).
- 464 Claing, A., Laporte, S. A., Caron, M. G. & Lefkowitz, R. J. Endocytosis of G protein-coupled receptors: roles of G protein-coupled receptor kinases and beta-arrestin proteins. *Progress in neurobiology* **66**, 61-79 (2002).
- 465 Shaulsky, G., Fuller, D. & Loomis, W. F. A cAMP-phosphodiesterase controls PKA-dependent differentiation. *Development* **125**, 691-699 (1998).
- 466 Yan, K., Gao, L. N., Cui, Y. L., Zhang, Y. & Zhou, X. The cyclic AMP signaling pathway: Exploring targets for successful drug discovery (Review). *Molecular medicine reports* **13**, 3715-3723, doi:10.3892/mmr.2016.5005 (2016).
- 467 Nishihara, H., Hwang, M., Kizaka-Kondoh, S., Eckmann, L. & Insel, P. A. Cyclic AMP promotes cAMP-responsive element-binding protein-dependent induction of cellular inhibitor of apoptosis protein-2 and suppresses apoptosis of colon cancer cells through ERK1/2 and p38 MAPK. *J Biol Chem* **279**, 26176-26183, doi:10.1074/jbc.M313346200 (2004).
- 468 Laroche-Joubert, N., Marsy, S., Michelet, S., Imbert-Teboul, M. & Doucet, A. Protein kinase A-independent activation of ERK and H,K-ATPase by cAMP in native kidney cells: role of Epac I. *J Biol Chem* **277**, 18598-18604, doi:10.1074/jbc.M201868200 (2002).
- 469 McLean, J. H. *et al.* A phosphodiesterase inhibitor, cilomilast, enhances cAMP activity to restore conditioned odor preference memory after serotonergic depletion in the neonate rat. *Neurobiology of learning and memory* **92**, 63-69, doi:10.1016/j.nlm.2009.02.003 (2009).
- 470 Narumiya, S., Sugimoto, Y. & Ushikubi, F. Prostanoid receptors: structures, properties, and functions. *Physiological reviews* **79**, 1193-1226, doi:10.1152/physrev.1999.79.4.1193 (1999).
- 471 Lewis, R. A. *et al.* Prostaglandin D2 generation after activation of rat and human mast cells with anti-IgE. *Journal of immunology* **129**, 1627-1631 (1982).

- 472 Roberts, L. J., 2nd, Sweetman, B. J., Lewis, R. A., Austen, K. F. & Oates, J. A. Increased production of prostaglandin D2 in patients with systemic mastocytosis. *The New England journal of medicine* **303**, 1400-1404, doi:10.1056/NEJM198012113032405 (1980).
- 473 Whittle, B. J., Hamid, S., Lidbury, P. & Rosam, A. C. Specificity between the anti-aggregatory actions of prostacyclin, prostaglandin E1 and D2 on platelets. *Advances in experimental medicine and biology* **192**, 109-125 (1985).
- 474 Narumiya, S. & Toda, N. Different responsiveness of prostaglandin D2-sensitive systems to prostaglandin D2 and its analogues. *British journal of pharmacology* **85**, 367-375 (1985).
- 475 Giles, H. & Leff, P. The biology and pharmacology of PGD2. *Prostaglandins* **35**, 277-300 (1988).
- 476 Wright, D. H., Ford-Hutchinson, A. W., Chadee, K. & Metters, K. M. The human prostanoid DP receptor stimulates mucin secretion in LS174T cells. *British journal of pharmacology* **131**, 1537-1545, doi:10.1038/sj.bjp.0703688 (2000).
- 477 Mizoguchi, A. *et al.* Dominant localization of prostaglandin D receptors on arachnoid trabecular cells in mouse basal forebrain and their involvement in the regulation of non-rapid eye movement sleep. *Proc Natl Acad Sci U S A* **98**, 11674-11679, doi:10.1073/pnas.201398898 (2001).
- 478 Yoshida, T. *et al.* Inhibitory effects of prostaglandin D2 against the proliferation of human colon cancer cell lines and hepatic metastasis from colorectal cancer. *Surgery today* **28**, 740-745 (1998).
- 479 Hirai, H. *et al.* Prostaglandin D2 selectively induces chemotaxis in T helper type 2 cells, eosinophils, and basophils via seven-transmembrane receptor CRTH2. *J Exp Med* **193**, 255-261 (2001).
- 480 Nagata, K. *et al.* CRTH2, an orphan receptor of T-helper-2-cells, is expressed on basophils and eosinophils and responds to mast cell-derived factor(s). *FEBS Lett* **459**, 195-199 (1999).
- 481 Watanabe, T. *et al.* Positive and negative regulation of cell proliferation through prostaglandin receptors in NIH-3T3 cells. *J Cell Physiol* **169**, 401-409, doi:10.1002/(SICI)1097-4652(199611)169:2<401::AID-JCP20>3.0.CO;2-A (1996).
- 482 Tsushita, K., Kozawa, O., Tokuda, H., Oiso, Y. & Saito, H. Proliferative effect of PGD2 on osteoblast-like cells; independent activation of pertussis toxin-sensitive GTP-binding protein from PGE2 or PGF2 alpha. *Prostaglandins, leukotrienes, and essential fatty acids* **45**, 267-274 (1992).
- 483 Tokuda, H., Kozawa, O., Harada, A. & Uematsu, T. Prostaglandin D2 induces interleukin-6 synthesis via Ca2+ mobilization in osteoblasts: regulation by protein kinase C. *Prostaglandins, leukotrienes, and essential fatty acids* **61**, 189-194, doi:10.1054/plef.1999.0089 (1999).
- 484 Sawyer, N. *et al.* Molecular pharmacology of the human prostaglandin D2 receptor, CRTH2. *British journal of pharmacology* **137**, 1163-1172, doi:10.1038/sj.bjp.0704973 (2002).
- 485 Ito, S. *et al.* Prostaglandin F2 alpha receptor is coupled to Gq in cDNA-transfected Chinese hamster ovary cells. *Biochem Biophys Res Commun* **200**, 756-762 (1994).
- 486 Breyer, R. M., Bagdassarian, C. K., Myers, S. A. & Breyer, M. D. Prostanoid receptors: subtypes and signaling. *Annual review of pharmacology and toxicology* **41**, 661-690, doi:10.1146/annurev.pharmtox.41.1.661 (2001).
- 487 Lupulescu, A. Hormonal regulation of epidermal tumor development. *The Journal of investigative dermatology* **77**, 186-195 (1981).

- 488 Wagner, E. F. & Nebreda, A. R. Signal integration by JNK and p38 MAPK pathways in cancer development. *Nature reviews. Cancer* **9**, 537-549, doi:10.1038/nrc2694 (2009).
- 489 Fang, J. Y. & Richardson, B. C. The MAPK signalling pathways and colorectal cancer. *The Lancet. Oncology* **6**, 322-327, doi:10.1016/S1470-2045(05)70168-6 (2005).
- 490 Qualtrough, D. *et al.* Prostaglandin F(2alpha) stimulates motility and invasion in colorectal tumor cells. *International journal of cancer* **121**, 734-740, doi:10.1002/ijc.22755 (2007).
- 491 Williams, T. J. Prostaglandin E2, prostaglandin I2 and the vascular changes of inflammation. *British journal of pharmacology* **65**, 517-524 (1979).
- 492 Renz, H., Gong, J. H., Schmidt, A., Nain, M. & Gemsa, D. Release of tumor necrosis factor-alpha from macrophages. Enhancement and suppression are dose-dependently regulated by prostaglandin E2 and cyclic nucleotides. *Journal of immunology* **141**, 2388-2393 (1988).
- 493 Hinson, R. M., Williams, J. A. & Shacter, E. Elevated interleukin 6 is induced by prostaglandin E2 in a murine model of inflammation: possible role of cyclooxygenase-2. *Proc Natl Acad Sci U S A* **93**, 4885-4890 (1996).
- 494 Abramovitz, M. *et al.* The utilization of recombinant prostanoid receptors to determine the affinities and selectivities of prostaglandins and related analogs. *Biochim Biophys Acta* **1483**, 285-293 (2000).
- 495 Castellone, M. D., Teramoto, H., Williams, B. O., Druey, K. M. & Gutkind, J. S. Prostaglandin E2 promotes colon cancer cell growth through a Gs-axin-beta-catenin signaling axis. *Science* **310**, 1504-1510, doi:10.1126/science.1116221 (2005).
- 496 Hebert, R. L., Jacobson, H. R. & Breyer, M. D. PGE2 inhibits AVP-induced water flow in cortical collecting ducts by protein kinase C activation. *The American journal of physiology* **259**, F318-325, doi:10.1152/ajprenal.1990.259.2.F318 (1990).
- 497 Watanabe, K. *et al.* Role of the prostaglandin E receptor subtype EP1 in colon carcinogenesis. *Cancer Res* **59**, 5093-5096 (1999).
- 498 Nishigaki, N., Negishi, M. & Ichikawa, A. Two Gs-coupled prostaglandin E receptor subtypes, EP2 and EP4, differ in desensitization and sensitivity to the metabolic inactivation of the agonist. *Mol Pharmacol* **50**, 1031-1037 (1996).
- 499 Desai, S., April, H., Nwaneshiudu, C. & Ashby, B. Comparison of agonist-induced internalization of the human EP2 and EP4 prostaglandin receptors: role of the carboxyl terminus in EP4 receptor sequestration. *Mol Pharmacol* **58**, 1279-1286 (2000).
- 500 Sheng, H., Shao, J., Washington, M. K. & DuBois, R. N. Prostaglandin E2 increases growth and motility of colorectal carcinoma cells. *J Biol Chem* **276**, 18075-18081, doi:10.1074/jbc.M009689200 (2001).
- 501 Fujino, H., Xu, W. & Regan, J. W. Prostaglandin E2 induced functional expression of early growth response factor-1 by EP4, but not EP2, prostanoid receptors via the phosphatidylinositol 3-kinase and extracellular signal-regulated kinases. *J Biol Chem* **278**, 12151-12156, doi:10.1074/jbc.M212665200 (2003).
- 502 Pozzi, A. *et al.* Colon carcinoma cell growth is associated with prostaglandin E2/EP4 receptor-evoked ERK activation. *J Biol Chem* **279**, 29797-29804, doi:10.1074/jbc.M313989200 (2004).
- 503 Bastepe, M. & Ashby, B. Identification of a region of the C-terminal domain involved in short-term desensitization of the prostaglandin EP4 receptor. *British journal of pharmacology* **126**, 365-371, doi:10.1038/sj.bjp.0702291 (1999).
- 504 Mutoh, M. *et al.* Involvement of prostaglandin E receptor subtype EP(4) in colon carcinogenesis. *Cancer Res* **62**, 28-32 (2002).
- 505 Negishi, M. *et al.* Opposite coupling of prostaglandin E receptor EP3C with Gs and G(o). Stimulation of Gs and inhibition of G(o). *J Biol Chem* **268**, 26067-26070 (1993).

- 506 Namba, T. *et al.* Alternative splicing of C-terminal tail of prostaglandin E receptor
subtype EP3 determines G-protein specificity. *Nature* **365**, 166-170,
doi:10.1038/365166a0 (1993).
- 507 Tanabe, Y., Masu, M., Ishii, T., Shigemoto, R. & Nakanishi, S. A family of metabotropic
glutamate receptors. *Neuron* **8**, 169-179 (1992).
- 508 Nishigaki, N. *et al.* Characterization of the prostaglandin E receptor expressed on a
cultured mast cell line, BNU-2cl3. *Biochemical pharmacology* **46**, 863-869 (1993).
- 509 Sonnenburg, W. K., Zhu, J. H. & Smith, W. L. A prostaglandin E receptor coupled to a
pertussis toxin-sensitive guanine nucleotide regulatory protein in rabbit cortical
collecting tubule cells. *J Biol Chem* **265**, 8479-8483 (1990).
- 510 Burkey, T. H. & Regan, J. W. Activation of mitogen-activated protein kinase by the
human prostaglandin EP3A receptor. *Biochem Biophys Res Commun* **211**, 152-158,
doi:10.1006/bbrc.1995.1790 (1995).
- 511 Amano, H. *et al.* Host prostaglandin E(2)-EP3 signaling regulates tumor-associated
angiogenesis and tumor growth. *J Exp Med* **197**, 221-232 (2003).
- 512 Shoji, Y. *et al.* Downregulation of prostaglandin E receptor subtype EP3 during colon
cancer development. *Gut* **53**, 1151-1158, doi:10.1136/gut.2003.028787 (2004).
- 513 Cattaneo F, Parisi M, Fioretti T, Esposito G & R, A. Intranuclear Signaling Cascades
Triggered by Nuclear GPCRs. *J Cell Signal* **1** (2016).
- 514 Bhattacharya, M. *et al.* Nuclear localization of prostaglandin E2 receptors. *Proc Natl
Acad Sci U S A* **95**, 15792-15797 (1998).
- 515 Bhattacharya, M. *et al.* Localization of functional prostaglandin E2 receptors EP3 and
EP4 in the nuclear envelope. *J Biol Chem* **274**, 15719-15724 (1999).
- 516 Wang, D. & Dubois, R. N. Eicosanoids and cancer. *Nature reviews. Cancer* **10**, 181-193,
doi:10.1038/nrc2809 (2010).
- 517 van Rees, B. P. *et al.* Expression of microsomal prostaglandin E synthase-1 in intestinal
type gastric adenocarcinoma and in gastric cancer cell lines. *International journal of
cancer* **107**, 551-556, doi:10.1002/ijc.11422 (2003).
- 518 Yoshimatsu, K. *et al.* Inducible microsomal prostaglandin E synthase is overexpressed
in colorectal adenomas and cancer. *Clinical cancer research : an official journal of the
American Association for Cancer Research* **7**, 3971-3976 (2001).
- 519 Hanaka, H. *et al.* Microsomal prostaglandin E synthase 1 determines tumor growth in
vivo of prostate and lung cancer cells. *Proc Natl Acad Sci U S A* **106**, 18757-18762,
doi:10.1073/pnas.0910218106 (2009).
- 520 Yoshimatsu, K. *et al.* Inducible prostaglandin E synthase is overexpressed in non-small
cell lung cancer. *Clinical cancer research : an official journal of the American
Association for Cancer Research* **7**, 2669-2674 (2001).
- 521 Zhou, J. *et al.* Interactions between prostaglandin E(2), liver receptor homologue-1,
and aromatase in breast cancer. *Cancer Res* **65**, 657-663 (2005).
- 522 Hanahan, D. & Weinberg, R. A. Hallmarks of cancer: the next generation. *Cell* **144**, 646-
674, doi:10.1016/j.cell.2011.02.013 (2011).
- 523 Pai, R. *et al.* PGE(2) stimulates VEGF expression in endothelial cells via ERK2/JNK1
signaling pathways. *Biochem Biophys Res Commun* **286**, 923-928,
doi:10.1006/bbrc.2001.5494 (2001).
- 524 Obermajer, N. *et al.* PGE(2)-driven induction and maintenance of cancer-associated
myeloid-derived suppressor cells. *Immunological investigations* **41**, 635-657,
doi:10.3109/08820139.2012.695417 (2012).
- 525 Chulada, P. C. *et al.* Genetic disruption of Ptgs-1, as well as Ptgs-2, reduces intestinal
tumorigenesis in Min mice. *Cancer Res* **60**, 4705-4708 (2000).

- 526 Harris, R. E. Cyclooxygenase-2 (cox-2) blockade in the chemoprevention of cancers of the colon, breast, prostate, and lung. *Inflammopharmacology* **17**, 55-67, doi:10.1007/s10787-009-8049-8 (2009).
- 527 Ng, K. *et al.* Aspirin and COX-2 inhibitor use in patients with stage III colon cancer. *Journal of the National Cancer Institute* **107**, 345, doi:10.1093/jnci/dju345 (2015).
- 528 Alshafie, G. A., Abou-Issa, H. M., Seibert, K. & Harris, R. E. Chemotherapeutic evaluation of Celecoxib, a cyclooxygenase-2 inhibitor, in a rat mammary tumor model. *Oncology reports* **7**, 1377-1381 (2000).
- 529 Robertson, F. M. *et al.* Ibuprofen-induced inhibition of cyclooxygenase isoform gene expression and regression of rat mammary carcinomas. *Cancer letters* **122**, 165-175 (1998).
- 530 Williams, C. S. *et al.* Celecoxib prevents tumor growth in vivo without toxicity to normal gut: lack of correlation between in vitro and in vivo models. *Cancer research* **60**, 6045-6051 (2000).
- 531 Goldman, A. P. *et al.* Meloxicam inhibits the growth of colorectal cancer cells. *Carcinogenesis* **19**, 2195-2199 (1998).
- 532 Tsujii, M., Kawano, S. & DuBois, R. N. Cyclooxygenase-2 expression in human colon cancer cells increases metastatic potential. *Proceedings of the National Academy of Sciences of the United States of America* **94**, 3336-3340, doi:10.1073/pnas.94.7.3336 (1997).
- 533 Waddell, W. R., Ganser, G. F., Cerise, E. J. & Loughry, R. W. Sulindac for polyposis of the colon. *American journal of surgery* **157**, 175-179 (1989).
- 534 Mann, M. *et al.* Targeting cyclooxygenase 2 and HER-2/neu pathways inhibits colorectal carcinoma growth. *Gastroenterology* **120**, 1713-1719 (2001).
- 535 Steinbach, G. *et al.* The effect of celecoxib, a cyclooxygenase-2 inhibitor, in familial adenomatous polyposis. *The New England journal of medicine* **342**, 1946-1952, doi:10.1056/NEJM200006293422603 (2000).
- 536 Pollard, M. & Luckert, P. H. Indomethacin treatment of rats with dimethylhydrazine-induced intestinal tumors. *Cancer treatment reports* **64**, 1323-1327 (1980).
- 537 Tsujii, M. *et al.* Cyclooxygenase regulates angiogenesis induced by colon cancer cells. *Cell* **93**, 705-716 (1998).
- 538 Seed, M. P. *et al.* The inhibition of colon-26 adenocarcinoma development and angiogenesis by topical diclofenac in 2.5% hyaluronan. *Cancer research* **57**, 1625-1629 (1997).
- 539 Kawamori, T., Rao, C. V., Seibert, K. & Reddy, B. S. Chemopreventive activity of celecoxib, a specific cyclooxygenase-2 inhibitor, against colon carcinogenesis. *Cancer research* **58**, 409-412 (1998).
- 540 Sheng, H. *et al.* Inhibition of human colon cancer cell growth by selective inhibition of cyclooxygenase-2. *The Journal of clinical investigation* **99**, 2254-2259, doi:10.1172/JCI119400 (1997).
- 541 Oshima, M. *et al.* Suppression of intestinal polyposis in Apc delta716 knockout mice by inhibition of cyclooxygenase 2 (COX-2). *Cell* **87**, 803-809 (1996).
- 542 Prescott, S. M. & White, R. L. Self-promotion? Intimate connections between APC and prostaglandin H synthase-2. *Cell* **87**, 783-786 (1996).
- 543 Romsing, J. & Moiniche, S. A systematic review of COX-2 inhibitors compared with traditional NSAIDs, or different COX-2 inhibitors for post-operative pain. *Acta anaesthesiologica Scandinavica* **48**, 525-546, doi:10.1111/j.0001-5172.2004.00379.x (2004).

- 544 Gabriel, S. E., Jaakkimainen, L. & Bombardier, C. Risk for serious gastrointestinal complications related to use of nonsteroidal anti-inflammatory drugs. A meta-analysis. *Annals of internal medicine* **115**, 787-796 (1991).
- 545 Bresalier, R. S. *et al.* Cardiovascular events associated with rofecoxib in a colorectal adenoma chemoprevention trial. *The New England journal of medicine* **352**, 1092-1102, doi:10.1056/NEJMoa050493 (2005).
- 546 Nussmeier, N. A. *et al.* Complications of the COX-2 inhibitors parecoxib and valdecoxib after cardiac surgery. *The New England journal of medicine* **352**, 1081-1091, doi:10.1056/NEJMoa050330 (2005).
- 547 Baron, J. A. *et al.* A randomized trial of rofecoxib for the chemoprevention of colorectal adenomas. *Gastroenterology* **131**, 1674-1682, doi:10.1053/j.gastro.2006.08.079 (2006).
- 548 Arber, N. *et al.* Celecoxib for the prevention of colorectal adenomatous polyps. *The New England journal of medicine* **355**, 885-895, doi:10.1056/NEJMoa061652 (2006).
- 549 Bertagnolli, M. M. *et al.* Celecoxib for the prevention of sporadic colorectal adenomas. *The New England journal of medicine* **355**, 873-884, doi:10.1056/NEJMoa061355 (2006).
- 550 Ahmetaj-Shala, B. *et al.* Evidence that links loss of cyclooxygenase-2 with increased asymmetric dimethylarginine: novel explanation of cardiovascular side effects associated with anti-inflammatory drugs. *Circulation* **131**, 633-642, doi:10.1161/CIRCULATIONAHA.114.011591 (2015).
- 551 Dai, P. *et al.* Efficacy and safety of COX-2 inhibitors for advanced non-small-cell lung cancer with chemotherapy: a meta-analysis. *OncoTargets and therapy* **11**, 721-730, doi:10.2147/OTT.S148670 (2018).
- 552 Edelman, M. J. *et al.* Phase III Randomized, Placebo-Controlled, Double-Blind Trial of Celecoxib in Addition to Standard Chemotherapy for Advanced Non-Small-Cell Lung Cancer With Cyclooxygenase-2 Overexpression: CALGB 30801 (Alliance). *Journal of clinical oncology : official journal of the American Society of Clinical Oncology* **35**, 2184-2192, doi:10.1200/JCO.2016.71.3743 (2017).
- 553 Lynch, P. M. *et al.* An international randomised trial of celecoxib versus celecoxib plus difluoromethylornithine in patients with familial adenomatous polyposis. *Gut* **65**, 286-295, doi:10.1136/gutjnl-2014-307235 (2016).
- 554 Chen, J. *et al.* Efficacy and safety profile of celecoxib for treating advanced cancers: a meta-analysis of 11 randomized clinical trials. *Clinical therapeutics* **36**, 1253-1263, doi:10.1016/j.clinthera.2014.06.015 (2014).
- 555 Mbalaviele, G. *et al.* Distinction of microsomal prostaglandin E synthase-1 (mPGES-1) inhibition from cyclooxygenase-2 inhibition in cells using a novel, selective mPGES-1 inhibitor. *Biochemical pharmacology* **79**, 1445-1454, doi:10.1016/j.bcp.2010.01.003 (2010).
- 556 Xu, D. *et al.* MF63 [2-(6-chloro-1H-phenanthro[9,10-d]imidazol-2-yl)-isophthalonitrile], a selective microsomal prostaglandin E synthase-1 inhibitor, relieves pyresis and pain in preclinical models of inflammation. *J Pharmacol Exp Ther* **326**, 754-763, doi:10.1124/jpet.108.138776 (2008).
- 557 Leclerc, P. *et al.* Characterization of a new mPGES-1 inhibitor in rat models of inflammation. *Prostaglandins & other lipid mediators* **102-103**, 1-12, doi:10.1016/j.prostaglandins.2013.03.005 (2013).
- 558 Guerrero, M. D. *et al.* Anti-inflammatory and analgesic activity of a novel inhibitor of microsomal prostaglandin E synthase-1 expression. *European journal of pharmacology* **620**, 112-119, doi:10.1016/j.ejphar.2009.08.007 (2009).

- 559 Beales, I. L. & Ogunwobi, O. O. Microsomal prostaglandin E synthase-1 inhibition blocks proliferation and enhances apoptosis in oesophageal adenocarcinoma cells without affecting endothelial prostacyclin production. *International journal of cancer* **126**, 2247-2255, doi:10.1002/ijc.24875 (2010).
- 560 Leclerc, P. *et al.* Characterization of a human and murine mPGES-1 inhibitor and comparison to mPGES-1 genetic deletion in mouse models of inflammation. *Prostaglandins & other lipid mediators* **107**, 26-34, doi:10.1016/j.prostaglandins.2013.09.001 (2013).
- 561 Montrose, D. C. *et al.* The role of PGE2 in intestinal inflammation and tumorigenesis. *Prostaglandins & other lipid mediators* **116-117**, 26-36, doi:10.1016/j.prostaglandins.2014.10.002 (2015).
- 562 Xu, Y. *et al.* Lysophosphatidic acid as a potential biomarker for ovarian and other gynecologic cancers. *Jama* **280**, 719-723 (1998).
- 563 Sutphen, R. *et al.* Lysophospholipids are potential biomarkers of ovarian cancer. *Cancer epidemiology, biomarkers & prevention : a publication of the American Association for Cancer Research, cosponsored by the American Society of Preventive Oncology* **13**, 1185-1191 (2004).
- 564 Zhou, X. *et al.* Identification of plasma lipid biomarkers for prostate cancer by lipidomics and bioinformatics. *PLoS One* **7**, e48889, doi:10.1371/journal.pone.0048889 (2012).
- 565 Skotland, T. *et al.* Molecular lipid species in urinary exosomes as potential prostate cancer biomarkers. *European journal of cancer* **70**, 122-132, doi:10.1016/j.ejca.2016.10.011 (2017).
- 566 Chen, X. *et al.* Plasma lipidomics profiling identified lipid biomarkers in distinguishing early-stage breast cancer from benign lesions. *Oncotarget* **7**, 36622-36631, doi:10.18632/oncotarget.9124 (2016).
- 567 Yang, L. *et al.* Comprehensive lipid profiling of plasma in patients with benign breast tumor and breast cancer reveals novel biomarkers. *Analytical and bioanalytical chemistry* **407**, 5065-5077, doi:10.1007/s00216-015-8484-x (2015).
- 568 Zhao, Z. *et al.* Plasma lysophosphatidylcholine levels: potential biomarkers for colorectal cancer. *Journal of clinical oncology : official journal of the American Society of Clinical Oncology* **25**, 2696-2701, doi:10.1200/JCO.2006.08.5571 (2007).
- 569 Joo, E. J. *et al.* Carbohydrate-containing molecules as potential biomarkers in colon cancer. *Omics : a journal of integrative biology* **18**, 231-241, doi:10.1089/omi.2013.0128 (2014).
- 570 Chiu, H. M. *et al.* Association between early stage colon neoplasms and false-negative results from the fecal immunochemical test. *Clinical gastroenterology and hepatology : the official clinical practice journal of the American Gastroenterological Association* **11**, 832-838 e831-832, doi:10.1016/j.cgh.2013.01.013 (2013).
- 571 Park, D. I. *et al.* Comparison of guaiac-based and quantitative immunochemical fecal occult blood testing in a population at average risk undergoing colorectal cancer screening. *The American journal of gastroenterology* **105**, 2017-2025, doi:10.1038/ajg.2010.179 (2010).
- 572 Brenner, H. & Tao, S. Superior diagnostic performance of faecal immunochemical tests for haemoglobin in a head-to-head comparison with guaiac based faecal occult blood test among 2235 participants of screening colonoscopy. *European journal of cancer* **49**, 3049-3054, doi:10.1016/j.ejca.2013.04.023 (2013).
- 573 Graser, A. *et al.* Comparison of CT colonography, colonoscopy, sigmoidoscopy and faecal occult blood tests for the detection of advanced adenoma in an average risk population. *Gut* **58**, 241-248, doi:10.1136/gut.2008.156448 (2009).

- 574 Zorzi, M. *et al.* Impact on colorectal cancer mortality of screening programmes based on the faecal immunochemical test. *Gut* **64**, 784-790, doi:10.1136/gutjnl-2014-307508 (2015).
- 575 Mellman, I. Endocytosis and molecular sorting. *Annual review of cell and developmental biology* **12**, 575-625, doi:10.1146/annurev.cellbio.12.1.575 (1996).
- 576 Sotelo, J. R. & Porter, K. R. An electron microscope study of the rat ovum. *The Journal of biophysical and biochemical cytology* **5**, 327-342 (1959).
- 577 Novikoff, A. B., Essner, E. & Quintana, N. Golgi Apparatus and Lysosomes. *Federation proceedings* **23**, 1010-1022 (1964).
- 578 Kirchhausen, T. Three ways to make a vesicle. *Nat Rev Mol Cell Biol* **1**, 187-198, doi:10.1038/35043117 (2000).
- 579 Lemmon, S. K. & Traub, L. M. Sorting in the endosomal system in yeast and animal cells. *Current opinion in cell biology* **12**, 457-466 (2000).
- 580 Felder, S. *et al.* Kinase activity controls the sorting of the epidermal growth factor receptor within the multivesicular body. *Cell* **61**, 623-634 (1990).
- 581 Mullock, B. M., Bright, N. A., Fearon, C. W., Gray, S. R. & Luzio, J. P. Fusion of lysosomes with late endosomes produces a hybrid organelle of intermediate density and is NSF dependent. *J Cell Biol* **140**, 591-601 (1998).
- 582 Futter, C. E., Collinson, L. M., Backer, J. M. & Hopkins, C. R. Human VPS34 is required for internal vesicle formation within multivesicular endosomes. *J Cell Biol* **155**, 1251-1264, doi:10.1083/jcb.200108152 (2001).
- 583 Kleijmeer, M. *et al.* Reorganization of multivesicular bodies regulates MHC class II antigen presentation by dendritic cells. *J Cell Biol* **155**, 53-63, doi:10.1083/jcb.200103071 (2001).
- 584 Fujita, Y., Kosaka, N., Araya, J., Kuwano, K. & Ochiya, T. Extracellular vesicles in lung microenvironment and pathogenesis. *Trends in molecular medicine* **21**, 533-542, doi:10.1016/j.molmed.2015.07.004 (2015).
- 585 They, C., Ostrowski, M. & Segura, E. Membrane vesicles as conveyors of immune responses. *Nature reviews. Immunology* **9**, 581-593, doi:10.1038/nri2567 (2009).
- 586 Gould, S. J. & Raposo, G. As we wait: coping with an imperfect nomenclature for extracellular vesicles. *Journal of extracellular vesicles* **2**, doi:10.3402/jev.v2i0.20389 (2013).
- 587 Harding, C., Heuser, J. & Stahl, P. Receptor-mediated endocytosis of transferrin and recycling of the transferrin receptor in rat reticulocytes. *J Cell Biol* **97**, 329-339 (1983).
- 588 Pan, B. T., Teng, K., Wu, C., Adam, M. & Johnstone, R. M. Electron microscopic evidence for externalization of the transferrin receptor in vesicular form in sheep reticulocytes. *J Cell Biol* **101**, 942-948 (1985).
- 589 Johnstone, R. M., Adam, M., Hammond, J. R., Orr, L. & Turbide, C. Vesicle formation during reticulocyte maturation. Association of plasma membrane activities with released vesicles (exosomes). *J Biol Chem* **262**, 9412-9420 (1987).
- 590 Trams, E. G., Lauter, C. J., Salem, N., Jr. & Heine, U. Exfoliation of membrane ectoenzymes in the form of micro-vesicles. *Biochim Biophys Acta* **645**, 63-70 (1981).
- 591 Johnstone, R. M., Bianchini, A. & Teng, K. Reticulocyte maturation and exosome release: transferrin receptor containing exosomes shows multiple plasma membrane functions. *Blood* **74**, 1844-1851 (1989).
- 592 Zakharova, L., Svetlova, M. & Fomina, A. F. T cell exosomes induce cholesterol accumulation in human monocytes via phosphatidylserine receptor. *J Cell Physiol* **212**, 174-181, doi:10.1002/jcp.21013 (2007).
- 593 Andreola, G. *et al.* Induction of lymphocyte apoptosis by tumor cell secretion of FasL-bearing microvesicles. *J Exp Med* **195**, 1303-1316 (2002).

- 594 Karlsson, M. *et al.* "Tolerosomes" are produced by intestinal epithelial cells. *European journal of immunology* **31**, 2892-2900, doi:10.1002/1521-4141(2001010)31:10<2892::AID-IMMU2892>3.0.CO;2-I (2001).
- 595 Wolfers, J. *et al.* Tumor-derived exosomes are a source of shared tumor rejection antigens for CTL cross-priming. *Nature medicine* **7**, 297-303, doi:10.1038/85438 (2001).
- 596 They, C. *et al.* Indirect activation of naive CD4+ T cells by dendritic cell-derived exosomes. *Nature immunology* **3**, 1156-1162, doi:10.1038/ni854 (2002).
- 597 Raposo, G. *et al.* B lymphocytes secrete antigen-presenting vesicles. *J Exp Med* **183**, 1161-1172 (1996).
- 598 Zitvogel, L. *et al.* Eradication of established murine tumors using a novel cell-free vaccine: dendritic cell-derived exosomes. *Nature medicine* **4**, 594-600 (1998).
- 599 Chaput, N. & They, C. Exosomes: immune properties and potential clinical implementations. *Seminars in immunopathology* **33**, 419-440, doi:10.1007/s00281-010-0233-9 (2011).
- 600 Valadi, H. *et al.* Exosome-mediated transfer of mRNAs and microRNAs is a novel mechanism of genetic exchange between cells. *Nature cell biology* **9**, 654-659, doi:10.1038/ncb1596 (2007).
- 601 Crescitelli, R. *et al.* Distinct RNA profiles in subpopulations of extracellular vesicles: apoptotic bodies, microvesicles and exosomes. *Journal of extracellular vesicles* **2**, doi:10.3402/jev.v2i0.20677 (2013).
- 602 Mathivanan, S. & Simpson, R. J. ExoCarta: A compendium of exosomal proteins and RNA. *Proteomics* **9**, 4997-5000, doi:10.1002/pmic.200900351 (2009).
- 603 They, C. *et al.* Molecular characterization of dendritic cell-derived exosomes. Selective accumulation of the heat shock protein hsc73. *J Cell Biol* **147**, 599-610 (1999).
- 604 They, C. *et al.* Proteomic analysis of dendritic cell-derived exosomes: a secreted subcellular compartment distinct from apoptotic vesicles. *Journal of immunology* **166**, 7309-7318 (2001).
- 605 Wubbolts, R. *et al.* Proteomic and biochemical analyses of human B cell-derived exosomes. Potential implications for their function and multivesicular body formation. *J Biol Chem* **278**, 10963-10972, doi:10.1074/jbc.M207550200 (2003).
- 606 Trajkovic, K. *et al.* Ceramide triggers budding of exosome vesicles into multivesicular endosomes. *Science* **319**, 1244-1247, doi:10.1126/science.1153124 (2008).
- 607 Carayon, K. *et al.* Proteolipidic composition of exosomes changes during reticulocyte maturation. *J Biol Chem* **286**, 34426-34439, doi:10.1074/jbc.M111.257444 (2011).
- 608 Laulagnier, K. *et al.* Mast cell- and dendritic cell-derived exosomes display a specific lipid composition and an unusual membrane organization. *Biochem J* **380**, 161-171, doi:10.1042/BJ20031594 (2004).
- 609 Melo, S. A. *et al.* Glypican-1 identifies cancer exosomes and detects early pancreatic cancer. *Nature* **523**, 177-182, doi:10.1038/nature14581 (2015).
- 610 Taylor, D. D. & Gercel-Taylor, C. MicroRNA signatures of tumor-derived exosomes as diagnostic biomarkers of ovarian cancer. *Gynecologic oncology* **110**, 13-21, doi:10.1016/j.ygyno.2008.04.033 (2008).
- 611 Royo, F. *et al.* Different EV enrichment methods suitable for clinical settings yield different subpopulations of urinary extracellular vesicles from human samples. *Journal of extracellular vesicles* **5**, 29497, doi:10.3402/jev.v5.29497 (2016).
- 612 Skog, J. *et al.* Glioblastoma microvesicles transport RNA and proteins that promote tumour growth and provide diagnostic biomarkers. *Nature cell biology* **10**, 1470-1476, doi:10.1038/ncb1800 (2008).

- 613 Peinado, H. *et al.* Melanoma exosomes educate bone marrow progenitor cells toward a pro-metastatic phenotype through MET. *Nature medicine* **18**, 883-891, doi:10.1038/nm.2753 (2012).
- 614 Hoshino, A. *et al.* Tumour exosome integrins determine organotropic metastasis. *Nature* **527**, 329-335, doi:10.1038/nature15756 (2015).
- 615 Zarini, S., Gijon, M. A., Ransome, A. E., Murphy, R. C. & Sala, A. Transcellular biosynthesis of cysteinyl leukotrienes in vivo during mouse peritoneal inflammation. *Proceedings of the National Academy of Sciences of the United States of America* **106**, 8296-8301, doi:10.1073/pnas.0903851106 (2009).
- 616 Laulagnier, K. *et al.* PLD2 is enriched on exosomes and its activity is correlated to the release of exosomes. *FEBS letters* **572**, 11-14, doi:10.1016/j.febslet.2004.06.082 (2004).
- 617 Matsuo, H. *et al.* Role of LBPA and Alix in multivesicular liposome formation and endosome organization. *Science* **303**, 531-534, doi:10.1126/science.1092425 (2004).
- 618 Xiang, X. *et al.* Induction of myeloid-derived suppressor cells by tumor exosomes. *International journal of cancer* **124**, 2621-2633, doi:10.1002/ijc.24249 (2009).
- 619 Subra, C. *et al.* Exosomes account for vesicle-mediated transcellular transport of activatable phospholipases and prostaglandins. *J Lipid Res* **51**, 2105-2120, doi:10.1194/jlr.M003657 (2010).
- 620 Llorente, A. *et al.* Molecular lipidomics of exosomes released by PC-3 prostate cancer cells. *Biochim Biophys Acta* **1831**, 1302-1309, doi:10.1016/j.bbaliip.2013.04.011 (2012).
- 621 Pienimaeki-Roemer, A. *et al.* Lipidomic and proteomic characterization of platelet extracellular vesicle subfractions from senescent platelets. *Transfusion* **55**, 507-521, doi:10.1111/trf.12874 (2015).
- 622 Haraszti, R. A. *et al.* High-resolution proteomic and lipidomic analysis of exosomes and microvesicles from different cell sources. *Journal of extracellular vesicles* **5**, 32570, doi:10.3402/jev.v5.32570 (2016).
- 623 Lydic, T. A. *et al.* Rapid and comprehensive 'shotgun' lipidome profiling of colorectal cancer cell derived exosomes. *Methods (San Diego, Calif)* **87**, 83-95, doi:10.1016/j.ymeth.2015.04.014 (2015).
- 624 Zeisig, R., Koklic, T., Wiesner, B., Fichtner, I. & Sentjurg, M. Increase in fluidity in the membrane of MT3 breast cancer cells correlates with enhanced cell adhesion in vitro and increased lung metastasis in NOD/SCID mice. *Arch Biochem Biophys* **459**, 98-106, doi:10.1016/j.abb.2006.09.030 (2007).
- 625 Montaudon, D., Louis, J. C. & Robert, J. Phospholipid acyl group composition in normal and tumoral nerve cells in culture. *Lipids* **16**, 293-297 (1981).
- 626 Perkins, R. G. & Scott, R. E. Differences in the phospholipid, cholesterol, and fatty acyl composition of 3T3 and SV3T3 plasma membranes. *Lipids* **13**, 653-657 (1978).
- 627 Van Hoeven, R. P., Emmelot, P., Krol, J. H. & Oomen-Meulemans, E. P. Studies on plasma membranes. XXII. Fatty acid profiles of lipid classes in plasma membranes of rat and mouse livers and hepatomas. *Biochim Biophys Acta* **380**, 1-11 (1975).
- 628 Ruggieri, S. *et al.* Lipid characteristics in metastatic cells. *Clinical & experimental metastasis* **17**, 271-276 (1999).
- 629 Norambuena, A. & Schwartz, M. A. Effects of integrin-mediated cell adhesion on plasma membrane lipid raft components and signaling. *Molecular biology of the cell* **22**, 3456-3464, doi:10.1091/mbc.E11-04-0361 (2011).
- 630 Marquez, M. G., Nieto, F. L., Fernandez-Tome, M. C., Favale, N. O. & Sterin-Speziale, N. Membrane lipid composition plays a central role in the maintenance of epithelial cell adhesion to the extracellular matrix. *Lipids* **43**, 343-352, doi:10.1007/s11745-008-3152-y (2008).

- 631 Marquez, M. G., Favale, N. O., Leocata Nieto, F., Pescio, L. G. & Sterin-Speziale, N. Changes in membrane lipid composition cause alterations in epithelial cell-cell adhesion structures in renal papillary collecting duct cells. *Biochim Biophys Acta* **1818**, 491-501, doi:10.1016/j.bbame.2011.11.018 (2012).
- 632 Kyriakos, M. The President's cancer, the Dukes classification, and confusion. *Archives of pathology & laboratory medicine* **109**, 1063-1066 (1985).
- 633 Martin, M. L. *et al.* Sustained activation of sphingomyelin synthase by 2-hydroxyoleic acid induces sphingolipidosis in tumor cells. *J Lipid Res* **54**, 1457-1465, doi:10.1194/jlr.M036749 (2013).
- 634 Neoptolemos, J. P., Husband, D., Imray, C., Rowley, S. & Lawson, N. Arachidonic acid and docosahexaenoic acid are increased in human colorectal cancer. *Gut* **32**, 278-281 (1991).
- 635 Barcelo-Coblijn, G. *et al.* Sphingomyelin and sphingomyelin synthase (SMS) in the malignant transformation of glioma cells and in 2-hydroxyoleic acid therapy. *Proc Natl Acad Sci U S A* **108**, 19569-19574, doi:10.1073/pnas.1115484108 (2011).
- 636 Doria, M. L. *et al.* Lipidomic analysis of phospholipids from human mammary epithelial and breast cancer cell lines. *J Cell Physiol* **228**, 457-468, doi:10.1002/jcp.24152 (2013).
- 637 Marien, E. *et al.* Non-small cell lung cancer is characterized by dramatic changes in phospholipid profiles. *International journal of cancer* **137**, 1539-1548, doi:10.1002/ijc.29517 (2015).
- 638 Roos, D. S. & Choppin, P. W. Tumorigenicity of cell lines with altered lipid composition. *Proc Natl Acad Sci U S A* **81**, 7622-7626 (1984).
- 639 Snyder, F. & Wood, R. Alkyl and alk-1-enyl ethers of glycerol in lipids from normal and neoplastic human tissues. *Cancer Res* **29**, 251-257 (1969).
- 640 Benjamin, D. I. *et al.* Ether lipid generating enzyme AGPS alters the balance of structural and signaling lipids to fuel cancer pathogenicity. *Proc Natl Acad Sci U S A* **110**, 14912-14917, doi:10.1073/pnas.1310894110 (2013).
- 641 Howard, B. V., Morris, H. P. & Bailey, J. M. Ether-lipids, -glycerol phosphate dehydrogenase, and growth rate in tumors and cultured cells. *Cancer Res* **32**, 1533-1538 (1972).
- 642 Albert, D. H. & Anderson, C. E. Ether-linked glycerolipids in human brain tumors. *Lipids* **12**, 188-192 (1977).
- 643 Smith, R. E. *et al.* A reliable biomarker derived from plasmalogens to evaluate malignancy and metastatic capacity of human cancers. *Lipids* **43**, 79-89, doi:10.1007/s11745-007-3133-6 (2008).
- 644 Fernandez, R. *et al.* Identification of Biomarkers of Necrosis in Xenografts Using Imaging Mass Spectrometry. *Journal of the American Society for Mass Spectrometry* **27**, 244-254, doi:10.1007/s13361-015-1268-x (2016).
- 645 Dressler, K. A., Kan, C. C. & Kolesnick, R. N. Sphingomyelin synthesis is involved in adherence during macrophage differentiation of HL-60 cells. *J Biol Chem* **266**, 11522-11527 (1991).
- 646 Olivera, A., Buckley, N. E. & Spiegel, S. Sphingomyelinase and cell-permeable ceramide analogs stimulate cellular proliferation in quiescent Swiss 3T3 fibroblasts. *J Biol Chem* **267**, 26121-26127 (1992).
- 647 Abe, M. *et al.* A role for sphingomyelin-rich lipid domains in the accumulation of phosphatidylinositol-4,5-bisphosphate to the cleavage furrow during cytokinesis. *Mol Cell Biol* **32**, 1396-1407, doi:10.1128/MCB.06113-11 (2012).
- 648 Patterson, N. H. *et al.* Assessment of pathological response to therapy using lipid mass spectrometry imaging. *Scientific reports* **6**, 36814, doi:10.1038/srep36814 (2016).

- 649 Balakrishnan, S., Goodwin, H. & Cumings, J. N. The distribution of phosphorus-containing lipid compounds in the human brain. *J Neurochem* **8**, 276-284 (1961).
- 650 Hack, M. H. & Helmy, F. M. Thin-layer chromatographic resolution of molecular species of ethanolamine plasmalogen quantitatively unique to myelin. *J Chromatogr* **135**, 229-234 (1977).
- 651 Boggs, J. M. & Rangaraj, G. Changes in the composition of two molecular species of ethanolamine plasmalogen in normal human myelin during development. *Biochim Biophys Acta* **793**, 313-316 (1984).
- 652 Getz, G. S., Bartley, W., Lurie, D. & Notton, B. M. The phospholipids of various sheep organs, rat liver and of their subcellular fractions. *Biochim Biophys Acta* **152**, 325-339 (1968).
- 653 Gottfried, E. L. Lipids of human leukocytes: relation to celltype. *J Lipid Res* **8**, 321-327 (1967).
- 654 MacDonald, J. I. & Sprecher, H. Distribution of arachidonic acid in choline- and ethanolamine-containing phosphoglycerides in subfractionated human neutrophils. *J Biol Chem* **264**, 17718-17726 (1989).
- 655 Blank, M. L., Smith, Z. L., Lee, Y. J. & Snyder, F. Effects of eicosapentaenoic and docosahexaenoic acid supplements on phospholipid composition and plasmalogen biosynthesis in P388D1 cells. *Arch Biochem Biophys* **269**, 603-611 (1989).
- 656 Chapkin, R. S. & Carmichael, S. L. Effects of dietary n-3 and n-6 polyunsaturated fatty acids on macrophage phospholipid classes and subclasses. *Lipids* **25**, 827-834 (1990).
- 657 Waku, K., Uda, Y. & Nakazawa, Y. Lipid composition in rabbit sarcoplasmic reticulum and occurrence of alkyl ether phospholipids. *Journal of biochemistry* **69**, 483-491 (1971).
- 658 Yamada, K., Imura, K., Taniguchi, M. & Sakagami, T. Studies on the composition of phospholipids in rat small intestinal smooth muscle. *Journal of biochemistry* **79**, 809-817 (1976).
- 659 Okano, G., Matsuzaka, H. & Shimojo, T. A comparative study of the lipid composition of white, intermediate, red and heart muscle in rats. *Biochim Biophys Acta* **619**, 167-175 (1980).
- 660 Bussolino, F. & Camussi, G. Platelet-activating factor produced by endothelial cells. A molecule with autocrine and paracrine properties. *European journal of biochemistry* **229**, 327-337 (1995).
- 661 Dueck, D. A. *et al.* The modulation of choline phosphoglyceride metabolism in human colon cancer. *Mol Cell Biochem* **162**, 97-103 (1996).
- 662 Nagan, N. & Zoeller, R. A. Plasmalogens: biosynthesis and functions. *Prog Lipid Res* **40**, 199-229 (2001).
- 663 Hossain, M. S. *et al.* Reduction of Ether-Type Glycerophospholipids, Plasmalogens, by NF-kappaB Signal Leading to Microglial Activation. *The Journal of neuroscience : the official journal of the Society for Neuroscience* **37**, 4074-4092, doi:10.1523/JNEUROSCI.3941-15.2017 (2017).
- 664 Bishop, J. E. & Hajra, A. K. Mechanism and specificity of formation of long chain alcohols by developing rat brain. *J Biol Chem* **256**, 9542-9550 (1981).
- 665 Honsho, M., Asaoku, S. & Fujiki, Y. Posttranslational regulation of fatty acyl-CoA reductase 1, Far1, controls ether glycerophospholipid synthesis. *J Biol Chem* **285**, 8537-8542, doi:10.1074/jbc.M109.083311 (2010).
- 666 Honsho, M. & Fujiki, Y. Plasmalogen homeostasis - regulation of plasmalogen biosynthesis and its physiological consequence in mammals. *FEBS Lett* **591**, 2720-2729, doi:10.1002/1873-3468.12743 (2017).

- 667 Emoto, K. *et al.* Redistribution of phosphatidylethanolamine at the cleavage furrow of
dividing cells during cytokinesis. *Proc Natl Acad Sci U S A* **93**, 12867-12872 (1996).
- 668 Marconescu, A. & Thorpe, P. E. Coincident exposure of phosphatidylethanolamine and
anionic phospholipids on the surface of irradiated cells. *Biochim Biophys Acta* **1778**,
2217-2224, doi:10.1016/j.bbamem.2008.05.006 (2008).
- 669 Stafford, J. H. & Thorpe, P. E. Increased exposure of phosphatidylethanolamine on the
surface of tumor vascular endothelium. *Neoplasia* **13**, 299-308 (2011).
- 670 Rizzo, W. B. Fatty aldehyde and fatty alcohol metabolism: review and importance for
epidermal structure and function. *Biochim Biophys Acta* **1841**, 377-389,
doi:10.1016/j.bbalip.2013.09.001 (2014).
- 671 Hossain, M. S. *et al.* Plasmalogens rescue neuronal cell death through an activation of
AKT and ERK survival signaling. *PLoS One* **8**, e83508,
doi:10.1371/journal.pone.0083508 (2013).
- 672 Shulga, Y. V., Anderson, R. A., Topham, M. K. & Epan, R. M. Phosphatidylinositol-4-
phosphate 5-kinase isoforms exhibit acyl chain selectivity for both substrate and lipid
activator. *J Biol Chem* **287**, 35953-35963, doi:10.1074/jbc.M112.370155 (2012).
- 673 Traynor-Kaplan, A. *et al.* Fatty-acyl chain profiles of cellular phosphoinositides.
Biochimica et biophysica acta. Molecular and cell biology of lipids **1862**, 513-522,
doi:10.1016/j.bbalip.2017.02.002 (2017).
- 674 da Silva, T. F. *et al.* Peripheral nervous system plasmalogens regulate Schwann cell
differentiation and myelination. *The Journal of clinical investigation* **124**, 2560-2570,
doi:10.1172/JCI72063 (2014).
- 675 Dihlmann, S., Kloor, M., Fallsehr, C. & von Knebel Doeberitz, M. Regulation of AKT1
expression by beta-catenin/Tcf/Lef signaling in colorectal cancer cells. *Carcinogenesis*
26, 1503-1512, doi:10.1093/carcin/bgi120 (2005).
- 676 Itoh, N. *et al.* Phosphorylation of Akt/PKB is required for suppression of cancer cell
apoptosis and tumor progression in human colorectal carcinoma. *Cancer* **94**, 3127-
3134, doi:10.1002/cncr.10591 (2002).
- 677 Johnson, S. M. *et al.* Novel expression patterns of PI3K/Akt/mTOR signaling pathway
components in colorectal cancer. *Journal of the American College of Surgeons* **210**,
767-776, 776-768, doi:10.1016/j.jamcollsurg.2009.12.008 (2010).
- 678 Jain, D. in *Gastrointestinal pathology and its clinical implications* Vol. 2 (eds Robert
Ridell & Jain Dhanpat) Ch. 16, 875-928 (Wolter Kluwers, 2014).
- 679 O'Leary, A. D. & Sweeney, E. C. Lymphoglandular complexes of the colon: structure
and distribution. *Histopathology* **10**, 267-283 (1986).
- 680 Menendez, J. A. & Lupu, R. Fatty acid synthase and the lipogenic phenotype in cancer
pathogenesis. *Nature reviews. Cancer* **7**, 763-777, doi:10.1038/nrc2222 (2007).
- 681 Merchant, T. E., Meneses, P., Gierke, L. W., Den Otter, W. & Glonek, T. 31P magnetic
resonance phospholipid profiles of neoplastic human breast tissues. *Br J Cancer* **63**,
693-698 (1991).
- 682 Merchant, T. E. *et al.* Phospholipid profiles of human colon cancer using 31P magnetic
resonance spectroscopy. *International journal of colorectal disease* **6**, 121-126 (1991).
- 683 Ogiso, H. *et al.* Comparative Analysis of Biological Sphingolipids with
Glycerophospholipids and Diacylglycerol by LC-MS/MS. *Metabolites* **4**, 98-114,
doi:10.3390/metabo4010098 (2014).
- 684 Record, M., Carayon, K., Poirot, M. & Silvente-Poirot, S. Exosomes as new vesicular
lipid transporters involved in cell-cell communication and various pathophysiology.
Biochim Biophys Acta **1841**, 108-120, doi:10.1016/j.bbalip.2013.10.004 (2014).

- 685 Skotland, T., Sandvig, K. & Llorente, A. Lipids in exosomes: Current knowledge and the way forward. *Progress in lipid research* **66**, 30-41, doi:10.1016/j.plipres.2017.03.001 (2017).
- 686 Denzer, K., Kleijmeer, M. J., Heijnen, H. F., Stoorvogel, W. & Geuze, H. J. Exosome: from internal vesicle of the multivesicular body to intercellular signaling device. *J Cell Sci* **113 Pt 19**, 3365-3374 (2000).
- 687 Delage, E., Puyaubert, J., Zachowski, A. & Ruelland, E. Signal transduction pathways involving phosphatidylinositol 4-phosphate and phosphatidylinositol 4,5-bisphosphate: convergences and divergences among eukaryotic kingdoms. *Prog Lipid Res* **52**, 1-14, doi:10.1016/j.plipres.2012.08.003 (2013).
- 688 Koberlin, M. S. *et al.* A Conserved Circular Network of Coregulated Lipids Modulates Innate Immune Responses. *Cell* **162**, 170-183, doi:10.1016/j.cell.2015.05.051 (2015).
- 689 MacDonald, J. I. & Sprecher, H. Phospholipid fatty acid remodeling in mammalian cells. *Biochim Biophys Acta* **1084**, 105-121 (1991).
- 690 Wang, B. *et al.* Phospholipid Remodeling and Cholesterol Availability Regulate Intestinal Stemness and Tumorigenesis. *Cell stem cell* **22**, 206-220 e204, doi:10.1016/j.stem.2017.12.017 (2018).
- 691 Miyazaki, M., Kim, Y. C., Gray-Keller, M. P., Attie, A. D. & Ntambi, J. M. The biosynthesis of hepatic cholesterol esters and triglycerides is impaired in mice with a disruption of the gene for stearoyl-CoA desaturase 1. *J Biol Chem* **275**, 30132-30138, doi:10.1074/jbc.M005488200 (2000).
- 692 Ntambi, J. M. & Miyazaki, M. Regulation of stearoyl-CoA desaturases and role in metabolism. *Prog Lipid Res* **43**, 91-104 (2004).
- 693 Kan, C. F., Singh, A. B., Dong, B., Shende, V. R. & Liu, J. PPARdelta activation induces hepatic long-chain acyl-CoA synthetase 4 expression in vivo and in vitro. *Biochim Biophys Acta* **1851**, 577-587, doi:10.1016/j.bbalip.2015.01.008 (2015).
- 694 D'Souza, K. & Epand, R. M. The phosphatidylinositol synthase-catalyzed formation of phosphatidylinositol does not exhibit acyl chain specificity. *Biochemistry* **54**, 1151-1153, doi:10.1021/bi5015634 (2015).
- 695 Ge, L., Gordon, J. S., Hsuan, C., Stenn, K. & Prouty, S. M. Identification of the delta-6 desaturase of human sebaceous glands: expression and enzyme activity. *The Journal of investigative dermatology* **120**, 707-714, doi:10.1046/j.1523-1747.2003.12123.x (2003).
- 696 Gale, S. E. *et al.* A regulatory role for 1-acylglycerol-3-phosphate-O-acyltransferase 2 in adipocyte differentiation. *J Biol Chem* **281**, 11082-11089, doi:10.1074/jbc.M509612200 (2006).
- 697 Gil-de-Gomez, L. *et al.* Cytosolic group IVA and calcium-independent group VIA phospholipase A2s act on distinct phospholipid pools in zymosan-stimulated mouse peritoneal macrophages. *Journal of immunology* **192**, 752-762, doi:10.4049/jimmunol.1302267 (2014).
- 698 Yan, W. *et al.* The highly selective production of 2-arachidonoyl lysophosphatidylcholine catalyzed by purified calcium-independent phospholipase A2gamma: identification of a novel enzymatic mediator for the generation of a key branch point intermediate in eicosanoid signaling. *J Biol Chem* **280**, 26669-26679, doi:10.1074/jbc.M502358200 (2005).
- 699 Matsumoto, H. *et al.* Concordant induction of prostaglandin E2 synthase with cyclooxygenase-2 leads to preferred production of prostaglandin E2 over thromboxane and prostaglandin D2 in lipopolysaccharide-stimulated rat peritoneal macrophages. *Biochem Biophys Res Commun* **230**, 110-114, doi:10.1006/bbrc.1996.5894 (1997).

- 700 Naraba, H. *et al.* Segregated coupling of phospholipases A2, cyclooxygenases, and terminal prostanoid synthases in different phases of prostanoid biosynthesis in rat peritoneal macrophages. *Journal of immunology* **160**, 2974-2982 (1998).
- 701 Sano, H. *et al.* Expression of cyclooxygenase-1 and -2 in human colorectal cancer. *Cancer Res* **55**, 3785-3789 (1995).
- 702 Kujubu, D. A., Reddy, S. T., Fletcher, B. S. & Herschman, H. R. Expression of the protein product of the prostaglandin synthase-2/TIS10 gene in mitogen-stimulated Swiss 3T3 cells. *J Biol Chem* **268**, 5425-5430 (1993).
- 703 O'Banion, M. K., Winn, V. D. & Young, D. A. cDNA cloning and functional activity of a glucocorticoid-regulated inflammatory cyclooxygenase. *Proc Natl Acad Sci U S A* **89**, 4888-4892 (1992).
- 704 Kujubu, D. A., Fletcher, B. S., Varnum, B. C., Lim, R. W. & Herschman, H. R. TIS10, a phorbol ester tumor promoter-inducible mRNA from Swiss 3T3 cells, encodes a novel prostaglandin synthase/cyclooxygenase homologue. *J Biol Chem* **266**, 12866-12872 (1991).
- 705 Piomelli, D. The molecular logic of endocannabinoid signalling. *Nature reviews. Neuroscience* **4**, 873-884, doi:10.1038/nrn1247 (2003).
- 706 Billah, M. M. & Lapetina, E. G. Rapid decrease of phosphatidylinositol 4,5-bisphosphate in thrombin-stimulated platelets. *J Biol Chem* **257**, 12705-12708 (1982).
- 707 Weiss, S. J., McKinney, J. S. & Putney, J. W., Jr. Receptor-mediated net breakdown of phosphatidylinositol 4,5-bisphosphate in parotid acinar cells. *Biochem J* **206**, 555-560 (1982).
- 708 Marte, B. M. & Downward, J. PKB/Akt: connecting phosphoinositide 3-kinase to cell survival and beyond. *Trends Biochem Sci* **22**, 355-358 (1997).
- 709 Cantley, L. C. & Neel, B. G. New insights into tumor suppression: PTEN suppresses tumor formation by restraining the phosphoinositide 3-kinase/AKT pathway. *Proc Natl Acad Sci U S A* **96**, 4240-4245 (1999).
- 710 Delcommenne, M. *et al.* Phosphoinositide-3-OH kinase-dependent regulation of glycogen synthase kinase 3 and protein kinase B/AKT by the integrin-linked kinase. *Proc Natl Acad Sci U S A* **95**, 11211-11216 (1998).
- 711 Huang, E. H. *et al.* Aldehyde dehydrogenase 1 is a marker for normal and malignant human colonic stem cells (SC) and tracks SC overpopulation during colon tumorigenesis. *Cancer Res* **69**, 3382-3389, doi:10.1158/0008-5472.CAN-08-4418 (2009).
- 712 Douville, J., Beaulieu, R. & Balicki, D. ALDH1 as a functional marker of cancer stem and progenitor cells. *Stem cells and development* **18**, 17-25, doi:10.1089/scd.2008.0055 (2009).
- 713 Zhou, J. *et al.* Activation of the PTEN/mTOR/STAT3 pathway in breast cancer stem-like cells is required for viability and maintenance. *Proc Natl Acad Sci U S A* **104**, 16158-16163, doi:10.1073/pnas.0702596104 (2007).
- 714 Sunayama, J. *et al.* Crosstalk between the PI3K/mTOR and MEK/ERK pathways involved in the maintenance of self-renewal and tumorigenicity of glioblastoma stem-like cells. *Stem cells* **28**, 1930-1939, doi:10.1002/stem.521 (2010).
- 715 Xia, P. & Xu, X. Y. PI3K/Akt/mTOR signaling pathway in cancer stem cells: from basic research to clinical application. *American journal of cancer research* **5**, 1602-1609 (2015).
- 716 Cao, Y., Dave, K. B., Doan, T. P. & Prescott, S. M. Fatty acid CoA ligase 4 is up-regulated in colon adenocarcinoma. *Cancer Res* **61**, 8429-8434 (2001).
- 717 Dong, M. *et al.* Inverse association between phospholipase A2 and COX-2 expression during mouse colon tumorigenesis. *Carcinogenesis* **24**, 307-315 (2003).

- 718 Eberhart, C. E. *et al.* Up-regulation of cyclooxygenase 2 gene expression in human
colorectal adenomas and adenocarcinomas. *Gastroenterology* **107**, 1183-1188 (1994).
- 719 Hao, X. *et al.* Early expression of cyclo-oxygenase-2 during sporadic colorectal
carcinogenesis. *The Journal of pathology* **187**, 295-301, doi:10.1002/(SICI)1096-
9896(199902)187:3<295::AID-PATH254>3.0.CO;2-Y (1999).
- 720 Pender-Cudlip, M. C. *et al.* Delta-6-desaturase activity and arachidonic acid synthesis
are increased in human breast cancer tissue. *Cancer science* **104**, 760-764,
doi:10.1111/cas.12129 (2013).
- 721 Nakanishi, M. *et al.* Genetic deletion of mPGES-1 suppresses intestinal tumorigenesis.
Cancer Res **68**, 3251-3259, doi:10.1158/0008-5472.CAN-07-6100 (2008).
- 722 Chen, L. *et al.* Stearoyl-CoA desaturase-1 mediated cell apoptosis in colorectal cancer
by promoting ceramide synthesis. *Scientific reports* **6**, 19665, doi:10.1038/srep19665
(2016).
- 723 Dimberg, J., Samuelsson, A., Hugander, A. & Soderkvist, P. Gene expression of
cyclooxygenase-2, group II and cytosolic phospholipase A2 in human colorectal cancer.
Anticancer research **18**, 3283-3287 (1998).
- 724 Heasley, L. E. *et al.* Induction of cytosolic phospholipase A2 by oncogenic Ras in human
non-small cell lung cancer. *J Biol Chem* **272**, 14501-14504 (1997).
- 725 Morioka, Y. *et al.* Potential role of group X secretory phospholipase A(2) in
cyclooxygenase-2-dependent PGE(2) formation during colon tumorigenesis. *FEBS Lett*
487, 262-266 (2000).
- 726 Takaku, K. *et al.* Suppression of intestinal polyposis in Apc(delta 716) knockout mice by
an additional mutation in the cytosolic phospholipase A(2) gene. *J Biol Chem* **275**,
34013-34016, doi:10.1074/jbc.C000585200 (2000).
- 727 Hong, K. H., Bonventre, J. C., O'Leary, E., Bonventre, J. V. & Lander, E. S. Deletion of
cytosolic phospholipase A(2) suppresses Apc(Min)-induced tumorigenesis. *Proc Natl
Acad Sci U S A* **98**, 3935-3939, doi:10.1073/pnas.051635898 (2001).
- 728 Brulet, M. *et al.* Lipid mapping of colonic mucosa by cluster TOF-SIMS imaging and
multivariate analysis in cfr knockout mice. *J Lipid Res* **51**, 3034-3045,
doi:10.1194/jlr.M008870 (2010).
- 729 Guo, S., Wang, Y., Zhou, D. & Li, Z. Significantly increased monounsaturated lipids
relative to polyunsaturated lipids in six types of cancer microenvironment are
observed by mass spectrometry imaging. *Scientific reports* **4**, 5959,
doi:10.1038/srep05959 (2014).
- 730 Kurabe, N. *et al.* Accumulated phosphatidylcholine (16:0/16:1) in human colorectal
cancer; possible involvement of LPCAT4. *Cancer science* **104**, 1295-1302,
doi:10.1111/cas.12221 (2013).
- 731 Chakrabarty, S., Radjendirane, V., Appelman, H. & Varani, J. Extracellular calcium and
calcium sensing receptor function in human colon carcinomas: promotion of E-
cadherin expression and suppression of beta-catenin/TCF activation. *Cancer Res* **63**,
67-71 (2003).
- 732 Brenner, B. M., Russell, N., Albrecht, S. & Davies, R. J. The effect of dietary vitamin D3
on the intracellular calcium gradient in mammalian colonic crypts. *Cancer letters* **127**,
43-53 (1998).
- 733 van der Flier, L. G. & Clevers, H. Stem cells, self-renewal, and differentiation in the
intestinal epithelium. *Annual review of physiology* **71**, 241-260,
doi:10.1146/annurev.physiol.010908.163145 (2009).
- 734 Maloberti, P. M. *et al.* Functional interaction between acyl-CoA synthetase 4,
lipooxygenases and cyclooxygenase-2 in the aggressive phenotype of breast cancer
cells. *PLoS One* **5**, e15540, doi:10.1371/journal.pone.0015540 (2010).

- 735 Qin, Y., Li, L., Pan, W. & Wu, D. Regulation of phosphatidylinositol kinases and metabolism by Wnt3a and Dvl. *J Biol Chem* **284**, 22544-22548, doi:10.1074/jbc.M109.014399 (2009).
- 736 Pan, W. *et al.* Wnt3a-mediated formation of phosphatidylinositol 4,5-bisphosphate regulates LRP6 phosphorylation. *Science* **321**, 1350-1353, doi:10.1126/science.1160741 (2008).
- 737 Sato, T. *et al.* Long-term expansion of epithelial organoids from human colon, adenoma, adenocarcinoma, and Barrett's epithelium. *Gastroenterology* **141**, 1762-1772, doi:10.1053/j.gastro.2011.07.050 (2011).
- 738 Calon, A., Tauriello, D. V. & Batlle, E. TGF-beta in CAF-mediated tumor growth and metastasis. *Seminars in cancer biology* **25**, 15-22, doi:10.1016/j.semcancer.2013.12.008 (2014).
- 739 Bennett, A. in *Prostaglandins: physiological, pharmacological and pathological aspects* (ed SMM Karim) 247-276 (1976).
- 740 Robert, A. R., M. in *Prostaglandins* (ed JB Lee) 113-176 (Elsevier, 1982).
- 741 DuBois, R. N., Awad, J., Morrow, J., Roberts, L. J., 2nd & Bishop, P. R. Regulation of eicosanoid production and mitogenesis in rat intestinal epithelial cells by transforming growth factor-alpha and phorbol ester. *The Journal of clinical investigation* **93**, 493-498, doi:10.1172/JCI116998 (1994).
- 742 Cohn, S. M., Schloemann, S., Tessner, T., Seibert, K. & Stenson, W. F. Crypt stem cell survival in the mouse intestinal epithelium is regulated by prostaglandins synthesized through cyclooxygenase-1. *The Journal of clinical investigation* **99**, 1367-1379, doi:10.1172/JCI119296 (1997).
- 743 Parfenova, H. *et al.* Dynamics of nuclear localization sites for COX-2 in vascular endothelial cells. *American journal of physiology. Cell physiology* **281**, C166-178, doi:10.1152/ajpcell.2001.281.1.C166 (2001).
- 744 Coffey, R. J. *et al.* Epidermal growth factor receptor activation induces nuclear targeting of cyclooxygenase-2, basolateral release of prostaglandins, and mitogenesis in polarizing colon cancer cells. *Proceedings of the National Academy of Sciences of the United States of America* **94**, 657-662, doi:10.1073/pnas.94.2.657 (1997).
- 745 Schievella, A. R., Regier, M. K., Smith, W. L. & Lin, L. L. Calcium-mediated translocation of cytosolic phospholipase A2 to the nuclear envelope and endoplasmic reticulum. *The Journal of biological chemistry* **270**, 30749-30754 (1995).
- 746 Spencer, A. G., Woods, J. W., Arakawa, T., Singer, II & Smith, W. L. Subcellular localization of prostaglandin endoperoxide H synthases-1 and -2 by immunoelectron microscopy. *The Journal of biological chemistry* **273**, 9886-9893 (1998).
- 747 D'Santos, C. S., Clarke, J. H. & Divecha, N. Phospholipid signalling in the nucleus. Een DAG uit het leven van de inositide signalering in de nucleus. *Biochimica et biophysica acta* **1436**, 201-232 (1998).
- 748 Ueno, N. *et al.* Coupling between cyclooxygenase, terminal prostanoid synthase, and phospholipase A2. *The Journal of biological chemistry* **276**, 34918-34927, doi:10.1074/jbc.M100429200 (2001).
- 749 Baron, M. An overview of the Notch signalling pathway. *Seminars in cell & developmental biology* **14**, 113-119 (2003).
- 750 Artavanis-Tsakonas, S., Rand, M. D. & Lake, R. J. Notch signaling: cell fate control and signal integration in development. *Science* **284**, 770-776 (1999).
- 751 Hasson, P. *et al.* EGFR signaling attenuates Groucho-dependent repression to antagonize Notch transcriptional output. *Nature genetics* **37**, 101-105, doi:10.1038/ng1486 (2005).

- 752 San Roman, A. K., Jayewickreme, C. D., Murtaugh, L. C. & Shivdasani, R. A. Wnt secretion from epithelial cells and subepithelial myofibroblasts is not required in the mouse intestinal stem cell niche in vivo. *Stem cell reports* **2**, 127-134, doi:10.1016/j.stemcr.2013.12.012 (2014).
- 753 East, J. E., Vieth, M. & Rex, D. K. Serrated lesions in colorectal cancer screening: detection, resection, pathology and surveillance. *Gut* **64**, 991-1000, doi:10.1136/gutjnl-2014-309041 (2015).
- 754 Levine, J. S. & Ahnen, D. J. Clinical practice. Adenomatous polyps of the colon. *The New England journal of medicine* **355**, 2551-2557, doi:10.1056/NEJMcp063038 (2006).
- 755 Snover, D. C. Update on the serrated pathway to colorectal carcinoma. *Human pathology* **42**, 1-10, doi:10.1016/j.humpath.2010.06.002 (2011).
- 756 Ringner, M. What is principal component analysis? *Nature biotechnology* **26**, 303-304, doi:10.1038/nbt0308-303 (2008).
- 757 Thomas, A., Charbonneau, J. L., Fournaise, E. & Chaurand, P. Sublimation of new matrix candidates for high spatial resolution imaging mass spectrometry of lipids: enhanced information in both positive and negative polarities after 1,5-diaminonaphthalene deposition. *Analytical chemistry* **84**, 2048-2054, doi:10.1021/ac2033547 (2012).
- 758 Xiong, X. *et al.* Data processing for 3D mass spectrometry imaging. *Journal of the American Society for Mass Spectrometry* **23**, 1147-1156, doi:10.1007/s13361-012-0361-7 (2012).
- 759 Fernandez, R. *et al.* Optimized Protocol To Analyze Changes in the Lipidome of Xenografts after Treatment with 2-Hydroxyoleic Acid. *Analytical chemistry* **88**, 1022-1029, doi:10.1021/acs.analchem.5b03978 (2016).
- 760 Liebisch, G., Lieser, B., Rathenberg, J., Drobnik, W. & Schmitz, G. High-throughput quantification of phosphatidylcholine and sphingomyelin by electrospray ionization tandem mass spectrometry coupled with isotope correction algorithm. *Biochim Biophys Acta* **1686**, 108-117 (2004).
- 761 Liebisch, G. *et al.* High throughput quantification of cholesterol and cholesteryl ester by electrospray ionization tandem mass spectrometry (ESI-MS/MS). *Biochimica et biophysica acta* **1761**, 121-128, doi:10.1016/j.bbalip.2005.12.007 (2006).
- 762 Liebisch, G., Drobnik, W., Lieser, B. & Schmitz, G. High-throughput quantification of lysophosphatidylcholine by electrospray ionization tandem mass spectrometry. *Clinical chemistry* **48**, 2217-2224 (2002).
- 763 Matyash, V., Liebisch, G., Kurzchalia, T. V., Shevchenko, A. & Schwudke, D. Lipid extraction by methyl-tert-butyl ether for high-throughput lipidomics. *Journal of lipid research* **49**, 1137-1146, doi:10.1194/jlr.D700041-JLR200 (2008).
- 764 Zemski Berry, K. A. & Murphy, R. C. Electrospray ionization tandem mass spectrometry of glycerophosphoethanolamine plasmalogen phospholipids. *Journal of the American Society for Mass Spectrometry* **15**, 1499-1508, doi:10.1016/j.jasms.2004.07.009 (2004).
- 765 Liebisch, G. *et al.* Quantitative measurement of different ceramide species from crude cellular extracts by electrospray ionization tandem mass spectrometry (ESI-MS/MS). *J Lipid Res* **40**, 1539-1546 (1999).
- 766 Horing, M., Ejsing, C. S., Hermansson, M. & Liebisch, G. Quantification of Cholesterol and Cholesteryl Ester by Direct Flow Injection High-Resolution Fourier Transform Mass Spectrometry Utilizing Species-Specific Response Factors. *Analytical chemistry* **91**, 3459-3466, doi:10.1021/acs.analchem.8b05013 (2019).
- 767 Husen, P. *et al.* Analysis of lipid experiments (ALEX): a software framework for analysis of high-resolution shotgun lipidomics data. *PloS one* **8**, e79736, doi:10.1371/journal.pone.0079736 (2013).

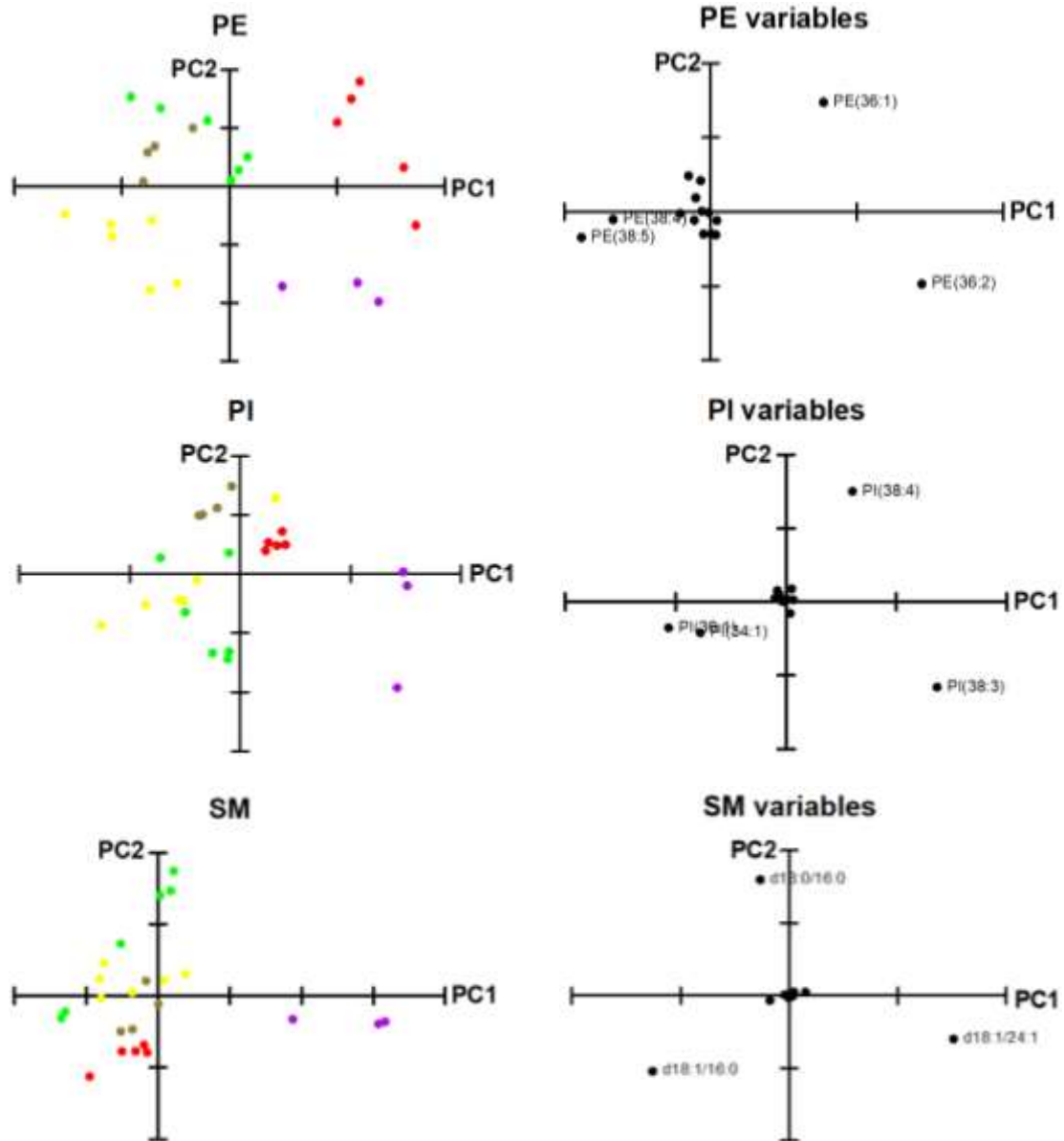
- 768 Sato, T. *et al.* Single Lgr5 stem cells build crypt-villus structures in vitro without a
mesenchymal niche. *Nature* **459**, 262-265, doi:10.1038/nature07935 (2009).
- 769 Yiben Gu, J. F., Pang-Kuo Lo, Shunqi Wang, Qian Wang, Hexin Chen. The effect of B27
supplement on promoting in vitro propagation of Her2/neu-transformed mammary
tumorspheres. *Journal of Biotech Research* **3**, 13 (2011).
- 770 Bottenstein, J. E. & Sato, G. H. Growth of a rat neuroblastoma cell line in serum-free
supplemented medium. *Proc Natl Acad Sci U S A* **76**, 514-517 (1979).
- 771 Zhang, F., Lau, S. S. & Monks, T. J. The cytoprotective effect of N-acetyl-L-cysteine
against ROS-induced cytotoxicity is independent of its ability to enhance glutathione
synthesis. *Toxicological sciences : an official journal of the Society of Toxicology* **120**,
87-97, doi:10.1093/toxsci/kfq364 (2011).
- 772 Vistica, D. T. *et al.* Tetrazolium-based assays for cellular viability: a critical examination
of selected parameters affecting formazan production. *Cancer research* **51**, 2515-2520
(1991).
- 773 Slater, T. F., Sawyer, B. & Straeuli, U. Studies on Succinate-Tetrazolium Reductase
Systems. Iii. Points of Coupling of Four Different Tetrazolium Salts. *Biochimica et
biophysica acta* **77**, 383-393, doi:10.1016/0006-3002(63)90513-4 (1963).
- 774 Taylor, S. C., Laperriere, G. & Germain, H. Droplet Digital PCR versus qPCR for gene
expression analysis with low abundant targets: from variable nonsense to publication
quality data. *Scientific reports* **7**, 2409, doi:10.1038/s41598-017-02217-x (2017).

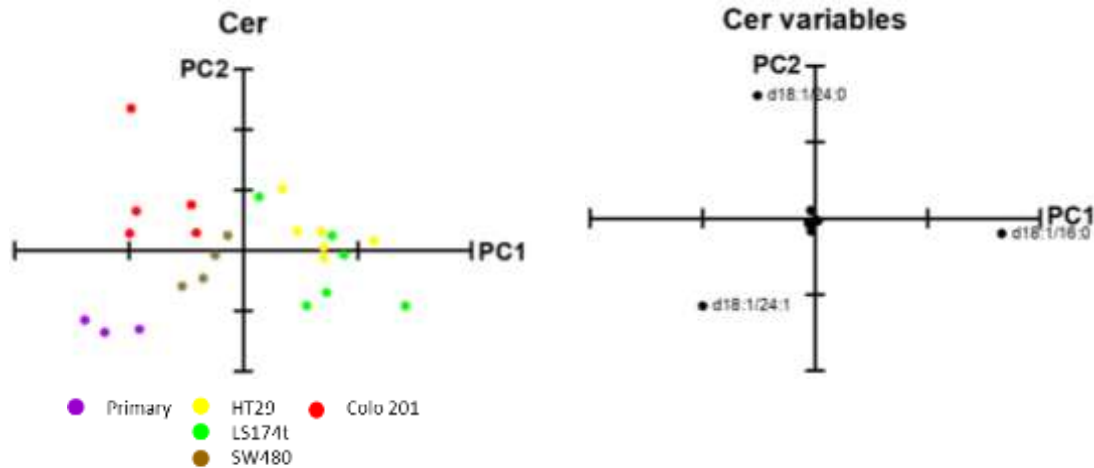
SUPPLEMENTAL MATERIAL

8 Supplemental material

3.1.1 Lipid markers for cellular malignization in cell culture model

PCA





Supplemental figure 1: PCA of each molecular lipid class separates the primary from the cancer cells. The analysis was made with the contribution in percentage of each molecule to the total amount of the family. Explained variances: PE 65.9%, PI 87.5%, SM 90.6%, Cer 96.4%. Only the most influential variables are indicated at each PCA variables graph. ● Primary, ● HT29, ● LS174t, ● SW480 and ● Colo201 cell lines.

Supplemental table 1

	Prim		HT29		LS174t		SW480		Colo 201	
Lipid classes										
	Mean	SD	Mean	SD	Mean	SD	Mean	SD	Mean	SD
PC	44.9	4.8	50.4 _a	2.9	49.2	0.7	53.6 _{aaa}	1.6	53.6 _{aaa}	1.2
SM	11.1	2.1	7.2 _{aa}	1.0	9.0	1.6	6.0 _{aaa c}	0.6	7.8 _a	0.9
Cer	1.4	0.7	1.8	0.5	1.2	0.2	1.5	0.2	0.6 _{bbb d}	0.0
PE	25.1	3.4	8.2 _{aaa}	1.3	11.7 _{aaa bb}	1.3	10.8 _{aaa}	0.7	11.6 _{aaa b}	1.0
PE-P	5.4	0.6	18.5 _{aaa}	1.4	14.8 _{aaa bbb}	0.9	13.4 _{aaa bbb}	1.1	13.9 _{aaa bbb}	1.0
PI	4.8	0.6	7.5 _{aaa}	1.1	5.6 _{bb}	0.8	6.4	0.6	5.4 _{bb}	0.4
PS	7.4	0.2	6.4	2.2	8.5	0.8	8.4	1.9	7.1	0.9

Supplemental table 1: Comprehensive lipidome analysis of Primary, HT29, LS174t, SW4380 and Colo 201 cells. Statistical significance was assessed using ANOVA followed by Bonferroni post-test analysis. a $P < 0.05$, aa $P < 0.01$, aaa $P < 0.001$, Primary vs HT29; b $P < 0.05$, bb $P < 0.01$, bbb $P < 0.001$, Primary vs LS174t; c $P < 0.05$, cc $P < 0.01$, ccc $P < 0.001$, Primary vs SW480; d $P < 0.05$, dd $P < 0.01$, ddd $P < 0.001$, Primary vs Colo 201.

Supplemental table 2

	Prim	HT29	LS174t	SE480	Colo 201
Lipid molecular species					
PC					

8. Supplemental material

	Mean	SD	Mean	SD	Mean	SD	Mean	SD	Mean	SD
32:0	6.3	1.0	9.5 aa	1.8	6.7 bb	0.3	3.8 a bbb c	0.7	5.3 bbb	0.4
34:2	13.1	3.4	10.0 a	1.0	7.1 aaa b	0.9	6.8 aaa b	0.3	7.9 aaa	0.5
34:1	34.7	0.8	39.1 a	2.8	43.6 aaa bb	1.9	51.0 aaa bb ccc	1.2	42.1 aaa ddd	1.4
36:4	1.5	0.1	2.8	1.2	1.9	0.6	2.3	0.2	0.7 bbb c d	0.1
36:3	5.5	1.0	4.2 aa	0.6	3.5 aaa	0.3	2.9 aaa bb	0.2	2.7 aaa bbb c	0.1
36:2	21.8	1.7	16.6 a	2.8	17.0	2.0	13.9 aa	1.2	27.3 a bbb ccc ddd	3.1
36:1	7.4	0.4	7.1	0.7	8.7	1.1	9.2	0.8	9.2	2.2
38:6	0.1	0.0	1.8 aaa	0.6	1.3 aa	0.3	1.5 aaa	0.1	0.5 bbb c dd	0.1
38:5	1.0	0.2	2.7 a	1.1	2.2	0.5	2.7 a	0.3	1.0 bb dd	0.2
38:4	4.1	0.6	2.3 a	1.3	2.8	0.5	2.1 a	0.2	0.7 aaa b cc	0.1
38:3	3.0	0.4	1.5 aaa	0.5	2.4 bb	0.4	1.4 aaa c	0.2	1.1 aaa ccc	0.2
40:7	0.1	0.0	0.6 aaa	0.1	0.5 aaa	0.1	0.5 aaa	0.0	0.3 aaa bbb d	0.0
40:6	0.2	0.0	1.0 a	0.5	0.9 a	0.3	0.8	0.1	0.4 b	0.2
40:5	0.5	0.0	0.9	0.4	1.0	0.3	1.0	0.1	0.6	0.1
40:4	0.8	0.1	0.2 aaa	0.1	0.3 aaa	0.1	0.2 aaa	0.1	0.2 aaa c	0.0
PE										
32:0	0.3	0.2	0.5	0.2	0.5	0.2	0.3	0.0	0.3	0.1
34:2	4.2	1.1	4.1	1.0	2.5 a bb	0.6	1.9 aa bbb	0.3	2.7 b	0.3
34:1	13.0	1.8	16.0	1.7	14.8	1.6	13.0 b	1.2	14.8	0.8
36:4	0.7	0.1	2.0 aaa	0.3	0.8 bbb	0.1	1.0 bbb	0.2	0.2 bbb cc ddd	0.1
36:3	4.9	1.5	4.8	0.9	2.1 aaa bbb	0.6	3.2 b	0.5	3.0 a bb	0.2
36:2	34.4	5.3	19.9 aa	3.8	19.7 aaa	4.5	17.9 aaa	0.8	32.1 bb cc ddd	5.4
36:1	14.1	2.2	9.9	2.0	18.0 bbb	1.1	16.7 bbb	1.7	25.5 aaa bbb	3.4

									ccc ddd	
38:5	3.1	0.3	15.1 aaa	2.9	6.6 bbb	1.3	10.1 aaa bb	1.9	3.7 bbb ddd	0.7
38:4	8.9	0.5	12.7 aa	1.7	12.5 a	1.3	14.3 aaa	1.8	4.7 aa bbb ccc ddd	1.0
38:3	10.6	0.9	3.7 aaa	1.1	6.3 aa b	2.0	5.3 aaa	0.6	2.5 aaa ccc d	0.5
40:7	0.3	0.1	3.0 aaa	0.1	2.9 aaa	0.7	3.0 aaa	0.1	2.7 aaa	0.4
40:6	0.5	0.1	3.5 aa	0.9	6.2 aaa bb	1.7	4.8 aaa	0.7	4.1 aa c	0.6
40:5	1.3	0.3	1.4	0.4	4.4 aaa bbb	1.4	4.2 aa bbb	0.5	2.7 c	0.5
40:4	3.4	1.6	0.2 aaa	0.2	1.0 aaa	0.5	1.4 aa b	0.3	0.3 aaa	0.1
PI										
34:2	0.7	0.4	1.3	0.3	1.7 a	0.3	1.6 a	0.5	1.9 aa	0.3
34:1	0.9	0.8	14.6 aaa	4.9	15.6 aaa	2.2	9.8 aa c	1.2	5.1 bbb ccc	0.4
36:4	0.6	0.1	1.8 a	0.5	1.8 a	0.9	2.5 aa	0.0	1.2 d	0.1
36:3	4.1	1.2	2.8	0.4	4.2 b	0.9	2.1 aa ccc	0.4	3.0	0.4
36:2	7.9	3.4	7.5	1.3	11.2 b	1.5	9.9	1.4	16.2 aaa bbb cc ddd	1.8
36:1	1.5	1.5	23.6 aaa	7.0	17.4 aaa	2.0	16.2 aaa	1.7	9.6 bbb c	0.9
38:6	0.1	0.0	0.7 aa	0.2	0.6 a	0.4	0.6 a	0.0	0.2 b	0.1
38:5	3.9	2.1	2.9	0.7	2.7	1.1	4.1	0.3	4.3	0.4
38:4	27.8	9.7	20.1	9.5	15.9	5.4	30.7 c	3.0	27.5	1.8
38:3	47.9	4.8	17.8 aaa	3.7	22.4 aaa	7.7	13.2 aaa c	1.0	23.3 aaa d	1.3
40:7	0.2	0.0	0.3	0.1	0.2	0.1	0.5 a cc	0.1	0.4 A cc	0.1
40:6	0.5	0.1	3.1 aaa	0.6	2.4 aa	1.2	2.1 a	0.2	2.3 aa	0.1
40:5	1.3	0.1	2.8 a	0.6	2.8 a	1.1	4.5 aaa bb cc	0.3	3.2 aa	0.3
40:4	2.6	0.1	0.7 aaa	0.4	1.2 aaa	0.2	2.1 bbb cc	0.5	1.6 aa bb	0.3
PS										
32:0	0.1	0.1	0.1	0.0	0.1	0.0	0.0 a	0.0	0.0 a	0.0
34:2	1.9	0.6	2.1	0.5	0.8 aa bbb	0.3	0.4 aaa bbb	0.1	0.7 aa bbb	0.2
34:1	10.0	1.9	16.7 aaa	2.3	7.6 bbb	1.4	6.9 bbb	0.6	7.8 bbb	0.6

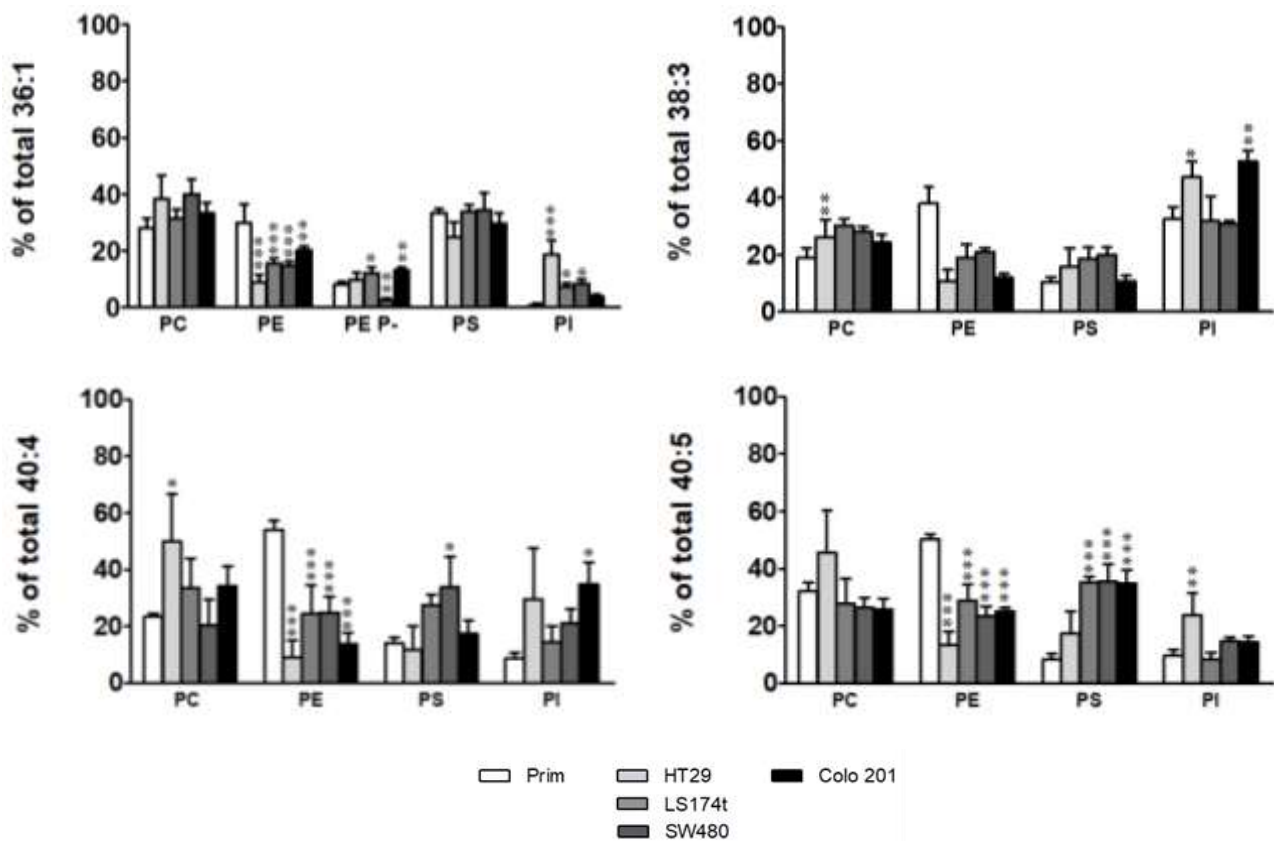
8. Supplemental material

36:4	0.2	0.0	0.6 aaa	0.1	0.1 aaa bbb	0.0	0.1 aa bbb	0.0	0.0 aaa bbb	0.0
36:3	1.5	0.2	2.9 aaa	0.1	0.4 aaa bbb	0.2	0.4 aaa bbb	0.2	0.4 aaa bbb	0.1
36:2	15.3	0.6	16.4	1.8	7.8 aaa bbb	1.9	9.7 aa bbb	0.8	11.1 a bbb c	1.7
36:1	53.7	2.0	38.0 aaa	2.2	54.2 bbb	2.3	51.0 bbb	2.3	60.5 aa bbb ccc ddd	0.4
38:6	0.0	0.0	0.2	0.2	0.1	0.1	0.2	0.0	0.0 b	0.0
38:5	0.4	0.0	2.5 aaa	1.0	0.4 bbb	0.1	0.8 bbb	0.2	0.2 bbb	0.1
38:4	3.2	0.1	6.0 a	2.1	2.6 bbb	0.4	3.2 bb	0.7	1.4 bbb	0.1
38:3	9.9	1.1	6.8 aa	1.1	8.2	1.1	6.6 aa	1.0	3.7 aaa bbb ccc dd	0.5
40:7	0.0	0.0	0.2 a	0.1	0.2 aa	0.0	0.4 aaa b c	0.1	0.4 aaa b	0.0
40:6	0.2	0.1	4.8 aaa	1.1	8.5 aaa bbb	2.2	9.5 aaa bbb	0.4	7.1 aaa	0.8
40:5	0.7	0.2	2.4	0.6	7.3 aaa bbb	1.4	8.4 aaa bbb	0.5	6.1 aaa bbb dd	0.8
SM										
d18:1/16:0	36.8	3.3	51.3 a	4.7	51.2 a	9.9	53.2 a	3.0	58.2 aa	3.8
d18:0/16:0	2.5	0.1	9.1	2.5	16.5 aaa bb	5.4	6.2 ccc	2.6	2.2 b ccc	0.2
d18:1/18:1	0.6	0.2	1.2 a	0.5	0.7 b	0.2	1.6 aa cc	0.1	1.0	0.2
d18:1/18:0	3.3	0.7	4.6	2.0	2.7	0.9	5.9 cc	0.7	3.7	0.3
d18:1/20:0	1.1	0.0	2.8 aa	0.8	1.8	0.7	1.9	0.2	2.6 a	0.4
d18:1/22:1	2.7	1.0	2.9	0.8	2.0	0.8	2.7	0.4	2.0	0.5
d18:1/22:0	6.8	0.5	5.7	1.2	4.6 a	1.1	4.7	0.7	4.8	1.2
d18:1/24:1	36.5	6.8	9.5 aaa	2.5	9.7 aaa	2.1	12.4 aaa	1.0	13.6 aaa	1.5
d18:1/24:0	7.0	0.8	7.7	0.9	6.0	1.2	5.4 b	0.7	6.8	1.4
d18:1/26:1	0.9	0.1	0.3 aaa	0.0	0.4 aaa	0.1	0.2 aaa	0.1	0.3 aaa	0.0
d18:1/26:0	0.2	0.1	0.3	0.1	0.3	0.1	0.1 bb cc	0.0	0.2	0.1
d16:1/18:1	1.7	0.6	4.7 aa	0.7	4.0 a	1.0	5.8 aaa c	0.4	4.6 aa	1.2
Ceramides										
d18:1/16:0	38.2	3.3	53.4 a	5.4	56.2 aa	7.9	38.2 bb ccc	2.5	30.3 bbb ccc	5.7
d18:1/18:0	1.6	0.1	2.7	0.9	1.1 bb	0.5	3.1 a ccc	0.4	0.8 bbb ddd	0.3

d18:1/20:0	0.6	0.0	1.7	2.7	0.4	0.2	0.3	0.1	0.2	0.1
d18:1/22:1	0.5	0.0	0.2	0.1	0.3	0.1	0.1 a	0.0	0.2	0.3
d18:1/22:0	6.2	0.6	6.3	1.3	5.9	1.9	6.8	1.0	4.6	1.4
d18:1/24:1	26.7	1.8	10.9 aaa	1.8	14.6 aaa	3.2	24.7 bbb cc	3.9	23.5 bbb cc	4.8
d18:1/24:0	24.8	3.2	24.3	4.0	20.3	7.1	25.9	2.2	37.2 a bb ccc d	7.4
d18:1/26:1	0.8	0.1	0.2 aa	0.0	0.2 aa	0.2	0.2 aa	0.1	0.8 bbb cc dd	0.3
d18:1/26:0	0.5	0.1	0.7	0.6	1.4	1.1	0.8	0.6	2.5 b	1.4

Supplemental table 2: Comprehensive lipidome analysis of Primary, HT29, LS174t, SW4380 and Colo 201 cells. Statistical significance was assessed using ANOVA followed by Bonferroni post-test analysis. a P < 0.05, aa P < 0.01, aaa P < 0.001, Primary vs HT29; b P < 0.05, bb P < 0.01, bbb P < 0.001, Primary vs LS174t; c P < 0.05, cc P < 0.01, ccc P < 0.001, Primary vs SW480; d P < 0.05, dd P < 0.01, ddd P < 0.001, Primary vs Colo 201.

Supplemental figure 2



Supplementary figure 2: Lipid distribution of species decreasing in PE. Total percentage of each fatty acid combination detected was calculated. The contribution of each lipid class to the total amount of fatty acid combination was calculated in order to evaluate how much is accumulated in each lipid class compared to the others. Values are expressed as percentage of total fatty acid (mole %) and represent mean \pm SD, n=3-6. **Statistical significance was assessed using one way ANOVA followed by Bonferroni post-test. Only significance respect primary cells are expressed.** * P<0.05; ** P<0.01; *** P<0.001.

3.1.2 Lipid markers for cellular malignization in human tissue

Supplementary table 3

Segment	% of total RI		
	Healthy epithelium		Adenoma
	Apical	Basal	
Assigned lipid species	Mean \pm SD	Mean \pm SD	Mean \pm SD
PI			
34:2	8.9 \pm 1.1	7.6 \pm 1.2	6.3 \pm 1.9
34:1	16.3 \pm 2.1	12.7 \pm 1.5	12.5 \pm 3.3
36:4	2.8 \pm 0.8 &	4.2 \pm 1.0	4.9 \pm 0.5
36:3	4.8 \pm 1.2	5.4 \pm 1.2	3.3 \pm 1.0
36:2	27.8 \pm 4.9 &	23.0 \pm 4.15	17.6 \pm 3.9
36:1	18.7 \pm 0.3 *,&	11.5 \pm 1.4	11.2 \pm 3.7
38:6	0.8 \pm 0.1	0.7 \pm 0.1	0.4 \pm 0.3
38:5	1.7 \pm 0.5	2.8 \pm 0.2	2.5 \pm 0.6
38:4	17.4 \pm 2.9 &	31.2 \pm 2.0	40.3 \pm 11.0
40:4	0.7 \pm 0.3	1.1 \pm 0.2	0.9 \pm 0.8
PE			
34:2	2.2 \pm 0.1	2.2 \pm 0.2	1.3 \pm 1.0
34:1	7.1 \pm 0.8	5.8 \pm 0.8	5.7 \pm 0.8
34:0	0.00 \pm 0.00	1.2 \pm 1.1	1.1 \pm 1.4
36:4	1.2 \pm 0.3	1.4 \pm 0.2	1.0 \pm 0.6
36:3	7.5 \pm 0.3 &&	8.2 \pm 0.5 ++	4.0 \pm 1.5
36:2	26.3 \pm 2.1	25.0 \pm 1.8	23.9 \pm 2.9
36:1	25.8 \pm 1.4	23.2 \pm 2.0	31.0 \pm 5.8
36:0	1.6 \pm 1.4	1.5 \pm 1.3	1.2 \pm 1.2
38:6	0.2 \pm 0.4	0.2 \pm 0.3	0.7 \pm 0.5
38:5	2.2 \pm 0.6	2.6 \pm 0.5	2.9 \pm 1.4
38:4	5.7 \pm 0.5	7.8 \pm 0.2	8.2 \pm 2.4
38:3	7.9 \pm 0.8	8.1 \pm 1.0	6.7 \pm 1.6
38:2	9.8 \pm 0.1	9.4 \pm 0.1	8.0 \pm 1.3
38:1	1.5 \pm 1.3	1.4 \pm 1.3	2.4 \pm 0.7
40:5	0.6 \pm 0.4	0.9 \pm 0.3	0.9 \pm 0.6
40:4	0.4 \pm 0.3	1.0 \pm 0.1	0.9 \pm 0.6
PC			
32:0	3.2 \pm 1.4 *	5,9 \pm 1,0 †	3.3 \pm 0.6
32:1	1.1 \pm 0.5	1,4 \pm 0,3	0.9 \pm 0.1

34:0	3.2 ± 0.5	2,4 ± 0,6 ++	4.6 ± 0.6
34:1	36.1 ± 2.8 &	31,9 ± 0,3 ++	47.1 ± 4.9
34:2	16.3 ± 3.8	17,4 ± 3,3	14.3 ± 2.3
34:3	1.3 ± 0.3 &	1,5 ± 0,2 ++	0.7 ± 0.1
36:0	0.4 ± 0.1	0,2 ± 0,1	0.4 ± 0.1
36:1	5.5 ± 0.3	4,5 ± 0,4	5.8 ± 1.3
36:2	17.1 ± 1.1	16,5 ± 1,0	12.7 ± 2.6
36:3	10.1 ± 1.9 &	10,8 ± 0,5 ++	5.6 ± 1.2
36:4	2.9 ± 0.6	3,9 ± 0,4	2.6 ± 1.4
36:5	0.2 ± 0.2	0,2 ± 0,1	0.1 ± 0.2
38:2	0.3 ± 0.3	0,2 ± 0,1	0.0 ± 0.0
38:3	0.4 ± 0.3	0,5 ± 0,4	0.2 ± 0.1
38:4	1.0 ± 0.4	1,4 ± 0,3	1.0 ± 0.8
38:5	0.6 ± 0.3	0,8 ± 0,4	0.5 ± 0.6
38:6	0.2 ± 0.2	0,2 ± 0,1	0.1 ± 0.2
40:5	0.01 ± 0.01	0,0 ± 0,1	0.0 ± 0.0
40:6	0.04 ± 0.02	0,2 ± 0,1	0.0 ± 0.0
PE plasmalogens			
PE P- 16:0/18:2	7.7 ± 1.3 &&	7.3 ± 1.4 ++	2.5 ± 1.8
PE P- 16:0/18:1	13.6 ± 1.7	11.6 ± 0.9	9.2 ± 3.3
PE P- 16:0/20:4	10.9 ± 1.1 &	14.4 ± 1.0	15.0 ± 2.2
PE P- 16:0/20:3, PE P- 18:1/18:2	5.4 ± 0.6 &&&	5.4 ± 1.0 +++	2.1 ± 0.2
PE P- 18:0/18:2, PE P- 18:1/18:1, PC P- 16:0/18:2	14.7 ± 2.9 &&&	11.8 ± 2.0 +	6.5 ± 2.0
PE P- 18:0/18:1, PC P- 16:0/18:1	11.1 ± 0.7 *,&&	8.1 ± 0.2	7.4 ± 1.5
PE P- 16:0/22:6	4.0 ± 0.9 &	4.0 ± 0.7 +	7.2 ± 1.5
PE P- 18:1/20:4, PE P- 16:0/22:5, PE P- 18:0/20:5	6.8 ± 1.5	8.2 ± 1.6	7.7 ± 1.0
PE P- 18:0/20:4, PE P- 16:0/22:4	16.0 ± 1.5	18.6 ± 0.7	25.5 ± 6.3
PE P- 40:7	0.9 ± 0.8	0.7 ± 0.7	1.3 ± 0.6
PE P- 18:0/22:6, PE P- 18:1/22:5, PC P- 16:0/22:6	4.5 ± 0.9	3.9 ± 0.6	8.8 ± 2.8
PE P- 18:0/22:5, PC P- 16:0/22:5	1.9 ± 0.5	2.3 ± 0.5	2.6 ± 0.5
PE P- 20:0/20:4, PE P- 18:0/22:4, PC P- 18:0/20:4	2.5 ± 0.4	3.7 ± 0.4	4.1 ± 1.5
Supplementary table 3: Comprehensive lipidome of colon epithelial clusters. All possible plasmalogen species assignments are indicated, although the most probable is marked in bold. Values are expressed as mean±SD, n=3-5. Statistical significance was assessed using ANOVA followed by Bonferroni post-test analysis. * P < 0.05, ** P < 0.01, apical vs. basal, & P < 0.05, && P < 0.01 apical vs. AD, and † P < 0.05, †† P < 0.001 basal vs. AD.			

Supplementary table 4

Lamina Propria	% of total RI			
	Healthy LP			Adenoma
	Apical	Central	Basal	
PI	Mean ± SD	Mean ± SD	Mean ± SD	Mean ± SD
34:2	0.3 ± 0.1	0.9 ± 0.1	1.6 ± 0.5	1.4 ± 1.2
34:1	1.2 ± 0.3	2.3 ± 0.2	3.5 ± 0.8	3.8 ± 3.3
36:4	2.1 ± 0.4 &&	2.2 ± 0.3 _§	2.3 ± 0.1	2.8 ± 0.3
36:3	0.7 ± 0.1 **	1.2 ± 0.1	2.2 ± 0.7	1.3 ± 0.7
36:2	4.1 ± 0.6 **	6.0 ± 1.1	11.1 ± 5.1	6.5 ± 2.6
36:1	2.3 ± 0.5	3.4 ± 0.6	5.7 ± 3.3	4.2 ± 3.1
38:5	3.4 ± 0.3	3.8 ± 0.6	3.7 ± 0.6	4.7 ± 1.7
38:4	68.0 ± 3.2	63.0 ± 2.4	53.4 ± 8.2	55.1 ± 11.4
38:3	13.2 ± 2.9	11.6 ± 3.3	8.7 ± 3.4	11.4 ± 1.1
40:6	1.4 ± 0.9	1.9 ± 1.1	3.1 ± 1.7	2.8 ± 1.2
40:5	1.8 ± 0.9	2.6 ± 1.4	3.6 ± 2.1	4.8 ± 2.6
40:4	1.4 ± 0.2	1.0 ± 0.6	1.1 ± 0.3	1.1 ± 0.8
PE				
34:1	3.2 ± 0.8 &&	4.2 ± 0.7	4.5 ± 1.1	5.2 ± 0.6
34:0	5.7 ± 0.4	5.5 ± 0.3	5.1 ± 0.3	6.1 ± 3.1
36:4	3.4 ± 0.6	2.7 ± 0.6	1.8 ± 0.4	1.2 ± 1.4
36:3	2.1 ± 0.9	2.8 ± 0.3	3.9 ± 1.5	1.5 ± 1.7
36:2	13.9 ± 1.8 *	16.7 ± 1.5	22.7 ± 4.4	17.2 ± 4.6
36:1	18.1 ± 2.2	21.6 ± 2.7	23.5 ± 4.3	24.9 ± 7.9
38:5	7.4 ± 0.8 *	5.4 ± 0.8	3.6 ± 0.7	5.9 ± 2.3
38:4	34.6 ± 1.5 *	29.2 ± 2.0	22.3 ± 2.8	26.6 ± 8.1
38:2	6.0 ± 0.7 ***	7.5 ± 0.9 €	9.8 ± 1.1 +++	6.5 ± 0.9
40:5	5.7 ± 0.6	4.4 ± 0.6	2.8 ± 0.5	4.9 ± 2.2
PC				
32:0	12.9 ± 1.6		11.7 ± 1.9	11.3 ± 5.7
32:1	1.6 ± 0.1		1.8 ± 0.1	1.7 ± 0.4
34:0	2.4 ± 0.5		2.4 ± 0.5	3.4 ± 0.9
34:1	26.9 ± 1.0 &		29.7 ± 1.9	37.3 ± 7.5
34:2	11.0 ± 2.7		13.4 ± 2.5	12.0 ± 1.6
34:3	0.8 ± 0.3		0.9 ± 0.2	0.6 ± 0.3
36:0	0.3 ± 0.1		0.3 ± 0.1	0.2 ± 0.1
36:1	3.8 ± 0.5		4.9 ± 0.4	4.5 ± 1.2
36:2	10.3 ± 1.1		12.6 ± 0.4	11.1 ± 2.7
36:3	5.8 ± 0.5		6.3 ± 0.5	5.5 ± 0.9
36:4	11.5 ± 2.4		6.7 ± 1.1	6.8 ± 4.7
36:5	0.7 ± 0.2 &&		0.4 ± 0.1	0.2 ± 0.3

38:2	0.1 ± 0.1		0.1 ± 0.1	ND
38:3	0.7 ± 0.7		0.7 ± 0.7	0.3 ± 0.2
38:4	6.4 ± 1.2 &		5.3 ± 0.8	3.1 ± 2.0
38:5	3.8 ± 1.4		2.1 ± 0.8	1.8 ± 1.5
38:6	0.8 ± 0.4 &		0.4 ± 0.2	0.2 ± 0.3
40:5	0.1 ± 0.1		0.1 ± 0.1	ND
40:6	0.1 ± 0.1		0.1 ± 0.1	ND
PE plasmalogens				
16:0/ 18:1	6.3 ± 0.9	7.2 ± 0.5	7.8 ± 0.7	6.4 ± 0.8
16:0/18:2	ND	1.0 ± 0.4	1.4 ± 0.5	0.7 ± 0.6
18:0/18:1, PC P- 16:0/18:1	3.4 ± 1.0	4.0 ± 0.3	4.0 ± 0.6	3.4 ± 1.0
18:0/18:2, PE P- 18:1/18:1, PC P- 16:0/18:2	3.4 ± 1.1	3.4 ± 0.6	4.2 ± 1.0	3.3 ± 0.6
16:0/20:3, PE P- 18:1/18:2	ND	0.7 ± 0.6	1.4 ± 0.7	1.1 ± 0.3
16:0/20:4	18.6 ± 2.0 *, &	20.4 ± 1.2	21.2 ± 2.7	22.7 ± 2.0
18:0/20:4, PE P- 16:0/22:4	28.4 ± 3.8	28.8 ± 3.0	29.5 ± 5.2	26.5 ± 1.3
18:1/20:4, PE P- 16:0/22:5, PE P- 18:0/20:5	13.1 ± 2.4	13.4 ± 2.1	12.3 ± 2.0	13.1 ± 2.1
16:0/22:6	6.5 ± 1.2	5.1 ± 0.9	4.1 ± 1.0 †	6.6 ± 1.4
20:0/20:4, PE P- 18:0/22:4, PC P- 18:0/20:4	7.6 ± 0.5 **, &	6.1 ± 0.7	5.4 ± 1.3	5.7 ± 0.6
18:0/22:5, PC P- 16:0/22:5	5.8 ± 1.0 *	4.3 ± 1.1	3.6 ± 1.4	4.6 ± 0.6
18:0/22:6, PE P- 18:1/22:5, PC P- 16:0/22:6	6.2 ± 0.8 *	4.5 ± 0.7	2.8 ± 2.0 †	5.8 ± 1.1

Supplemental table 4: Comprehensive lipidome of colon lamina propria clusters. All possible plasmalogen species assignments are indicated, although the most probable is marked in bold. Values are expressed as mean±SD, n=3-5. Statistical significance was assessed using ANOVA followed by Bonferroni post-test analysis. * P < 0.05, ** P < 0.01, apical vs. basal, & P < 0.05, && P < 0.01 apical vs. AD, and † P < 0.05, †† P < 0.001 basal vs. AD.

3.1.3 Extracellular vesicles lipids as biomarkers of malignization in cell culture model

Supplemental table 5

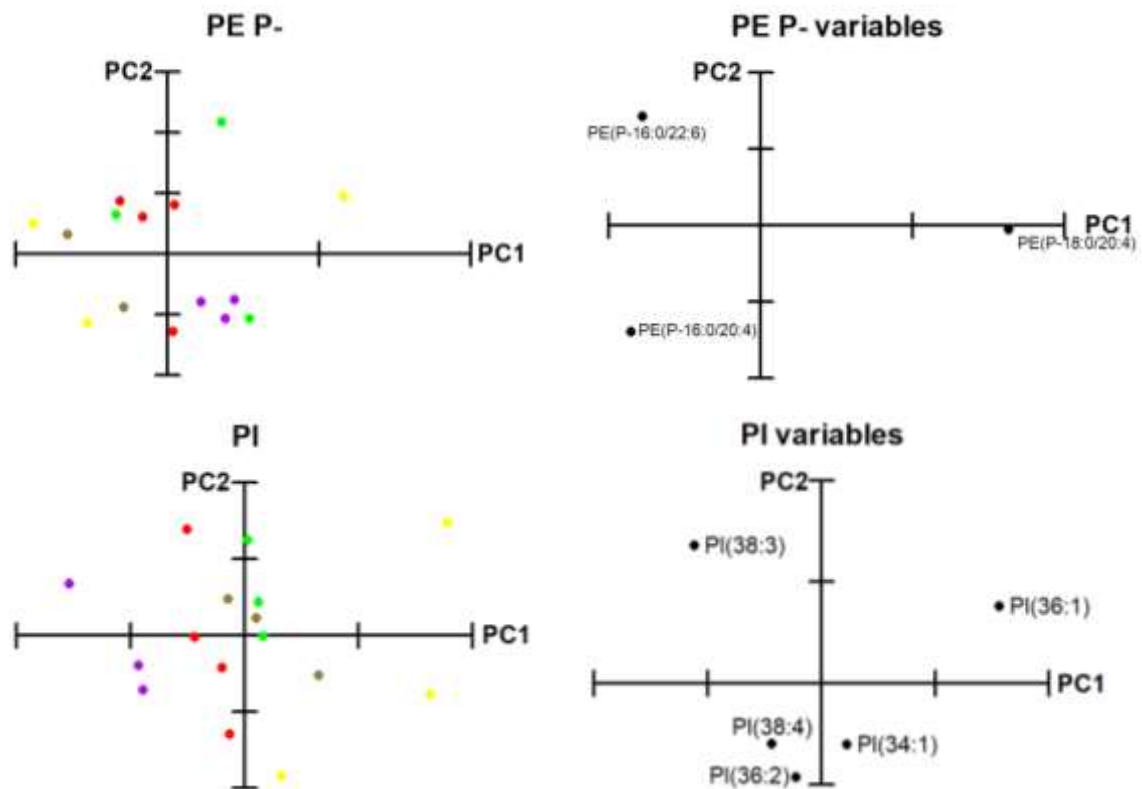
	Prim		HT29		LS174t		SW480		Colo201	
Lipid classes										
	Mean	SD	Mean	SD	Mean	SD	Mean	SD	Mean	SD
PC	29.8	8.0	61.6 _{aa}	1.5	58.4 _{aa}	4.1	60.3 _{aa}	5.8	48.6 _a	9.6

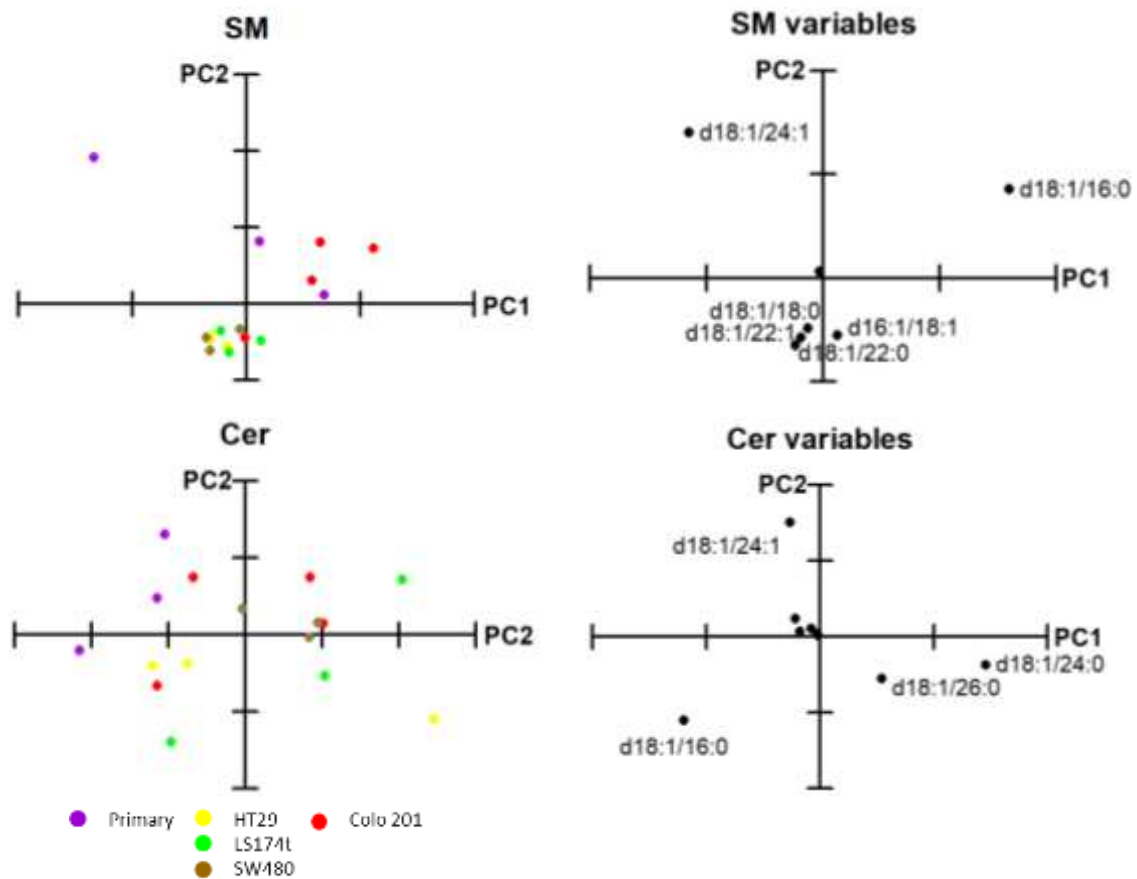
SM	34.8	5.5	34.0	2.7	35.4	2.1	34.0	1.8	28.4	2.8
Cer	3.4	0.5	1.0 aaa	0.3	1.3 aaa	0.6	0.8 aaa	0.4	0.6 aaa	0.2
PE	10.3	2.5	0.9 aaa	0.4	1.3 aaa	0.6	1.3 aaa	0.9	3.3 aaa	1.3
PE P-	6.3	1.2	0.9	0.7	1.1	0.9	1.2	1.7	7.9	5.9
PI	4.1	1.8	0.4 aa	0.2	0.6 aa	0.2	1.1 a	0.9	0.9 aa	0.4
PS	11.3	4.7	1.4 a	0.3	1.9	0.7	1.3 a	1.0	10.3	5.2

Supplemental table 5: Lipid classes analysis of EVs isolated from the supernatant of Primary, HT29, LS174t, SW4380 and Colo 201 cells. Statistical significance was assessed using ANOVA followed by Bonferroni post-test analysis. a P < 0.05, aa P < 0.01, aaa P < 0.001, Primary vs HT29; b P < 0.05, bb P < 0.01, bbb P < 0.001, Primary vs LS174t; c P < 0.05, cc P < 0.01, ccc P < 0.001, Primary vs SW480; d P < 0.05, dd P < 0.01, ddd P < 0.001, Primary vs Colo 201.

Supplemental figure 3

PCA:





Supplemental figure 3: PCA of lipid species analysed in cell culture derived EVs. Only the most influential variables are indicated at each variables PCA analysis. Explained variances: PE plasmalogens 100%, PI 68.6%, SM 76.0%, Cer 57.7%. ● Primary, ● HT29, ● LS174t, ● SW480 and ● Colo201 cell lines.

Supplemental table 6

	Prim		HT29		LS174t		SW480		Colo201	
Lipid molecular species										
PC										
	Mean	SD	Mean	SD	Mean	SD	Mean	SD	Mean	SD
32:0	12.6	5.5	5.6	0.1	5.7	0.6	5.3 A	1.7	7.1	2.2
34:2	12.0	1.3	2.2 Aaa	0.0	2.5 aaa	0.1	2.5 aaa	0.3	2.8 aaa	0.7
34:1	30.5	6.1	28.3	0.6	28.5	0.9	28.4	3.3	34.7	4.3
36:4	1.2	0.3	1.9 A	0.1	2.0 aa	0.0	2.0 aa	0.2	1.7	0.3
36:3	3.6	0.8	2.9	0.2	2.9	0.1	3.1	0.2	2.7	0.4
36:2	19.9	5.8	9.4 Aa	1.9	8.3 aa	0.3	7.8 aa	0.3	9.6 aa	1.9
36:1	11.8	1.7	17.5 aaa	0.8	17.5 aaa	0.4	16.8 aaa	0.3	14.8 a b c	1.0
38:6	0.2	0.0	2.7 aaa	0.1	2.7 aaa	0.1	2.9 aaa	0.4	2.4 aaa	0.6
38:5	0.6	0.1	5.2 aaa	0.2	5.1 aaa	0.2	5.4 aaa	0.8	4.6 aaa	1.0

8. Supplemental material

38:4	3.1	0.7	6.7 aaa	0.2	6.9 aaa	0.3	7.0 aaa	0.9	5.4 A	1.1
38:3	3.0	2.3	6.0	0.3	6.2	0.5	6.4 A	1.1	4.9	1.1
40:7	0.0	0.0	0.6 aaa	0.1	0.6 aaa	0.0	0.7 aaa	0.1	0.5 aaa	0.1
40:6	0.2	0.0	5.3 aaa	0.4	5.0 aaa	0.3	5.7 aaa	1.1	4.1 aaa	1.0
40:5	0.5	0.1	5.2 aaa	0.1	5.4 aaa	0.3	5.5 aaa	0.9	4.2 aaa	0.8
40:4	0.6	0.2	0.6	0.1	0.5	0.0	0.6	0.2	0.5	0.1
PE										
32:0	0.4	0.1	18.3	11.5	8.5	7.3	10.0	7.1	3.3	3.6
34:2	11.6	3.8	9.3	9.9	7.7	2.7	8.3	8.8	2.0	0.6
34:1	10.5	0.8	30.3 aa	5.3	37.1 aaa	1.6	29.8 aa	7.0	24.1 a c	6.0
36:2	37.5	2.9	24.8	8.1	24.0	6.2	26.2	5.8	42.4 b	5.2
36:1	18.5	0.4	23.7	5.2	15.7	3.8	21.0	2.5	21.9	5.0
38:6	0.5	0.3	3.5	3.1	0.5	0.9	0.5	0.8	0.5	0.8
38:5	3.5	0.5	2.2	1.9	1.2	2.0	1.0	1.7	1.8	0.8
38:4	8.0	0.9	5.6	1.5	3.3	1.7	3.3	2.3	3.1 A	0.9
38:3	9.4	1.6	0.5 aaa	0.9	2.0 aaa	2.3	0.0 aaa	0.0	0.9 aaa	0.4
PE plasmalogens										
p16:0/20:4	42.6	3.1	38.4	34.1	25.8	22.5	51.9	6.2	36.5	12.7
p16:0/22:6	6.4	3.5	28.7	18.5	30.6	26.8	31.0	17.3	31.3	16.7
p18:0/20:4	50.9	4.7	32.9	44.4	43.7	19.1	17.2	11.1	32.2	7.2
PS										
34:2	1.7	0.5	0.5 aa	0.1	0.1 aaa	0.1	0.1 aaa	0.1	0.3 aaa	0.2
34:1	9.1	0.8	15.7	3.5	7.2 b	2.5	7.2 b	4.5	7.9 b	1.1
36:3	1.3	0.5	0.4	0.6	0.0 aa	0.1	0.1 a	0.1	0.3 A	0.2
36:2	16.0	1.9	16.3	1.5	6.5 aaa bbb	2.0	9.2 aa bb	2.6	10.8 a b	0.5
36:1	52.6	3.6	54.6	5.1	65.1 aa b	3.0	66.1 aa bb	0.4	65.4 aa bb	2.3
38:5	0.4	0.1	0.5	0.3	0.1	0.1	0.2	0.2	0.1	0.1
38:4	3.2	0.2	5.1	2.0	2.1 b	0.7	3.6	0.8	1.9 bb	0.3
38:3	8.5	1.1	3.9 a	0.8	4.3 a	2.7	4.5 a	1.6	3.8 A	0.5
40:6	0.9	0.7	1.7	1.3	7.4 aaa bbb	2.3	4.2 A	0.7	5.0 aa b	0.3
40:5	1.7	0.1	1.3	0.9	6.8 a bb	2.3	4.5	1.6	4.0	1.5
40:4	4.5	0.8	0.0 aaa	0.1	0.5 aaa	0.3	0.2 aaa	0.2	0.6 aaa	0.3
PI										
34:1	3.5	2.1	9.9	8.6	10.0	1.4	11.3	5.1	7.0	2.4
36:2	11.9	5.3	4.9	4.6	1.1	1.2	4.7	1.7	10.7	9.0

36:1	4.4	3.1	40.4 aa	18.8	24.8	1.1	24.5	3.7	16.6 b	1.7
38:4	36.8	3.3	29.9	12.9	29.4	4.8	29.1	2.5	30.3	2.4
38:3	43.5	8.7	14.9 aa	6.2	34.7	5.7	30.4	7.7	35.4 b	9.0
SM										
d16:1/18:1	1.6	0.5	4.9 aaa	0.1	4.9 aaa	0.8	4.7 aaa	0.2	5.3 aaa	0.8
d18:1/16:0	40.2	6.1	36.8	0.6	38.2	1.5	36.9	1.4	45.4	5.0
d18:0/16:0	6.9	3.2	2.6 a	0.1	3.1 a	0.2	2.6 a	0.3	2.4 aa	0.2
d18:1/18:1	1.6	0.7	2.3	0.1	2.3	0.2	2.4	0.3	1.7	0.3
d18:1/18:0	7.0	1.2	7.8	0.4	7.8	0.1	7.9	0.8	5.9	1.3
d18:1/20:0	1.7	0.0	3.1 aa	0.2	3.0 aa	0.3	3.0 aa	0.2	2.2	0.6
d18:1/22:1	2.9	0.4	5.3 a	0.4	5.3 a	0.3	5.4 aa	0.5	3.4 b c d	1.2
d18:1/22:0	7.4	0.6	10.8 aaa	0.4	10.3 aa	0.4	10.2 aa	0.3	8.3 bb c d	1.0
d18:1/24:1	23.2	9.7	19.1	0.7	18.0	1.1	19.0	0.7	17.4	1.1
d18:1/24:0	6.6	0.8	7.0	0.4	6.8	0.2	7.4	0.6	7.4	0.8
d18:1/26:1	0.6	0.2	0.2	0.1	0.3	0.1	0.4	0.3	0.5	0.3
d18:1/26:0	0.1	0.0	0.1	0.1	0.1	0.0	0.1	0.1	0.1	0.1
Ceramides										
d18:1/16:0	39.9	7.5	37.4	10.9	33.2	15.6	30.7	2.5	36.4	10.5
d18:1/18:0	11.3	1.5	5.1	5.1	1.3 aa	1.6	1.5 aa	2.1	2.3 aa	2.0
d18:1/22:0	12.2	1.2	9.1	5.6	8.1	4.6	12.0	2.1	7.7	2.3
d18:1/24:1	18.4	6.3	8.6	7.5	11.0	7.7	14.3	0.8	18.2	4.5
d18:1/24:0	16.5	3.3	32.1	15.6	34.3	9.5	32.9	3.3	31.7	6.5
d18:1/26:0	1.6	0.7	7.7	3.3	12.0	6.2	8.6	3.9	3.8	4.3

Supplemental table 6: Comprehensive lipidome analysis of EVs isolated from the supernatant of Primary, HT29, LS174t, SW4380 and Colo 201 cells. Statistical significance was assessed using ANOVA followed by Bonferroni post-test analysis. a P < 0.05, aa P < 0.01, aaa P < 0.001, Primary vs HT29; b P < 0.05, bb P < 0.01, bbb P < 0.001, Primary vs LS174t; c P < 0.05, cc P < 0.01, ccc P < 0.001, Primary vs SW480; d P < 0.05, dd P < 0.01, ddd P < 0.001, Primary vs Colo 201.

3.1.4 Extracellular vesicles lipidome as clinical CRC biomarker

Supplemental table 7

	Healthy		HP		AD		Neo	
	Lipid classes							
	Mean	SD	Mean	SD	Mean	SD	Mean	SD
PC	36.7	4.7	45.0	14.1	48.0 a	13.3	46.9 a	9.0
SM	33.5	6.3	25.1	6.6	28.5	10.1	28.5	6.6

Cer	3.0	1.2	2.6	0.4	2.7	1.2	3.4	1.1
PE	7.7	2.4	7.5	2.4	5.8	3.0	7.2	2.4
PS	1.4	0.4	1.8	0.7	2.0_a	0.6	1.8	0.5
PI	14.9	6.1	15.8	6.4	10.8	3.9	10.1_a	3.2
LPC	2.8	0.9	2.1	0.5	2.1	1.1	2.1	0.9

Supplemental table 7: Lipid classes analysis of EVs isolated from the serum of healthy patients, patients with hyperplastic polyps (HP), adenomatous polyps (AD) and with carcinomas (Neo). Statistical significance was assessed using ANOVA followed by Bonferroni post-test analysis. a P<0.05, aa P<0.01, aaa P<0.001, Healthy vs. HP; b P<0.05, bb P<0.01, bbb P<0.001, Healthy vs AD; c P<0.05, cc P<0.01, ccc P<0.001, Healthy vs Neo.

Supplemental table 8

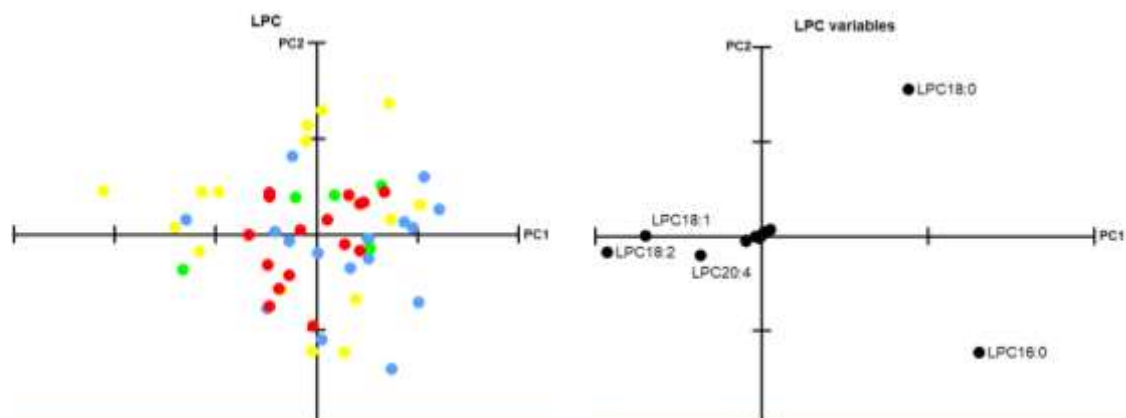
Healthy Patients Group				
Sex	Age	Location		
M	37	Rectum		
F	37	Rectum		
F	39	Rectum		
F	39	Rectum		
F	44	Rectum		
F	49	Rectum		
M	50	Rectum		
F	51	Rectum		
F	52	Rectum		
F	59	Rectum		
M	61	Rectum		
F	62	Rectum		
F	66	Rectum		
F	69	Rectum		
Hyperplastic polyps				
Sex	Age	Location		
M	43	Transverse		
F	45	Transverse, descendent		
M	52	Transverse		
M	75	Descendent		
M	83	Ascendent		
Adenomatous Polyps Group				
Sex	Age	Location	Histologic details ^a	Nº of polyps
F	54	Sigma	TV	1
M	56	Ascendent	Tubular	6
F	57	Descendent	Tubular	>20
M	58	Rectum	Tubular	>20
M	61	Ascendent	TV	4
M	61	Sigma	TV	3
F	61	Descendent	Tubular	1
M	63	Rectum	TV	1
M	65	Transverse	Tubular	3

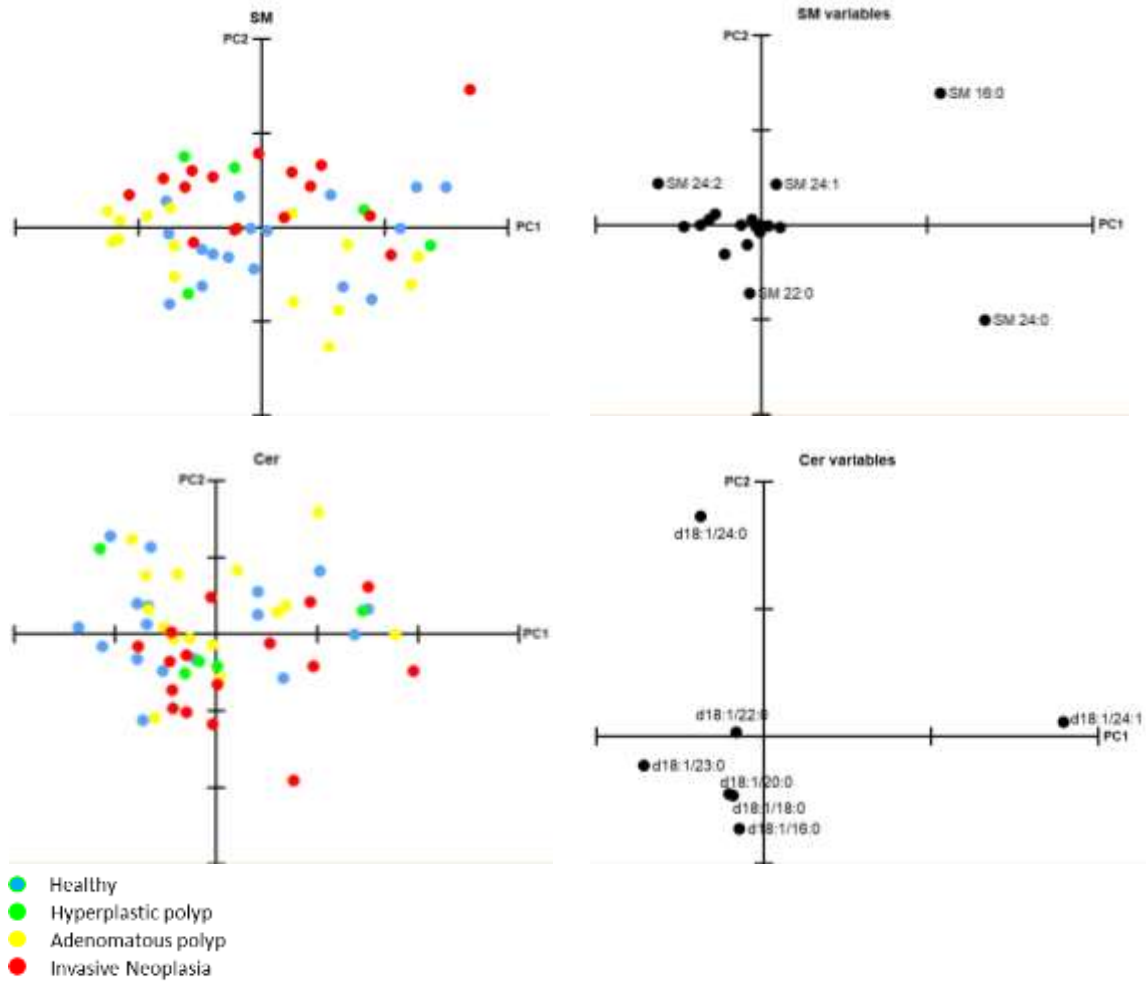
F	65	Sigma	?	1
M	67	Transverse	TV	2
F	67	Ascendent-cecum	Tubular	2
F	68	Tranverse	TV	1
M	74	Rectum	TV with ADC	3
M	78	Ascendent	Tubular	-
F	82	Cecum	Without HGD	3

Invasive neoplasia

Sex	Age	Location	Anatomic stage/ TNM classification ^b
M	59	Recto	T ₃ N ₀ -N ₁
F	78	Sigma	T ₃ N _{2a}
F	65	Sigma	T ₃ N ₀
F	58	Rectum	T ₄
F	66	Rectum	T ₃ N ₀ M _x
M	72	Sigma	T ₁ N ₀
F	60	Sigma	T ₂
M	66	Sigmoide	T ₂ N ₀
M	47	Sigma	T ₄ M ₂
M	53	Ascendent	T ₄ N ₀
F	77	Sigma	T ₂ N ₀
F	65	Sigma-descendent	T ₃ N ₀ b M _{1a}
F	54	Descendent	T ₄ N ₀
M	74	Splenicus	T ₃ N ₀
M	70	Rectum	T ₃ N ₀
M	71	Descendent	T ₃ N _{1b}
M	54	Rectum	T ₃ N ₃
M	69	Sigma	T ₃ N _{1b}
M	87	Rectum	T ₃ N ₀

Supplemental table 8: Clinical information of the patients participating in this study ^(a) Adenomas are divided into three subtypes based depending on the percentage of villous component into: (1) tubular (<25%), (2) tubulovillous (TV, 25-75%), and (3) villous (>75%). Villous adenomas are associated more often with larger adenomas and more severe degrees of dysplasia. HGD: High Grade Dysplasia. ^(b) NOS: not otherwise specified, i.e., conventional adenocarcinoma.

Supplemental figure 4



Supplemental figure 4: PCA of % of each species lipid family in patients serum derived Evs. Explained variances: LPC 92.9, SM 69.9%, Cer 89.4%,.

Supplemental table 9

	Healthy		HP		AD		Neo	
Lipid molecular species								
PC								
	Mean	SD	Mean	SD	Mean	SD	Mean	SD
30:0	1.7	0.4	1.5	0.8	1.0 _{aa}	0.6	1.0 _{aa}	0.5
32:2	0.2	0.1	0.2	0.1	0.2	0.1	0.2 _a	0.1
32:1	2.0	0.7	1.8	0.7	1.5	0.6	1.3 _a	0.5
32:0	5.5	2.0	3.6	1.6	3.8	2.5	4.2	2.3
34:3	0.6	0.2	0.7	0.2	0.7	0.3	0.7	0.2
34:2	14.0	2.8	17.5	6.8	18.2	5.0	20.0 _{aa}	4.5
34:1	32.5	4.3	28.9	5.4	26.0 _a	7.9	26.1 _a	6.2

34:0	1.3	0.6	0.7	0.4	0.8	0.8	0.8	0.6
36:5	0.3	0.1	0.3	0.1	0.4	0.3	0.4	0.2
36:4	1.8	1.0	3.5	2.1	5.6_a	4.6	4.9	3.3
36:3	2.6	0.9	4.1	1.7	4.5_A	2.3	4.3	1.7
36:2	9.2	1.3	10.9	2.8	10.6	1.7	11.9_{aa}	2.6
36:1	10.1	1.9	7.3	2.8	7.1	4.2	6.4_a	2.9
36:0	5.0	0.8	3.6	1.8	3.0_a	2.0	2.9_a	2.0
38:6	1.9	0.4	2.6	1.4	2.6	1.6	2.2	1.0
38:5	1.6	0.4	1.7	0.5	1.9	0.9	1.6	0.5
38:4	1.5	0.7	2.7	1.3	4.3_a	3.4	3.9	2.5
38:3	1.3	0.4	1.9	0.2	2.1_{aa}	0.8	2.0_a	0.7
38:2	1.6	0.4	1.7	0.9	1.5	0.4	1.5	0.5
38:1	3.1	0.6	2.3	1.1	2.0	1.4	1.7_{aa}	1.2
40:6	1.1	0.4	1.3	0.2	1.1	0.4	1.1	0.4
40:5	0.7	0.2	0.7	0.3	0.5	0.2	0.5	0.1
40:4	0.4	0.1	0.5	0.3	0.5	0.3	0.5	0.3
PE								
34:2	4.4	1.3	4.3	1.7	4.5	1.2	4.8	1.3
34:1	23.7	12.5	13.4	12.3	19.8	15.3	17.6	12.3
36:2	6.7	1.6	6.8	3.9	7.4	1.7	7.7	1.7
36:1	7.3	2.4	6.0	3.2	6.2	4.0	6.5	3.1
38:6	2.7	1.0	4.1	2.7	5.2	4.0	4.9	3.3
38:5	2.7	1.0	4.2	1.4	4.5	2.7	4.2	1.9
38:4	5.5	2.9	9.1	6.9	13.5_a	9.0	14.5_{aa}	8.1
32:2	1.3	0.6	1.5	0.7	0.8_{a b}	0.3	0.8_b	0.3
32:1	1.6	0.5	1.5	0.6	1.0_{aa}	0.3	1.1_{aa}	0.3
32:0	2.3	0.6	1.8_{d e}	0.9	1.6	0.8	1.6	0.8
34:3	1.3	0.5	1.4	0.6	0.9	0.3	1.1	0.4
34:0	1.4	0.6	1.4	1.1	0.9	0.5	0.8_a	0.4
36:5	0.9	0.4	1.0	0.3	0.7	0.2	0.7	0.2
36:4	1.3	0.4	1.8	0.7	2.4_{aa}	0.9	2.4_{aa}	1.0
36:3	1.7	0.3	2.0	0.4	1.9	0.3	2.1_a	0.5
38:3	2.9	1.0	3.8	1.1	2.6	1.0	2.7	0.9
38:2	4.4	0.8	3.6	1.1	3.2_a	1.0	3.3	1.2
38:1	3.0	0.9	2.9	0.9	2.2	0.8	2.2_a	0.6
40:6	2.6	2.2	1.9	2.9	4.3	3.4	3.2	2.7

8. Supplemental material

40:5	3.0	1.3	4.1	1.7	2.7	1.2	3.0	1.0
40:4	3.0	1.2	3.2	0.8	2.5	0.8	2.8	1.0
40:3	3.2	1.3	3.6	1.8	2.1	1.0	2.5	1.0
42:7	7.8	3.4	10.2 _d _e	5.9	5.1 _b	2.4	5.7 _b	2.7
42:6	3.0	1.8	3.0	1.7	2.0	1.1	1.9	0.9
42:5	2.7	1.2	3.4 _d	1.7	1.7 _b	0.7	2.0	0.9
PI								
32:0	10.9	2.8	9.0	4.4	5.6 _{aaa}	3.4	6.6 _{aa}	3.1
34:2	6.8	1.1	5.2	0.9	4.8 _{aaa}	1.4	5.5 _a	1.1
34:1	14.0	4.3	10.8	4.7	8.9 _a	4.3	8.9 _{aa}	3.8
36:4	3.2	2.1	4.1	1.1	3.9	0.8	3.5	1.2
36:3	3.6	1.8	3.9	2.6	4.0	1.0	3.6	1.0
36:2	15.5	3.6	16.2	3.4	15.8	3.5	18.3	2.2
36:1	12.7	2.7	10.8	3.3	8.3 _a	4.2	8.9 _a	4.2
36:0	10.0	3.0	8.2	3.6	5.2 _{aaa}	3.0	6.6 _a	3.0
38:4	16.1	6.9	23.0	11.9	33.6 _{aa}	14.8	30.1 _a	12.8
38:3	5.6	1.7	7.0	1.9	7.5	1.8	6.7	2.4
38:2	1.5	1.7	1.8	2.3	2.4	1.1	1.3	1.2
LPC								
15:0	0.7	0.1	0.7	0.2	0.6	0.2	0.6	0.2
16:1	1.2	0.3	1.3	0.3	1.3	0.3	1.2	0.2
16:0	57.1	3.9	55.6	5.9	51.0 _{aa}	6.2	54.3	3.0
18:3	0.4	0.1	0.4	0.1	0.3	0.1	0.4	0.1
18:2	5.3	2.7	7.3	4.7	8.3	4.3	6.8	2.3
18:1	10.0	2.2	11.7	3.3	13.2 _{aa}	3.0	11.5	2.1
18:0	19.4	3.4	16.3	5.0	17.1	4.9	17.7	3.2
20:5	0.3	0.1	0.3	0.1	0.4	0.1	0.4	0.1
20:4	1.4	0.9	2.3	1.4	3.1 _a	2.1	2.9	1.3
20:3	0.5	0.2	0.8	0.4	0.9 _a	0.5	0.7	0.2
20:0	0.6	0.2	0.5	0.1	0.5	0.3	0.5	0.2
22:6	0.4	0.2	0.6	0.3	0.9 _a	0.6	0.7	0.3
22:5	0.2	0.1	0.3	0.1	0.3	0.1	0.3	0.1
22:4	0.2	0.1	0.3	0.1	0.3	0.1	0.3 _a	0.1
22:0	2.2	0.7	1.7	0.6	1.7	0.9	1.7	0.8
SM								
d18:1/14:0	3.8	0.7	4.1	1.3	3.6	0.5	3.2	0.6
d18:1/15:0	1.9	0.2	2.1	0.5	1.8	0.3	1.7	0.3

d18:1/16:1	3.0	0.6	3.2	0.7	3.2	0.9	3.1	0.5
d18:1/16:0	37.9	2.6	39.4	2.7	36.5	2.7	39.0	2.9
d16:0/ 16:0	1.9	0.3	1.6	0.4	1.5	0.4	1.8	0.3
d18:1/16:1-OH	1.3	0.2	1.3	0.3	1.1_a	0.2	1.1_{aa}	0.2
d18:1/16:0-OH	0.6	0.1	0.5	0.2	0.4_a	0.1	0.5	0.1
d18:1/18:1	2.4	0.6	2.4	0.6	2.5	0.9	2.4	0.6
d18:1/18:0	7.4	1.0	7.2	1.1	7.0	1.5	7.4	1.2
d18:0/ 18:0	0.5	0.3	0.4	0.3	0.4	0.2	0.6	0.2
d18:1/20:1	1.1	0.3	1.1	0.2	1.1	0.3	1.0	0.3
d18:1/20:0	3.4	0.9	3.2	1.2	3.2	1.0	2.9	0.8
d18:1/22:2	0.1	0.1	0.2	0.2	0.1	0.1	0.1	0.1
d18:1/22:1	3.4	0.9	3.7	0.6	4.1	1.3	3.5	0.8
d18:1/22:0	8.1	1.0	7.3	1.1	7.9	1.2	7.3	1.3
d22:0/ 22:0	0.1	0.2	0.0	0.0	0.1	0.1	0.1	0.1
d18:1/24:3	0.1	0.1	0.2	0.1	0.3	0.3	0.2	0.2
d18:1/24:2	2.8	0.7	3.5	1.5	4.0	2.2	3.8	1.4
d18:1/24:1	11.2	1.2	11.8	2.3	12.6	1.7	12.7_a	1.2
d18:1/24:0	8.8	2.7	6.7	2.6	8.5	3.8	7.4	2.7
Cer								
d18:1/16:0	7.5	1.3	8.8	1.2	7.5	1.4	9.0	2.3
d18:1/18:0	4.8	1.4	5.3	1.4	4.2	1.0	5.0	1.2
d18:1/20:0	4.5	1.7	4.9	1.3	4.1	1.1	4.9	1.2
d18:1/22:0	13.5	1.1	13.3	0.7	12.9	1.3	12.8	1.8
d18:1/23:0	9.6	4.0	10.0	2.1	9.2	3.6	8.8	2.8
d18:1/24:1	29.6	8.3	26.7	6.3	30.3	7.8	31.0	7.0
d18:1/24:0	30.6	3.5	31.1	2.3	31.9_f	3.3	28.4_c	3.1

Supplemental table 9: Lipid molecular species analysis of EVs isolated from the serum of healthy patients, patients with hyperplastic polyps (HP), adenomatous polyps (AD) and with carcinomas (Neo). Unless indicated, as major sphingoid base, we assumed that all SM backbones were 18:1 carbon chains, although this was not checked and other minority sphingoid base could be present at SM molecular species. Statistical significance was assessed using ANOVA followed by Bonferroni post-test analysis. a P<0.05, aa P<0.01, aaa P<0.001, Healthy vs. HP; b P<0.05, bb P<0.01, bbb P<0.001, Healthy vs AD; c P<0.05, cc P<0.01, ccc P<0.001, Healthy vs Neo; d P<0.05, dd P<0.01, ddd P<0.001, HP vs AD; e P<0.05, ee P<0.01, eee P<0.001, HP vs Neo; f P<0.05, ff P<0.01, fff P<0.001, AD vs Neo.

3.2.1 Lipidome as biomarker of the physiopathological state of the cell

Supplemental table 10

Gradual distribution					
Lipid class	Assigned lipid	R ²	Adjustment	Gradient ^(b)	RI basal / apical

	species		mode ^(a)		values ^(c)
PI					
	32:1	0.62	Log	+	0.2/0.6
	34:1	0.89	lineal	+	8.0/17.0
	34:2	0.76	Log	+	5.0/8.0
	36:1	0.98	lineal	+	6.0/20.0
	36:2	0.94	Log	+	5.7/27.0
	36:3	0.76	2 nd	-	
	36:4	0.94	Log	-	8.2/2.5
	38:4	0.97	Log	-	71.6/15.0
	38:5	0.81	lineal	-	2.5/1.5
	40:4	0.82	lineal	-	1.4/0.4
PE					
	34:1	0.80	Log	+	4.3/7.2
	36:3	0.85	2 nd	-	
	36:4	0.42	lineal	-	1.8/1.0
	38:1	0.56	2 nd	+	
	38:4	0.79	Log	-	20.0/5.4
	38:5	0.40	lineal	-	3.6/1.6
PE-P					
	16:0/18:1	0.70	Log	+	8.3/14.4
	18:0/18:1 PC-O 16:0/18:1	0.82	Log	+	5.6/13.0
	18:0/18:2 18:1/18:1 PC-O 16:0/18:2	0.63	Log	+	8.3/15.5
	16:0/20:4	0.91	Log	-	21.3/9.7
	18:0/20:4 16:0/22:4	0.77	Log	-	28.6/16.1
	20:0/20:4 18:0/22:4 PC-O 18:0/20:4	0.84	Log	-	8.1/1.9
PC					
	32:0	0.69	lineal	-	6.5/4.6
	38:2	0.68	lineal	-	0.7/0.4
	38:3	0.68	lineal	-	1.0/0.5
	38:4	0.43	Log	-	2.8/1.1
	38:5	0.26	Log	-	1.1/0.7
Even distribution					
Lipid class	Assigned lipid species	Mean	SD	%	
PE					
	36:1	24.23	1.34	5.53	
	36:2	25.41	1.97	7.74	
	38:2	9.99	0.91	9.12	
	38:3	7.29	0.70	9.68	
PE-P					

	16:0/18:2	8.4	0.9	10.71
	16:0/20:3 18:1/18:2	4.8	0.6	12.50
	18:1/20:4 16:0/22:5 18:0/20:5	8.8	1.5	17.05
	16:0/22:6	4.4	0.6	13.64
	18:0/22:6 18:1/22:5 PC-O 16:0/22:6	4.7	0.6	12.77
PC				
	32:1	1.50	0.11	7.00
	34:1	37.17	1.52	4.10
	34:2	16.40	0.62	4.00
	34:3	1.50	0.10	7.00
	36:2	17.10	0.40	2.00
	36:3	10.40	0.74	7.00
Scattered distribution				
Lipid class	Assigned lipid species	mean	SD	%
PI				
	32:0	0.53	0.06	11.25
	38:6	0.99	0.20	20.71
PE				
	34:2	2.27	0.31	13.56
PC				
	36:1	4.44	0.49	10.94
	36:4	3.20	0.43	13.30
Supplemental table 10: (a) Changes in RI along the crypt were fitted to linear equation, a polynomial equation of second grade (2 nd) or to a logarithmic equation (log). (b) Slope was considered positive when RI increased from the base of the crypt towards the lumen and negative if the opposite. (c) To indicate the magnitude of the change, IR values at the first and last pixel corresponding to the base and top are included. Values are expressed as percentage of total RI for a particular lipid class and represent the IR mean value of five different crypts obtained in four independent experiments measurements. Those species following the strictest patterns appear shadowed in grey.				

Supplemental table 11

Healthy enterocytes			
Protein	P-value^(a)	η^2	Gradient^(b)
PGE2S	0.0001	0.484	+
SCD1	0.0001	0.39	+
CB1	0.0001	0.331	+
COX1	0.001	0.343	+
FAR1	0.001	0.377	+
AGPS	0.003	0.337	+
PLA2G4	0.003	0.461	+
FAD2	0.008	0.483	+
Pi3K	0.011	0.293	+

ACS4	0.02	0.469	+
COX2	0.039	0.271	+
MBOAT7	0.191	0.088	+
CDS	0.467	0.0134	+
PIP2	0.674	0.005	+
CB2	0.72	0.003	+
FAR2	0.785	0.006	+
AGPA _{T2}	0.827	0.002	-
iPLA2G6	0.838	0.002	-
GNPAT	0.843	0.003	-

Supplemental table 11: Statistical analysis showing a gradual distribution of lipid enzymes along the crypt. **a)** Once obtained the IF images, complete crypts were divided in three areas: basal, central and apical as it is described in Materials and Methods. IF values were obtained in at least 12 different sections of 3-4 different patients. To evaluate statistically the differences in protein expression along the crypt, repeated measurement ANOVAs were computed for IF values in healthy and for adenomatous tissue in separated analysis using IBM SPSS Statistics 22. Results are reported using a significance level (P-value) of 0.05 and eta-square (η^2) to indicate the magnitude of the difference. **b)** Slope was considered positive when IF values increased from to base of the crypt towards the lumen and negative if the opposite. ACS4: Acyl-CoA synthase 4; CDS2: CDP-Diacylglycerol Synthase 2; COX1/2: cyclooxygenase 1/2; PLA2G4: Ca²⁺ dependent phospholipase A2; iPLA2: Ca²⁺-independent phospholipase A2; FAD2: fatty acid desaturase 2; PGE2S: prostaglandin E2 synthase; SCD1: stearoyl-CoA desaturase 1; CB1/2: cannabinoid receptor 1/2; PI3K: phosphatidyl inositol 3-kinase; PIP2: phosphatidyl inositol 3 phosphate MBOAT7: acyltransferase_{AA} specific; AGPA_{T2}: acyltransferase; FAR 1 and FAR2, fatty acid reductase 1 and 2; GNPAT: glycerone-phosphate O-acyltransferase; AGPS: alkylglycerone-phosphate synthase.

Supplemental table 12

Adenomatous colonocytes			
Protein	P-value ^(a)	η^2	Gradient ^(b)
PI3K	0.011	0.224	-
ACS4	0.052	0.154	+
CB2	0.063	0.127	+
COX1	0.134	0.135	+
iPLA2G6	0.148	0.143	+
PIP2	0.209	0.046	+
CDS2	0.214	0.08	+
AGPS	0.22	0.113	+
FAD2	0.273	0.07	+
FAR1	0.333	0.156	+
PLA2G4	0.477	0.015	-
PGE2S	0.539	0.035	-
SCD1	0.614	0.009	-
CB1	0.646	0.011	-
FAR2	0.707	0.012	+
COX2	0.736	0.006	+

GNPAT	0.771	0.007	-
MBOAT7	0.790	0.003	=
AGPA _{T2}	0.935	0	=

Supplemental table 12: Statistical analysis showing a gradual distribution of lipid enzymes along the adenomatous crypt. **a)** Once obtained the IF images, complete crypts were divided in three areas: basal, central and apical as it is described in Materials and Methods. IF values were obtained in at least 12 different sections of 3-4 different patients. To evaluate statistically the differences in protein expression along the crypt, repeated measurement ANOVAs were computed for IF values in healthy and for adenomatous tissue in separated analysis using IBM SPSS Statistics 22. Results are reported using a significance level (P-value) of 0.05 and eta-square (η^2) to indicate the magnitude of the difference. **b)** Slope was considered positive when IF values increased from base of the crypt towards the lumen and negative if the opposite. ACS4: Acyl-CoA synthase 4; CDS2: CDP-Diacylglycerol Synthase 2; COX1/2: cyclooxygenase 1/2; PLA2G4: Ca²⁺ dependent phospholipase A2; iPLA2: Ca²⁺-independent phospholipase A2; FAD2: fatty acid desaturase 2; PGE2S: prostaglandin E2 synthase; SCD1: stearoyl-CoA desaturase 1; CB1/2: cannabinoid receptor 1/2; Pi3K: phosphatidyl inositol 3-kinase; PIP2: phosphatidyl inositol 3 phosphate MBOAT7: acyltransferase AA specific; AGPA_{T2}: acyltransferase ; FAR 1 and FAR2, fatty acid reductase 1 and 2; GNPAT: glycerone-phosphate O-acyltransferase; AGPS: alkylglycerone-phosphate synthase.

Supplemental table 13

Gradual Distribution				
Lipid class	Assigned lipid species	R ² (a)	Gradient ^(b)	RI basal / apical values ^(c)
PI				
	34:1	0.20	-	3.3/1.9
	36:1	0.28	-	7.3/2.4
	36:2	0.29	-	13.2/2.4
	36:3	0.36	-	2.5/1.1
	36:4	0.18	-	2.5/2.0
	38:4	0.45	+	60.1/77.8
	38:5	0.28	-	4.6/2.4
PE				
	34:1	0.24	-	4.6/3.7
	36:1	0.55	-	24.3/23.6
	36:2	0.22	-	19.6/14.3
	36:4	0.55	+	2.0/2.3
	38:2	0.44	-	9.2/7.2
	38:4	0.55	+	21.9/27.5
	38:5	0.70	+	3.8/5.6
	40:5	0.49	+	3.4/4.8
PC				
	32:0	0.32	-	13.5/13.3
	34:2	0.63	-	16.6/12.3
	34:3	0.39	-	1.1/0.9
	36:2	0.42	-	11.7/10.8
	36:4	0.24	+	4.9/10.5
	36:5	0.01	-	0.3/0.7

	38:3	0.32	+	0.4/0.6
	38:4	0.47	+	4.1/5.9
	38:5	0.65	+	1.4/3.6
	38:6	0.42	+	0.5/0.9
PE plasmalogens				
	PE P-40:4/PE O-40:5	0.6	+	7.6/5.4
	PE P-40:5/PE O-40:6	0.6	+	5.8/3.6
Even distribution				
Lipid class	Assigned lipid species	mean	SD	%
PE				
	34:0	5.10	0.76	14.90
	38:3	6.23	0.70	0.28
PC				
	32:1	1.88	0.21	11.00
	34:1	29.52	2.02	6.84
	36:1	3.86	0.85	22.01
	36:3	4.33	1.03	23.88
Scattered distribution				
Lipid class	Assigned lipid species	mean	SD	%
PI				
	34:2	1.17	0.56	48.32
PE				
	34:2	1.30	0.42	32.60
	36:3	2.90	0.75	25.94
PE-P				
	PE P- 34:1/PE O-34:2	7.3	2.21	30.24
	PE P- 34:2/PE O-34:3	1.61	1.21	75.4
	PE P-36:1/PE O-36:2	3.97	1.76	44.43
	PE P-36:2/PE O-36:3	4.04	2.16	53.52
	PE P-36:3/PE O-36:4	1.04	0.99	94.83
	PE P-36:4/PE O-36:5	20.62	3.74	18.12
	PE P-38:4/PE O-38:5	27.62	5.41	19.58
	PE P-38:5/PE O-38:6	13.44	3.38	25.11
	PE P-38:6/PE O-38:7	5.26	2.05	38.97
	PE P-40:6/PE O-40:7	4.45	2.41	54.06
	PE P-40:7/PE O-40:8	1.18	1.05	88.44
PC				
	38:2	0.30	0.10	43.90
Supplemental table 13: (a)Changes in RI along the crypt were fitted to linear equation. (b) Slope was considered positive when RI increased from the base of the crypt towards the lumen and negative if the opposite. (c) To indicate the magnitude of the change, IR values at the first and last pixel corresponding to the base and top of the mucosa are included. Values are expressed as percentage of total IR for a particular lipid class and represent the IR mean value of four independent experiments measurements. PtdCho: phosphatidylcholine, PtdEtn: phosphatidylethanolamine, PtdIns: phosphatidylinositol. Those species following the strictest patterns appear shadowed in grey.				

Supplemental table 14

Healthy lamina propria			
Protein	P-value ^(a)	η^2	Gradient ^(b)
PLA ₂ G4	0.0001	0.408	+
CB2	0.005	0.159	-
MBOAT7	0.005	0.165	-
COX2	0.007	0.181	+
iPLA ₂ G6	0.012	0.073	+
COX1	0.025	0.088	-
FAR2	0.047	0.291	+
SCD	0.053	0.061	-
FAR1	0.177	0.094	+
FADS2	0.218	0.03	-
PGE ₂ S	0.248	0.021	+
PIP2	0.284	0.025	=
ACS4	0.287	0.022	+
AGPA _{T2}	0.33	0.152	-
GNPAT	0.392	0.029	+
PI3IK	0.529	0.009	+
AGPS	0.54	0.165	+
CDS	0.545	0.013	-
CB1	0.488	0.013	+

Supplemental table 14: Statistical analysis showing a gradual distribution of lipid enzymes along the healthy lamina propria. (a) Once obtained the IF images, complete crypts were divided in three areas: basal, central and apical as it is described in Materials and Methods. IF values were obtained in at least 12 different sections of 3-4 different patients. To evaluate statistically the differences in protein expression along the crypt, repeated measurement ANOVAs were computed for IF values in healthy and for adenomatous tissue in separated analysis using IBM SPSS Statistics 22. Results are reported using a significance level (P-value) of 0.05 and eta-square (η^2) to indicate the magnitude of the difference. (b) Slope was considered positive when IF values increased from to base of the crypt towards the lumen and negative if the opposite. ACS4: Acyl-CoA synthase 4; CDS2: CDP-Diacylglycerol Synthase 2; COX1/2: cyclooxygenase 1/2; PLA2G4: Ca²⁺ dependent phospholipase A2; iPLA2: Ca²⁺-independent phospholipase A2; FAD2: fatty acid desaturase 2; PGE2S: prostaglandin E2 synthase; SCD1: stearoyl-CoA desaturase 1; CB1/2: cannabinoid receptor 1/2; Pi3K: phosphatidyl inositol 3-kinase; PIP2: phosphatidyl inositol 3 phosphate MBOAT7: acyltransferase AA specific; AGPA_{T2}: acyltransferase; FAR 1 and FAR2, fatty acid reductase 1 and 2; GNPAT: glycerone-phosphate O-acyltransferase; AGPS: alkylglycerone-phosphate synthase.

Supplemental table 15

Adenoma lamina propria			
Protein	P-value ^(a)	η^2	Gradient ^(b)
PGE ₂ S	0.0001	0.64	+
PIP2	0.002	0.191	+
FAR2	0.006	0.432	+
PI3K	0.007	0.266	-

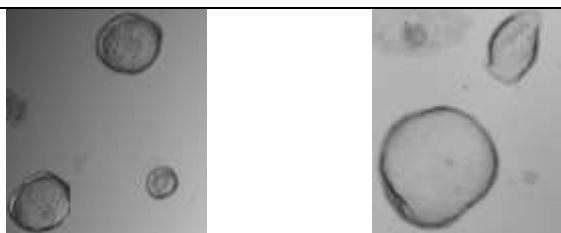
FAR1	0.019	0.316	+
AGPA _{T2}	0.038	0.155	+
AGPS	0.052	0.326	+
COX2	0.069	0.103	-
MBOAT7	0.107	0.105	-
iPLA ₂ G6	0.122	0.101	+
FADS2	0.157	0.129	-
ACS4	0.244	0.029	+
GNPAT	0.302	0.151	+
CB2	0.581	0.016	+
COX1	0.645	0.017	-
CDS2	0.724	0.009	+
CB1	0.738	0.006	=
PLA ₂ G4	0.785	0.003	=

Supplemental table 15: Statistical analysis showing a gradual distribution of lipid enzymes along the healthy lamina propria. (a) Once obtained the IF images, complete crypts were divided in three areas: basal, central and apical as it is described in Materials and Methods. IF values were obtained in at least 12 different sections of 3-4 different patients. To evaluate statistically the differences in protein expression along the crypt, repeated measurement ANOVAs were computed for IF values in healthy and for adenomatous tissue in separated analysis using IBM SPSS Statistics 22. Results are reported using a significance level (P-value) of 0.05 and eta-square (η^2) to indicate the magnitude of the difference. (b) Slope was considered positive when IF values increased from to base of the crypt towards the lumen and negative if the opposite. ACS4: Acyl-CoA synthase 4; CDS2: CDP-Diacylglycerol Synthase 2; COX1/2: cyclooxygenase 1/2; PLA2G4: Ca²⁺ dependent phospholipase A2; iPLA2: Ca²⁺-independent phospholipase A2; FAD2: fatty acid desaturase 2; PGE2S: prostaglandin E2 synthase; SCD1: stearoyl-CoA desaturase 1; CB1/2: cannabinoid receptor 1/2; PI3K: phosphatidyl inositol 3-kinase; PIP2: phosphatidyl inositol 3 phosphate MBOAT7: acyltransferase ^{AA} specific; AGPA_{T2}: acyltransferase; FAR 1 and FAR2, fatty acid reductase 1 and 2; GNPAT: glycerone-phosphate O-acyltransferase; AGPS: alkylglycerone-phosphate synthase.

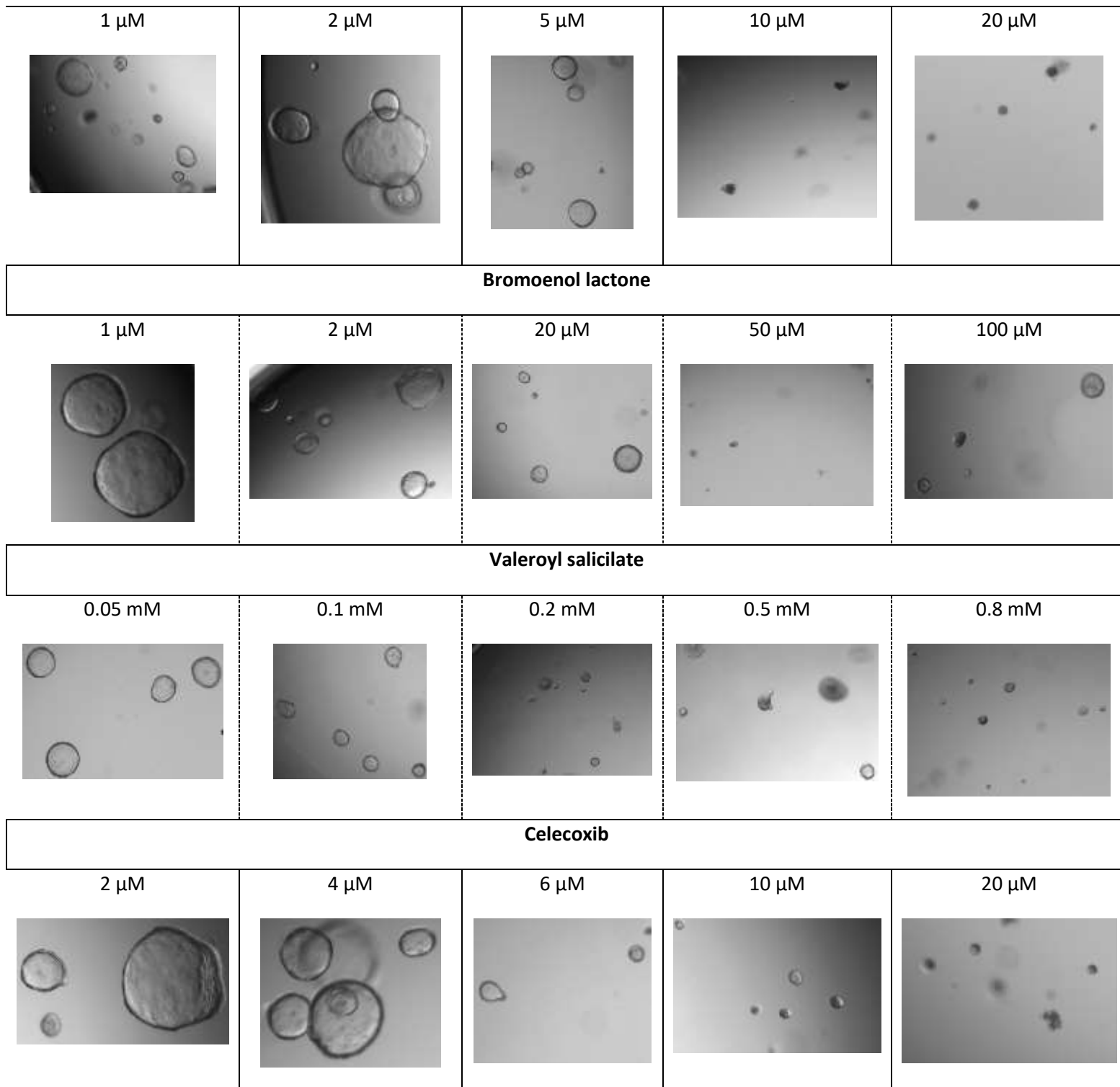
3.2.2 Prostaglandin signaling in colon proliferation

Supplemental figure 5

Vehicle (DMSO 0.3%)

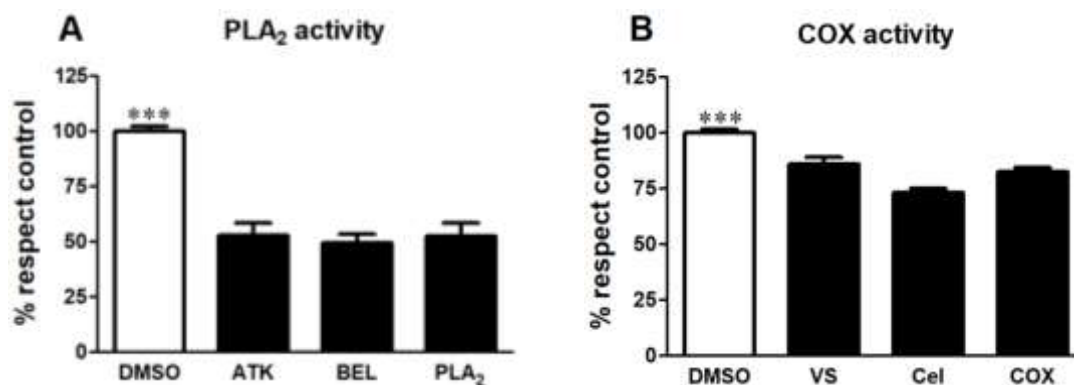


Arachidonyl trifluoromethyl ketone



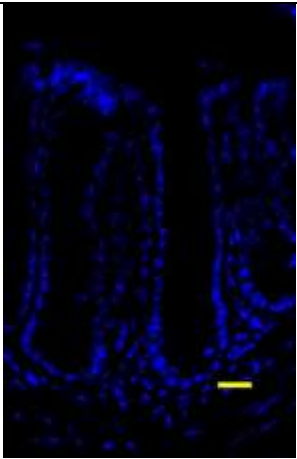
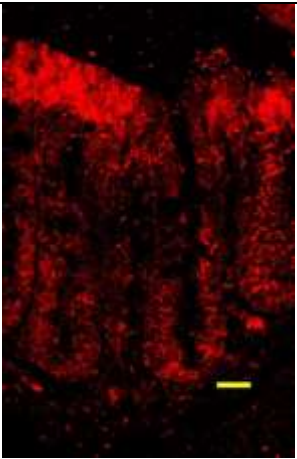
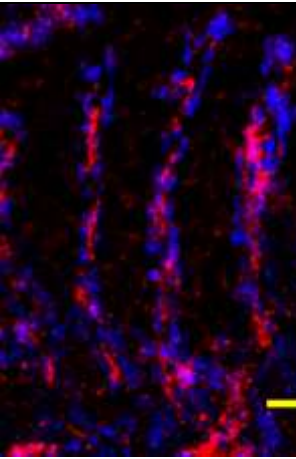
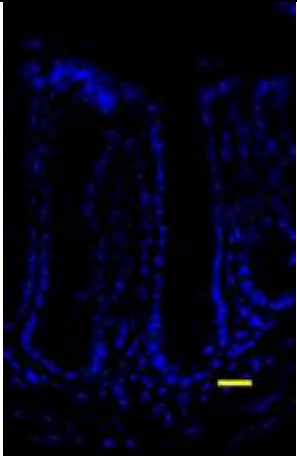
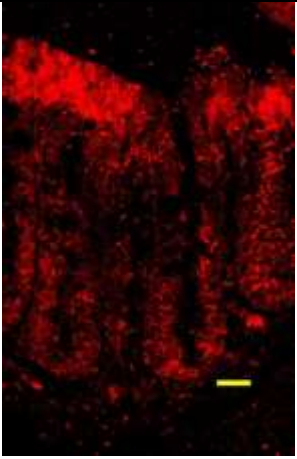
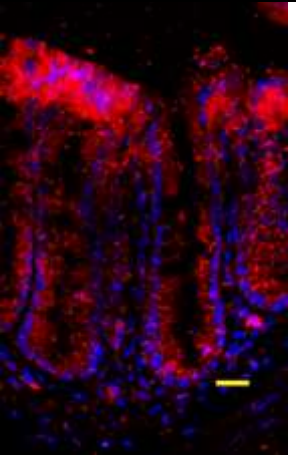
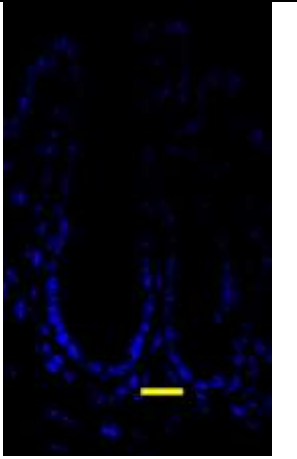
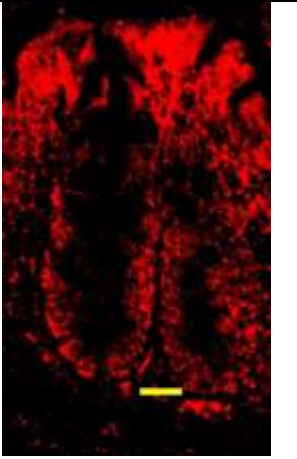
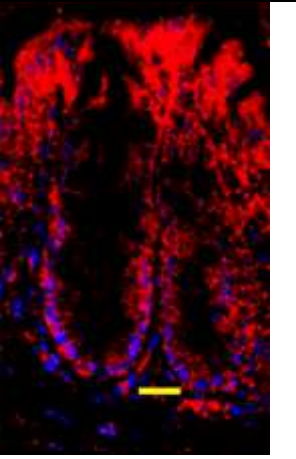
Supplemental figure 5: Representative images of the organoids cultured at different PLA₂ and COX inhibitors concentration. The maximum concentration of each inhibitor before organoid development impairment compared to control conditions was: 5 μ M for ATK, 20 μ M for BEL, 0.1 mM for VS and 4 μ M for Cel.

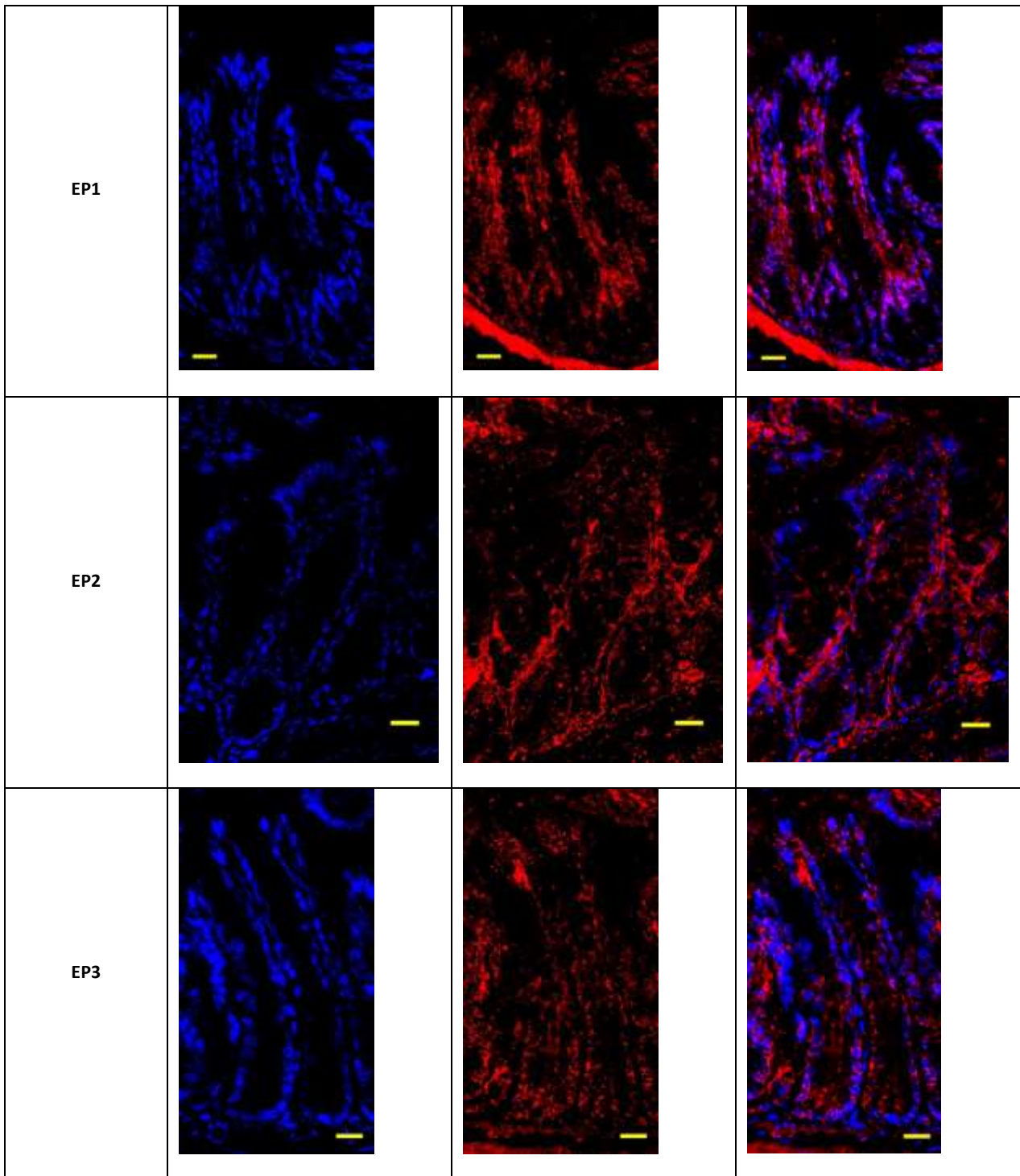
Supplemental figure 6

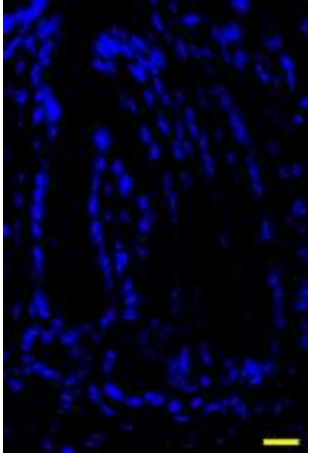
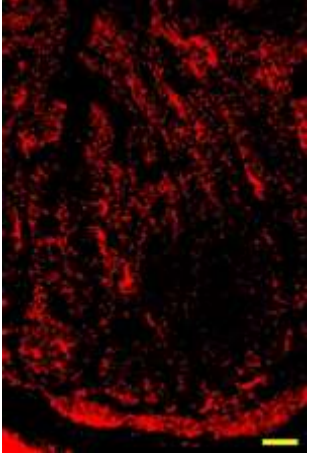
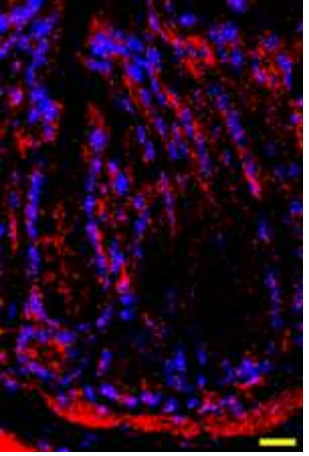


Supplemental figure 6: Assessment of the PLA₂ and COX inhibition capacity of the compounds used. . Statistical significance was assessed using ANOVA followed by Bonferroni post-test analysis. *** P<0.001. **A)** Assessment of PLA₂ activity after treatment with PLA₂ inhibitors using the EnzChek Phospholipase A₂ assay kit of Invitrogen. The concentrations used for each inhibitor was: 5 μM for ATK and 20 μM for BEL. **B)** Assessment of COX activity after treatment with COX inhibitors using the COX Activity Assay kit of Abcam. The concentrations used for each inhibitor was: 0.1 mM for VS and 4 μM for Cel. DMSO: dimethylsulfoxide, ATK: arachidonyl trifluoromethyl ketone, BEL: bromoenol lactone, PLA₂: combination of ATK and BEL, VS: valerolyl salicylate, Cel: celecoxib, COX: combination of VS and Cel.

Supplemental figure 7

<p>ATPase Na⁺/K⁺</p>			
<p>PGF_{2α} receptor</p>			
<p>PGD₂ receptor</p>			



EP4			
	DAPI	Antibody	Merge
Supplemental figure 7: Representative immunofluorescence assay of each prostaglandin receptor tested and the ATPase Na ⁺ /K ⁺ as a negative control of nuclear presence.			